Camel fossils from the El Kowm Basin, Syria. Diversity and evolution

Inauguraldissertation

Zur
Erlangung der Würde eines Doktors der Philosophie
vorgelegt der
Philosophisch-Naturwissenschaftlichen Fakultät
der Universität Basel

von

Pietro Martini

aus Cavergno, Tessin

Locarno, 2019

Genehmigt von der Philosophisch-Naturwissenschaftlichen Fakultät

auf Antrag von

Prof. Dr. Jean-Marie Le Tensorer
Dr. Peter Schmid

Basel, den 12. Dezember 2017

Prof. Dr. Martin Spiess
Dekan

Acknowledgements

This doctoral thesis was supported by the Swiss National Foundation, the Isaac Dreyfus-Bernheim Stiftung, and the Freiwillige Akademische Gesellschaft Basel. The material studied herein was obtained from excavation in the El Kowm Basin, which are funded by the Swiss National Foundation, the Tell Arida Foundation and the Freiwillige Akademische Gesellschaft Basel.

I am glad to have the occasion to express my deep gratitude to the people who made this study possible. In first place, Prof. Jean-Marie Le Tensorer offered me the chance of pursuing a PhD under his supervision and always provided me with means, advice, patience and most of all his friendship. Dr. Loïc Costeur kindly took me under his care, followed me and supported me through most of the research, leading me to endure some of the most challenging times. Prof. Peter Schmid trusted me with the study of El Kowm camelids from the very beginning, in the form of my Master's thesis. Only with the help and encouragement of these three outstanding people have I been able to arrive were I am now.

For their participation in the committee of my doctoral exam, I am thankful to Prof. Dieter Ebert, who accepted the position of Vorsitzender, and to Dr. Jan van der Made who joined from Madrid. They shared this duty and share my gratitude with the already mentioned Prof. Jean-Marie Le Tensorer, Dr. Loïc Costeur and Prof. Peter Schmid.

Several others have contributed to my work, and I extend my heartly gratitude to them. The fellow researchers in the El Kowm Project have been most friendly and helpful, enlightening me in the nuances of the stratigraphy: Reto Jagher, Dorota Wojtczak, Thomas Hauck, the late Daniel Schumann, Fabio Wegmüller, and the many students and colleagues involved in the project. Daniel had particular regards for me both in El Kowm and during my revision of the collection records, and his tragic, premature departure is sorely regretted. I am thankful to Hélène Le Tensorer and to Vera von Falkenstein for their supportive encouragement. I also wish to mention the staff of the IPNA Institute and of the Tell Arida research center, led by Ahmed Taha, whose work was foundational to any lab or field research we carried on. Ahmed lost his battle with cancer as this thesis was going in print; his invaluable collaboration with all visitors since the dawn of researches in El Kowm will not be forgotten.

The Naturhistorisches Museum Basel opened its door to me and gave me a second working place, where I ended up spending most of my time: I'm grateful to all the staff who helped me, and especially to the directors Christian Meier and Basil Thüring for the hospitality, to Markus Weick and Tandra Fairbanks for tutoring me on the preparation of fossils, and to the fellow paleontologists Vanessa De Pietri, Yannick Mary, and Bastien Mennecart for sharing thoughts and drinks in moments of enlightenment and darkness, respectively.

Outside of my closest work circle, I wish to remember and thank the collaboration and scientific support of Denis Geraads and John Rowan. My gratitude goes to all curators that granted me access to the collections in their care: in temporal order, Barbara Oberholzer and Marianne Haffner (Zoologisches Museum der Universität Zürich), Paul Schmid (Naturhistorisches Museum des Burgergemeindes Bern), Jacqueline Studer (Muséum d'Histoire Naturelle de la Ville de Genève), Michela Podestà and Giorgio Bardelli (Museo Civico di Storia Naturale Milano), and Denis Geraads (Muséum National d'Histoire Naturelle Paris). The camel project was started as a Master thesis at the Anthropological Institute and Museum of the University of Zürich: I am grateful to the staff and to the director, Prof. Carel van Schaik. Other people who shared ideas, information and literature are also thanked: Jan van der Made, Jorge Morales, Grégoire Métais, Anneke Van Heteren, Donna Rush and Huig de Groot. Inna Popko greatly helped with the translation of Russian and Ukrainian literature, and Marin Mikelin was instrumental in the production of photographs and other pictures: both deserve my warmest appreciation.

Finally, I want to express my highest gratitude and affection to my family and friends who have been close to me in all or part of this long, challenging, sometimes frustrating endeavor. I would probably have lost my sanity if they hadn't been around: my parents Luca and Michela, my siblings Gori and Giulia, Irene, Ana and Elisa, Lars and the "Disagio" friends, the pals from AIM and UZH, Marco and all the Vio's, Flaminia and Sempronia. It's a short list which definitely suffers from recency bias, therefore I'll add in a classic conclusion: "… e tutti quelli che mi conoscono!"

Table of contents

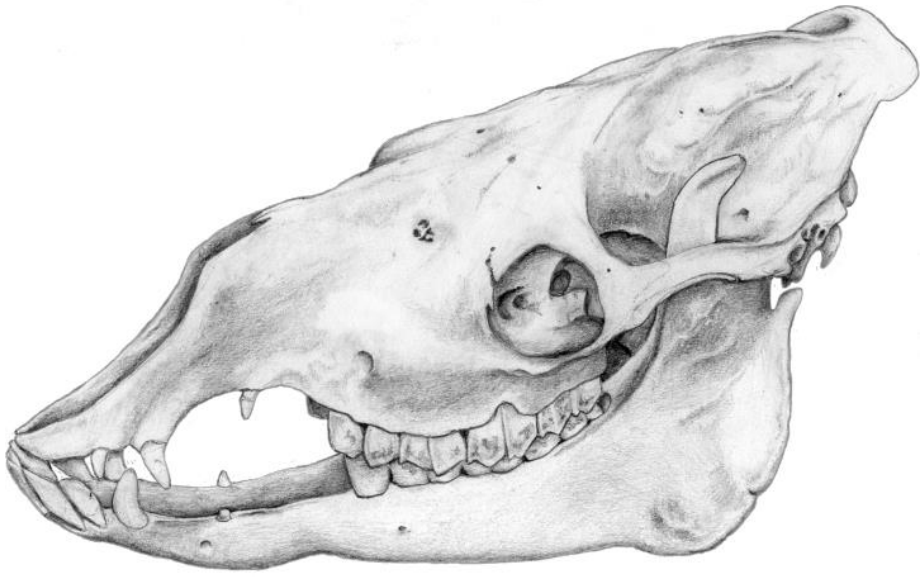

Fig. 00 Cranium of female *C. bactrianus* ZM 17685, drawing by the author

Summary

Camelidae is a family of Artiodactyla which includes a depleted diversity of extant species, divided into two tribes: the Camelini consist of two domestic species (Bactrian camel, *Camelus bactrianus*, and dromedary, *C. dromedarius*; the former is also represented by a wild subspecies, *C. bactrianus ferus*), and the Lamini consist of two domestic (*Lama glama* and *Vicugna pacos*) and two wild species (*Lama guanicoe* and *Vicugna vicugna*). The natural distribution of Camelini is in Eurasia and Africa, while Lamini are endemic of South America and are not part of this work. However, the family has a rich fossil record, amounting to dozens of extinct species, from its origins in the middle Eocene (~45 Ma) of North America to the dispersal of Camelini into the Old World towards the end of the Miocene (~6 Ma).

After their immigration, the evolutionary history of camels in Eurasia is unclear. Several Pliocene and Pleistocene species have been named within the genera *Paracamelus* and *Camelus*, but the relationships among them are poorly understood, in particular within the last two million years. Consequently, no direct ancestor of either extant species is known. As a matter of fact, until the turn of the millennium it was not even clear if Bactrian camel and dromedary are actually different species, or only domestic forms of the same wild precursor, and osteological differences between them were hardly known. This paucity of knowledge depends in equal measure from a lack of fossils and from a lack of evolutionary investigations over these animals, which contrasts with the great historical, cultural, and economic importance that they have in the arid regions of Africa and Asia. Thus, a better understanding of Old World camels will depend both on discovery of new fossils, and on improved description of already known species, including extant ones.

A rich collection of camel fossils has been found in the oasis of El Kowm, central Syria. This locality is a 10-km wide basin where numerous artesian wells have dotted the otherwise arid plain over the span of the Pleistocene, creating as many archaeological sites. The springs were not only attractive for the steppe fauna, but also for the ancient human population which are continuously recorded since their first expansion out of Africa: the most ancient lithic assemblage, from the site Aïn al Fil, is dated to the Olduvai subchron at about 1.8 Ma, while the most recent industries grade into the Neolithic and historical periods. The El Kowm Basin has been extensively studied from an archaeological point of view, and three sites have been excavated systematically: Nadaouiyeh Aïn Askar, Umm el Tlel and Hummal. However, the stratigraphy does not record only the human presence, but also a rich macrofauna. All layers of the site present similar animal assemblages: the

dominant taxa are camels, equids and bovids of different size classes, indicating an arid steppe habitat and the absence of important climatic changes. The abundance of fossils and the long, detailed stratigraphic sequence obtained by combining the major sites give to the El Kowm Basin a prominent place among Middle East paleontological localities, which are concentrated on the humid coast or the northern mountains and rarely sample faunas adapted to arid climates. More specifically, this deep and rich record of camelids is unmatched in the Middle East and in the Pleistocene of the Old World, providing a unique window through which the origins of their charismatic extant relatives can be studied.

In this doctoral thesis, I tackle the study of the El Kowm in two steps: first, I lay some necessary comparative foundations by gathering data on the osteology of extant *Camelus* species and describing the yet unpublished type sample of *Camelus thomasi*, a terminal Early Pleistocene species from Algeria which is suspected to occur in the Middle East as well. Then I proceed with the description of the camelid samples from the sites of Nadaouiyeh, Hummal, and Aïn al Fil in the El Kowm Basin.

To compare the osteology of both extant camel species, *Camelus bactrianus* and *Camelus dromedarius*, I elected to focus on simple morphometric methods. Previous observations gave rise to the suspect that qualitative traits are poorly indicated to diagnose these two closely related species, but several skeletal parts might differ in proportions between them. In order to apply the data and methods on the fossil record, I found necessary to choose simple statistical analyses which can be applied even on highly fragmentary or poorly preserved specimens. Therefore, I developed a reliable measurement system and a data transformation called Harmonic Scores, which is a combination of standardizing and scaling. The chosen methods gave satisfying result: we were able to identify and quantify several consistent interspecific differences, some of which are univocal and highly diagnostic, while others are only slightly significant and noticeable only at a population level. In addition to the descriptive results and the measurement database that were generated, some distinctive traits are suggestive of previously unknown biological adaptation: in particular, the cranial anatomy of Bactrian camels shows characters correlated with increased grazing, while its limb muscle attachments may indicate additional need for lateral stability in a heavier animal. The presence and number of humps is reflected in the vertebral column, with several differences in the lumbar region that will be helpful in the reconstruction of fossil species.

The only fossil species which has been mentioned in the Middle East is *Camelus thomasi* POMEL 1893, described from the Algerian locality Tighennif. Unfortunately, only few skeletal part

of this species have been published by its author (a maxilla, a fragment of mandibula, and a metatarsal), and the original description was not very detailed. Additional specimens have been referred to *C. thomasi* on the basis of weak arguments, usually large size and geographical proximity. However, a much larger fossil sample from Tighennif has been recovered by Arambourg in 1954-56 but never published. The remains are housed at the Musée National d'Histoire Naturelle in Paris and have long been unavailable to researchers. We finally elucidate the morphology of *C. thomasi* by describing this collection, including a complete cranium, several mandibles and postcranial bones. Our study shows that this animal was larger than extant camels, but not as much as some remains assigned to it; that currently, no identification outside of the Maghreb can be considered reliable; and that its relationships with either extant species are not very close, unlike what has been proposed by several authors.

The sites of the El Kowm Basin which have been included in this study are Aïn al Fil, Hummal and Nadaouiyeh Aïn Askar, all excavated by the University of Basel. The combined stratigraphy starts with Aïn al Fil, which is a small site dated at 1.8 Ma. It has yielded only four camelid specimens, but two very different specimens of the same bone (the scaphoideum) give reasons to accept the existence of two unnamed species in its time span; one of them is a giant form.

The temporal sequence in Nadaouiyeh covers a time span from 0.55 to 0.15 Ma, and is bracketed between the lower and the upper sections of Hummal. The important assemblage from this site is described and assigned to a new species, named *Camelus roris*. A rather complete cranium is chosen as the holotype, and a left maxilla as the paratype; this form is characterized by average size, broad cranial proportions, unique orbital shape, presence of maxillar crest, posterior placement of the palatine foramina, upper dentition with relatively large M1 and small M3, and a pachyostotic mandible comparable to *C. thomasi*. More than hundred dental and postcranial specimens are assigned to this species, but rare instances of bones with a strongly different morphology suggest that a second species sporadically visited the locality in this period.

The stratigraphy of Hummal site starts in the late Early Pleistocene but does not have an absolute dating; the entire lower section (unit G) is estimated within 1.2 and 0.8 Ma. In this time span, abundant camelid material is found and is shown to differ from other named species, either in El Kowm or elsewhere. It also differs from the material in Aïn al Fil. Unfortunately, there are not enough well-preserved cranial specimens to warrant the definition of a new species for this assemblage.

An important hiatus divides the lower layers in Hummal from the upper section (units A-F), whose age is considered middle to late Pleistocene; unit E is possibly as old as 0.325 Ma, and the uppermost units extends into historic times. This section is subdivided into several units, corresponding to different archaeological and camelid assemblages. The largest collection is found in the Mousterian industry-bearing unit C (layer 5). Here, the material demonstrates clearly that two species existed side by side within the interval from 0.150 to 0.045 Ma, one of slightly smaller size than the extant dromedary, the other of gigantic proportions, comparable to the largest Old World camelid known. Both species could be defined on adequate material: the small camel was named *Camelus concordiae*, and the large one *Camelus moreli*.

The situation is less clear in the units D, E, and F, representing a period intermediate between Nadaouiyeh and the Mousterian layers. Our study concluded that this material cannot be divided into discrete forms, nor can it be separated from neither the older *C. roris* nor the younger *C. concordiae*. We interpret this as a period of either admixture or alternance between these two species or their close relatives; anagenetic change is not impossible but seems unlikely.

The descriptive work performed within the scope of this thesis has produced abundant data over the morphology of extant and extinct camel species, both known and new. The comparative morphometry of living *Camelus* species answers a century-old debate and provides a necessary reference for any further studies. The publication of a large collection of *C. thomasi* fossils sheds clarity over this often misunderstood species. The analysis of the El Kowm record brought to light an unexpected and vast diversity, created by a pattern of dynamic evolutionary change, with at least six species represented here: more than the number previously described worldwide.

Introduction

Scope of the study

This thesis is built on 6 chapters, corresponding to as many independent academic articles that are presently in different stages; two have been published, one has been accepted for publication, one is approaching submission, and two are complete and undergoing final preparation. The manuscript can be divided into two parts: the first two chapters consist of preliminary studies which lay the necessary comparative base for further advances. The second part, composed of four chapters, presents and interprets results concerning the actual subject of this thesis, namely the camelid fossils from El Kowm, Syria.

In addition to gathering and publishing the comparative data mentioned, study of the fossil collection required two additional tasks: revision of the collection documentation, and laboratory preparation of the specimens. Both endeavors needed a significant time. The Hummal collection has been excavated over twelve field campaigns (1997-2011 except 1998), and its faunal record had not been investigated until the start of this thesis; hence, some mistakes, inconsistencies and incomplete corrections in the documentation of fossils have accumulated over this time but had not yet been systematically reviewed. The results of the collection revision are not included; they have been integrated in the official database of the El Kowm research group, and here only data regarding the studied material is presented. Preparation of the fossils (from both Hummal and Nadaouiyeh collections) was necessary in order to allow manipulation, description and measurement of several specimens. The two most challenging items were the cranium Nad F14-671 and the left scapula Nad H14-755, both very delicate and almost completely covered in hard sediments that had to be removed carefully. Once the study material and its documentation were appropriately restored, I moved on to their investigation.

A significant issue during the course of my work was the political unrest in Syria, which has been qualified as civil war and has prevented any access to the research station of Tell Arida since 2011. We have been informed that belligerent parts had occupied the structure, and some of the buildings have been damaged by the hostilities. About two-thirds of the fossil collection from Hummal (as well as large amounts of archaeological remains) were preserved in this location: it is presently impossible to know the state of the collections, and it is possible or even likely that some or all of them were removed, destroyed, damaged, admixed or in other ways confused so that scientific studies will be prevented or greatly impaired. Fortunately, I have been able to gather

preliminary data during the field campaign of 2009, and I have included these and other sources of information in the analyses, as they might represent the only knowledge ever available regarding the important material in that collection. In the not so near future, hypothetical recovery of that collection or further excavations in the El Kowm Basin might be able to provide additional details concerning the assemblages I describe here.

Originally, I intended to include also a phylogenetic analysis of Old World camels in my thesis. I decided that this project was unfeasible after realizing that the El Kowm material is inadequate, and that the knowledge on other camel fossils is insufficient to obtain a meaningful result. On the one hand, although each species described here is known though many skeletal elements, most of the elements are known for only few species: for example, the cranium is known in two species and the symphysis only in one. The dentition is very conservative in camelids, and does not offer many characters. Hence, limiting an analysis to the elements known in all or most species would yield only a weak phylogenetic hypothesis. On the other hand, there is a lack of descriptive data concerning fossil species not reviewed in this thesis, such as *C. knoblochi*, *"C." sivalensis* and all *Paracamelus* species. In order to include these species, additional descriptions and original observations would be necessary. Considering these challenges, I concluded that a meaningful phylogenetic analysis would have exceeded the scope of this thesis, and I limited myself to accurate, abundant descriptions of the new material. This work lays some fundaments on which future studies of Old World camelids will be build.

Content of the chapters

All chapters are presented in the form of manuscript. Slight differences in the structure and formatting of each chapter (in particular concerning figures) might be due to different requirement of the pertinent journals. Chapter 4 and Chapter 5 mention new names for three new species ascribed to the genus *Camelus*: these chapters are conceived as manuscripts for publication, upon which the names shall be considered valid.

Chapter 1

This chapter consists of a published article which compares both extant species of camel, with a focus on morphometric data. The study was started as my Master's thesis, but the dataset was expanded, the statistical analysis refined, and the results were published within the scope of my doctoral thesis. The reference to the article is:

Martini, P., P. Schmid, and L. Costeur (2017). *Comparative morphometry of Bactrian Camel and Dromedary*. **Journal of Mammalian Evolution** (19 pgg and electronic supplementary material). https://doi.org/10.1007/s10914-017-9386-9

The detailed comparison of extant *Camelus* species was a necessary requisite to any study of fossils. Only few authors had tried to compare both species, but none of their study was considered as an adequate starting point for the analysis of the El Kowm fossils. In particular, we focused on gathering a statistically significant sample of morphometric data, something which was never done before.

Camel species only show few qualitative distinctions in osteology, but our work was able to find a large number of statistically different proportions in the majority of skeletal elements. We paid special attention to elements abundant in the El Kowm fossil record, but often neglected in paleontology, such as carpals, tarsals, and long bone diaphysis. Conversely, dentition is often the best diagnostic element or even the only preserved part of fossil mammals, but it turned out to have a limited taxonomic value in our study group. The published descriptions and measurement data set will provide a fundamental reference for any morphological study of camels from now on.

In addition, a novelty is represented by the statistical analysis of data: in order to compare two animals of different but overlapping size, we developed a transformation which was called harmonic score and can be thought of as an average of all indices relative to the other measurements of a specimen. All measurements are expressed as a proportion of the reference value (here, the interspecific average of both extant species) and then scaled by an estimation of size (here, the harmonic mean of all proportional values of the specimen). This calculation can also be performed using incomplete measurement sets, such as those obtained from fragmentary fossil specimens. Comparable common approaches (e.g. Simpson's log-ratio transformation) do not take size into consideration, hence cannot be directly interpreted in terms of shape but need further comparisons. On the other hand, more refined morphometric methods (e.g. Principal Component Analysis or Discriminant Analysis) require complete dataset and well-preserved specimens. Therefore, harmonic scores combine standardizing, size scaling, and simplicity in a way which is innovative in paleontology. This transformation was applied extensively in this and in subsequent studies (chapters 6-8); the scores are then analyzed and compared using basic statistical test (such as Student's t-test), or visualized with bivariate scatterplots (to compare small samples). The method was found to be very useful in both detecting and quantifying differences (which could then be confirmed visually), and might have promising applications in other studies.

Chapter 2

This chapter consists of a published article which describes for the first time a large sample of *Camelus thomasi* fossils from its type locality Tighennif, Algeria. The reference to the article is:

Martini, P., and D. Geraads (2018). Camelus thomasi *Pomel, 1893, from the Pleistocene type-locality Tighennif (Algeria). Comparisons with modern* Camelus. **Geodiversitas** 40 (5): 115-134 (19 pgg). https://doi.org/10.5252/geodiversitas2018v40a5.

This species is the only known fossil camel species which, for geographic and temporal distribution, might be expected to appear in the El Kowm Basin. It is known from Northern Africa, was reported from locations in the Middle East, and the age of its type material is estimated at 1 Ma, within the El Kowm temporal depth. Other fossil camel species are either much older (*C. grattardi* and *C. sivalensis* are Pliocene; *Paracamelus* is known until 2 Ma), geographically remote (*C. grattardi* is known from Ethiopia, *C. sivalensis* from India, *C. knoblochi* and most *Paracamelus* from central Eurasia and Siberia; not to mention the North American camelid diversity) or ecologically distinct (*C. knoblochi* and several *Paracamelus* species are known only from boreal habitats, which were significantly colder or had greater tree cover than the steppe reconstructed in El Kowm). Unfortunately, *Camelus thomasi* was poorly known; the original description (Pomel 1893) included only a maxilla, a fragmentary mandible and a metatarsal. Later excavations the locality have yielded a larger sample, including a well-preserved cranium, but this material was yet undescribed.

I visited and studied the Tighennif collection in 2016 for comparative purposes: however, it became apparent that a complete description and publication of this material was also necessary. In our study, we illustrate the anatomy of this species, showing its distinctiveness within the Old World camelid record. We argue that no identification of this species outside the Maghreb is substantiated, rejecting in particular any previous report from the Middle East.

Although this study is concerned only with Algerian material, it is nonetheless highly relevant to the study of the El Kowm camelid. Together, chapter 1 and chapter 2 establish a reference against which the fossils sample that form the subject of this thesis has to be compared and evaluated.

Chapter 3

This chapter consists of a published article which presents an overview of the study and its preliminary results. It was developed as the abstract of an oral presentation held at the UISPP in Burgos, 2014 (hence, it was written before chapter 4). The proceedings of that conference session were then gathered in a special volume of l'Anthropologie. The reference to the article is:

Martini, P., L. Costeur, J.-M. Le Tensorer, and P. Schmid (2015). *Pleistocene camelids from the Syrian Desert: The diversity in El Kowm*. **L'Anthropologie** 119: 687-693 (7 pgg). http://dx.doi.org/10.1016/j.anthro.2015.10.005

This article in its final form was written in early 2015 when the morphometric study was already completed, but most of the fossil sample was yet unstudied. Only preliminary observation on the Hummal material (gathered during my Master's thesis, in 2010) and on the Nadaouiyeh cranium were available; the Tighennif material and the remaining specimens from Nadaouiyeh and Hummal were still unknown. Being a preliminary report, some statements and suggestions have been refined, corrected or contradicted in the following chapters; in particular, the doubts about the validity and integrity of the Algerian species *C. thomasi* have been proved to be unfounded, according the description of the complete Tighennif sample (chapter 4).

Chapter 4

This chapter consists of a manuscript in preparation for submission to the Journal of Vertebrate Paleontology. It describes the camelid collection from Nadaouiyeh Aïn Askar. The provisional reference to the article is:

Martini, P., L. Costeur, R. Jagher, and J.-M. Le Tensorer (in preparation). *A new species from Nadaouiyeh Aïn Askar (Syria) contributes to the diversity of Pleistocene Camelidae*.

This study is the first part of the description of the El Kowm camelid record. We concern ourselves with this locality first, because it covers a shorter temporal span that the other major locality, Hummal, and it appears to contain a restricted diversity of camelid. Indeed, we show that most specimens can be assigned to one new species, although a few isolated remains suggest the occasional presence of at least another form. A complete cranium is chosen as the holotype.

Chapter 5

This chapter consists of a manuscript in preparation. It describes the camelid collection from the sediments containing Mousterian industry (layer 5) of Hummal. The provisional reference to the article is:

Martini, P., L. Costeur, J.-M. Le Tensorer, and P. Schmid (in preparation). *A giant and a small camel lived side by side in the Late Pleistocene of Syria*.

This study is the second part of the description of the El Kowm camelid record. The Mousterian-containing layers are the paleontologically richest horizon of Hummal, and are particularly interesting because they bear evidence for the existence of two different-sized species of camel over a short geological time span. Their description finds evidence that both form represent new species, further expanding the diversity known in the genus *Camelus*. An overview of previous finds from the Levant shows that this coexistence was hinted at by other authors, whose suspicions can here be confirmed.

Chapter 6

This chapter consists of a manuscript in preparation. It describes the remaining camelid fossils from Hummal and Aïn al Fil, and presents an overview of the complete temporal sequence in the El Kowm Basin. The provisional reference to the article is:

Martini, P., R. Jagher, D. Wojtczak, F. Wegmüller, L. Costeur and J.-M. Le Tensorer (in preparation). *The diversity of Camelidae in El Kowm and in the Levant*.

This study is the third and last part of the description of the El Kowm camelid record. The remaining samples are less rich than those described in Chapter 6 and 7; we find indication of additional diversity, but overall the remains are not abundant or well-preserved enough to define other species. We review and discuss the complete collection included in the study (Nadaouiyeh Aïn Askar, Hummal, and Aïn al Fil), arguing that six camel species can be discerned over the 1.8 Ma deep sequence: two unnamed in Aïn al Fil, one unnamed in the Oldowan-bearing layers of Hummal (Early Pleistocene), one named from Nadaouiyeh, likely coexistence of two species in the Yabroudian and Hummalian layers of Hummal, and finally two named species in the Mousterian layers of Hummal. The results presented in this final chapter bring this thesis to a conclusion.

Chapter 1

Comparative morphometry of Bactrian camel and Dromedary

Pietro Martini, Peter Schmid, Loïc Costeur (2017)

Journal of Mammalian Evolution

Abstract

There are two living species of Old World camelids (Camelidae, Artiodactyla): the Bactrian camel (*Camelus bactrianus*) and the dromedary (*Camelus dromedarius*). Differences in osteology between them are poorly known, and this lack of knowledge hinders archaeological and paleontological research. Previous comparative studies have focused on subtle qualitative differences, which are subject to great intraspecific variation and interspecific overlap.

In this study, we use simple morphometric methods and statistical analyses to compare the skeleton of Old World camels. Over the entire skeleton we were able to find several consistent differences, some univocal and highly diagnostic, others only slightly significant and noticeable only at a population level. Some of the distinctive traits are suggestive of previously unknown biological adaptations. In particular, the cranial anatomy of Bactrian camels shows characters correlated with increased grazing, while its limb muscle attachments may indicate additional need for lateral stability in a heavier animal. The presence and number of humps is reflected in the vertebral column, with several differences that will be helpful in the reconstruction of fossil species.

Camelus – Camelidae – Morphometry – Osteology

Introduction

The extant Old World camelids can be divided into two forms: one-humped and two-humped camels. Traditionally, they have been considered different species, named dromedary or Arabian camel (*Camelus dromedarius* Linnaeus, 1758), and Bactrian or Asian camel (*Camelus bactrianus* Linnaeus, 1758), respectively (Nowak 1999). Both are common domestic animals in desert regions of Eurasia and northern Africa, but there is only one endangered population of wild two-humped camels that survives in the Gobi desert (Hare 2008), while wild one-humped camels are unknown in the present and unrecorded in human history. There have been populations of feral dromedaries in

the southwestern USA, in Spain, in Namibia (Epstein and Mason 1971; Nowak 1999), and at least one million individuals live currently in Australia (Saalfeld and Edwards 2010).

The specific status of the two forms has been a long-standing matter of debate (Peters and Driesch 1997; Steiger 1990). A series of arguments was put forward to claim that both forms are only domestic breeds with a common wild ancestor: the apparent absence of a wild ancestor of the dromedary, the incomplete reproductive isolation, a supposed embryological similarity, and lack of clarity on osteological differences (Driesch and Obermaier 2007; Peters and Driesch 1997; Potts 2004; Wapnish 1981). Each of these objections has been refuted in the last two decades, leading to a growing consensus on the validity of both species (Burger 2016; Driesch and Obermaier 2007; Köhler-Rollefson 1993; Peters 1998).

A common wild ancestor for the two domestic camels was postulated because no wild ancestor of the dromedary was known in human history. Reports by the Greek geographer Strabo of wild camels from the Nabatean region (northwestern Saudi Arabia and Jordan), and uncertain reports from the colonial age in Sudan, both from regions where domestic camels were already present at the time, are dismissed as more likely to refer to feral dromedaries (Mikesell 1955; Spassov and Stoytchev 2004). Archaeological remains of possible wild dromedaries were also long missing (Köhler-Rollefson 1993); only recently, pictographic (Spassov and Stoytchev 2004) and abundant osteological evidence of one-humped camel hunting was found in Arabia (Beech et al. 2009; Curci et al. 2014; Driesch and Obermaier 2007; Peters 1998; Uerpmann and Uerpmann 2002), which is interpreted as supporting the idea that dromedaries have been domesticated there from a wild population. However, the domestication process is still poorly understood, and it is premature to suggest that domestication caused size reduction in this species (Curci et al. 2014). The first documented use of domestic camels was indeed associated with Arabian nomadic tribes, like the biblical Midianites (Köhler-Rollefson 1993).

The reproductive isolation between the two forms is evidently incomplete, because they interbreed easily: in the past, hybrids were regularly produced for their large size and good working abilities (Burger 2016; Lesbre 1903; Potts 2004; Uerpmann 1999). However, contradictory statements were provided by the literature regarding the fertility of hybrids, leading to the suspicion that parental forms might not be distinct at the specific level (Hare 2008; Köhler-Rollefson 1989; Lesbre 1903). This confusion has been clarified in more recent publications, indicating that hybrids can breed up to the fourth generation, but undergo a loss of fertility (Köhler-Rollefson 1993; Manefield and Tinson 1996; Potts 2004), and therefore that the parent species are indeed distinct

(Mikesell 1955). On the other hand, new genetic studies have shown that the divergence between the two species is old (Almathen et al. 2016; Cui et al. 2007; Wu et al. 2014).

A further issue was raised by an embryological study claiming that the embryos of the dromedary initially develop two humps, which later fuse in a single one (Lombardini 1879). Curiously, for 130 years this statement was accepted as a proof of the conspecificity of the two camel forms, without further verification (Peters 1998; Spassov and Stoytchev 2004; Steiger 1990). Only recently an experiment proved that the embryos of the dromedary have only a single hump (Kinne et al. 2010).

The existence of significant osteological differences between the two camel forms has often been questioned (Driesch and Obermaier 2007; Olsen 1988; Peters 1998; Wapnish 1984), and the lack of adequate descriptive work has often been bemoaned (Lesbre 1903; Olsen 1988; Steiger 1990). Several authors have therefore described the anatomy of camels and tried to find reliable diagnostic characters in osteology. Lesbre (1903) compared the whole anatomy, Köhler-Rollefson (1989) the cranium, and Steiger (1990) the postcranial skeleton. Wapnish (1984), Olsen (1988), Studer and Schneider (2006), and Harris et al. (2010) suggested additional diagnostic characters. Smuts and Bezuidenhout (1987) described the anatomy of the dromedary. All these works have consistently been able to describe enough differences to warrant distinction at a specific level.

While some authors found that these comparative studies were satisfying in the description of diagnostic characters between both species, in particular the work of Steiger (1990) (Driesch and Obermaier 2007; Peters and Driesch 1997), others had trouble applying the criteria to the identification of isolated bones (De Grossi Mazzorin 2006; Pigière and Henrotay 2012; Uerpmann 1999), were able to apply the criteria only to a small part of their sample (Grigson 2012), found both species in the same bone assemblage (Reynaud Savioz and Morel 2005), or felt that additional diagnostic criteria were still needed (Studer and Schneider 2006).

A possible reason for this disagreement is that the traditional morphological approach may not be fully appropriate to diagnose the two species. Most of the characters suggested in previous works are continuous and have qualitative definitions, not definitions based on statistically significant differences or clear-cut thresholds. As Bactrian camels and dromedaries are close in morphology and have a large intraspecific variation in size and shapes (Köhler-Rollefson 1991; Olsen 1988; Steiger 1990), several characters are also likely to show substantial interspecific overlap. As a consequence, most qualitative criteria cannot be consistently and reliably used to identify bones, nor can they be applied to fossil species, which may show mosaic characters or

shapes unknown in recent camels. An additional problem is that some museum specimens used to establish the criteria may have been misidentified. In particular, hybrid camels may have been labelled as dromedaries (Köhler-Rollefson 1989; Studer and Schneider 2006), casting doubt on the results of all the works that did not consider this issue.

In this study we propose a comparative metrical characterization of camel osteology, aiming at a quantitative description of the morphological differences between the two camel species. We do not exclusively seek univocal diagnostic characters, but rather search for consistent distinctions on a statistical basis, taking into consideration variation and overlap. To do so, we suggest a set of linear measurements and we test the significance of differences in intraspecific averages. We investigate the cranium and most of the postcranial skeleton, and we suggest some interpretations of the main differences. Our results cover a lack of knowledge about interspecific differences, which are relevant to the description and identification of archaeological and paleontological remains of *Camelus* species.

Material and Methods

Comparative materials

Partial and complete skeletons of 21 Bactrian camels and 24 dromedaries have been measured and included in the sample (see Online Resource 2).

The cranium is represented by 17 Bactrian camels and 14 dromedaries; samples of postcranial bones are more limited. Only fully grown specimens (with M3 partly or totally erupted, or epiphyses completely fused if no cranial material was present; exceptions are indicated and justified) were included in the study.

Sexual dimorphism in camel osteology is limited. Males are bigger, have larger canines, and differ in the shape of the pelvis (Driesch and Obermaier 2007; Smuts and Bezuidenhout 1987; Steiger 1990), but the postcranial skeleton does not show other differences (Steiger 1990). In our sample, the total of individual of each sex was variable from one bone to the other, but always similar between the two species. In light of this, we explicitly controlled for sexual dimorphism within each species in the cranium and dentition, but not in the mandibula or postcranium. The dentition is also expected to show age variation, due to both growth and wear. We separately controlled for age variation among three groups, defined by the degree of wear in upper M1 and M3. Interspecific dental differences were then studied separately within each sex, within all

individuals excluding older adults, and within all individuals excluding younger adults (see Online Resource 3).

Putative dromedary specimens kept in European zoos may represent camel hybrids, which have one hump and resist better humid and cool climates (1991, 1989). In addition, old museum specimens might be mislabeled. Most of the dromedary specimens in our sample originate from countries within the current domestic distribution of this species (Mali, Jordan, Sudan, and Syria), thus representing typical individuals. Questionable individuals (nine dromedaries of unknown origin and two specimens labeled as dromedaries, but apparently Bactrian camels) were compared with the remaining individuals of certain origins. The univocal diagnostic characters found in cranium, mandibula, atlas, and axis allowed confidently assigning all individuals to one of the two species and including them in the analysis; no individual was considered to be a possible hybrid.

The parts of the skeleton that were measured include: cranium, mandibula, dentition, first and second cervical vertebrae, all seven lumbar vertebrae, sacrum, scapula, humerus, radioulnare, carpalia (scaphoideum, lunatum, triquetrum, pisiforme, trapezoideum, capitatum, hamatum), metacarpale, anterior proximal phalanx, anterior intermediate phalanx, femur, patella, tibia, fibula, tarsalia (astragalus, calcaneus, cuboideum, naviculare, medial cuneiforme, intermediolateral cuneiforme), metatarsale, posterior proximal phalanx, posterior intermediate phalanx. The terminology follows Barone (Barone 1999) and Smuts and Bezuidenhout (Smuts and Bezuidenhout 1987) with Latin nouns and anglicized adjectives.

Measurements

The system of measurements was derived from the standard suggested by von den Driesch (1976), adapted and completed to the aim of this study. The morphometric analysis of Caprinae by Crégut-Bonnoure (2002) was taken as a term of comparison, and the final set of measurements of the two studies were similar in scope. See Online Resource 1 for the illustration of measurements and Online Resources 3-8 for the complete dataset.

The measurements have been taken using a slide gauge caliper, rounded to the next 0.5 mm, using straight measurements between easily defined endpoint and maximal or minimal dimensions, as often as possible. This simple protocol was intended to be easy to implement. All measurements were taken by the first author. In addition to measurements, we scored 18 qualitative characters on the cranium, two on the mandible, and one on the axis. Each character was scored in two or three

states; when three states were used, one represented an intermediate or ambiguous state. The results were integrated with those of the metric study.

Statistical analyses

The morphological and size proximity of the two camels causes a substantial overlap in raw measurements; hence these have a reduced discriminative power. Even when statistically significant differences are found, they may often depend on the larger average size of the Bactrian camel (Grigson 1983; Steiger 1990), and not on a real difference in shape. Bivariate proportions provide a better diagnosis, but a large number of proportions or indices is necessary to describe the shape of a complex object, because each can represent only a two-way contrast. Further issues with the use of ratios are the effects of allometry and the normality of distribution. (Mendoza et al. 2002; Palmqvist et al. 1999).

To address these problems and obtain variables proportional to the size of a bone, the following transformation was performed (Fig. 1). Each measurement was scaled by the interspecific mean of that variable, in order to have values with the same average (equal to 1) for every variable. Afterwards, the size of each specimen was calculated as the harmonic mean of all available scaled measurements. Then, each scaled measurement was divided by the harmonic mean, to obtain a value proportional to the size of the bone. The value resulting from this transformation was called harmonic score (HS). All raw measurements and the corresponding HS are provided in Online Resources 3-8.

We chose to use the harmonic mean as size estimate, because the final results (the HS) are equivalent to the arithmetic means of all possible bivariate proportions, which is obtained dividing the scaled value of interest by each other scaled values and by itself. The HS were found to be normally distributed. The HS are more accurate if the harmonic mean is obtained using many variables, but can be calculated also from an incomplete set of measurements, such as for many specimens in the present sample. The interspecific mean for each variable was obtained as the average of both intraspecific means of all individuals. In some instances, the harmonic mean was calculated excluding variables that showed extreme variation, because this random variation was independent of the actual size of the specimen, but would nevertheless have a strong leverage on the harmonic mean. This correction was applied to the anterior dentition (strongly dimorphic) and to small, irregular features of the atlas, axis, sacrum, and tibia.

To investigate morphological differences between the two camel species, we compared the mean HS using a two-tailed Student's t test. The cranial, mandibular, and vertebral qualitative characters were investigated using chi-squared test in the software PAST (Hammer et al. 2001). We restricted our analyses to within-bone comparisons. Measurements and characters with a significantly different average (defined as p-value < 0.05) are discussed and interpreted in terms of morphological features and proportions. Variables without a significant difference are reported when it is relevant to indicate that certain features are not diagnostic.

All data generated and analyzed in this study (measurements and HS transformations) are included in the Online Resources of this article.

Results

All measurements and analyses are provided in Online Resources 3-8. The relevant metric variables are indicated in the text using an abbreviation for each element and number code for each measurement. Description of the overall size refers to the harmonic mean. The statistical strength of a difference (p-values for metric and qualitative characters) is indicated by asterisks (°, >0.05; *, < 0.05; **, < 0.01; ***, <0.001) unless when the difference is measured by several p-values.

After the description of each element, the results are compared with those of previous qualitative analyses (Harris et al. 2010; Köhler-Rollefson 1989; Lesbre 1903; Olsen 1988; Steiger 1990; Wapnish 1984).

Cranium

There are a high number of interspecific differences in the cranium (Online Resource 3; Figs. 2-4). Out of 77 metric variables, as many as 35 variables have a significantly different average. In addition, 12 morphologic characters out of 18 differ between the two species. The cranium is significantly larger in Bactrian camels (variable Hmean***), but longer in dromedaries (variables C1**, C9*). We note that an adult individual can easily be identified on the basis of its skull shape: Bactrian camels have a regular shape with a smoother outline, while dromedaries appear rostrocaudally compressed and more angular, with a steeper nose and concave forehead (Fig. 2). The impression that the crania are morphologically distinct is confirmed by several quantitative characters, some of which are univocal and not overlapping.

Only one intersexual difference was found in both Bactrian camel (C6*, C75°) and dromedary (C6**, C75°) samples: males have a longer (but not broader) foramen magnum than females. Male

Bactrian camels also show shorter palate (C10*), broader glenoid fossa (C46*), broader incisive bone (C49*), and broader occipital condyles (C73°, C74*) than females. In male dromedaries, the cheek tooth row is shifted caudally relatively to the prosthion (C29*, C30*), the zygomatic arch is thicker (C23**), and the oval foramina are farther apart (C68*). In neither species could we identify any difference in the placement of the canines.

Our results indicate that the crania of the two camel species are consistently different, in agreement with Köhler-Rollefson (1991) but in contrast with Olsen (1988), who suggested that crania can barely be separated.

Frontal region

The rostral part of the face (anterior to the cheek tooth row) is longer in dromedaries (C13***, C29**, C30**). The infraorbital foramen is in the same position in both species (°), in most cases above the contact line of P4-M1. In dromedaries, the orbit is in a lower and more rostral position, closer to both the infraorbital foramen (C15**) and the alveolar border (C24**). In this species, the orbit is (dorsoventrally) taller (C19**): its highest part is the rostral half, while in the other species it is the caudal half (***). In Bactrian camels, the frontal orbital process is broader (C21***). The lateral suture of the zygomatic arch does not get as close to the orbit as in dromedaries (C22**). The zygomatic arch is thinner in dromedaries (C23***). Bactrian camels have a well-developed maxillar crest under the orbit, which is greatly reduced or absent in the other species (***).

In dromedaries, the nasal bones are narrower caudally (C50***) while the medial ends of the incisive-maxillary sutures (very close to the distal end of nasals) are farther apart (C51**). This indicates that the nasal opening is wider; it is also longer (C2***). The ethmoidal fissure is very irregular in shape, but is often larger in Bactrian camels (C20*). The frontal region is clearly concave in dromedaries, rather flat in Bactrian camels (***).

The braincase is broader in Bactrian camels (C57***); the squamotemporal foramina on its sides are farther apart (C58*). The postorbital constriction is farther backwards in this species than in the other (*). The nuchal crest is rather straight and flat, while in dromedaries it is dorsally convex (**). Although the sagittal crest tends to be more developed in dromedaries, the difference was not significant when controlling for sex (°).

Köhler-Rollefson (1989) noted that dromedaries have a longer face. Our results suggest that the rostrum is longer, even though the orbits are placed forward, closer to the infraorbital foramen.

Lesbre (1903) considered the nasal opening to be broader in dromedaries, which is confirmed here. He also found the nasal bones to be broader caudally than rostrally in the latter, and the opposite in Bactrian camels; our results are slightly different and indicate that in dromedaries the nasals are caudally narrower and rostrally broader than in Bactrian camels. Some previous studies (Lesbre 1903, Köhler-Rollefson 1989) noted that the ethmoidal fissure is larger in Bactrian camels. Lesbre (1903) and Olsen (1988) commented on how the profile of dromedaries is concave over the frontal region. We confirm both these observations.

Only Lesbre (1903) noticed that the maxillary crest is well developed in the Bactrian camel but not in the dromedary.

Lesbre (1903) further suggested that horizontal and vertical diameters of the orbits are subequal in dromedaries, while in Bactrian camel the vertical diameter is larger. Our results rather indicate that Bactrian camels have a larger horizontal diameter in raw measurements: the vertical diameter is therefore relatively greater in dromedaries. However, we agree with Lesbre (1903) on the larger breadth of the orbital process of the frontal, the greater distance from the orbit to the alveolar border, and the greater thickness of the zygomatic arch in Bactrian camels. He also correctly observed that the braincase is broader in Bactrian camels.

We cannot confirm that the sagittal and nuchal crests are more pronounced in Bactrian camels, as found by all previous studies (Lesbre 1903, Olsen 1988, Köhler-Rollefson 1989); in our sample the difference was present, but not significant.

Palatal region

The palate is distinctly longer in dromedaries (C10***, C11***). The palatine foramina are more rostrally placed in dromedaries (C25***); in our sample, they are usually found at the level of the premolars, while they are never found rostral to the first molars in the other species (***). The canines are more distal (caudal) and the caniniform P1 is more mesial (rostral) in dromedaries (C27**, C28***); it follows that in the latter, canines and P1 are closer to each other. Male dromedaries have a cheek tooth row shifted caudally, in comparison to Bactrian camels but also to female dromedaries (C29**, C30**). The palate is wider between the caniniform P1 in dromedaries (C61**), but between other teeth there are no differences.

At the basis of the perpendicular palatine blade, a small, rugged concavity faces downwards (is placed horizontally) in Bactrian camels, while it faces sidewards (is oblique) in dromedaries (***).

The choana is broader (C67***) and normally bears a caudal nasal spine on a rounded rostral border in dromedaries; in the other species, the choana is narrower and often has a pointed rostral border (*), lacking a caudal nasal spine (**).

Köhler-Rollefson (1991) noted that dromedaries have a longer palate. Lesbre (1903) and Harris et al. (2010) both reported that the extension of the palatine differs between the two species, but contradicted each other about which species reaches farther rostrally. We caution that the palatine suture can be impossible to see in adult camels, and we instead suggest focusing on the position of palatine foramina, which differ consistently between both species in our sample. However, Geraads (pers. comm. 2016) noted that exceptions in the position of palatine foramina are rare but possible.

The glenoid fossa differs substantially between the two camels, in the way that already Lesbre (1903) had suggested. Our metric analysis is supported by the qualitative description provided.

Basicranium

The basicranium is on average longer in Bactrian camels (C7°, C8***). In this species, the pterygoid processes (C36*) and the spine of the optic foramen are longer (C39***). The oval foramina (C68*) and the mastoid foramina are farther apart in dromedaries (C76**).

The glenoid fossa is rostrocaudally longer (C47**) and has a taller postglenoid process in dromedaries (C48**). Its shape can be described as rectangular in Bactrian camels, and as triangular in dromedaries (***).

The occipital condyles are larger, longer (C45*), and broader in dromedaries (C73***, C74***). Their rostral border is clearly constricted in Bactrian camels, while the constriction is usually weak or absent in dromedaries (**). Caudodorsal to the condyles, the nuchal tubercle is strong and prominent in Bactrian camels, low or absent in dromedaries (***). The foramen magnum is longer in dromedaries (C6***). This difference is also found when comparing males to females within both species, and when comparing only members of the same sex between species.

Only Lesbre (1903) advanced some observations regarding basicranial features. We were able to test metrically if the sphenomaxilloid foramen is larger in the Bactrian camel, and if the process found lateral to the base of the sphenoid blades is more prominent in that species. In neither case could we find a significant difference. Lesbre (1903) also suggested that the caudal palatine foramen is much closer to the sphenomaxilloid foramen in dromedaries. We were occasionally able to observe this difference, although we did not verify this character metrically.

Mandibula

Like the cranium, the mandible is larger in Bactrian camels (**) and presents many diagnostic characters; most of the measurements show a significant interspecific difference (Online Resource 3).

Bactrian camels have a longer mandible, which can be seen in most of the rostrocaudal measurements (M1***, M2***, M3***, M4**, M5**, M7**, M12***). The increase in length depends mainly on the cheek tooth row (M7**), as the rostral part of the dentition (from p4 to the incisive arcade) does not differ between species (M8°). On the other hand, the symphysis is relatively longer in dromedaries (M9***).

The position of the caniniform p1 is more rostral in dromedaries (compare M6° with M5** and M7**); the same condition is found in the upper dentition. The rostral mental foramen has a similar position in both species (M10°), but the caudal mental foramen is shifted caudally in dromedaries (M11***). In our sample, it was always found under m1 or m2 in dromedaries, but more often under p4 or m1 in Bactrian camels, although placement under m2 happened as well and the difference was not significant (°).

The body is normally broader in Bactrian camels, especially in the middle of the cheek tooth row, but some dromedary specimens can be robust as well, preventing the differences from being more significant (M15**, M16°). The height of the body has a large variation in Bactrian camels, where it can be very low especially in the caudal region; therefore, the body is equally tall at the level of the premolar, but it is taller in dromedaries at the level of m3 (M19°, M20*, M21**)

The mandibular condyles are broader but shorter in Bactrian camels (M17***, M18**). This different shape corresponds to the differences found in the glenoid fossa. The condyles and the angular process are equally tall in both species, but in Bactrian camels the coronoid process is much

longer (M22***) and is curved backwards, forming the shape of a hook; in dromedaries it is short and ends abruptly, with a squared apex (***)

Köhler-Rollefson (1989) suggested that the distal part of the mandibular corpus is tilted dorsally in Bactrian camels. We agree and point out that this correlates with the shape of the maxilla, which is tilted ventrally in dromedaries. Geraads (pers. comm. 2016) noted that exceptions in the position of caudal mental foramina are possible. Both Lesbre (1903) and Köhler-Rollefson (1989) found the symphysis to be longer in dromedaries; we obtained the same result.

These authors also correctly observed that the coronoid process is longer and curved in two-humped camels, but seemed not to fully appreciate the importance of this character. Besides being an extremely reliable diagnostic trait, it might have ecological implications discussed later in this section.

Dentition

Sexual dimorphism is expressed in similar ways within both species (Online Resource 3). Both sets of canines and the caniniform upper I3, upper P1, and lower p1 are more massive in males. The difference is more significant in upper I3 and upper C for Bactrian camels (Ds1***, Ds2***, Ds3***, Ds4***, Ds5°, Ds6*), but more in upper P3 and lower C for dromedaries (Ds1*, Ds2°, Ds3*, Ds4*, Ds5**, Ds6**; Di1*, Di2***, Di3*, Di4°). Sexual dimorphism was not studied in the lower dentition of Bactrian camels, because measurements were available for only one male. As the sexual differences are strong, all measurements of the caniniform teeth were excluded from the harmonic mean.

In general, wear is irrelevant for premolar proportions but causes molars to become significantly shorter and wider. The lower I1 becomes narrower, but there was no age difference in the other incisors (Di5**). The upper P3 does not change shape with wear, while both upper P4 and lower p4 have a broader occlusal surface in older adults (Ds14**, Di11*). Upper M1 becomes broader and shorter on the occlusal surface, and usually also at the alveolar level (especially the distal lobe) (Ds17-22). Lower m1 shows the same development, but it is the alveolar mesial lobe to become wider, not the distal one (Di13-19). Upper M2 becomes broader and shorter both at the occlusal and alveolar level (Ds23-31). Lower m2 undergoes the same change of shape; however, the alveolar breadth is not always different (Di20-27). Upper M3 becomes broader; its mesial lobe becomes shorter, but its distal lobe becomes longer (Ds32-38). Lower m3 becomes broader but not

shorter, except for the occlusal surface of the mesial lobe (Di29-38). As the effect of sex is preponderant, age effect was not studied on caniniform teeth.

In spite of our effort to control for age and sex, we were not able to identify any interspecific differences in the dentition, except for the overall larger size of Bactrian camels (***, **, **, ° in different analyses). Few measurements were found to have a barely significant difference in some of the separate comparisons, but as there was no strongly significant difference and no pattern across the sample, we conclude that the dentition of both camel species is very similar, without significant specific differences.

The dentition shows no interspecific differences, in line with Lesbre's (1903) observations. Clutton-Brock (1962) and Morales et al. (1980) also considered the dentition to be of limited diagnostic value. We are not able to confirm the few dental morphological differences listed by Köhler-Rollefson (1989) and Harris et al. (2010).

Atlas

The best diagnostic character of this bone is the size of the ventral foramen (single opening in the atlantid fossa), which is so large in Bactrian camels that there is no interspecific overlap of its diameter in our sample (at17***) (Online Resource 4; Fig. 5). The harmonic mean was calculated excluding the diameter of the ventral foramen.

Other differences can be found in the dorsal foramina; in dromedaries, the cranial (alar) foramina are more distant from each other (at5**), have the same distance from the cranial border (at4°), and a greater distance from the caudal (transversal) foramina (at3***), suggesting that the last can be closer to the caudal border. In Bactrian camels the vertebral channel is normally higher: this can be seen in the taller cranial and caudal articular opening (at8**, at14*), and the greater diagonal height of the cranial and caudal articular cavities (at9**, at15°).

All previous analyses (Lesbre 1903; Steiger 1990; Wapnish 1984) recognized the diagnostic importance of the ventral foramen in the atlantal fossa. Steiger (1990) suggested that the wings are caudally more developed in Bactrian camels, but we found that they are barely longer in dromedaries. Lesbre (1903) observed that the transversal foramina are closer to the caudal border in dromedaries, which is consistent with our analysis. We also found that the vertebral channel is dorsoventrally taller in the Bactrian camel.

Axis

The axis presents one of the best qualitative diagnostic characters overall: the common opening of the lateral and the transversal foramina is covered by a bony bridge in dromedaries, but not in Bactrian camels (Fig. 5). We found two dromedaries with the bridge incompletely developed (not closed) and one Bactrian camel with initial development. Even these exceptions were more similar to the regular morphology of their own species than to the other species (***; Online Resource 3).

As for the morphometric differences (Online Resource 4), the most important one is that Bactrian camels have a greater maximal breadth (ax8***), but at the same time a smaller minimal breadth (ax7**). The length of both arch (ax2*) and body (ax3**) is greater in dromedaries. In this species, the body is caudally narrower (ax11°), while the caudal breadth of the spine is on average greater (ax10°); this variable has a high variation and was excluded from the calculation of the harmonic mean. The overall size is greater in Bactrian camels (*).

Both Lesbre (1903) and Steiger (1990) saw the presence of a divided lateral foramen in the axis as a reliable distinction. We were able to show that even unusual morphologies are closer to the standard of their own species, than to the other species.

Thoracic vertebrae

The thoracic vertebrae were not included in the morphometrical study. However, we were able to notice some characters worth mentioning.

The thoracic vertebrae usually amount (but not always) to twelve and they intergrade morphologically along the spine, hence only the first and some of the last ones can be identified in isolation. Otherwise, it is necessary to have the complete column in order to rank them by number.

The spinous processes of the thoracic vertebrae are thick and strong in Bactrian camels, slenderer and bladelike in dromedaries. The orientation of the processes differs; they are in general more inclined in Bactrian camels, and the outline of the complete column is suggestive of the number and position of the humps. The transition from a thoracic morphology to a lumbar morphology of the zygapophyseal facets (from horizontal to vertical orientation) takes place between the 11^{th} and 12^{th} vertebrae in dromedaries, but already between the 10^{th} and 11^{th} in Bactrian camels.

The different position of the transition from thoracic to lumbar morphology was not noticed in previous studies.

Lumbar vertebrae

The seven lumbar vertebrae (the number can vary) share a common structure, which allows them to be measured following the same protocol (Online Resource 4). We discuss the interspecific variations of all variables along the lumbar column, from lumbar I to lumbar VII (one immature but adult-sized Bactrian camel was included to increase sample size). Lumbar vertebrae are prone to interlock through the zygapophyses and to have corpora fused between them or with the sacrum.

The length of the body is never significantly different (lu1). It is however generally stronger in Bactrian camels: it is significantly taller in lumbar VI cranial, in lumbar III-VII caudal, broader in lumbar II-V cranial, and broader in lumbar I-VI caudal (lu7, lu8, lu12, lu13). Therefore, the central part of the lumbar section shows a significant difference in body massiveness, while the extremes (lumbar I and VII) show a difference much weaker.

The neural arch is longer in Bactrian camels (except in lumbar V, VI) (lu2). There is no obvious difference in height (lu6, lu11 must be compared to lu7, lu12).

The zygapophyses are in general craniocaudally more prominent in dromedaries (lumbar II, III, and V) (lu3). In this species they also are wider in the posterior part (lumbar IV to VII) (lu9, lu14).

The spinal processes are longer in dromedaries between lumbar II and V, but shorter in lumbar VII (lu4). In lumbar I, this process is cranially taller in dromedaries. In lumbar III to V and again VII, however, the process is taller in the other species (lu5, lu10).

In summary, Bactrian camels tend to have more massive bodies, longer neural arches, and taller but shorter spinal processes. Dromedaries have broader, more prominent zygapophyses. These interspecific differences are stronger in the central part, while lumbar I and VII can have less strongly expressed or even opposite proportions.

The greater craniocaudal length of the spines of lumbar vertebrae was observed by Lesbre (1903). Both he and Steiger (1990) observed that the height of the spines decreases constantly from the first to the last in dromedaries, while it rises until the 3rd or 4th in Bactrian camels. We did not compare measurements between different bones; however, we found that the height of the spine of

lumbar I is greater in dromedaries, while those of the III, IV, and V lumbar are greater in the other species. We add that the body is stronger and the zygapophyses are narrower in Bactrian camels.

Sacrum

The sacrum usually consists of four fused vertebrae. The first free vertebra caudal to it is considered the first caudal vertebra by Steiger (1990), but both Lesbre (1903) and Smuts and Bezuidenhout (1987) considered it the fifth sacral. Occasionally, the last lumbar vertebrae or the fifth sacral are fused to the sacrum.

The neural arch and the wings are both longer in Bactrian camels, but not the body itself (sa1*, sa4**; Online Resource 4). The distance between the sacral foramina can have a large variation, but it appears significantly wider between the third dorsal foramina in dromedaries (sa7*) and between the first and second ventral foramina in the other species (sa8*, sa9***). Cranially, the articular head (the body) is broader in the two-humped camel, but the articular processes are narrower, like in the lumbar vertebrae (sa13*, sa14***). The height of the spine shows a large variation, hence it was excluded from the calculation of the harmonic mean.

Steiger (1990) maintained that the sacrum is shorter and broader in Bactrian camels, but we could not observe this difference.

Scapula

The two species are distinct by the relative size of the supraspinatous and infraspinatous fossa: the latter is usually much deeper in the Bactrian camel, but the difference is marginal in dromedaries (sc5**, sc6*; Online Resource 5). To put this in other words, the scapular spine is usually closer to the cranial border in two-humped camels, almost central in the other species.

While Lesbre (1903) and Steiger (1990) contradicted each other regarding the general proportions of the scapula (narrower in dromedaries after the former, the opposite after the latter), we did not find any significant difference in the general outline. Nevertheless, we agree with Lesbre (1903) in observing that the spine is closer to the cranial border in Bactrian camels, causing different relative sizes of the supraspinatous and infraspinatous fossae. We also confirm the observations of Lesbre (1903) and Steiger (1990) that the spine is more prominent in Bactrian camels, with a clearer median tuberosity and a longer acromion.

Humerus

The greater tubercle is laterally more prominent in dromedaries (hu7**; Online Resource 5). At the level of the nutritional foramen, the diaphysis is rounded in Bactrian camels and flattened in dromedaries: the latter has a larger maximal diameter (hu12*) but a smaller minimal diameter (hu13**). The olecranon fossa is taller in dromedaries (hu22**).

Although previous studies described the humerus as more massive in Bactrian camels, as is the case for other long bones (Lesbre 1903; Steiger 1990), we were not able to replicate this result with morphometric data. As the humerus has a twisted shaft, we used different shaft diameter measurements from those for other long bones (choosing largest and smallest diameters at specific points instead of largest and smallest diameters in specific directions), and this may explain our result. However, other authors have observed that the proximal limb bones (humerus and femur) differ less in proportions between species than distal limb bones (radioulnare, tibia, and especially metapodia) (Olsen 1988; Peters and Driesch 1997), in accordance with our data suggesting no difference.

Radioulnare

The radioulnare is longer and slenderer in dromedaries (ru1***, ru2***; Online Resource 5). The maximal breadth of the olecranon is greater in Bactrian camels (ru5***). The trochlear notch is longer in dromedaries (ru8*), while the coronoid process is deeper in Bactrian camels (ru13*); the lateral radial articular facet is wider and deeper in the latter species (ru11*, ru12°; small sample size). The minimal breadth of the diaphysis is larger in the two-humped camel (ru16**), but the minimal depth does not differ (ru15°). Distally, the medial (radial) articular surface is deeper (ru17*, ru22*) but narrower in dromedaries (ru25**).

In agreement with previous works (Lesbre 1903, Steiger 1990), we found the radioulnare to differ significantly in several proportions between the two camels. In particular, the Bactrian camels are overall massive and have a large olecranon.

Scaphoideum

The proximal facet (Ks6*, Ks7***; Online Resource 6) and the palmar distal facet are significantly broader in Bactrian camels (Ks11*), but the dorsal distal facet is broader in dromedaries (Ks10*). In the latter species, the distal aspect of the bone is deeper (Ks8*); the height in the middle of the bone is usually greater (Ks2°).

Our morphometric analysis was able to distinguish several differences in the carpal bones, unlike previous authors who found them not to be remarkably different (Lesbre 1903) or suggested fewer criteria than for other bones (Steiger 1990). The scaphoideum does not offer major differences, but we concur with Steiger (1990) who suggested it is broader in Bactrian camels.

Lunatum

The proximal facet of the lunatum is medially deeper in Bactrian camels (Kl3**; Online Resource 6). It also tends to be narrower (Kl4*) and to have a deeper lateral side, but not significantly so (Kl2°). The distal lateral process is often placed more palmarly in Bactrian camels (Kl10**, Kl11°).

Steiger (1990) noted similar differences as we noticed in the shape of the proximal facet of the lunatum, although using a different formulation to describe it. The position of the distal lateral process was not observed before our study.

Triquetrum

The distal facet of the triquetrum is broader in Bactrian camels (Kq8**; Online Resource 6). The distance between the two dorsal tips of the proximal and distal facets is greater in dromedaries (Kq2*).

The narrower distal facet of the triquetrum in dromedaries was also mentioned by Steiger (1990).

Pisiform

The pisiform is the most diagnostic of all carpal bones. It can often be identified at first sight as a Bactrian camel, if the tuberosity is roughly triangular, or as a dromedary, if the tuberosity is rather globular. Even when the shape is intermediate, the difference is easily made by metrical data: the diameter of the tuberosity (Kp1***; Online Resource 6) and the height of the bone (Kp4*) are larger in Bactrian camels, while the proximal depth (Kp2**) is larger in dromedaries. The articular facet is also clearly distinct; it is broader and taller in dromedaries (Kp5*, Kp6***).

Lesbre (1903) already noted that the pisiform shows the clearest interspecific distinctions. He and Steiger (1990) recognized differences in the shape of the tuberosity but not in that of the articular facet.

Trapezoideum

The distal facet of the trapezoideum has a larger maximal diameter in dromedaries (Kt3*; Online Resource 6), but the proximal facet is broader in Bactrian camels (Kt4*).

Steiger's (1990) observations on the trapezoideum proportions were close to ours.

Capitatum

The capitatum of Bactrian camels has a larger maximal diameter (Kc3**; Online Resource 6), but on average a smaller dorsomedial height (Kc2*)

Previous authors were unable to find measurable differences in the capitatum.

Hamatum

In dromedaries, the palmar process (hamulus) is more prominent, as shown by the maximal diameter (Kh3*; Online Resource 6). In Bactrian camels, the distal facet is deeper (Kh5*). The palmar region is usually taller in the former species (Kh2°), and the dorsal region in the latter (Kh1*).

We can support Steiger's (1990) observation that the palmar process is more developed in dromedaries.

Metacarpale

Metapodia were found to complete development earlier than other skeletal parts; therefore, three adult-sized specimens from immature individuals were included in the sample. The metacarpale is longer and slenderer in dromedaries, as happens for most of the long bones (mp1***, mp2***; Online Resource 5). The proximal articulation is broader in Bactrian camels (mp5*), with a comparatively deeper lateral part (mp4*). The minimal breadth of the diaphysis is larger in Bactrian camels (mp12**), but the minimal depth is not different (mp11°). The lateral condyle (distal articular surface) is deeper and narrower in the dromedaries (mp14***, mp16*), while the medial one does not differ significantly (mp13°, mp15°) (Fig. 6). Overall, the distal part of the metacarpale is broader in Bactrian camels (mp17*).

Observations made by previous studies about differences found in the metacarpale are considered together with the metatarsale.

Anterior proximal phalanx

The anterior medial and anterior lateral phalanges are identical in morphology. The only known difference is that within an individual the lateral phalanx is slightly larger than the medial one (Steiger 1990). The data for medial and lateral phalanges can be analyzed separately or can be pooled, allowing the inclusion of isolated specimens and thus increasing sample size. The results are qualitatively the same; hence, we present here only the statistically stronger results from the pooled sample. The same observations are valid about the posterior proximal phalanx, to which we apply the same analysis.

The proximal articular surface is broader in Bactrian camels (pp4***; Online Resource 8). The lips of the distal trochlea (both axial and abaxial) are longer in the dromedary (pp9***, pp10***) (Fig. 7).

Observations made by previous studies about differences found in anterior proximal phalanges are considered together with the posterior proximal phalanx.

Anterior intermediate phalanx

The distinction of lateral and medial intermediate phalanges is even subtler than for the proximal phalanges. Moreover, it is equally hard to differentiate anterior and posterior intermediate phalanges (Steiger 1990): usually the anterior ones can be identified by the slightly larger size, but in our sample there were individuals with complete phalanx sets for which it was impossible to convincingly identify their position. Hence, we analyzed all intermediate phalanges in a pooled sample only (including only one averaged value for each individual and each variable).

The diaphysis is on average broader in dromedaries, unlike in the long bones (ip6*; Online Resource 8). The distal articulation is usually broader in this species, too (ip8*), but the abaxial lip is shorter (ip10*). We observed that in Bactrian camels, this phalanx often appears curved toward the axis, while it is straight in dromedaries.

The intermediate phalanx is found to be broader in dromedaries than in Bactrian camel, unlike most other limb bones. Previous work (Lesbre 1903, Steiger 1990) indicated the opposite. Our results appear therefore surprising and cannot be considered conclusive on this issue.

Femur

The femur is longer and slenderer in dromedaries, as seen in three length variables (fe1***, fe2***, fe3**; Online Resource 5). This species has a broader proximal part of the femur (from head to greater trochanter) (fe6*). The neck is usually deeper in Bactrian camels (fe7*). The minimal breadth of the diaphysis is on average larger in the latter (fe10*). The distal trochlea is broader in dromedaries (fe14***). Although the condyles do not differ significantly, the breadth across both condyles is clearly larger in Bactrian camels, suggesting that the distance between them is greater (fe17**). The overall size is larger in Bactrian camels (*).

Like for most long bones, we agree with previous authors that dromedaries have a longer and slenderer femur. Steiger (1990) found that the greater trochanter of Bactrian camels is larger. Although our measurements are ultimately not appropriate to decide this, it would fit in a group of other enlarged muscular attachments that could have an adaptive value for this species (see Discussion).

Patella

The articular surface (caudal) is proximally broader in Bactrian camels (pa5***; Online Resource 5), but distally broader in dromedaries (pa6**) (Fig. 8). The maximal depth is greater in the latter species (pa3**).

Lesbre (1903) already proposed that dromedaries have a thicker patella, and that the relative proximal and distal breadth differ between species. We are able to confirm both observations. The differences shown by the patella are clear and consistent, even though this bone has a very simple form.

Tibia

Following the pattern found in other long bones, the tibia is longer in dromedaries (ti1***, ti2***, ti3***; Online Resource 5) and the minimal breadth (but not the minimal depth) of the diaphysis is larger in Bactrian camels (ti13***). The proximal epiphysis as a whole is broader in Bactrian camels (ti4*). Dromedaries have a more prominent proximal medial condyle, as the distance from it to the tibial tuberosity is greater (ti10*), but the tuberosity itself is not more prominent (ti11°). The lateral fossa of the distal cochlea (which articulates with the malleolar bone) is deeper (ti16***) and wider in the Bactrian camel (ti21**) (Fig. 9). The overall size is larger in the

latter species (*). The breath of the intercondylar eminences' tips showed a high variation; hence, it was excluded from the calculation of the harmonic mean.

While previous studies have noted the greater slenderness of the tibia in dromedaries (Lesbre 1903, Steiger 1990), we report for the first time the difference in the shape of the distal cochlea. Our observations on fossil specimens (in preparation) suggest that its proportions have a promising taxonomic value.

Fibula

The main interspecific difference is the larger average size of this bone in Bactrian camels (***; Online Resource 7). All raw measurements, except the height of the proximal process, are significantly larger in the two-humped camels. When size is removed from the measurements, dromedaries have a taller proximal process (fi2*) and a taller plantar region (fi3*) with a narrower proximal facet (fi8*). The size and shape of the fibula correlate with the proportions of the tibial cochlea.

Astragalus

The proximal part is usually wider in dromedaries; however, two Bactrian camel outliers prevent this variable from reaching a significant difference (Ta7°; Online Resource 7). The calcaneal surface is broader in Bactrian camels (Ta8**). The lateral side of the bone is taller in dromedaries (Ta1*), while the medial side height is not significantly different (Ta3°); however, plotting these two correlated variables together produces two well separated species group, where Bactrian camels always have either a shorter lateral side or a longer medial side than dromedaries (Fig. 10). The distal articular surface has different breadth proportions: the lateral part is larger in the dromedary (Ta14*), the medial part in the Bactrian camel (Ta15**; small samples).

Steiger (1990) and Uerpmann (1999) observed that the astragalus of dromedaries has a proximally more prominent lateral lip of the proximal trochlea and a less prominent medial lip: we provide direct statistical support for the first character and are able to indirectly observe the second. On the other hand, Steiger (1990) found that the proximal trochlea is broader in Bactrian camels, while our result shows the opposite. Wapnish (1984) and Steiger (1990) both noticed that in the astragalus the fibular salient (lateral spine) is more prominent and horizontal in dromedaries. Although we observe the same difference, its quantification was not statistically significant. We

also confirm the greater breadth of the calcaneal surface in Bactrian camels, and the wider lateral part of the distal trochlea in dromedaries, again in accordance with Steiger (1990).

Calcaneus

In Bactrian camels, the calcaneus is larger (**) and more massive, but not as long as in the other species (Tc1***; Online Resource 7). In dromedaries, the tubercle is deeper (Tc2*) but has a narrower constriction (Tc4**); the sustentaculum is placed closer to the plantar border (Tc5***); the fibular trochlea is placed higher (Tc11***), but is laterally less prominent (Tc8*); the plantar border is wider (Tc12***); and the distal facet is shorter (Tc13*).

Lesbre (1903) and Steiger (1990) suggested that the fibular trochlea of the calcaneus may be broader in Bactrian camels, but we found no difference in that respect. However, we can support Steiger's (1990) observation that the fibular trochlea is proximally more protruding in dromedaries. We also agree with Steiger (1990) in noting that the plantar border of the calcaneus is broader in the latter species. The calcaneus stands out among postcranial bones for its large number of independent and clear diagnostic characters.

Cuboideum

The cuboideum has a taller dorsal region (Tq1***) with a narrower dorsal proximal facet in Bactrian camels (Tq18**; Online Resource 7). Additionally, it is usually larger in this species (*), with a broader proximal side (Tq13*) and broader lateral proximal facet (Tq16*).

The proportional differences of the dorsal part of the cuboideum are proposed here for the first time. Unlike Steiger (1990), we did not find the proximal process of the cuboideum to be significantly taller.

Naviculare

The naviculare is on average larger in Bactrian camels (*; Online Resource 7). Its overall shape is deeper (Tn4**) but narrower in dromedaries (Tn5***). The distal plantar facet is deeper in dromedaries (Tn8***).

The proportional differences of the naviculare are proposed here for the first time.

Medial cuneiforme

The medial cuneiforme, which is actually found in laterodorsal position, is a small simple bone which is often missing from collections, yielding a small comparative sample (one immature dromedary was included to increase sample size; Online Resource 7). Bactrian camels are larger (**) and might also have a larger distal facet, but this character fails to reach the significance level (Tm5°).

Intermediolateral cuneiforme

The intermediolateral cuneiforme, which is found in lateroplantar position, is larger in Bactrian camels (*; Online Resource 7). The dorsal lateral facet is always large in this species, while it has a large size variation and can be much smaller in dromedaries (Tl5**).

Metatarsale

Metapodia were found to complete development earlier than other skeletal parts; therefore, two adult-sized specimens from immature individuals were included in the sample. The metatarsale is longer and slenderer in dromedaries (mp1***, mp2***; Online Resource 5). The proximal end of the bone is deeper in this species (mp8*). Its articulation bears a triangular plantar process that is shorter (mp18***) but broader (mp19*) in Bactrian camels, with some exceptionally broad specimens among dromedaries. The maximal depth of the diaphysis (including the borders of the plantar side) is greater in dromedaries (mp10*); the minimal depth instead does not differ, and the minimal breadth is smaller than in the other species (mp12**). Both condyles are broader in the Bactrian camel, but only the lateral one significantly so (mp15°, mp16***); no difference in depth was detected (mp13°, mp14°) (Fig. 6). The distal breadth across the condyles is greater in the Bactrian camel (mp17**). Overall, the interspecific differences are similar to those found in the metacarpale.

Several previous studies already showed the differences in length and slenderness for both metapodia (Lesbre 1903; Olsen 1988; Peters and Driesch 1997; Steiger 1990).

The proximal process formed by metatarsal V was found by Steiger (1990) to be longer, narrower and more pointed in dromedaries, which is confirmed here.

Wapnish (1984) found that the metapodial condyles are deeper than broad in dromedaries, while in Bactrian camels they are broader than deep. We cannot agree with these categorical

observations, but instead we find a general tendency to deeper and narrower condyles in dromedaries. This is significant in metacarpale IV, and true but less significant in metacarpale III and both metatarsals. These observations contrast with Steiger's (1990) suggestion that metapodial condyles are both broader and deeper in Bactrian camels.

Grigson (1983) claimed that medial condyles can be recognized from lateral ones because of their square shape in distal view, and that in metacarpal condyles the anterior facet projects more than in metatarsal. In our view, these characters vary far too much to be diagnostic. We are not able to provide criteria to identify isolated medial from lateral condyles. To separate metacarpal from metatarsal condyles, the size difference is usually sufficient.

Harris et al. (2010) reported that distal metapodia are more divergent in Bactrian camels. We find that the total distal breadth of both metapodia is relatively larger in this species, which is congruent with this statement.

Posterior proximal phalanx

The posterior medial and posterior lateral phalanges are identical in morphology. The only known difference is that within an individual the lateral phalanx is slightly larger than the medial one (Steiger 1990). The medial and lateral phalanges can be analyzed separately or can be pooled, forming a sample with a larger number of individuals (including only one averaged value for each individual and each variable). As the results are qualitatively the same, we present only the statistically stronger results from the pooled sample. The same observations are valid about the anterior proximal phalanx, to which we apply the same analysis.

The same metric differences found in the anterior proximal phalanx are retrieved in the posterior proximal phalanx (Online Resource 8): the proximal articular surface is broader in Bactrian camels (pp4***), and both the axial (pp9***) and the abaxial lip (pp10***) of the distal trochlea are longer in the dromedary (Fig 7). Further distinctions are significant only in the posterior proximal phalanx: the diaphysis is both broader (pp5*) and deeper in the Bactrian camel (pp6*).

Lesbre (1903) observed correctly that anterior and posterior proximal phalanges are very similar and show the same interspecific differences, although we find the posterior phalanges to be more diagnostic. Indeed, only the posterior phalanges present a significant difference in slenderness as suggested by Lesbre (1903) and Steiger (1990). The latter also noticed that the proximal facet is

broader in Bactrian camels. Neither author observed the different lengths of the distal condyle lips, which are highly significant in our study.

Posterior intermediate phalanx

The data have been pooled with the anterior intermediate phalanx.

Size differences

The average size (the harmonic mean of all measurements, each scaled by the interspecific mean) of Bactrian camel bones was higher than the average size of all dromedary bones, except for one of the carpal bones. However, not all the size values differed significantly. The size differences in the cranium (***) and the mandible (**) were strongly significant, but this was not the case for the dentition and the cervical vertebrae. Neither did the axial skeleton show any size difference. In the anterior limb, no bone was significantly larger, and the triquetrum was (although not significantly) larger in dromedaries. In contrast, in the posterior limb significant size difference were found in the femur (*), the tibia (*), the fibula (***), and five of the six tarsal bones (calcaneus **, cuboideum *, naviculare *, medial cuneiforme **, and intermediolateral cuneiforme *).

Discussion

Our univariate morphometric analysis identifies a number of significant quantitative differences between Bactrian camels and dromedaries, consistent with a species level distinction between both forms. Comparing our results with those of previous qualitative analyses (Harris et al. 2010; Köhler-Rollefson 1989; Lesbre 1903; Olsen 1988; Steiger 1990; Wapnish 1984) allowed us to confirm several suggested diagnostic characters, but also to correct or refute others, and to propose some distinctive traits not identified before. However, not all of the differences found by our analysis are equally clear and significant. Low confidence results, indicated by * in the previous section, might be either confirmed or disproved in an even larger sample, while high confidence results, indicated by ** and ***, are expected to indicate real and clear differences.

Many cranial variables were distinct. Thirty-five out of 77 transformed metric variables for the cranium, 15 out of 25 transformed metric variables for the mandible, and 14 out of 20 morphological characters were found to be statistically different. In contrast, in the dentition there were no diagnostic traits once accounted for sex and age (wear stages). The head is smaller in dromedaries, although the cervical vertebrae do not differ in size. The braincase is also smaller in the latter.

Cranial sexual dimorphism is found in a small number of characters. The only difference found in both species is that the foramen magnum is longer, but not broader, in males. Other cranial traits did not differ. Males develop larger canines and caniniform premolars and incisors. No sexual dimorphism is known in postcranial bones, except in the pelvis which was not included in this study (Smuts and Bezuidenhout 1987; Steiger 1990).

The atlas and the axis do not differ in size but differ clearly in shape between the two camel species: the diagnostic characters are size, position, and shape of the foramina. The lumbar vertebrae show strong metric differences that vary from the first to the seventh.

Scapular and pelvic limb bones do not show the same amount of differences. The posterior limb bones tend to differ significantly both in shape and size: eight out of 12 bones are larger in Bactrian camels. The anterior limb bones are more conservative in shape, and none differs significantly in overall size. This is generally true for all limb parts: long bones, short bones, metapodia, and phalanges as well.

Nevertheless, some differences are comparable between the anterior and posterior limbs. Long bones and metapodia are relatively longer and more slender in the dromedary, while epiphyseal breadth and depth variables are relatively larger in Bactrian camels. The diaphysis of these bones is always significantly broader (transversal diameter); however, it does never differ in depth (craniocaudal, respectively dorsopalmar or dorsoplantar diameter).

Among the large number of cranial and mandibular interspecific differences, several concern structures involved in the mastication process. A key to their interpretation is provided by a study comparing cranial adaptation for grazing and browsing (Mendoza et al. 2002): among the typical traits of grazers, some also are diagnostic characters that separate the Bactrian camel from the dromedary. These include the development of a masseteric prominence or maxillary crest, orbits positioned relatively high and backwards, strong mandibular body, and relatively larger head. Further interspecific differences, which could also underlie different feeding adaptations, include the broader and shorter mandibular condyle, the corresponding different shape of the glenoid fossa, the longer and curved coronoid process, and the lesser development of the sagittal and occipital crests in the Bactrian camel.

Population ecology of camels is not well known, in part because these animals are studied mostly as domesticated forms. Both species are supposed to live in similar habitats, except for the different geographic distribution and temperature tolerance, and feeding differences are so far

unknown (Nowak 1999). Both species are mixed feeders; they prefer browsing on shrubs but can eat grass up to 30% of their diet, and need salty plants unpalatable to other animals (Feranec 2003; Nowak 1999; Semprebon and Rivals 2010). Both species are equally hypsodont (Semprebon and Rivals 2010).

In light of this consensus, it is quite surprising to find such strong differences in the morphological feeding adaptations between the two species of modern camels. However, the behavior and biology of the wild ancestors of domestic camels is unknown: extant wild Bactrian camels are genetically different from domestic camels, and likely represent a separate subspecies (Burger 2016; Hare 2008; Ji et al. 2009), while only feral populations of dromedaries are available for studies. Moreover, there is a lack of comparative ecological studies on camels, including wild and feral populations, which may reveal possible differences. We suggest that the set of cranial morphological differences described in our study represents adaptation to a feeding regime more inclined toward grazing in the Bactrian camel and more toward browsing in the dromedary. Therefore, the ecological separation between these species may be deeper than often assumed.

Recently, it was suggested that because *Camelus* is less hypsodont than its closest fossil relatives in North America, it could descend from a species adapted to high latitude forests (Rybczynski et al. 2013). However, extant camels are considered relatively hypsodont ungulates, whose dentition is adapted to browsing in dusty landscapes (Semprebon and Rivals 2010). In addition, even the oldest and most brachydont fossil camelid are reconstructed as open plain dwellers (Feranec 2003; Honey et al. 1998). Further, the first Eurasian camelids (in the genus *Paracamelus*) dispersed rapidly during the arid Messinian period, not through forested habitat, but rather along semi-desertic regions including China, northern Africa, and Spain (Likius et al. 2003; Van der Made et al. 2002). Hence, we consider it quite unlikely that the recent direct ancestors of *Camelus* and *Paracamelus* went through a forest-dwelling stage.

The most widely recognized character of camels is their characteristic humps. They consist of a fat reserve for periods of underfeeding, as present in many other animals; but unlike other species, camels concentrate all their fatty tissues in one body area to facilitate heat dissipation (Köhler-Rollefson 1991). The humps are formed only by soft tissues and it is as yet unclear if and how their presence, number, and position relate to the morphology of the vertebral column. The issue is relevant to the reconstruction of fossil species, which is necessary in attempting to reconstruct the phylogenetic development and relevance of these structures.

Olsen (1988) claimed that the presence of one or two humps is not reflected at all in the skeleton. Peters and von den Driesch (1997) argued the opposite, and provided a reconstruction of the vertebral column of both animals that clearly shows where and how the humps influence it. Our observations agree with the latter study. Many differences found by our analysis in the thoracic and lumbar vertebrae may be directly related to the presence of one or two humps. The two species differ in the outline of the spinal processes, which reflects the outline of the back in living animals. The Bactrian camel also has lumbar vertebrae with taller and broader corpora, but narrower zygapophyses. In this species, the transition from a thoracic (horizontal) to a lumbar (vertical) morphology of the intervertebral articulation occurs between the 10^{th} and the 11^{th} thoracal vertebra, one articulation later in the dromedary. All these characters are possibly related to the presence of a second hump in the Asian camel. Nevertheless, we warn that few isolated vertebrae are of no use in assessing the number of humps; an articulated vertebral sequence complete with spines would be necessary to discuss this issue, in particular for the reconstruction of a fossil species. As the humps of camels are an adaptation to life in deserts (Köhler-Rollefson 1991), they do not need to be expected in extinct species from other habitats.

Another well-known feature of camels is the pacing gait, which is an uncommon mode of locomotion allowing an increased stride in long-legged mammals. Camelids are the only wild animals using a high-speed running pace (Janis et al. 2002; Pfau et al. 2011; Van der Sluijs et al. 2010). The disadvantage of the pacing gait is a reduction in lateral stability, which is mitigated by a series of derived traits: in particular broad, splayed feet and enlarged proximal limb abductor attachment areas. Our results point out that some of these adaptations are more strongly developed in the Bactrian camel than in dromedary. For this species, we could observe a more prominent scapular spine and a broadened greater trochanter of the femur. Most of the long bone diaphyses are transversally (but not anteroposteriorly) broader than in the dromedary, which could also help in lateral stabilization. It appears therefore possible that Bactrian camels have an increased need for stabilization, which could derive simply from the larger body mass or from the addition of a second hump.

Both extant camel species have been domesticated, which might have impacted their present morphology. Typically, domesticated animal show important cranial differences from their wild relatives (Drake and Klingenberg 2010; Owen et al. 2014) and in particular they undergo a reduction of encephalization, calculated as brain size relatively to body mass (Zeder 2012). For instance, llamas (related to camels) have a 17.6% smaller brain and horses (similar to camels in how they are used under domestication) have a 14% smaller brain than their respective domestic

ancestors (Zeder 2012). We suggest that a comparable degree of encephalization loss should be expected in camels, too. This morphologic change happens swiftly after domestication, sometimes in less than 100 years (Zeder 2012); therefore, the larger braincase size of Bactrian camels cannot be explained as a differential domestication effect. Additional effects of domestication, such as variation in size and massiveness, are present in different camel breeds of both species, together with changes in soft character attributes like hair quality and coloring; but neoteny and variability in cranial shape are not apparent. To confirm the presence of morphological changes due to domestication, comparisons with their putative ancestor are necessaries. Unfortunately, morphological descriptions of the extant wild camel (*Camelus ferus*) are lacking; this taxon is considered a distinct subspecies from the one that is at the origin of domestic Bactrian camels (Burger 2016; Ji et al. 2009), which itself remains morphologically unknown. Archaeological material of two-humped camels has hardly been described (Peters and Driesch 1997). On the other hand, archaeological samples of supposed wild dromedaries exist but no morphologic or size differences is known (Curci et al. 2014; Driesch and Obermaier 2007).

Conclusions

Our analysis found several morphological differences distributed over the entire skeleton, consistent with a species distinction between *Camelus bactrianus* and *Camelus dromedarius*. Only a few bones did not differ in any measurement. According to our results, the univocal diagnostic characters in the cranium and mandibula (but not in the dentition) are numerous. Among postcranial bones, the most reliable characters are the size of the ventral foramen of the atlas (larger in Bactrian camels) and the presence of a bony bridge over the lateral foramen of the axis (only in dromedaries). Morphological characters of other bones are prone to at least some interspecific overlap, but several metric and proportional differences are significant at a population level. We show that if used in combination, several characters would allow the identification of a large number of isolated specimens with ease. However, it is equally important to recognize the extent of variation of these animals in the study of their extinct relatives. Although the fossil record of Old World camelids is poor, there is a substantial number of species named on fragmentary specimens (Kostopoulos and Sen 1999). We consider it likely that the intraspecific variation has been underestimated in paleontological analyses. We suggest that a review of known Pliocene and Pleistocene camelid species could recognize a number of synonyms, and is therefore highly necessary.

Acknowledgements

We would like to thank the curators that granted access to the collections in their care: B. Oberholzer and M. Haffner (Zoologisches Museum der Universität Zürich), Pa. Schmid (Naturhistorisches Museum des Burgergemeindes Bern), J. Studer (Muséum d'Histoire Naturelle de la Ville de Genève), M. Podestà and G. Bardelli (Museo Civico di Storia Naturale Milano). P. Martini is especially grateful to the Anthropologisches Institut und Museum der Universität Zürich, where this project was started as a Master thesis (Martini 2011). We thank the colleagues whose comments improved the manuscript: Y. Mary and V. De Pietri and in particular the reviewer D. Geraads. M. Mikelin helped prepare the illustrations. This study is part of P. Martini's doctoral thesis, which is supported by the Swiss National Foundation, the Isaac Dreyfus-Bernheim Stiftung, and the Freiwillige Akademische Gesellschaft Basel.

References

ALMATHEN, F., et al. 2016. Ancient and modern DNA reveal dynamics of domestication and cross-continental dispersal of the dromedary. Proceedings of the National Academy of Sciences of the United States of America.

BARONE, R. 1999. Anatomie comparée des mammifères domestiques. 4th ed. Vigot Frères, Paris. 1:1-761.

BEECH, M., M. MASHKOUR, M. HUELS, and A. ZAZZO. 2009. Prehistoric camels in south-eastern Arabia: the discovery of a new site in Abu Dhabi's Western Region, United Arab Emirates. Proceedings of the Seminar for Arabian Studies 39:17-30.

BURGER, P. A. 2016. The history of Old World camelids in the light of molecular genetics. Tropical animal health and production.

CLUTTON-BROCK, J. 1962.Analysis of mammalian faunas from prehistoric sites in India and western Asia. Ph.D. dissertation, University of London, London.

CREGUT-BONNOURE, E. 2002.Les Ovibovini, Caprini et Ovini (Mammalia, Artiodactyla, Bovidae, Caprinae) du Plio-Pléistocène d'Europe: systématique, évolution et biochronologie. Ph.D. dissertation, Université Claude Bernard, Lyon.

CUI, P., et al. 2007. A complete mitochondrial genome sequence of the wild two-humped camel (*Camelus bactrianus ferus*): an evolutionary history of Camelidae. BMC genomics 8:241.

CURCI, A., M. CARLETTI, and M. TOSI. 2014. The camel remains from site HD-6 (Ra's al-Hadd, Sultanate of Oman): an opportunity for a critical review of dromedary findings in eastern Arabia. Anthropozoologica 49:207-22.

DE GROSSI MAZZORIN, J. 2006. Cammelli nell'antichità: le presenze in Italia. Pp. 231-242 in Archaeozoological Studies in Honour of Alfredo Riedel (B. Sala and U. Tecchiati, eds.). Ufficio Beni Archeologici, Provincia di Bolzano, Bolzano.

DRAKE, A. G., and C. P. KLINGENBERG. 2010. Large-scale diversification of skull shape in domestic dogs: disparity and modularity. The American Naturalist 175:289-301.

DRIESCH, A. V. D. 1976. A guide to the measurement of animal bones from archaeological sites. Harvard University, Cambridge. 1:1-136.

DRIESCH, A. V. D., and H. OBERMAIER. 2007. The hunt for wild dromedaries during the 3rd and 2nd millennia BC on the United Arab Emirates coast. Camel bone finds from the excavations at Al Sufouh 2, Dubai, UAE. Pp. 133-167 in Skeletal Series and their Socio-economic Context (J. Grupe and J. Peters, eds.). Leidorf, Rahden.

EPSTEIN, H., and I. L. MASON. 1971. The Origin of the Domestic Animals of Africa. Africana Publishing Corporation, New York1-1292.

FERANEC, R. S. 2003. Stable isotopes, hypsodonty, and the paleodiet of *Hemiauchenia* (Mammalia: Camelidae): a morphological specialization creating ecological generalization. Paleobiology 29:230-242.

GRIGSON, C. 1983. A very large camel from the upper Pleistocene of the Negev Desert. Journal of Archaeological Science 10:311-316.

GRIGSON, C. 2012. Camels, copper and donkeys in the Early Iron Age of the southern Levant: Timna revisited. Levant 44:82-100.

HAMMER, Ø., D. A. T. HARPER, and P. D. RYAN. 2001. PAST: Paleontological Statistics software package for education and data analysis. Version 2.17c. Paleontologia Electronica 4:9.

HARE, J. 2008. *Camelus ferus*in IUCN 2013. IUCN Red List of Threatened Species. Version 2013.1.

HARRIS, J. M., D. GERAADS, and N. SOLOUNIAS. 2010. Camelidae. Pp. 815-820 in Cenozoic Mammals of Africa (L. Werdelin and W. J. Sanders, eds.). University of California Press, London.

HONEY, J. J., J. A. HARRISON, D. R. PROTHERO, and M. S. STEVENS. 1998. Camelidae. Pp. 439-462 in Evolution of Tertiary Mammals of North America: Terrestrial Carnivores, Ungulates, and Ungulatelike Mammals (C. M. Janis, K. Scott and L. L. Jacobs, eds.). Cambridge University Press, Cambridge.

JANIS, C. M., J. M. THEODOR, and B. BOISVERT. 2002. Locomotor evolution in camels revisited: a quantitative analysis of pedal anatomy and the acquisition of the pacing gait. Journal of Vertebrate Paleontology 22:110-121.

JI, R., et al. 2009. Monophyletic origin of domestic bactrian camel (*Camelus bactrianus*) and its evolutionary relationship with the extant wild camel (*Camelus bactrianus ferus*). Animal genetics 40:377-82.

KINNE, J., N. A. WANI, U. WERNERY, J. PETERS, and C. KNOSPE. 2010. Is there a two-humped stage in the embryonic development of the dromedary? Anatomia, histologia, embryologia 39:479-80.

KÖHLER-ROLLEFSON, I. U. 1989. Zoological analysis of camel skeletons. Pp. 142-164 in Pella of the Decapolis. Vol. 2, Final Report on the College of Wooster Excavations in Area IX, the Civic Complex, 1979-1985 (R. H. Smith and L. P. Day, eds.). The College of Wooster, Wooster.

KÖHLER-ROLLEFSON, I. U. 1991. *Camelus dromedarius*. Mammalian species 375:1-8.

KÖHLER-ROLLEFSON, I. U. 1993. Camels and camel pastoralism in Arabia. The Biblical Archaeologist 56:180-188.

KOSTOPOULOS, D. S., and S. SEN. 1999. Late Pliocene (Villafranchian) mammals from Sarikol Tepe, Ankara, Turkey. Mitteilungen der Bayerischen Staatssammlung für Paläontologie und Historische Geologie 39:165-202.

LESBRE, F.-X. 1903. Recherches anatomiques sur les Camélidés. Pp. 1-196 in Archives du Muséum d'Histoire Naturelle de Lyon (H. Georg, ed.), Lyon.

LIKIUS, A., M. BRUNET, D. GERAADS, and P. VIGNAUD. 2003. Le plus vieux Camelidae (Mammalia, Artiodactyla) d'Afrique: limite Mio-Pliocène, Tchad. Bulletin de la Société Géologique de France 174:187-193.

LOMBARDINI, L. 1879. Monografia dei Cammelli. Annali delle Università Toscane 259:147-187.

MANEFIELD, G. W., and A. H. TINSON. 1996. Camels: A Compendium. University of Sydney Post Graduate Foundation in Veterinary Science376.

MARTINI, P. 2011.A metrical analysis of the morphological variation in extant and fossil camels. Master's thesis, University of Zürich, Zürich.

MENDOZA, M., C. M. JANIS, and P. PALMQVIST. 2002. Characterizing complex craniodental patterns related to feeding behaviour in ungulates: a multivariate approach. Journal of Zoology 258:223-246.

MIKESELL, M. W. 1955. Notes on the dispersal of the Dromedary. Southwestern Journal of Anthropology 11:231-245.

MORALES, J., D. SORIA, and E. AGUIRRE. 1980. Camelido finimioceno en Venta del Moro. Primera cita para Europa Occidental. Estudios Geológicos 36:139-142.

NOWAK, R. M. 1999. Walker's Mammals of the World. The Johns Hopkins University Press, Baltimore1-1936.

OLSEN, S. J. 1988. The camel in Ancient China and an osteology of the camel. Proceedings of the Academy of Natural Sciences of Philadelphia 140:18-58.

OWEN, J., K. DOBNEY, A. EVIN, T. CUCCHI, G. LARSON, and U. STRAND VIDARSDOTTIR. 2014. The zooarchaeological application of quantifying cranial shape differences in wild boar and domestic pigs (*Sus scrofa*) using 3D geometric morphometrics. Journal of Archaeological Science 43:159-167.

PALMQVIST, P., A. ARRIBAS, and B. MARTÍNEZ-NAVARRO. 1999. Ecomorphological study of large canids from the lower Pleistocene of southeastern Spain. Lethaia 32:75-88.

PETERS, J. 1998. *Camelus thomasi* Pomel, 1893, a possible ancestor of the one-humped camel? Zeitschrift für Säugetierkunde 63:372-376.

PETERS, J., and A. V. D. DRIESCH. 1997. The two-humped camel (*Camelus bactrianus*): new light on its distribution, management and medical treatment in the past. Journal of Zoology 242:651-679.

PFAU, T., E. HINTON, C. WHITEHEAD, A. WIKTOROWICZ-CONROY, and J. R. HUTCHINSON. 2011. Temporal gait parameters in the alpaca and the evolution of pacing and trotting locomotion in the Camelidae. Journal of Zoology 283:193-202.

PIGIÈRE, F., and D. HENROTAY. 2012. Camels in the northern provinces of the Roman Empire. Journal of Archaeological Science 39:1531-1539.

POTTS, D. T. 2004. Camel hybridization and the role of *Camelus bactrianus* in the ancient Near East. Journal of the Economic and Social History of the Orient 47:143-165.

REYNAUD SAVIOZ, N., and P. MOREL. 2005. La faune de Nadaouiyeh Aïn Askar (Syrie centrale, Pléistocène moyen) : aperçu et perspectives. Revue de Paléobiologie, Genève 10:31-35.

RYBCZYNSKI, N., J. C. GOSSE, C. R. HARINGTON, R. A. WOGELIUS, A. J. HIDY, and M. BUCKLEY. 2013. Mid-Pliocene warm-period deposits in the High Arctic yield insight into camel evolution. Nature communications 4:1550.

SAALFELD, W. K., and G. P. EDWARDS. 2010. Distribution and abundance of the feral camel (*Camelus dromedarius*) in Australia. The Rangeland Journal 32:1-9.

SEMPREBON, G. M., and F. RIVALS. 2010. Trends in the paleodietary habits of fossil camels from the Tertiary and Quaternary of North America. Palaeogeography, Palaeoclimatology, Palaeoecology 295:131-145.

SMUTS, M. M. S., and A. J. BEZUIDENHOUT. 1987. Anatomy of the Dromedary. Oxford University Press, Oxford 1-230.

SPASSOV, N., and T. STOYTCHEV. 2004. The dromedary domestication problem: 3000 BC rock art evidence for the existence of wild One-humped camel in Central Arabia. Historia naturalis bulgarica 16:151-158.

STEIGER, C. 1990.Vergleichend morphologische Untersuchungen an Einzelknochen des postkranialen Skeletts der Altweltkamele. Ph.D. dissertation, Ludwig-Maximilians-Universität München, München.

STUDER, J., and A. SCHNEIDER. 2006. Camel use in the Petra Region, Jordan: 1st century BC to 4th century AD. Pp. 581-596 in Archaeozoology of the Near East VIII. Proceedings of the International Symposium on the Archaeozoology of Southwestern Asia and Adjacent Areas (E. Vila, L. Gourichon, A. M. Choyke and H. Buitenhuis, eds.). Maison de l'Orient et de la Méditerranée, Lyon.

UERPMANN, H.-P. 1999. Camel and horse skeletons from protohistoric graves at Mleiha in the Emirate of Sharjah (U.A.E.). Arabian archaeology and epigraphy 10:102-118.

UERPMANN, M., and H.-P. UERPMANN. 2002. The appearance of the domestic camel in south-east Arabia. Journal of Oman Studies 12:235-260.

VAN DER MADE, J., J. MORALES, S. SEN, and F. ASLAN. 2002. The first camel from the upper Miocene of Turkey and the dispersal of the camels into the Old World. Comptes Rendus Palevol 1:117-122.

VAN DER SLUIJS, L., M. GERKEN, and H. PREUSCHOFT. 2010. Comparative analysis of walking gaits in South American camelids. Journal of Zoology 282:291-299.

WAPNISH, P. 1981. Camel caravans and camel pastoralists at Tell Jemmeh. JANES 13:101-121.

WAPNISH, P. 1984. The dromedary and Bactrian camel in Levantine historical settings: The evidence from Tell Jemmeh. Pp. 171-200 in Animals and Archaeology: 3. Early Herders and their Flocks (J. Clutton-Brock and C. Grigson, eds.). British Archaeological Reports, International Series, Oxford.

WU, H., et al. 2014. Camelid genomes reveal evolution and adaptation to desert environments. Nature communications 5:5188.

ZEDER, M. A. 2012. Pathways to animal domestication. Pp. 227-259 in Biodiversity in Agricolture: Domestication, Evolution, and Sustainability (P. Gepts, et al., eds.). Cambridge University Press, Cambridge.

Online Resources

Supplementary figures and tables (including measurement tables and measurent procedures) are available under the electronic version of this published article (doi:10.1007/s10914-017-9386-9), or on request from the first author.

Figures

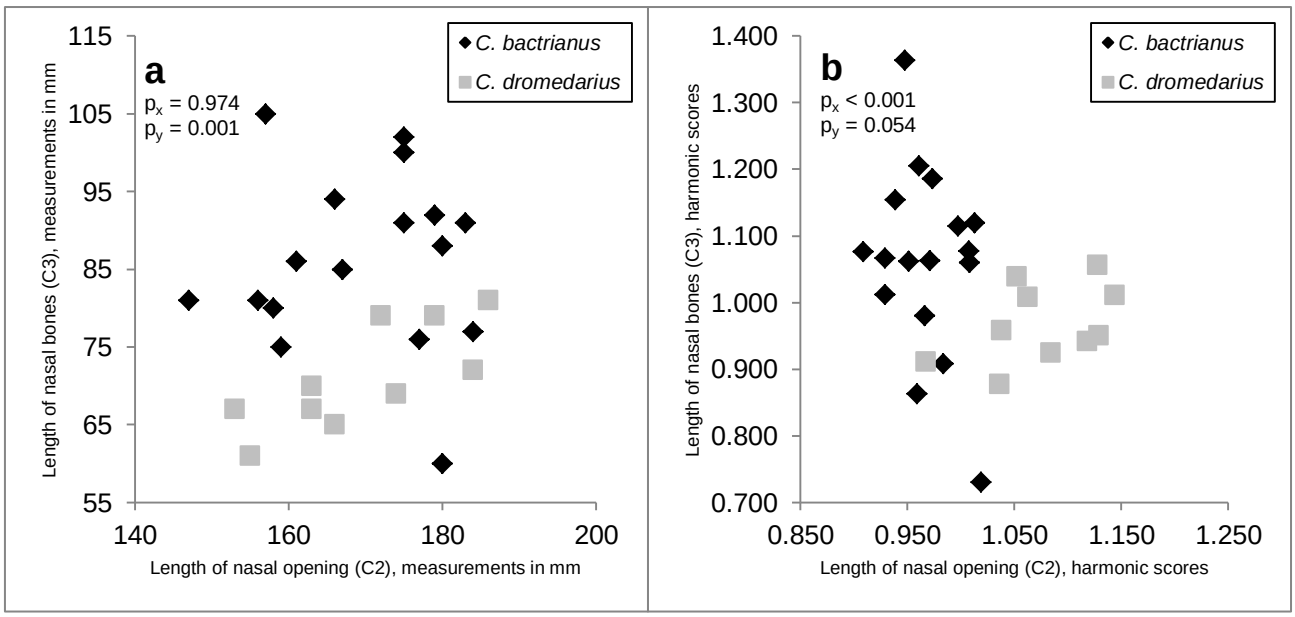

Fig. 1 An example of the use of harmonic scores: bivariate plot showing length of nasal opening (C2) vs. length of nasal bones (C3). **a** In raw measurements (mm), the nasal opening has the same length in both species, and the nasal bones are longer in *C. bactrianus*. **b** Harmonic scores (HS) are scaled by an estimation of the specimen's size, which on average is significantly larger in *C. bactrianus* crania. As a consequence, the nasal opening is shown to be relatively longer in all but one *C. dromedarius*, while the length of nasal bones has a large variation in *C. bactrianus* making this difference not significant ($p>0.05$)

Fig. 2 Comparison of cranium, in lateral view. Not to scale. Top: *C. bactrianus* MHNG 1063.089, bottom: *C. dromedarius* NMB 2128. Both individuals are males of a similar age

Fig. 3 Comparison of cranium, in dorsal view. Not to scale. Top: *C. bactrianus*, bottom: *C. dromedarius*. Same individuals as in Fig. 2

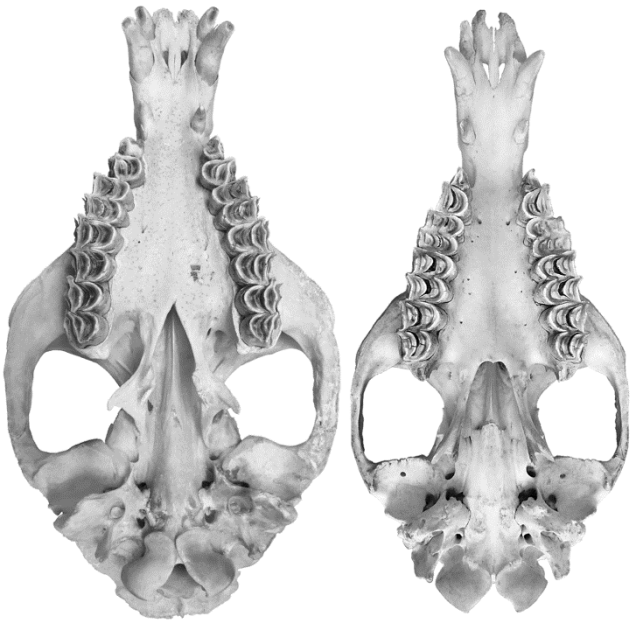

Fig. 4 Comparison of cranium, in basal view. Not to scale. Top: *C. bactrianus*, bottom: *C. dromedarius.* Same individuals as in Fig. 2

Fig. 5 Comparison of atlas (left, in ventral view) and axis (right, in lateral view). Not to scale. Top: *C. bactrianus* NMB 10902, bottom: *C. dromedarius* ZM 13130

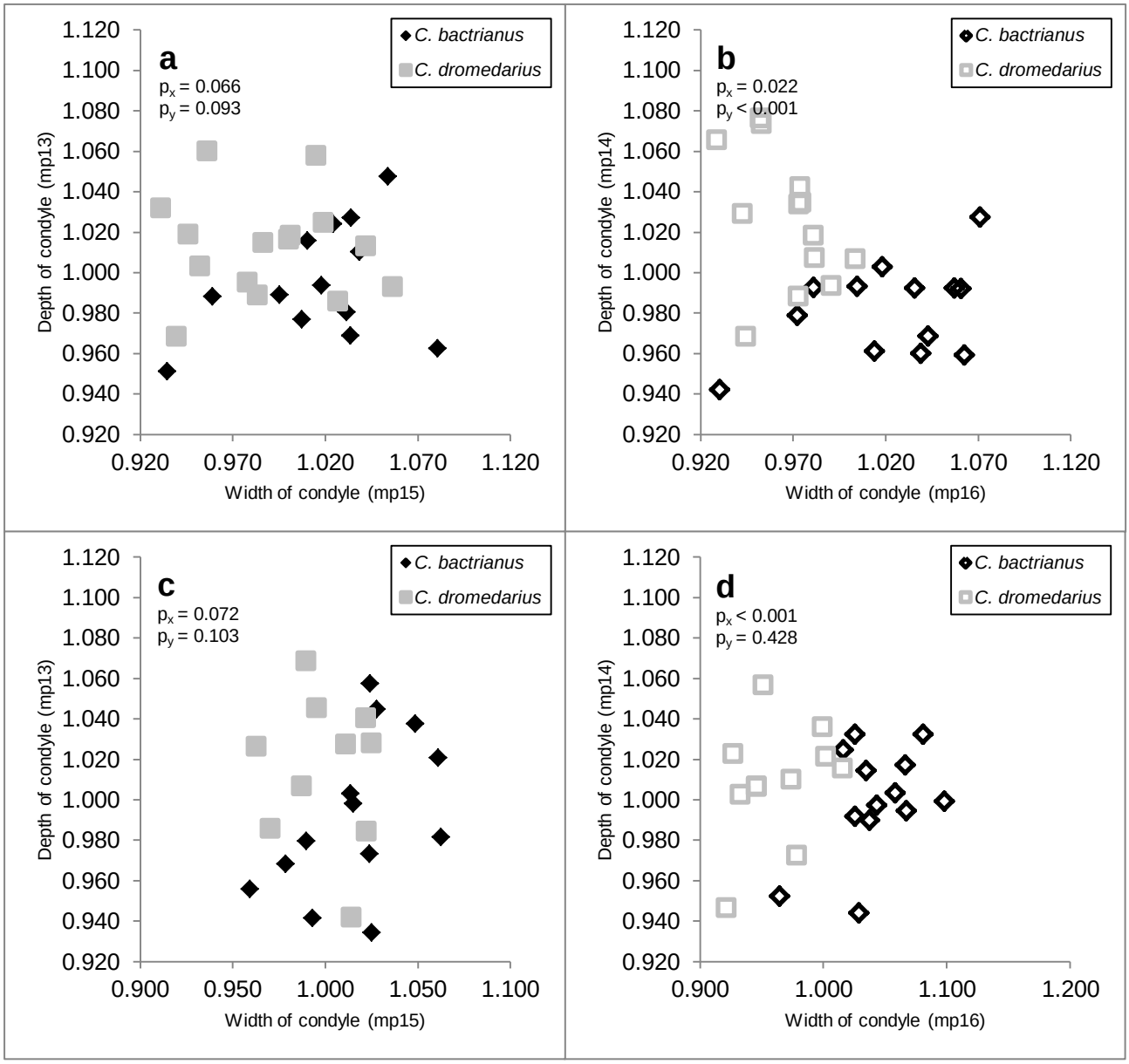

Fig. 6 Bivariate plots of harmonic scores showing proportions of metapodial condyles: transversal width (mp15/16) versus anteroposterior depth (mp13 /14). **a** Metacarpal medial **b** Metacarpal lateral **c** Metatarsal medial **d** Metatarsal lateral

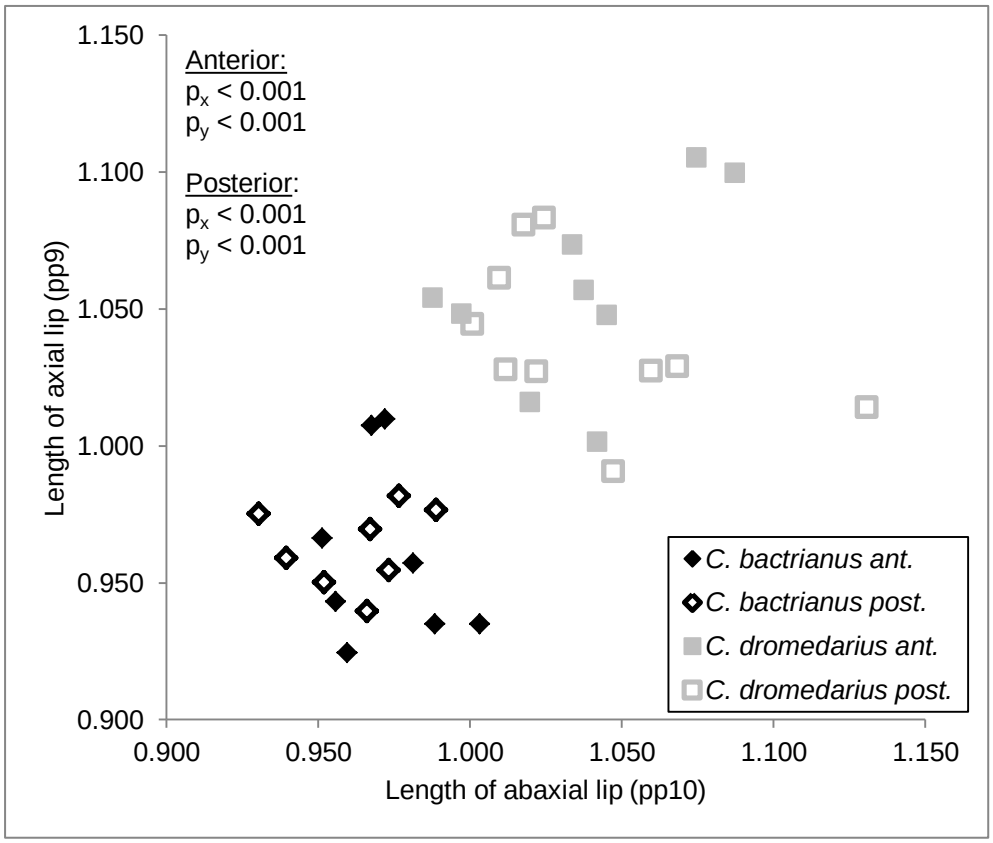

Fig. 7 Bivariate plot of harmonic scores showing proportions of condylar lips of anterior (=ant.) and posterior (=post.) proximal phalanx: length of abaxial lip (pp10) vs. length of axial lip (pp9)

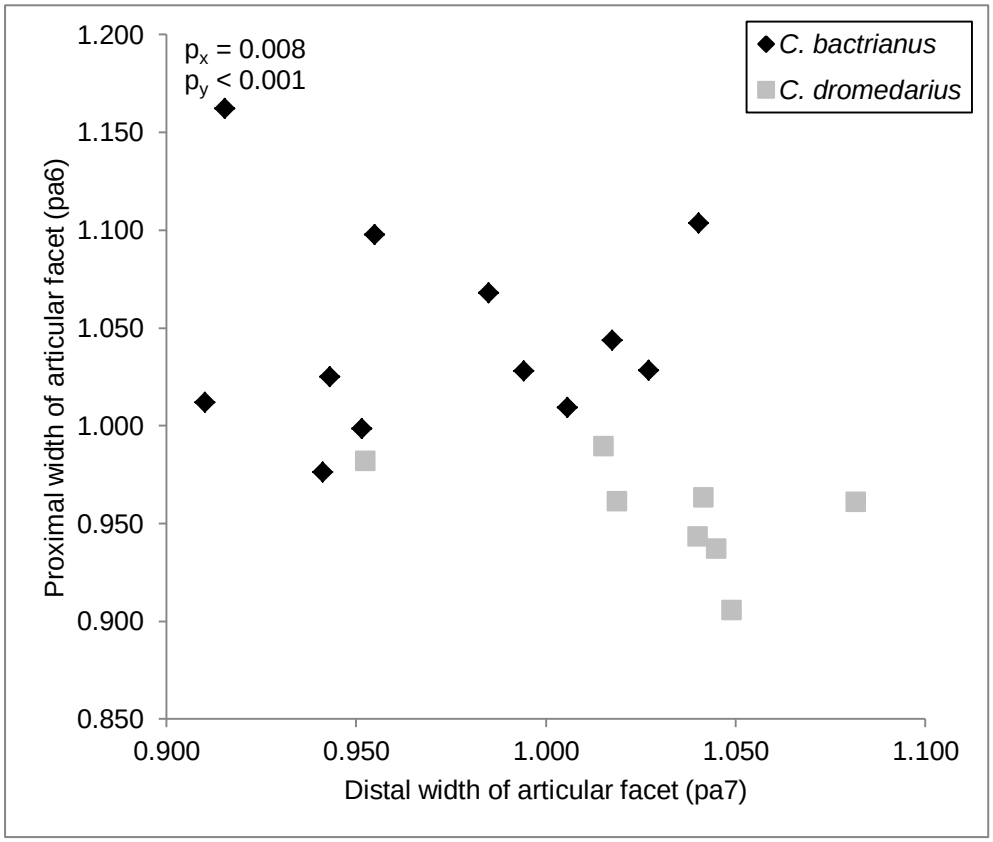

Fig. 8 Bivariate plot of harmonic scores showing proportions of the articular facet of the patella: distal transversal width (pa7) vs. proximal transversal width (pa6)

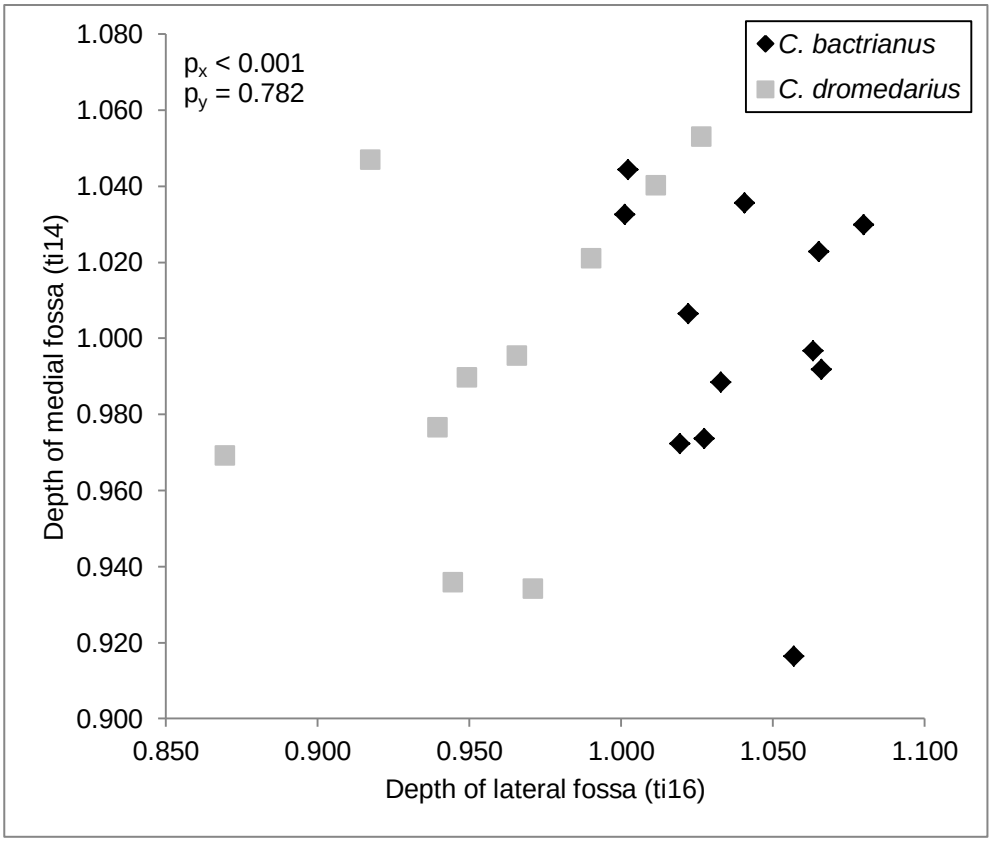

Fig. 9 Bivariate plot of harmonic scores showing proportions of the distal cochlea of the tibia: dorsoplantar depth of lateral fossa (ti16) vs. dorsoplantar depth of medial fossa (ti14)

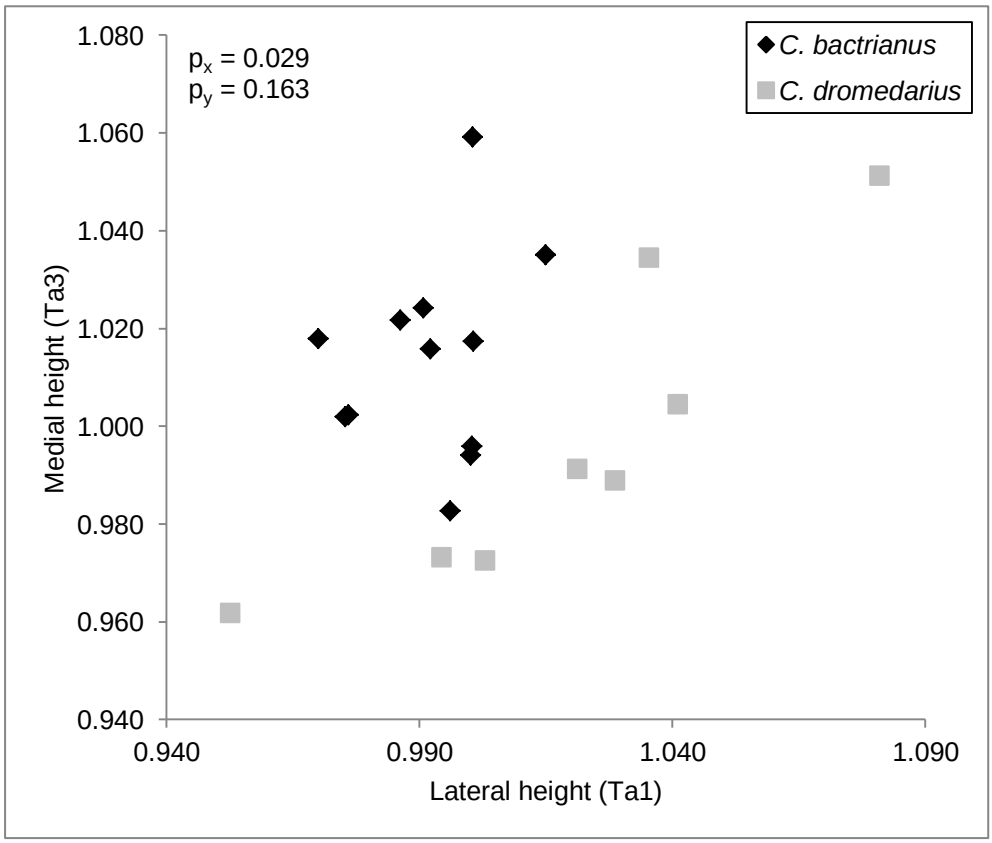

Fig. 10 Bivariate plot of harmonic scores showing proportions of the astragalus: Ta1, lateral height (Ta1) versus medial height (Ta3)

Chapter 2

Camelus thomasi Pomel, 1893, from the Pleistocene type-locality Tighennif (Algeria): Comparisons with modern *Camelus*

Pietro Martini, Denis Geraads (2018)

Geodiversitas 40 (5): 115-134

Abstract

We describe here the whole collection of *Camelus thomasi* from its type-locality, Tighennif (Ternifine) in Algeria. Detailed morphological and metric comparisons with the two species of modern *Camelus*, *C. bactrianus* and *C. dromedarius*, show that it is clearly distinct from both of them. It is mainly characterized by pachyostosis especially marked in the mandible, a size slightly greater than modern forms, broad molars with strong styles, and several unique cranial features. The species seems restricted to the terminal Early Pleistocene and is not definitely known outside Northwestern Africa. A phylogenetic analysis is premature, but *C. thomasi* does not appear to be particularly close to either modern species, and there is no support to regard it as an ancestor of the dromedary.

Keywords: Mammalia – Camelidae – Pleistocene – Algeria – morphometrics

Introduction

In one of his important monographs dealing with fossil mammals from Algeria, Pomel (1893) described a new species of camel as *Camelus thomasii*, based upon a fragment of maxilla, a piece of mandible and an incomplete metatarsal, from the locality then called Palikao, but better known in the literature as Ternifine (now Tighennif; Geraads [2016], and references therein). He noted that the type maxilla differs from that of the modern dromedary in the shape of the maxillo-palatine suture and in the horizontal orbital floor, supposedly giving the animal a less stupid look ['un air moins stupide'] than the dromedary, in which the orbits face more downwards. Further excavations at the site, mostly by C. Arambourg in 1954-56 (Arambourg and Hoffstetter 1963; Geraads et al. 1986), much increased the camel collection, which is now by far the richest sample of African fossil camels. However, in spite of its importance, this collection remained unstudied, besides short

descriptions by Harris et al. (2010). That explains why the species has been erroneously reported from a number of other sites and, most regrettably, its systematic position discussed without reference to the material from the type-locality. Here we describe the whole collection of *C. thomasi* from Tighennif, and discuss its relationships with the extant dromedary *C. dromedarius* and Bactrian camel *C. bactrianus*.

Materials and methods

Most of the material of *C. thomasi* described below (Table 1) is housed in MNHN; in addition, we have seen photos of the specimens (including the type) kept in the Algiers Museum, kindly provided by Y. Chaïd-Saoudi. A few other potential specimens of *C. thomasi* are from the 'Grotte des Rhinocéros' in Casablanca (Geraads & Bernoussi 2016). We have compared them to a good sample of modern camels: *C. bactrianus* (28 skulls), *C. dromedarius* (31 skulls), hybrids or unidentified (3 skulls), housed in MNHN, CCEC, ZIN, ZM, NMBE, NMB, MHNG, MSNM, and EK using the measurements of Martini et al. (2017). We have not attempted to distinguish taxonomically wild, feral and domestic forms of *C. bactrianus*, because such information is almost always missing in osteological collections.

Abbreviations

CCEC, Centre de Conservation et d'Etudes des Collections, Lyon

EK, Tell Arida research centrum, El Kowm, Syria

INSAP, Institut National des Sciences de l'Archéologie et du Patrimoine, Rabat

IPH, Institut de Paléontologie Humaine, Paris

MGA, Musée de Géologie, Algiers

MHNG, Muséum d'Histoire Naturelle de la Ville de Genève

MNHN, Muséum National d'Histoire Naturelle, Paris

MSNM, Museo Civico di Storia Naturale, Milano

NMB, Naturhistorisches Museum, Basel

NMBE, Naturhistorisches Museum des Burgergemeindes Bern

ZIN, Zoological Institute, Russian Academy of Sciences, Saint Petersburg

ZM, Zoologisches Museum der Universität Zürich

Systematic Paleontology

Family CAMELIDAE Gray, 1821

Genus *Camelus* L., 1758

Type species *Camelus bactrianus* Linnaeus, 1758.

Camelus thomasi Pomel, 1893

The name *Camelus thomasii* was first published by Pomel in 1886 but remained a *nomen nudum* until 1893.

Holotype (by original designation).

Right maxilla with M1–M2 and part of the palatine bone, N° 7236001 in the Musée de Géologie, Algiers, Algeria (Fig. 2E); also Pomel, 1893, pl.3, figs. 2−5 (note that Pomel's figures are inverted, and that the association of a M3 with this maxilla is tentative). From the late/terminal Early Pleistocene of Tighennif (formerly spelled Tighenif, also known as Ternifine or Palikao), near Mascara, Algeria.

Referred material

The whole collection of *Camelus* from Tighennif is referred to this species; the full list of specimens housed in MNHN and their measurements are given in the Appendix. In addition, we tentatively ascribe to the same species some specimens from the Middle Pleistocene of Oulad Hamida I quarry in Morocco, but they do not contribute to the definition of the species.

Diagnosis

A *Camelus* slightly larger than the modern species; pachyostosis weakly indicated in cranium (thick nasalia, thickening of the zygomatic arch posteriorly) and strongly so in the mandible; marked sexual dimorphism; V-shaped choanae; palatine foramina located anteriorly, at the level of P3 or P4; facial crest present; low placement of orbits; paroccipital process far from condyles; teeth small relatively to skull size; P1 located anteriorly, P3 with a complete lingual crescent; molars

alveolarly broad with strong styles; mandible thick and low, especially anteriorly; coronoid process short, massive, slightly twisted and bent backwards; caudal mental foramen located anteriorly, or absent; p1 absent or located more anteriorly than in modern forms; p4 long, with a long metaconid; limb bones long; tibial tuberosity slender and very prominent; phalanges robust.

Age of the site

Historical data on the excavations and research at Tighennif can be found in Geraads (2016), who provided a faunal list, and concluded that the site is probably older than the Middle Pleistocene, as also assumed by Sahnouni and van der Made ((2007); it can tentatively be dated to c. 1 Ma. It is best known for its hominin remains (Arambourg and Hoffstetter 1963), either referable to *Homo rhodesiensis* Woodward, 1921 (according to Hublin, 2001) or closer to *H. ergaster* (Martinón-Torres et al., 2007).

Description and comparisons with modern forms.

The best specimen is a relatively complete cranium, TER-1689 (Fig. 1), first figured by Lhote (1987). Its description can be complemented with that of other cranial elements: the maxilla with imperfectly preserved teeth TER-1816 (Fig. 2A), and the type-specimen MGA-7236001 (on the basis of photos kindly provided by Y. Chaïd-Saoudi, Fig. 2B). Unfortunately, TER-1689 is strongly dorso-ventrally crushed, so that the cranial surface consists of a mosaic of bone fragments among which sutures and details are hard to recognize. This crushing prevents reconstruction of the dorsal cranial profile and of the position of the front teeth relative to the occlusal plane of the cheek teeth. The basicranium is also poorly preserved and the right zygomatic arch is missing. In addition, the premaxillae are somewhat shifted posteriorly, and probably lack a few mm at their tips. By contrast, the moderately worn cheek-teeth are nicely preserved, but all teeth anterior to P3 are missing, except the left canine.

Overall size is close to the maximum seen in extant species (Table 2). The maximal length (measurement C1) of 575 mm exceeds that of all 31 measured *C. dromedarius*, and was surpassed (by less than 10 mm) in only two individuals out of 28 *C. bactrianus*; given that this measurement is certainly underestimated because of the preservation of the premaxillae, it can reasonably be assumed that this skull was longer than that of all modern *Camelus* in our sample. Beside the larger size, the only proportions that differ significantly from those of the modern forms are the ones that indicate a shorter face and rostrum; considering the imperfect preservation of the premaxilla, these differences can probably be ignored. Dorso-ventral crushing prevents fully reliable estimates of

breadth at orbital and post-orbital levels, but on the whole there is no evidence that general cranial proportions differed much from modern forms.

The premaxillae taper anteriorly, so that the rostrum appears pointed but it is certainly partly eroded; in both modern forms, its shape is variable, from similar to that of TER-1689 to distinctly broadened. The nasal opening looks small, but this is probably an impression given by the medial folding of the maxilla and misplacement of the premaxilla. Because of this crushing, the topographic relationships of the premaxillae cannot be definitely ascertained. Their most remarkable feature is their thickness throughout their length, which contrasts with their slenderness in the modern forms.

The infra-orbital foramen is located above the limit between P4 and M1; it occupies the same position in the maxilla TER-1816, and usually also in extant forms.

The front border of the orbit is located above the posterior half of M2, thus much like in modern forms, in which it is almost always located above that tooth as well. The orbit itself is too crushed for its real shape and measurements to be estimated, but it was located rather close to the tooth-row (Fig.3). A long facial crest runs more or less parallel to its ventral border, about 25 mm below it; it fades out anteriorly and posteriorly, without connecting the ventrolateral edge of the zygomatic arch; the maxilla TER-1816 is imperfectly preserved below the orbit, but the facial crest was probably absent. It is almost always wholly absent in *C. dromedarius* (CCEC 5000-2069 being the single exception), but it is at least incipient in *C. bactrianus*, although it usually talks the shape of a tubercle below the anterior orbital border. Another crest underlines the ventral orbital border, about 10 mm below it, and proceeds posteriorly into the ventro-lateral edge of the zygomatic arch, as in modern *Camelus*. The front end of the squamosal is located about 25 mm behind the orbit. As mentioned above, the shape of the nasals cannot be determined. The ethmoid fissure was at most very small, and probably absent; in *C. bactrianus* its size ranges from large to extremely small, in *C. dromedarius* from medium-sized to absent. Around their position, on either side of the posterior part of the nasals, the dorsal part of the skull bears two symmetrical depressions due to post-mortem crushing but whose formation was certainly facilitated by the thinness of bones in this area, and underlying sinuses. The supra-orbital foramina are located not far apart (46 mm), as in modern forms, where they are often multiple.

The sagittal crest suffered no major distortion; it starts behind the post-orbital constriction but remains low and, even in its caudal portion, never becomes blade-like as often occurs in male *C. dromedarius*. As it now stands, the nuchal crest is thin and convex in occipital view, but it is

probably incompletely preserved. In the sagittal plane, the occipital crest is stronger than in most recent *Camelus*. There was certainly no large nuchal tubercle above the foramen magnum, as sometimes occurs in *C. bactrianus*.

The ventral view confirms the tapering rostrum and short, pointed premaxillae. The large canine identifies the skull as that of a male. The P1 is missing, and its alveolus cannot be identified, but the individual was probably too young for having shed this tooth, as happens in senile individuals of the modern form. However, if present, this tooth was certainly closer to the canine than to P3, a position closer to the state of *C. dromedarius*, whereas in *C. bactrianus* this tooth is more posterior.

The palate is slightly crushed transversally, so that the outline of the choanae is imperfectly preserved; however, it was certainly much closer to the V shape that is most common in *C. bactrianus*, but is never found in *C. dromedarius*. TER-1816 almost certainly also had narrow V-shaped choanae. The choanae reach the level of the front of M3, which is not rare in *C. bactrianus*, but which we observed in a single, very old specimen of *C. dromedarius*. The course of the maxillo-palatine suture cannot be followed, as is normal in adult camels.

In TER-1689, the palatine foramina open at the level of P4, which is the most common position in *C. dromedarius*, whereas those of *C. bactrianus* almost always open at the level of M1 or M2. They are even more anterior in TER-1816, at the level of the posterior part of P3.

The pterygoid wings are missing, but the pterygoid processes of the basisphenoid consist of thick blades that emerge at the level of the middle of the glenoid fossae; in modern *Camelus*, they remain instead fully anterior to these fossae. The processes lateral to the foramen orbitorotundum are robust.

The glenoid fossae are incompletely preserved; they are deeply concave and bordered laterally by a thick, but low tubercle that is less lateral than in modern forms, because some thickening of the posterior root of the zygomatic arch occurred, laterally to this tubercle.

The auditory region is too poorly preserved for description, but a sharp difference with both modern species is that the paroccipital processes are located much farther from the occipital condyles, from which they are separated by a long, deep fossa, which is much shorter in modern camels; consequently, the tips of the paroccipital processes are farther apart than in modern forms. The condyles are broad (Fig. 4) and markedly extend onto the basioccipital, as in most

C. bactrianus, whereas they may be shorter antero-posteriorly in *C. dromedarius*, but the morphology of *C. thomasi* is within the variation of both modern species.

In contrast to skull length, length M1−M3 of the complete skull (C34 = 114 mm), is close to the mean value for *C. bactrianus*, but it is even distinctly lower (102 mm) in TER-1816, close to the mean of *C. dromedarius*. The cheek-teeth are little worn and very well preserved. Although no tooth is quite fresh, the slight wear of the premolars, and of the M3 tentatively associated with the type-maxilla, show that the degree of hypsodonty was very similar to that of modern *Camelus*. No cement cover is preserved on any tooth, in contrast to modern forms in which it is present; it was probably destroyed during fossilization, or removed during preparation, because it is present in some lower teeth, and because Pomel (1893, pl. 4, fig. 1) figured cement on an upper molar from Tighennif. The P3 has a complete lingual wall; the central valley is fully closed lingually, and opens mesially 13 mm above the cervix. The lingual crescent is never complete in *C. dromedarius*, and very rarely complete in *C. bactrianus*; in these forms, P3 is usually a reduced tooth, quite different from P4, whereas they are similar in *C. thomasi*. Thus, although this tooth is present only in TER-1689, the difference with modern forms is clear. P4 differs from P3 only in being larger and more symmetrical; on both teeth the buccal central rib is quite weak, and the mesial and distal styles are buccally prominent. M1 has a small basal cingulum along the lingual side; this tooth is distinctly smaller than M2, which is about as large as M3. On all molars, the buccal paracone rib is better indicated than the vestigial metacone rib, the parastyle is thicker than the mesostyle but both are quite prominent bucally, in contrast to the metastyle, which is distinct on M3 only. All these dental features are similar on the other specimens TER-1816 and MGA-7236001. In modern forms, the styles are less prominent buccally, especially the parastyle, which is not stronger than the mesostyle; there is variation in this regard, but the fact that both the type and TER-1816 also have prominent styles suggest that this is a valid difference.

In addition, the molars differ from those of modern forms in being broader, in particular the mesial lobe of M1 and M2 (Figs. 5-6); although these can be accurately measured only in TER-1689, this was clearly also true in the smaller maxilla TER-1816 (Fig. 1H).

Pomel (1893, pl. 4, fig. 3–4) tentatively ascribed to *C. thomasi* a mandible not found *in situ*, and now preserved in MGA; it fails to show the typical characters of the species, described below, and is probably of a historical *C. dromedarius* instead. The MNHN collection of *C. thomasi* from Tighennif includes seven partial mandibles, of which five are illustrated here: TER-1683 (Fig. 2F; almost certainly of the same individual as TER-1684); TER-1685 (Fig. 2G); 1900-27, collected by

Pallary (Fig. 2C); TER-1686 (Fig.2E); and TER-1688 (Fig. 2D). Two additional mandibles are stored in IPH and MGA.

Their most obvious character is the strong pachyostosis, the corpus being low but extremely thick below the cheek-teeth, and even thicker than deep below p4-m1 (Fig. 7); this thickening extends to the ascending ramus. The coronoid process is rather cylindrical with a flattened anterior surface, not blade-like. It is slanted backwards, with a weak curvature; its apex is transversally compressed, antero-posteriorly deeper than the base and has a slight lateral twist. This morphology contrasts with both species of modern *Camelus*, which are also different from each other. The condyle is preserved on TER-1685; it is rectangular, and antero-posteriorly short. This contributes, in addition to the shape of the coronoid process and reduction of the sigmoid notch, to the antero-posterior narrowness of the ramus at this level, in the three specimens in which this part is preserved.

TER-1683 (Fig. 2F) preserves a large part of the corpus anterior to p4, up to about 1 cm in front of the anterior mental foramen, and there is no evidence of a p1, so that this tooth was either absent, or more anterior. In modern *Camelus*, p1 is almost always present, and can be shed only in individuals distinctly older than TER-1683; it is never as anterior as it must have been if present in TER-1683.

The posterior mental foramen is located below the anterior part of m1 in TER-1685, but is certainly absent in TER-1683/1684. It is not visible in the other specimens, which preserve only the posterior part of the mandible, but if present it was always anterior to the middle of m1, a position more similar to that observed in *C. bactrianus*, whereas it is more posterior in *C. dromedarius*.

The only preserved p4 is that of TER-1685. It is longer than that of modern form; the metaconid is antero-posteriorly expanded to form a complete lingual wall; this sometimes occurs in *C. bactrianus*, but never in *C. dromedarius*.

In all camel species, the upper part of the lingual wall of the lower molars is concave between the stylids, but as wear proceeds, the styles fade away, and the lingual walls become more or less flat; they may even become slightly convex, perhaps especially so in *C. thomasi*. There is some variation in the shape of the third lobe of m3, but its lingual wall is less oblique than the average condition of modern forms.

There are a number of post-cranial bones in the Tighennif sample but preservation of most of them is imperfect, and precise measurements can seldom be taken (Table 3-4). Still, it is clear that

they are larger than those of living *Camelus*; in particular, all long bones whose length can be measured or reasonably estimated are longer than the modern maxima.

The scapula, humerus, radio-ulna, and carpals are not represented. There are some, mostly incomplete metacarpals (Fig. 8A); those of the Bactrian camel differ from those of the dromedary in being shorter and stouter; those of *C. thomasi* are significantly longer than all of them, but the diaphyses are relatively as robust as in *C. bactrianus*. In contrast, the distal articulation is narrow. TER-1652 is aberrant in its wide distal condyle, but the morphology of this part suggests plastic distortion. Other individuals show condyles which are deeper than wide, closer in this respect to dromedaries.

There is no femur, but there is an almost complete tibia TER-1682 (Fig. 8B) and two incomplete distal epiphyses. This bone is also longer than all modern ones, and distinctly more gracile than those of the Bactrian camel (Fig. 9). The proximal epiphysis differs clearly from both modern species in the narrow, transversely compressed but antero-posteriorly expanded anterior tuberosity (Fig. 8B2); it is much thicker and much less prominent in modern forms.

The single fibula is large and it is in particular wide. Although the distal tibiae are poorly preserved, the lateral facet of the distal cochlea appears to agree with the proportions of the fibula.

The calcanei (Fig. 8D) are large and overall similar to *C. bactrianus*, particularly in their shorter and less constricted tuber and the anterior placement of the sustentaculum; but the fibular trochlea is smaller and less prominent, and the plantar border is broad (except in TER-1665 that may not be fully adult), more like in the dromedary.

There are four astragali, of which only one is well-preserved (Fig. 8C). The proximo-lateral lip ranges from short as in *C. bactrianus*, to long as in *C. dromedarius* (Steiger 1990). Distally, the facet for the navicular (the lateral part of the trochlea) is relatively small (Fig. 10), more similar to *C. bactrianus* than to *C. dromedarius* (in which this facet is more similar in width to the facet for the cuboid).

A single cuboid (Fig. 8E), collected in 1982 (Geraads et al. 1986) is large and high; the astragalar facet is narrow, as in *C. bactrianus*. On the lateral side, the groove for the tendon of the m. peroneus longus is shallower than in modern forms.

The navicular (Fig.8F) is represented by two specimens that are low and wide, with proportions rather similar to *C. bactrianus*. Other known small bones include the trapezoideum and the intermedio-lateral cuneiform, which are similar to extant species.

The two metatarsals whose length can be estimated are, like the metacarpals, much longer than in modern *Camelus* (Fig. 11). The proximal epiphysis is relatively small. The facet for the cuboid is transversally wide, while the facet for the medial cuneiform is shortened. The distal articulation of the metatarsal is narrower than in *C. bactrianus*.

There are four anterior and one posterior phalanges. They are longer than in modern forms, and more massive, being less constricted at mid-length. The condyles appear narrow and seem to have less asymmetric lips than in extant species, where the abaxial lip is longer.

Discussion

The first issue regarding the Tighennif camel sample is that of its species homogeneity. Although size variation of the post-cranial remains can be accommodated within a single species, there are important size differences between, e.g., skull TER-1689 and maxilla TER-1816, or between the mandibles TER-1683/1684 and all other mandibles. However, all mandibles share the same remarkable pachyostosis and related features, and both TER-1689 and TER-1816 share strong styles, broad molars, and anteriorly located palatine foramina. We therefore conclude that the whole collection belongs to a single species, whose important size variation can be explained by sexual dimorphism.

The most remarkable feature of *C. thomasi* is its pachyostosis, which strongly affects the mandible, moderately the skull, but not the postcranials. This tissue distribution is similar to what is found in several megacerine Cervidae (see references in Morales et al. 1993), in which the mandible is also the most affected part, but not to what occurs in the lower Miocene *Lorancameryx* from Spain (Morales et al. 1993), in which it is the anterior limb that underwent the most spectacular pachyostosis. Besides some aquatic forms, in which it is obviously related to the need for increasing density, pachyostosis (defined as deposition of extra bone, by comparison with closely related forms) is rare in mammals and restricted, as far as we know, to a few Cetartiodactyla and *Homo* of the *erectus* group, so that general explanations are unlikely to be valid. The occurrence of pachyostosis in Cervidae, in which large amounts of bone are deposited every year, might be explained as a side-effect of antler formation, but its origin in *C. thomasi* remains obscure. Clearly, the heavy mandible of all camels, compared with similar-sized selenodont Cetartiodactyla, provided

a basis for this hyper-ossification. This pachyostosis might be dependent of environmental conditions and therefore it might be limited to the Tighennif population, but since this is the type locality we include this character in the diagnosis of this species

Some of the other morphological and metric features described above are closer to those of *C. dromedarius*, more of them are closer to *C. bactrianus*, but there are also some major features which unambiguously demonstrate that *C. thomasi* is distinct from both modern species, as listed in the diagnosis. Pending full study of recently collected material from Syria and Ethiopia, critical to the history of Old World Camelidae, a phylogenetic analysis would be premature, but now that *C. thomasi* is satisfactorily characterized, some conclusions regarding the distribution of the species can be drawn.

From the 'Grotte des Rhinocéros' near Casablanca, dated to c. 0.5 Ma, Geraads and Bernoussi (2017) reported some remains that they assigned to this species. Two upper molars OH1-GDR F14-87 do not have strong styles but are broader than in modern forms, as at Tighennif; a m3 E12-26 is broad as well. A virtually complete metacarpal GDR-5271 is about as long as the largest Tighennif bones, and remarkably robust, as several of its measurements even exceed the Tighennif ones. We can assume that these remains represent an advanced form of *C. thomasi*, which further increased the size and robustness of its bones, but positive identification cannot be reached without cranial or mandibular material.

Gautier (1966) reported *C. thomasi* from Northern Sudan, in a site dated to c. 22,000 BP. He estimated, on the basis of field photographs, that the length of some limb-bones was about 1.2-1.4 times longer than in modern forms (compared to one individual of each species). In fact, some of the bones (distal tibia, calcaneum) indicate that this animal was significantly larger than *C. thomasi*. This large size is partly confirmed by a mandible (not figured) whose measurements are slightly above those of modern *Camelus*. Moreover, Gautier's identification was not supported by any morphological feature, and in particular there is no mention of mandibular pachyostosis. Unfortunately, this paper led the way to numerous mentions of *C. thomasi* in the African and Arabian Late Pleistocene to Holocene, giving the deceitful impression that this species was widespread and persisted until historic times. For instance, Grigson (1983) suggested that a very large camel from the late Pleistocene of Israel might represent *C. thomasi*; again, the measurements that she provided are much larger than those of this species (e.g., breadth of distal metapodial condyle = c. 58 mm, vs. 36−52 mm at Tighennif; breadth of proximal metacarpal = c. 90 mm vs. 63−80 mm), and this identification must be rejected. Peters (1998) restudied the material seen by

Gautier, accepting his identification as *C. thomasi*, and concluded that this species was morphologically identical to the domestic dromedary and might be considered its wild ancestor. Later authors accepted and reinforced his proposal (Von den Driesch & Obermaier 2007). However, no morphological or metric comparison with the material from the type-locality of *C. thomasi* had ever been conducted, thus any discussion of the affinities of this species were lacking a sound basis. Our detailed study shows instead that *C. thomasi* differs clearly from both extant forms, rejecting other opinions found in the literature.

Conclusion

The material of *Camelus thomasi* from the type-locality Tighennif is sufficient to satisfactorily define the species, even though several bones remain unknown. Besides perhaps in the Thomas - Oulad Hamida cave complex in Morocco, there is no published convincing evidence of this species elsewhere. The hypothesis that *C. thomasi* was a widespread species from which the modern dromedary derives is not supported by the current morphological evidence.

The history of fossil camels in Afro-Arabia and the Near East remains poorly documented; hopefully, recently collected material from Syria and Ethiopia will shed new light on their evolution.

Acknowledgments

We are grateful to C. Argot and J. Lesur (MNHN), G. Baryshnikov (ZIN), D. Berthet (CCEC), D. Lefèvre and J.-P. Raynal (CNRS), B. Oberholzer and M. Haffner (ZM), P. Schmid (NMBE), J. Studer (MHNG), M. Podestà and G. Bardelli (MSNM), and L. Costeur (NMB) for access to collections, to P. Loubry for the photos of *C. thomasi* in the MNHN, and to Y. Chaïd-Saoudi for photos of the Algiers material. Thanks also to the reviewers, J. Morales and J. van der Made, for their helpful comments.

References

ARAMBOURG C. & HOFFSTETTER R. 1963. — Le gisement de Ternifine. *Archives de l'Institut de Paléontologie Humaine* 32: 1−190.

GAUTIER A. 1966. — *Camelus thomasi* from the Northern Sudan and its bearing on the relationship *C. thomasi – C. bactrianus*. *Journal of Paleontology* 40: 1368–1372.

GERAADS D. 2016. — Pleistocene Carnivora (Mammalia) from Tighennif (Ternifine), Algeria. *Geobios* 49: 445-458.

GERAADS D. & BERNOUSSI R. 2017. — La faune de vertébrés du Pléistocène moyen de la Grotte des Rhinocéros, Casablanca, Maroc : 6 – Hippopotamidae, Suidae and Camelidae, *in* RAYNAL J.-P. & MOHIB A. (eds.), Préhistoire de Casablanca 1 - La Grotte des Rhinocéros *(fouilles 1991 et 1996).* Villes et Sites Archéologiques du Maroc 6: 133−134.

GERAADS D., HUBLIN J-J., JAEGER J.-J., TONG H., SEN S. & TOUBEAU P. 1986. — The Pleistocene Hominid site of Ternifine, Algeria: new results on the environment, age and human industries. *Quaternary Research* 25: 380−386.

GRAY J. E. 1821. — On the natural arrangment of vertebrose animals. *London Medical Repository* 15: 296–310.

GRIGSON C. 1983. — A very large camel from the Upper Pleistocene of the Negev desert. *Journal of Archaeological Science* 10: 311–316.

HARRIS J. M., GERAADS D. & SOLOUNIAS N. 2010. — 41 – Camelidae, *in* Werdelin L. & Sanders W. J. (eds.), *Cenozoic Mammals of Africa*. University of California Press, Berkeley: 815–820.

HUBLIN J.-J. 2001. — Northwestern African Middle Pleistocene hominids and their bearing on the emergence of *Homo sapiens*, *in* Barham L. & Robson-Brown K. (eds.), *Human Roots. Africa and Asia in the Middle Pleistocene*. Western Academic and Specialist Press, Bristol: 99–121.

LHOTE H. 1987. — *Chameau et Dromadaire en Afrique du Nord et au Sahara: Recherches sur leurs Origines.* Office national des approvisionnements et des services agricoles (ONAPSA), Alger, Algeria, 161 pp.

LINNÆUS C. 1758. — *Systema naturæ per regna tria naturæ, secundum classes, ordines, genera, species, cum characteribus, differentiis, synonymis, locis. Tomus I.* Editio decima, reformata. Salvii, Stockholm, 824 pp.

MARTINI P., SCHMID P. & COSTEUR L.J. 2017. — Comparative morphometry of Bactrian camel and Dromedary. *Journal of Mammalian Evolution* doi:10.1007/s10914-017-9386-9.

MARTINÓN-TORRES M., BERMÚDEZ DE CASTRO J.M., GÓMEZ-ROBLES A., ARSUAGA J. L., CARBONELL E., LORDKIPANIDZE D., MANZI G. & MARGVELASHVILI A. 2007. — Dental evidence on the hominin dispersals during the Pleistocene. *Proceedings of the National Academy of Sciences of the USA* 104: 13279–13282.

MORALES J., PICKFORD M. & SORIA D. 1993. — Pachyostosis in a Lower Miocene giraffoid from Spain, *Lorancameryx pachyostoticus* nov. gen. nov. sp. and its bearing on the evolution of bony appendages in artiodactyls. *Geobios* 26: 207–230.

PETERS J. 1998. — *Camelus thomasi* Pomel, 1893, a possible ancestor of the one-humped camel ?

Zeitschrift für Säugetierkunde 63: 372–376.

POMEL A. 1886. — Station préhistorique de Ternifine (Mascara). *Comptes rendus de l'association française pour l'avancement des Sciences* 14: 504–505.

POMEL A. 1893. — *Paléontologie - Monographies - Caméliens et Cervidés.* Carte géologique de l'Algérie, Alger, Algeria, 50 pp.

SAHNOUNI M. & VAN DER MADE J. 2009. — The Oldowan in North Africa within a biochronological framework, in Schick K. & Toth N. (eds.), *The cutting edge: new approaches to the archaeology of human origins.* Stone Age Institute Press, Gosport: 179–210.

STEIGER C. 1990. — *Vergleichend morphologische Untersuchungen an Einzelknochen des postkranialen Skeletts der Altweltkamele.* Dissert. Ludwig-Maximilians Univ. München, 106 pp.

VON DEN DRIESCH A. & OBERMAIER H. 2007. — *The hunt for wild dromedaries during the 3rd and 2nd millennia BC on the United Arab Emirates coast. Camel bone finds from the excavations at Al Sufouh 2, Dubai, UAE.* Skeletal Series and their Socio-economic Context. J. Grupe and J. Peters.

WOODWARD A.S. 1921. — A New Cave Man from Rhodesia, South Africa. *Nature* 108: 371–372.

Figures

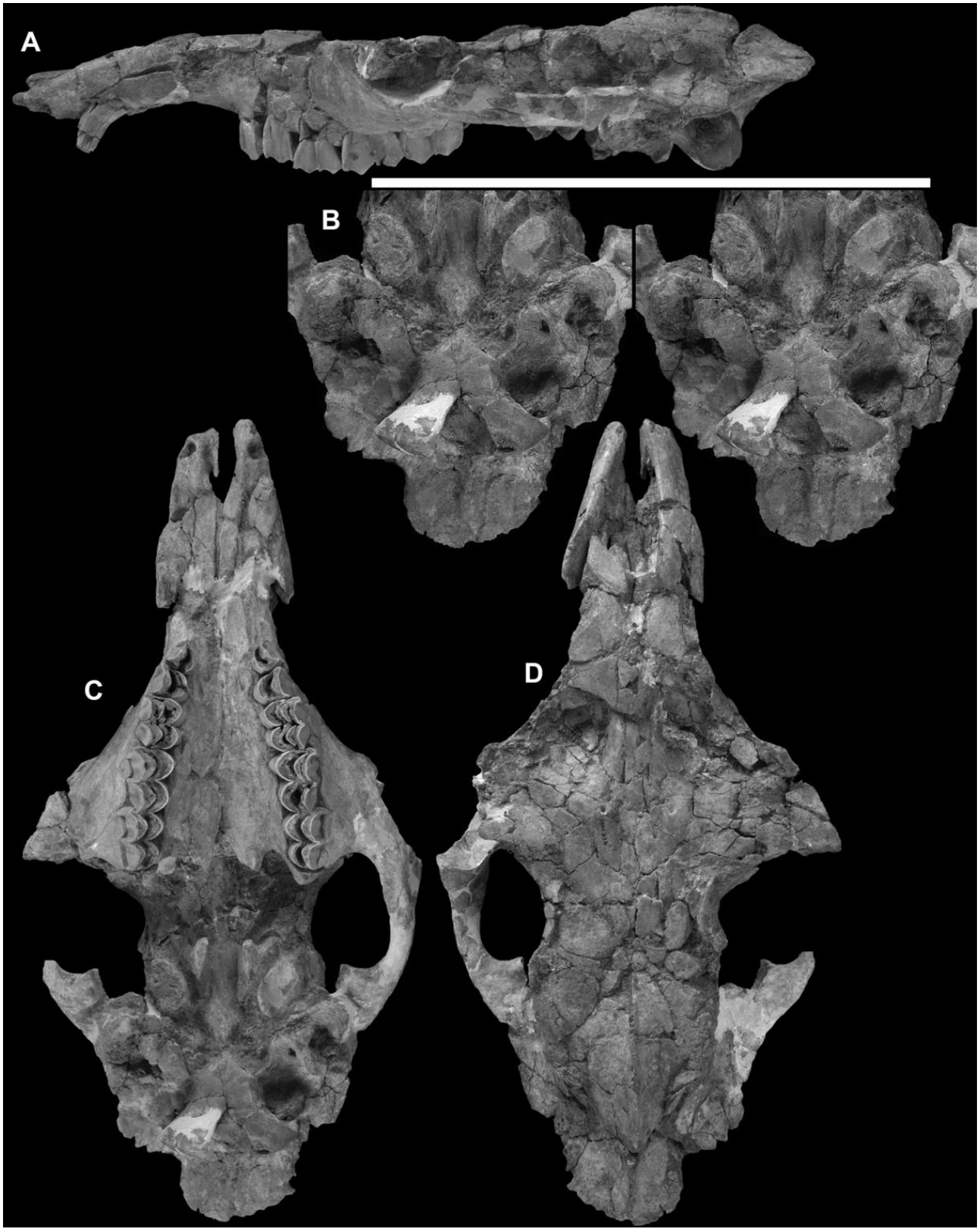

Figure 1. *Camelus thomasi*, Tighennif, cranium MNHN-TER-1689. A: left lateral view, B: ventral view of the cranial basis (stereo), C: ventral view, D: dorsal view. Scale bar = 40 cm.

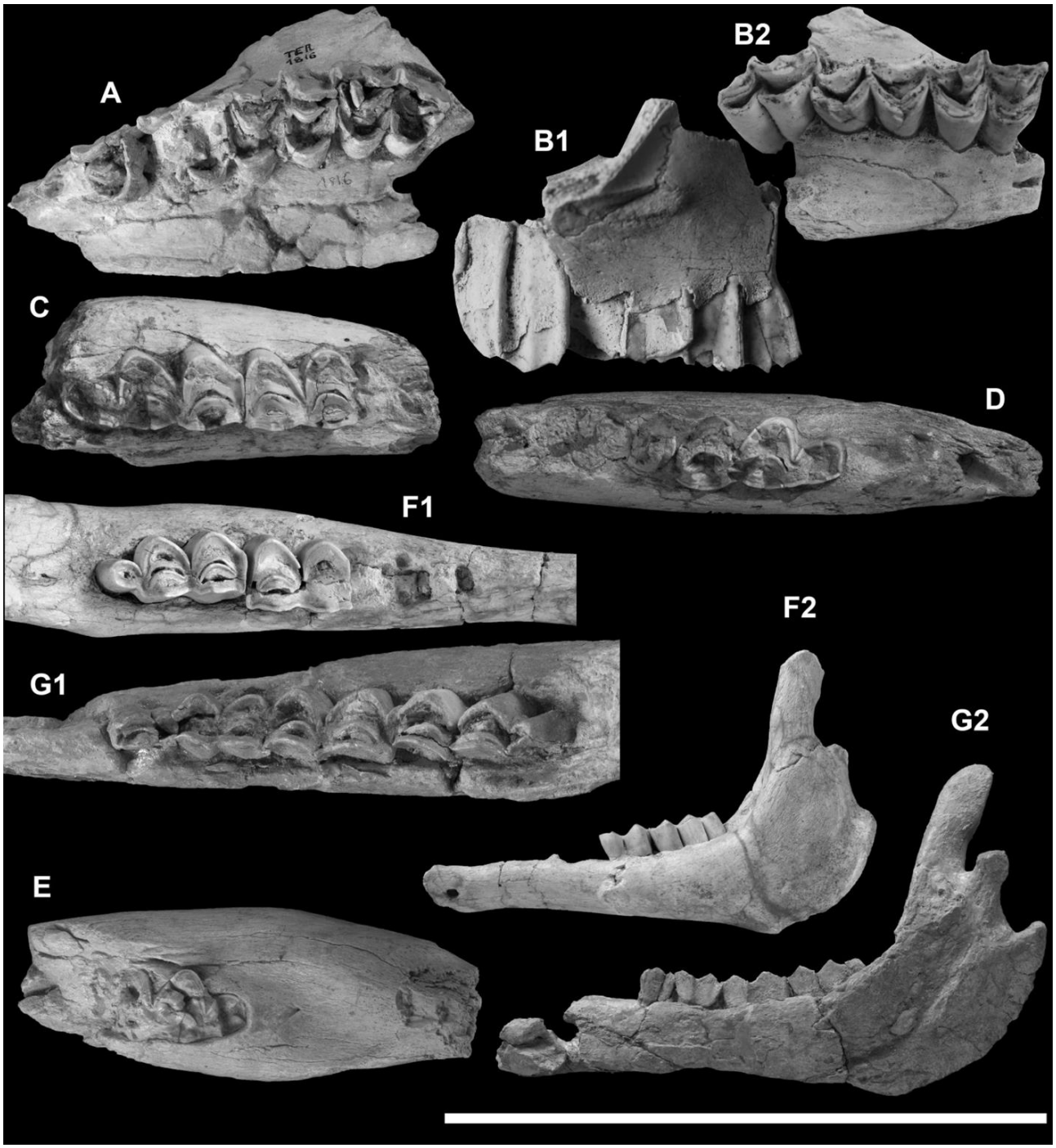

Figure 2. *Camelus thomasi*, Tighennif. A: maxilla TER-1816, occlusal view. B: maxilla with M1−M2 and tentatively associated M3, holotype n°7236001 (B1: right lateral view, B2: occlusal view). C: partial mandible 1900-27, dorsal view. D: partial mandible TER-1688, dorsal view. E: partial mandible TER-1686, dorsal view. F: mandible TER-1683 (F1: dorsal view, F2: lateral view). G: mandible TER1685 (G1: dorsal view, G2: medial view). Fig. B in Musée de Géologie, Alger, all others in MNHN. Scale bar = 40 cm for Figs. F2 and G2, 20 cm for all others.

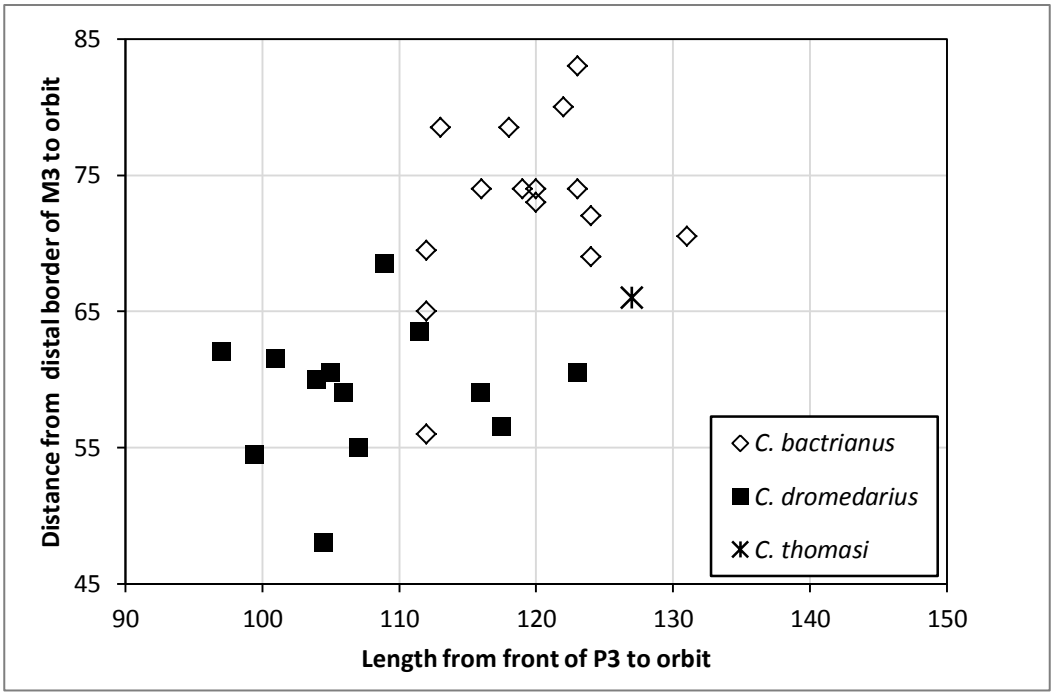

Figure 3. Bivariate plot of cranial measurements showing the position of the orbit (C24 vs. C14 of Martini et al. 2017).

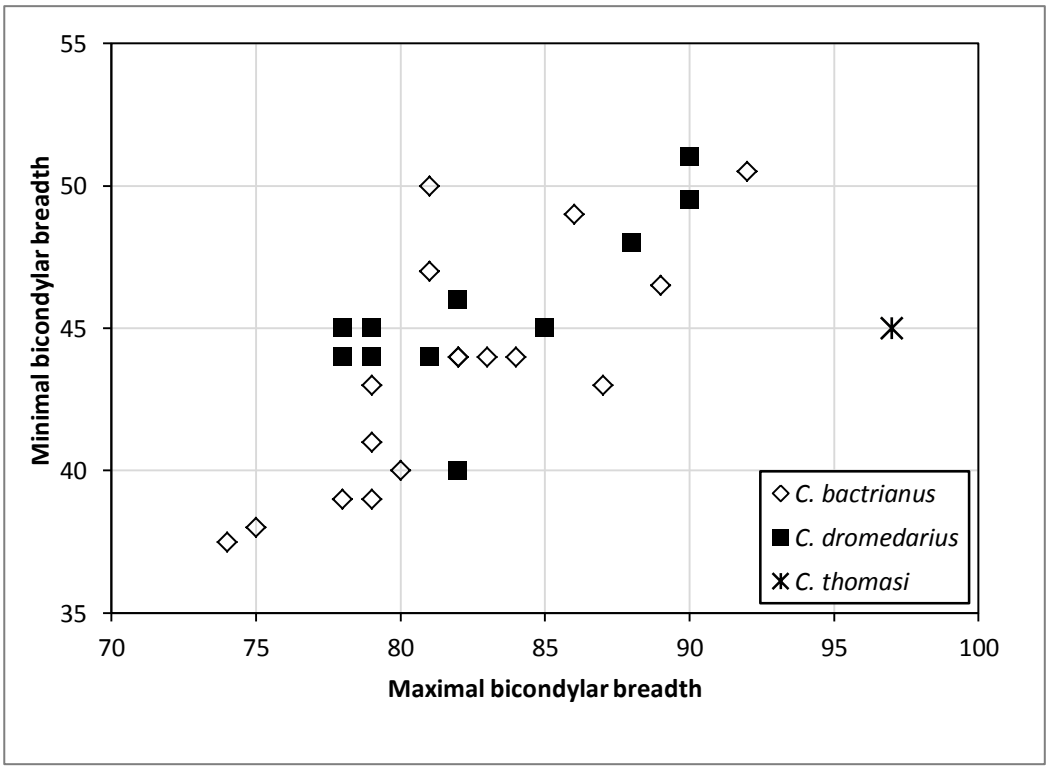

Figure 4. Bivariate plot of measurements of occipital condyles (C74 vs. C73 of Martini et al. 2017).

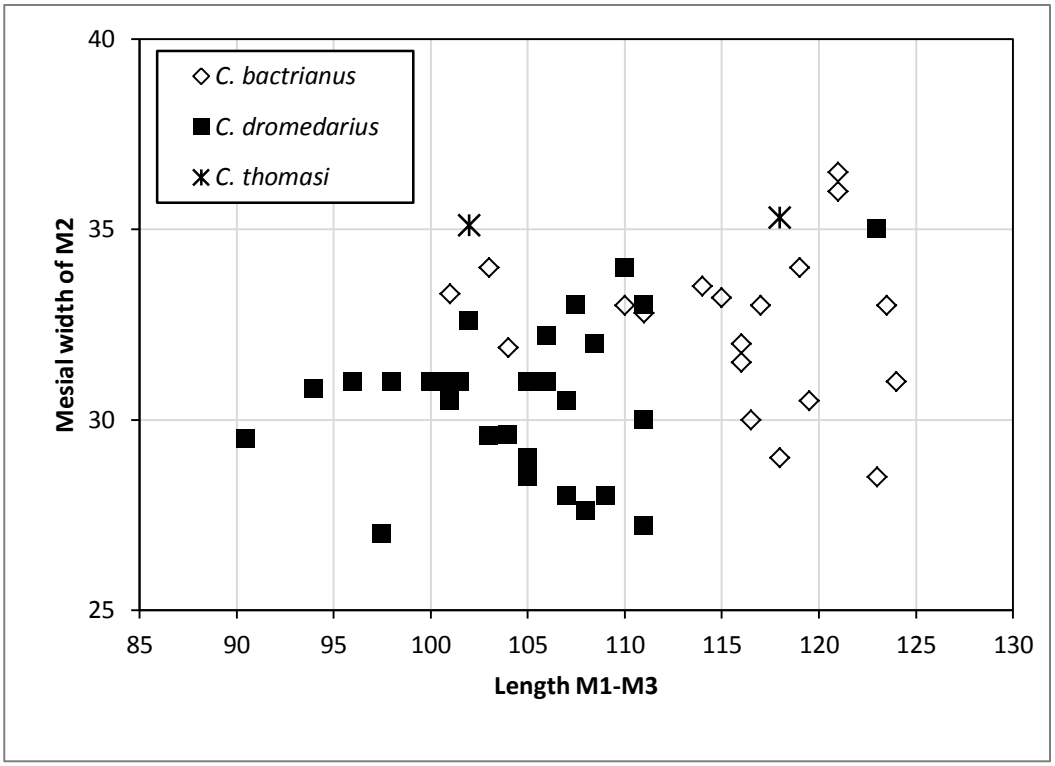

Figure 5. Bivariate plot of M2 mesial width vs. length of molar row (C34 vs. Ds24 of Martini et al. 2017).

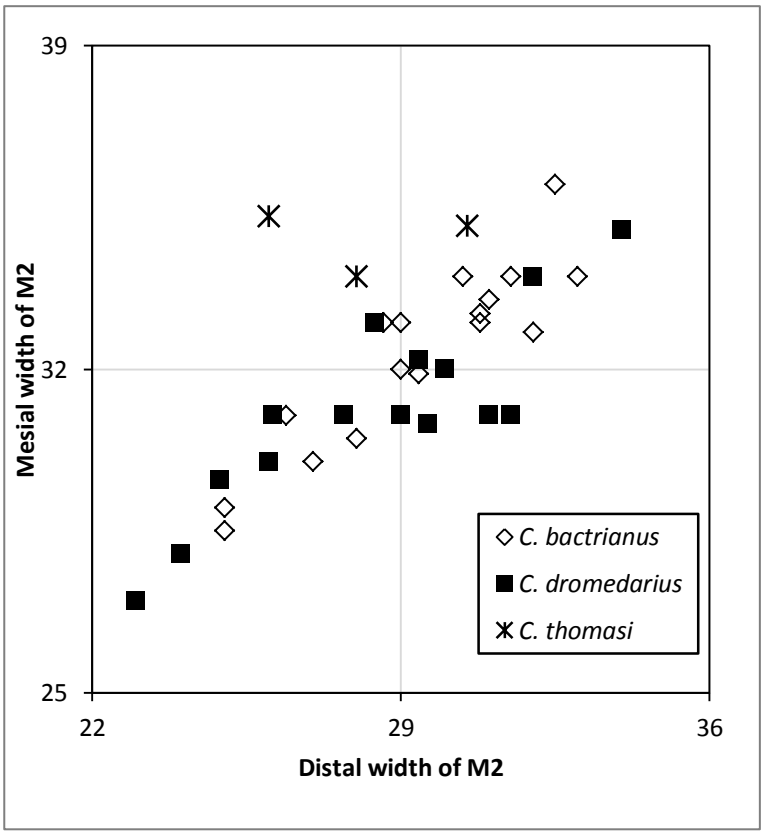

Figure 6. Bivariate plot of mesial vs. distal widths of M2 (Ds24 vs. Ds25 of Martini et al. 2017).

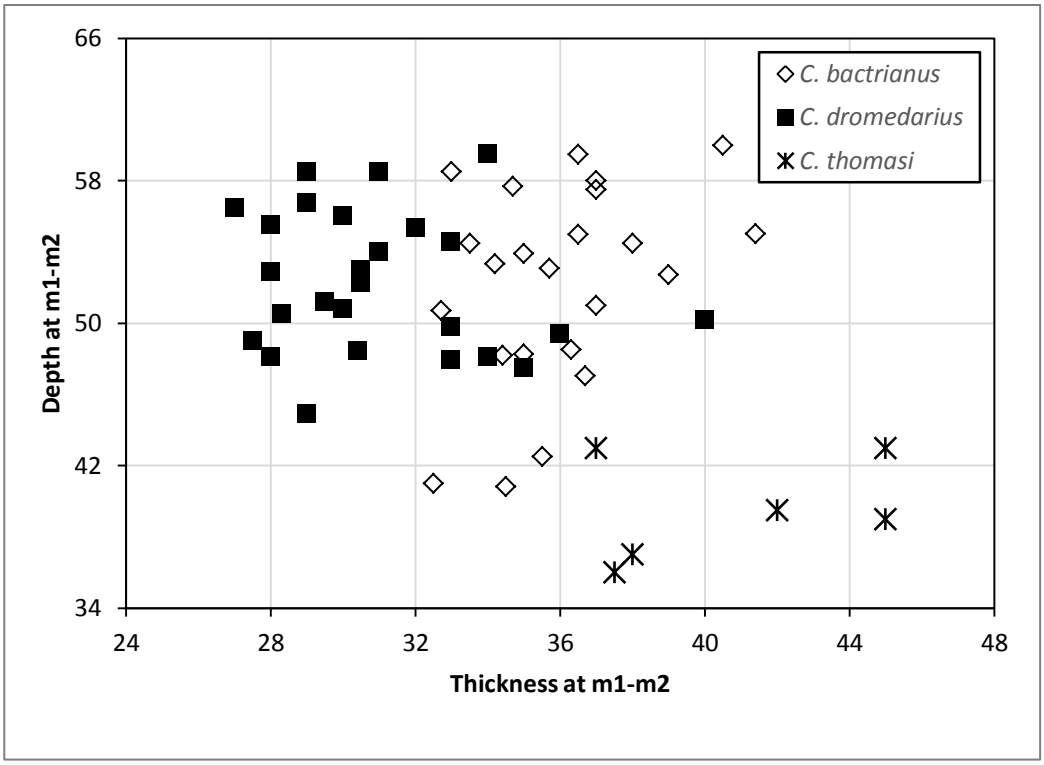

Figure 7. Bivariate plot of depth vs. thickness of the mandibular corpus (M20 vs. M15 of Martini et al. 2017).

Figure 8 (Next page). *Camelus thomasi*, Tighennif. A: metapodials; from left to right metatarsals TER-1664, TER-1690, and metacarpals TER-1648, TER-1681, and TER-1652. B: right tibia TER-1682 (B1: lateral view, B2: proximal view). C: left astragalus TER-1670 (C1: anterior view, C2: plantar view, C3: medial view, C4: distal view). D: left calcaneus TER-1666 (D1: anterior view, D2: plantar view, D3: medial view). E: left cuboid 1982-5-60 (E1: proximal view, E2: distal view, E3: medial view). F: right navicular TER-1679 (F1: proximal view, F2: distal view, F3: lateral view). Scale bar = 40 cm for Figs. A and B, 20 cm for all others.

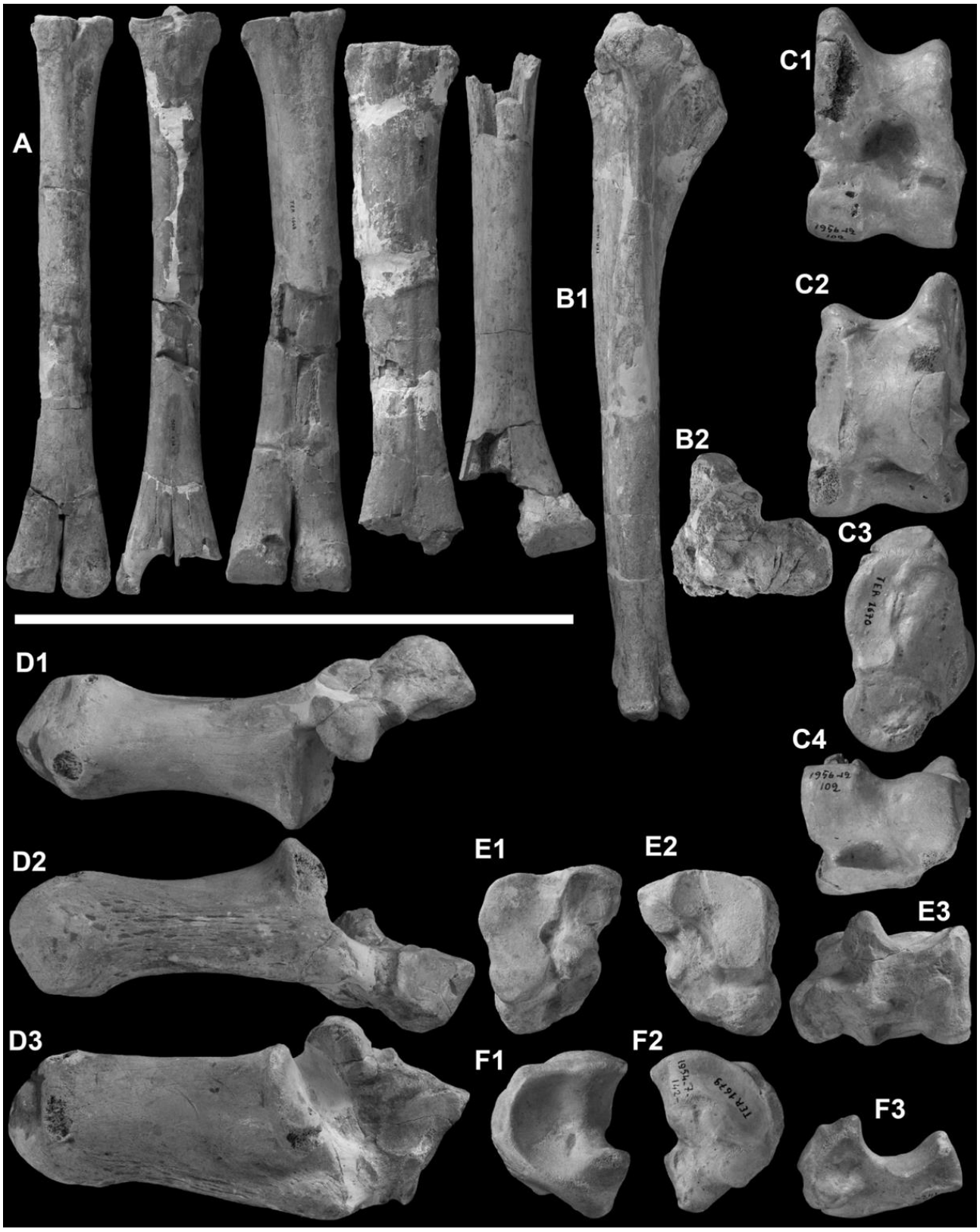

Figure 8. (Caption on previous page)

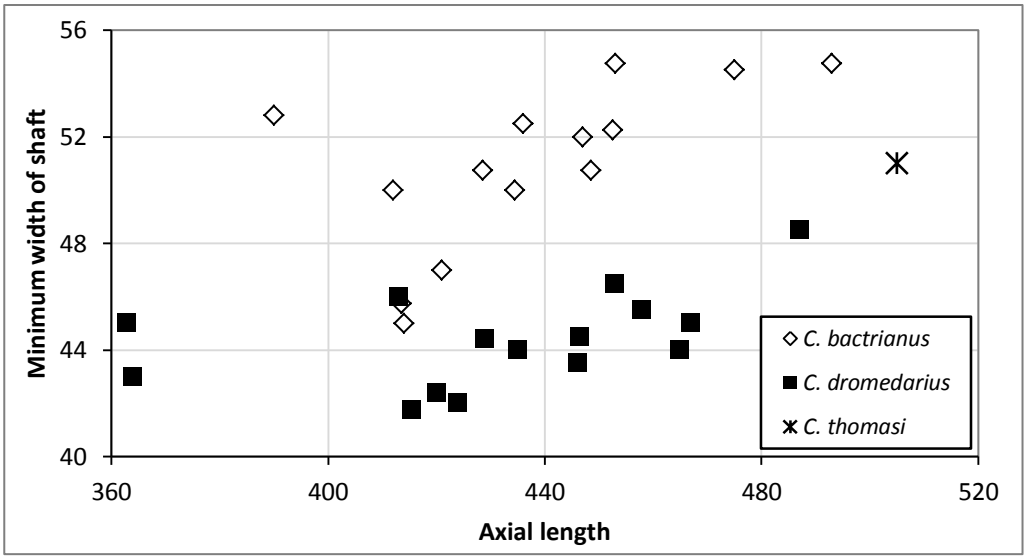

Figure 9. Bivariate plot of width of shaft vs. length of the tibia (Ti13 vs. Ti3 of Martini et al. 2017).

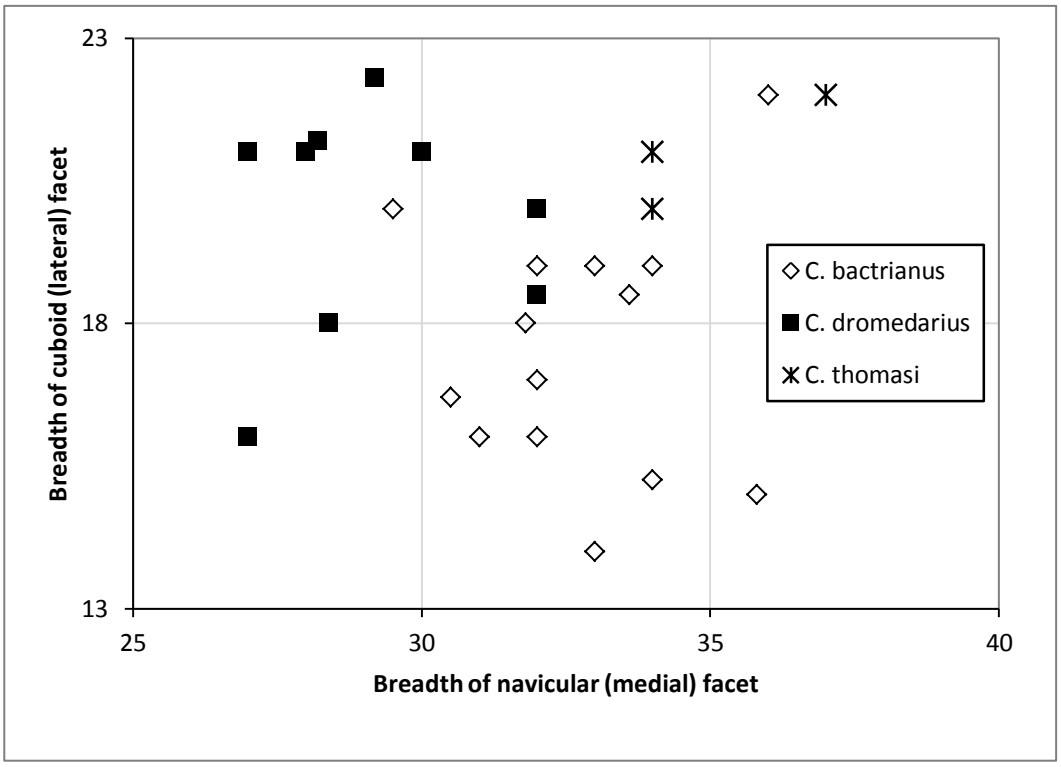

Figure 10. Bivariate plot of the widths of the cuboid facet vs. navicular facet of the astragalus (Ta15 vs. Ta14 of Martini et al. 2017).

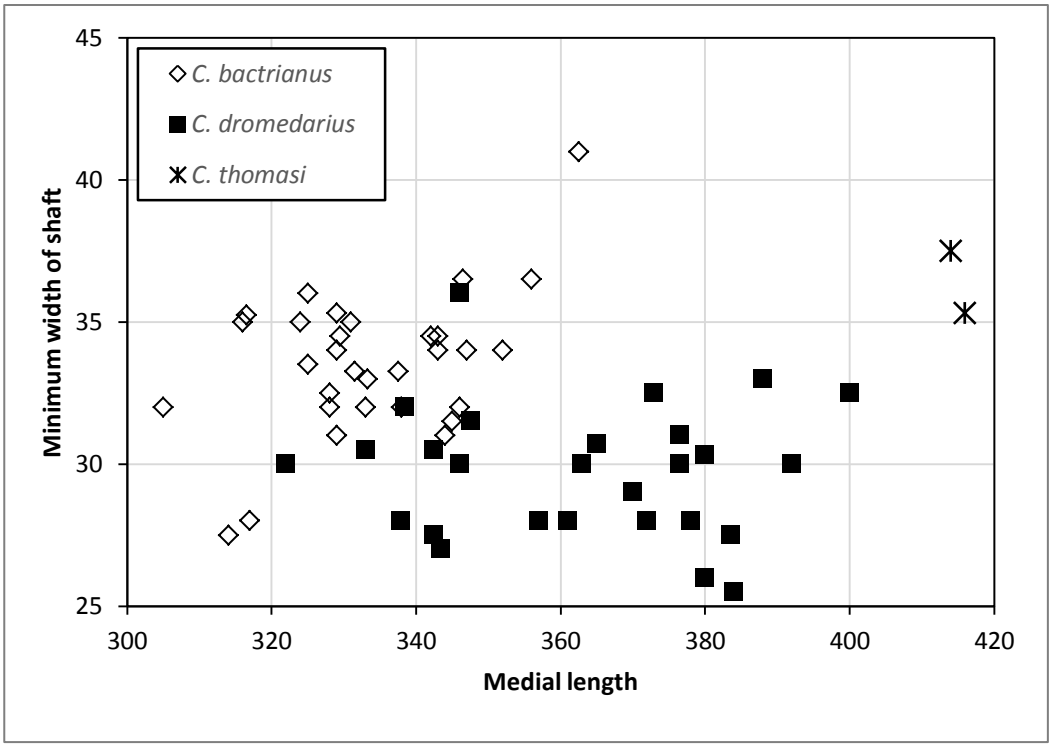

Figure 11. Figure 8. Bivariate plot of width of shaft vs. length of the metatarsus (Mp12 vs. Mp1 of Martini et al. 2017).

Tables

Table 1. List of specimens of *C. thomasi* described in this study.

Specimen	Side	Element	Preservation
OH F14.87		maxilla	fragment, with M1-M2
TER-1647	sin	metacarpale	proximal fragment
TER-1648	dex	metacarpale	complete
TER-1649	sin	tibia	distal fragment
TER-1650	dex	tibia	distal fragment
TER-1651	dex	metatarsale	distal fragment
TER-1652		metacarpale	diaphysis and left condyle
TER-1653		metacarpale	distal fragment
TER-1654		metacarpale	distal fragment
TER-1655	sin	metatarsale	proximal fragment
TER-1656	dex	metatarsale	proximal fragment
TER-1657	dex	metatarsale	proximal fragment
TER-1658	dex	metatarsale	proximal fragment
TER-1659		metacarpale	distal condyle
TER-1660	sin	fibula	lateral malleolus
TER-1661		metacarpale	proximal fragment
TER-1662	dex	metatarsale	proximal fragment with diaphysis
TER-1663	sin	metatarsale	proximal fragment with diaphysis
TER-1664	dex	metatarsale	complete
TER-1665	dex	calcaneus	
TER-1666	sin	calcaneus	
TER-1667	dex	calcaneus	
TER-1668	sin	calcaneus	
TER-1669	dex	astragalus	
TER-1670	dex	astragalus	
TER-1671	sin	astragalus	
TER-1672	dex	astragalus	
TER-1673		phalanx proximal posterior	complete
TER-1674		phalanx proximal anterior	complete
TER-1675		phalanx proximal anterior	complete
TER-1676		phalanx proximal anterior	complete
TER-1677		phalanx proximal anterior	complete
TER-1678	dex	naviculare	
TER-1679	dex	naviculare	
TER-1680	dex	ectomesocuneiforme	
TER-1681	sin	metacarpale	complete but missing distal condyles
TER-1682	dex	tibia	complete with damaged distal cochlea
TER-1683	sin	hemimandibula	with complete ramus, m2-m3, and alveoles of p4-m1; likely the same individuals as TER-1684
TER-1684	dex	hemimandibula	with damaged ramus, m2-m3, broken at the level of the alveoles of m1; likely the same individuals as TER-1683
TER-1685	dex	hemimandibula	with complete ramus and p4-m3
TER-1686	dex	hemimandibula	fragment, with fragment of ramus and broken m3
TER-1687	sin	hemimandibula	fragment, with highly damaged m3
TER-1688	dex	hemimandibula	fragment, with highly damaged m2-m3
TER-1689		cranium	complete, showing strong dorsoventral compression, with C sin and P3-M3 from both sides
TER-1690	sin	metatarsale	complete with damaged distal condyles
TER-1816	sin	maxilla	with damaged P3-M3
TER-1900-27	sin	hemimandibula	fragment, including m2-m3 and roots of m1
Tig82-560	sin	cuboideum	
(Unlabeled)		trapezoideum	

Table 2. Cranial measurements of *Camelus thomasi*. Abbreviations refer to the measurements in Martini et al. (2017). Data in mm; ~ indicates approximate measurements; * indicates remarks in the text.

	CRANIUM	TER-1689 sin	TER-1816 sin
C1	Maximal length (prosthion to akrokranion)	575 * ~	
C5	Occipital height (akrokranion to opisthion)	70 ~	
C6	Length of foramen magnum (opisthion to basion)	37 ~	
C8	Basicranial length (basion to staphilion)	190 ~	
C9	Basal length (basion to prosthion)	490 ~	
C10	Palatal length (staphilion to prosthion)	305 ~	
C11	Shorter palatal length (staphilion to intermaxillare)	243 ~	
C12	Lateral postorbital length (orbita to akrokranion)	295 ~	
C13	Lateral preorbital length (orbita to prosthion)	272 ~	
C14	Cheek length (predentale to orbita)	127	111 ~
C15	Infraorbital length (infraorbital foramen to orbita)	70	65 ~
C18	Orbital length (maximal horizontal diameter)	77 ~	
C22	Distance from zygomatic process of temporal to orbita	24	
C23	Transversal thickness of zygomatic arch	12	
C24	Suborbital height (orbita to M3 distal)	66	55 ~
C25	Position of palatine foramina (from staphylion)	107 ~	
C26	Position of incisive (prosthion to incisive, rostral)	23	
C27	Position of canine (prosthion to canine, rostral)	58	
C28	Position of P1 (prosthion to P1, rostral)	106	
C29	Position of cheek tooth (prosthion to P3, rostral)	168	
C30	Position of M1 (prosthion to M1, rostral buccal)	215	
C31	Postdental position (prosthion to M3 distal	330 ~	
C32	Oral length (prosthion to uranion)	343 ~	
C33	Cheek tooth length (P3-M3, included; buccal side)	161	140.5
C34	Molar row length (M1-M3, included; buccal side)	114	102
C35	Basidental length (basion-P3, rostral)	325 ~	
C45	Maximal diameter of condyle	60	
C46	Breadth of glenoid fossa (maximal)	72 ~	
C51	Breadth of nasal opening (between nasointermaxillares)	50 ~	
C52	Breadth between infraorbital foramina (lateral border)	101	
C54	Minimal biorbital breadth (between medial borders)	225 ~	
C56	Breadth of postorbital constriction (minimal)	120	
C57	Breadth of the braincase (maximal)	131	
C58	Breadth between squamotemporal foramina	121	
C59	Breadth between incisors (rostral)	50	
C60	Breadth between canines (rostral)	59	
C62	Breadth between P3's (rostral)	60	52 ~
C63	Breadth between M1's (rostral, buccal side)	117	116 ~
C64	Breadth between postdentales (M3 distal)	133	112 ~
C73	Maximal bicondylar breadth	97	
C74	Minimal bicondylar breadth	45	
C75	Breadth of foramen magnum (between condyles)	35	

	MANDIBULA	TER-1683 sin	TER-1684 dex	TER-1685 dex	TER-1686 dex	TER-1687 sin	TER-1688 dex	TER-1900-27 sin
M7	Length from p4 to m3 distal	126		161				
M11	Position of caudal mental foramen: from p4 mesial to caudal mental foramen	58 ~						
M12	Length from p4 mesial to angular process	220 ~		275 ~				
M13	Length from m3 distal to angular process	99		117				
M14	Length from m3 distal to condylar process	100 ~		121				
M15	Thickness of the corpus measured between m1 and m2	35.5	35	40 ~			34 ~	43
M16	Thickness of the corpus measured between m2 and m3	41	42	51	51 ~	48 ~	39	48 ~
M17	Breadth of the condylus			39				
M19	Height of the corpus mesial to p4	32		48				
M20	Height of the corpus between m1 and m2	37	36	39.5		39	43	43
M21	Height of the corpus distal to m3	65	65	72	85 ~	78 ~	74 ~	
M22	Height of the ramus from coronoid process to ventral border	189	191	230 ~				
M23	Height of the ramus from rostral notch to ventral border	127 ~	136	160				
M24	Height of the ramus from condylar process to ventral border			181				
M25	Height of the ramus from caudal notch to ventral border	102		138				

	UPPER DENTITION	TER-1689 sin	OH F14.87	TER-1816
Ds1	Alveolar length of I3	17		
Ds2	Alveolar breadth of I3	15		
Ds3	Alveolar length of C	35		
Ds4	Alveolar breadth of C	21		
Ds7	Alveolar length of P3	20		16
Ds8	Alveolar breadth of P3	20		
Ds9	Occlusal length of P3	20		18
Ds10	Occlusal breadth of P3	13		
Ds11	Alveolar length of P4	22		21
Ds12	Alveolar breadth of P4	28		25
Ds13	Occlusal length of P4	22		20
Ds14	Occlusal breadth of P4	17		21
Ds15	Alveolar length of M1	26	29	24
Ds16	Alveolar breadth of mesial lobe of M1	33	35 ~	29 ~
Ds17	Alveolar breadth of distal lobe of M1	31	33	33
Ds18	Occlusal length of M1	36	36 ~	30
Ds19	Occlusal length of mesial lobe of M1	18	18 ~	
Ds20	Occlusal length of distal lobe of M1	19	18	
Ds21	Occlusal breadth of mesial lobe of M1	22.5		
Ds22	Occlusal breadth of distal lobe of M1	20	24	28
Ds23	Alveolar length of M2	37	33	33
Ds24	Alveolar breadth of mesial lobe of M2	34.5	34	35
Ds25	Alveolar breadth of distal lobe of M2	26	28	30.5
Ds26	Occlusal length of M2	47	38	36
Ds27	Occlusal length of mesial lobe of M2	27	20	20
Ds28	Occlusal length of distal lobe of M2	23.5	20 ~	21
Ds29	Occlusal breadth of mesial lobe of M2	23	24	25
Ds30	Occlusal breadth of distal lobe of M2	18	19	22
Ds31	Alveolar length of M3	44		40
Ds32	Alveolar breadth of mesial lobe of M3	26		32
Ds33	Alveolar breadth of distal lobe of M3	22		29
Ds34	Occlusal length of M3	43		43
Ds35	Occlusal length of mesial lobe of M3	22 ~		23
Ds36	Occlusal length of distal lobe of M3	22		23
Ds37	Occlusal breadth of mesial lobe of M3	19		24
Ds38	Occlusal breadth of distal lobe of M3	14		19.5

	LOWER DENTITION	TER-1683 sin	TER-1684 dex	TER-1685 dex	TER-1686 dex	TER-1687 sin	TER-1688 dex	TER-1900-27 sin
Di8	Alveolar length of P4			24				
Di9	Alveolar breadth of P4			15				
Di10	Occlusal length of P4			22				
Di11	Occlusal breadth of P4			13				
Di12	Alveolar length of M1			30				
Di13	Alveolar breadth of mesial lobe of M1			23				
Di14	Alveolar breadth of distal lobe of M1			23				
Di15	Occlusal length of M1			34				
Di16	Occlusal length of mesial lobe of M1			15				
Di17	Occlusal length of distal lobe of M1			19				
Di18	Occlusal breadth of mesial lobe of M1			18				
Di19	Occlusal breadth of distal lobe of M1			20				
Di20	Alveolar length of M2	28	30	40				34
Di21	Alveolar breadth of mesial lobe of M2	24	24	26				27
Di22	Alveolar breadth of distal lobe of M2	25	25	25.5		26		27.5
Di23	Occlusal length of M2	35	35	44				37
Di24	Occlusal length of mesial lobe of M2	17	16	19.5				16
Di25	Occlusal length of distal lobe of M2	18.5	18.5	25				19
Di26	Occlusal breadth of mesial lobe of M2	24	25	20				25 ~
Di27	Occlusal breadth of distal lobe of M2	24	24.5	21				25
Di28	Alveolar length of M3	46	48	58	51 ~	55	52 ~	57
Di29	Alveolar breadth of mesial lobe of M3	24	24.5	23	27	25 ~	26 ~	28 ~
Di30	Alveolar breadth of central lobe of M3	23	23	24	26.5	24	26	25
Di31	Alveolar breadth of distal lobe of M3	11.5	13	14	14	14	15	13.5
Di32	Occlusal length of M3	45	46	48				57
Di33	Occlusal length of mesial lobe of M3	18	18	20				20
Di34	Occlusal length of central lobe of M3	17	18	20				
Di35	Occlusal length of distal lobe of M3	11.5	11	11				
Di36	Occlusal breadth of mesial lobe of M3	21	20.5	18				24 ~
Di37	Occlusal breadth of central lobe of M3	21	20.5	17				
Di38	Occlusal breadth of distal lobe of M3	10	10	8				

Table 3. Measurements of long bones, metapods and phalanges in *Camelus thomasi*. Abbreviations refer to the measurements in Martini et al. (2017). Data in mm; ~ indicates approximate measurements; § indicates measurements that might be either mesial or lateral.

	TIBIA	**TER-1649 sin**	**TER-1650 dex**	**TER-1682 dex**						
ti2	Length axial (from epicondylar eminence)			535 ~						
ti3	Length lateral (condyle to lateral fossa)			500 ~						
ti5	Depth of the lateral condyle			51						
ti8	Breadth of the lateral condyle			62 ~						
ti12	Minimal depth of the diaphysis	35		33						
ti13	Minimal breadth of the diaphysis			51						
ti14	Depth of the medial fossa of the cochlea (maximal)	45 ~	41 ~							
ti15	Depth of the axial fossa of the cochlea (maximal)	46 ~		43 ~						
ti16	Depth of the lateral fossa of the cochlea	41 ~		46 ~						
ti17	Dorsal breadth of the cochlea	87	88							
ti18	Palmar breadth of the cochlea	97.5								
ti19	Breadth of the medial fossa of the cochlea	29 ~	27 ~							
ti20	Breadth of the axial fossa of the cochlea	25 ~	26 ~							
ti21	Breadth of the lateral fossa of the cochlea	20 ~		20						
	METACARPALE	**TER-1647 sin**	**TER-1648 dex**	**TER-1652**	**TER-1653**	**TER-1654**	**TER-1659**	**TER-1661**	**TER-1681 sin**	
mp1	Length on the medial side		420 ~							
mp2	Length on the lateral side		400 ~							
mp3	Medial depth of the proximal articulation	62	51 ~					56	54	
mp4	Lateral depth of the proximal articulation							53	50 ~	
mp5	Breadth of the proximal articulation		78 ~					79	85	
mp6	Breadth of the medial proximal facet	41						34		
mp7	Breadth of the lateral proximal facet							31 ~		
mp8	Depth of the proximal articulation							52	50 ~	
mp9	Depth of the medial proximal facet	56						50		
mp10	Maximal depth of the diaphysis		41	38						
mp11	Minimal depth of the diaphysis		26	23	28	24			32	
mp12	Minimal breadth of the diaphysis		47	41					48	
mp13	Depth of the medial condyle			41 * §	44 ~	44	56 §			
mp14	Depth of the lateral condyle		49	41 * §		44	56 §			
mp15	Breadth of the medial condyle		42 ~	55 * §	42	44	52 §			
mp16	Breadth of the lateral condyle		44	55 * §	44	44	52 §			
mp17	Maximal distal breadth		89		99	91.5				
	METATARSALE	**TER-1651 dex**	**TER-1655 sin**	**TER-1656 dex**	**TER-1657 dex**	**TER-1658 dex**	**TER-1662 dex**	**TER-1663 sin**	**TER-1664 dex**	**TER-1690 sin**
mp1	Length on the medial side								420 ~	415 ~
mp2	Length on the lateral side								410 ~	
mp18	Length of the triangular process			25.5						27
mp19	Breadth of the triangular process		29 ~	31	26					32
mp20	Depth of the medioplantar proximal facet		18 ~	23	20	18.5	16			19
mp21	Depth of the medial proximal facet		36	33	34	39	33		38 ~	33
mp22	Depth of the lateral proximal facet		44	45	42	46	43			43
mp5	Breadth of the proximal articulation		68	71	70	80	67	74	63 ~	67
mp6	Breadth of the medial proximal facet		25	23.5	22 ~	30.5	27.5		25 ~	25
mp7	Breadth of the lateral proximal facet		27	27 ~	26 ~	29 ~	28			24
mp8	Depth of the proximal articulation		57.5	55	52	59	51		56.5	54
mp10	Maximal depth of the diaphysis						41	43.5	42	40
mp11	Minimal depth of the diaphysis	22.5							26	26.5
mp12	Minimal breadth of the diaphysis						35	37 ~	36	35
mp13	Depth of the medial condyle	40								
mp14	Depth of the lateral condyle	41.5							38 ~	
mp15	Breadth of the medial condyle	40								
mp16	Breadth of the lateral condyle	40							36 ~	
mp17	Maximal distal breadth	89							77 ~	
	PHALANX PROXIMAL ANTERIOR	**TER-1674**	**TER-1675**	**TER-1676**	**TER-1677**					
pp1	Length of the axial side	122	126	120	126					
pp2	Length of the abaxial side	120		117	123					
pp3	Proximal depth (articular surface)	43	43 ~	40 ~	43					
pp4	Proximal breath (articular surface)	53	51 ~	52	54					
pp5	Depth of the diaphysis	22.5	22.5	22.5	23					
pp6	Breadth of the diaphysis	27	27	29	29					
pp7	Depth of the condyle	31.5	31.5	31	35					
pp8	Breadth of the condyle	46 ~	46 ~	45 ~	44 ~					
pp9	Length of the axial lip of the condyle	40 ~	40 ~	38 ~	40.5 ~					
pp10	Length of the abaxial lip of the condyle	42 ~	39 ~	40 ~	42 ~					
	PHALANX PROXIMAL POSTERIOR	**TER-1673**								
pp1	Length of the axial side	103								
pp2	Length of the abaxial side	103								
pp3	Proximal depth (articular surface)	33								
pp4	Proximal breath (articular surface)	41								
pp5	Depth of the diaphysis	17								
pp6	Breadth of the diaphysis	21.5								
pp7	Depth of the condyle	24								
pp8	Breadth of the condyle	34.5 ~								
pp9	Length of the axial lip of the condyle	32 ~								
pp10	Length of the abaxial lip of the condyle	33 ~								

Table 4. Measurements of short bones (carpals and tarsals) in *Camelus thomasi*. Abbreviations refer to the measurements in Martini et al. (2017). Data in mm; ~ indicates approximate measurements.

	TRAPEZOIDEUM	**Unlabeled**			
Kt1	Maximal height	19			
Kt2	Maximal diagonal	25			
Kt3	Maximal diameter of the distal facet	24			
Kt4	Breadth of the proximal facet	16			
Kt5	Minimal diameter of the distal facet	13			
	FIBULA	**TER-1660 sin**			
fi1	Height dorsal	39			
fi2	Height in the middle (height of the process)	36			
fi4	Maximal depth	52 ~			
fi5	Depth of the proximal facet	43.5			
fi6	Depth of the distal facet	38 ~			
fi7	Dorsal breadth of the proximal side	32			
fi8	Plantar breadth of the proximal facet	25			
fi9	Breadth of the distal facet	25			
fi10	Depth of the medial (astragalar) facet	41 ~			
	TALUS	**TER-1669 dex**	**TER-1670 dex**	**TER-1671 sin**	**TER-1672 dex**
Ta1	Height of the lateral side	90	84		82 ~
Ta2	Height axial	67	64.5	65	65
Ta3	Height of the medial side	80	76	76.5	77
Ta4	Proximal depth of the lateral side	36	34		36
Ta5	Distal depth of the lateral side	31	29		25
Ta6	Middle depth of the lateral side	43	42		41 ~
Ta7	Proximal breadth	51	48		49
Ta8	Breadth of the calcaneal surface	36 ~	35	34	32 ~
Ta9	Breadth at the lateral (calcaneal) process	61	59	58	61 ~
Ta10	Distal breadth	58	53	56 ~	57
Ta11	Greater maximal diameter (dorsolateral-distomedial)	100	98		96
Ta12	Lesser maximal diameter (dorsomedial-distolateral)	90	85	87 ~	87
Ta13	Minimal depth of the proximal trochlea (groove)	25.5	25	23	24.5
Ta14	Breadth of the medial part of the distal trochlea	37	34	34	
Ta15	Breadth of the lateral part of the distal trochlea	22	20	21 ~	
Ta16	Medial depth of the distal trochlea	30	32	28.5	29
Ta17	Axial depth of the distal trochlea (groove)	22	21.5	21	19
Ta18	Lateral depth of the distal trochlea	30	29		25
Ta19	Height of the calcalneal surface	60 ~	54		53 ~
	CALCANEUS	**TER-1665 dex**	**TER-1666 sin**	**TER-1667 dex**	**TER-1668 sin**
Tc1	Maximal height (greatest length)		170	170 ~	162
Tc2	Depth of the tubercle		52 ~		46.5
Tc3	Maximal breadth of the tubercle		47		46.5
Tc4	Minimal breadth of the tubercle	24	31	31	26
Tc5	Depth medial (plantar border to substentaculum)	72	75		72
Tc6	Breadth of the substentaculum	50	50.5	52.5	49
Tc7	Medial distal height	80	83	85	77
Tc8	Depth lateral (plantar border to fibular trochlea)	75	75		72
Tc9	Height of the fibular trochlea	37	35	39	33
Tc10	Breadth of the fibular trochlea	21	21	25	20
Tc11	Distal lateral height (fibular trochlea to distal facet)	65	64	65	59
Tc12	Breadth of the plantar border	22	26		25
Tc13	Height of the distal (cuboid) facet	48.5	48	52	47
Tc14	Breadth of the distal (cuboid) facet	24.5	26	30	26 ~
	CUBOIDEUM	**Tig82-560 sin**			
Tq1	Dorsal height	41.5			
Tq2	Medial height (proximal process to centrodistal medial facet)	37 ~			
Tq3	Plantar diagonal (proximal process to plantar tuberosity)	56			
Tq4	Proximal depth (proximal dorsal border to plantar tuberosity)	74			
Tq5	Distal depth (distal dorsal border to plantar tuberosity)	65			
Tq6	Lateral depth (proximal dorsolateral border to plantar tuberosity)	62			
Tq7	From the plantar border of the proximal facet, to the dorsal border of the distal facet	64.5			
Tq8	From the dorsal border of the proximal facet, to the plantar border of the distal facet	62			
Tq9	Depth of the proximal facet	60			
Tq10	Depth of the distal facet	43			
Tq11	Length of the lateral groove (laterodorsal border of the proximal facet to distal facet)	48			
Tq12	Length of the plantar tubercle (centrodistal medial facet to plantar tuberosity)	42			
Tq13	Proximal breadth (centrodistal medial facet to lateral border of proximal facet)	52			
Tq14	Distal breadth (centrodistal medial facet to lateral border of distal facet)	46			
Tq15	Maximal diagonal breadth (proximal process to lateral border of distal facet)	60 ~			
Tq16	Breadth of the main proximal facet	42			
Tq17	Breadth of the distal facet	29			
Tq18	Breadth of the dorsal proximal facet	20			

	NAVICULARE	TER-1678 dex	TER-1679 dex
Tn1	Dorsal height	22	23
Tn2	Lateral height	19.5	20
Tn3	Plantar height	33	38
Tn4	Maximal depth	54	61.5
Tn5	Maximal breadth	41.5	42 ~
Tn6	Depth of the distal dorsal and lateral facet	48	55
Tn7	Depth of the distal dorsal facet	41	45
Tn8	Depth of the distal plantar facet	15 ~	16 ~
Tn9	Breadth of the distal dorsal facet	24	26
	ECTOMESOCUNEIFORME	**TER-1680 dex**	
Tl1	Maximal breadth	39	
Tl2	Proximal breadth	27	
Tl3	Proximal depth	38	
Tl4	Diameter of the plantar lateral facet	10 ~	
Tl5	Diameter of the dorsal lateral facet	19	
Tl6	Lateral depth	32 ~	
Tl7	Lateral height	21 ~	
Tl8	Breadth of distal facet	27	
Tl9	Depth of distal facet	36	

Chapter 3
Pleistocene camelids from the Syrian Desert: The diversity in El Kowm

Pietro Martini, Loïc Costeur, Jean-Marie Le Tensorer, Peter Schmid (2015)
L'anthropologie 119: 687-693

Abstract

The family Camelidae is known in Eurasia since the latest Miocene, and several species are recognized, but their evolution is poorly known. The region of El Kowm, central Syria, includes several sites spanning from the early to the late Pleistocene and provides the only abundant fossil record of camelids in the Middle East. Our preliminary results show that several species are present over the sequence, revealing some surprising evolutionary trends.

Introduction

The family Camelidae (Artiodactyla, Mammalia) includes a large diversity of extinct species, but few representatives survived into recent times. These are gathered in the subfamily Camelinae and split into the tribes Lamini and Camelini (Harrison 1985; Honey et al. 1998). Four South American species belong to the former: the guanaco (*Lama guanicoe*) and the vicuña (*Vicugna vicugna*), as well as their domestic descendants, the llama (*Lama glama*) and the alpaca (*Vicugna pacos*) (Feranec 2003; Stanley et al. 1994; Wheeler 2012). Modern Camelini are limited to the Old World. They include the one-humped dromedary (*Camelus dromedarius*) and the two-humped Bactrian camel (*Camelus bactrianus*) (Nowak 1999).

Camelids originated in North America during the Uintan NALMA stage of the middle Eocene (46.2-40.4 Ma) (Honey et al. 1998). The family was successful and developed a great diversity during the Miocene, allowing the coeval existence of at least 13 genera and 20 species (Semprebon and Rivals 2010). At the end of the Miocene, some Camelini dispersed though the Bering land bridge into the Old World (Rybczynski et al. 2013). Later, the Lamini tribe colonized South America during the Great American Biotic Interchange (Webb and Meachen 2004). At the end of the Pleistocene, the family went extinct in North America.

Early Old World camelids are united in the widespread genus *Paracamelus*. The oldest remains are dated from the late Turolian (MN 13, ca. 6 Ma) of China (Van der Made et al. 2002), Spain (Morales et al. 1980; Pickford et al. 1995) and Chad (Likius et al. 2003), pointing to a rapid dispersal over the arid Eurasian belt. Previous reports from Turkey have been disproved (Sen 2010; Van der Made et al. 2002). Suggestions that camelids were already present in the Pontic region by MN 12 are questionable (Sen 2010; Titov and Logvynenko 2006). The Late Miocene species were remarkable for their very large size. During the Pliocene and early Pleistocene, this genus was common in the steppe of central Eurasia, where it is recorded until 2.0 Ma (Kostopoulos and Sen 1999; Logvynenko 2001; Titov 2003; Vislobokova 2008). At the same time the first species assigned to the modern genus *Camelus* is found in India, under the name *C. sivalensis* FALCONER & CAUTLEY 1836 (Falconer and Murchison 1868). It is very similar to advanced *Paracamelus* species, from which it most likely evolved. In the middle and late Pleistocene, two other species are recognized: *C. thomasi* POMEL 1983 from Algeria (Harris et al. 2010; Pomel 1893), and *C. knoblochi* NEHRING 1901 in southern Russia and central Asia (Nehring 1901; Titov 2008). The most recently described species is the African *Camelus grattardi* GERAADS 2014, from the Member G of the Shungura Formation (Ethiopia, 2.2 Ma) (Gentry and Gentry 1969; Geraads 2014) Unfortunately, none of the fossil *Camelus* species is well known in the literature, and there is no phylogenetic scenario for the evolution of the modern species. (Geraads 2014; Kostopoulos and Sen 1999)

Contemporary Old World camels are usually divided into two species: the domestic, one-humped dromedary (*Camelus dromedarius* L. 1758) and the two-humped Bactrian camel, mainly known as a domestic animal (*Camelus bactrianus* L. 1758) but also existing as a wild form (*Camelus ferus* PRZEWALSKI 1883) (Hare 2008; Nowak 1999). However, taxonomic controversy has surrounded the recent Camelini, as they have often been lumped in a single species (Mason 1984; Peters 1998; Potts 2004). One argument for this was the lack of known wild one-humped camels that could be ancestral to the dromedary, but more recent archaeological discoveries have proven the distinctiveness of both species (Driesch and Obermaier 2007; Peters and Driesch 1997; Spassov and Stoytchev 2004). In addition to ontogenetic (Kinne et al. 2010) and morphological differences, which are slight but consistent (Köhler-Rollefson 1989; Lesbre 1903; Martini 2011; Steiger 1990; Wapnish 1984) (Martini, in prep.), it is relevant to point out that there is only little ecological and geographic interspecific overlap: the dromedary is found in hot deserts of North Africa and Middle East, while the Bactrian camel lives in cold deserts of central Asia (Köhler-Rollefson 1991).

A good opportunity to study the diversity and evolutionary trends of Eurasian camelids is provided by the faunal record of the El Kowm Basin, Central Syria (Jagher and Le Tensorer 2011). The many Palaeolithic archaeological sites of this region have provided abundant mammalian fossils, among which camelid remains are the most frequent faunal elements over the whole sequence. In fact, the El Kowm basin is presently the only site rich in fossil camelids in the whole Middle East, and therefore it can be a key site to the understanding of this family.

Results and discussion

Here we present an overview of the very first results from the analysis of this camelid succession; further studies are ongoing (Martini, in prep). The material included in this study was excavated by the University of Basel in three sites of the El Kowm Basin (Aïn al Fil, Hummal and Nadaouiyeh Aïn Askar) located within few kilometers from each other. Taken together they form an adequately complete stratigraphic sequence starting with the Early Paleolithic, in the Olduvai subchron of the Early Pleistocene (ca. 1800 Ka) and ending with the Mousterian, in the Upper Pleistocene (ca. 50 Ka) (Jagher and Le Tensorer 2011; Richter et al. 2011). The fauna is remarkably uniform throughout the sequence and is typical for an arid steppe habitat, showing little environmental change. The dominant taxa are Camelidae, small Bovidae (gazelles) and Equidae; Rhinocerotidae, larger Bovidae (oryxes and buffaloes), and Carnivora are important but less frequent elements (Reynaud Savioz 2011) (personal data).

Aïn al Fil is the smallest and newest of the three sites. Excavations were started only in 2008 and were interrupted after the 2010 campaign. The Olduvai-Matuyama reversal is identified in the sequence, which is therefore dated to the early Pleistocene, at ca. 1800 Ka. The name of the site is Arabic for "Well of the Elephant", referring to the first fossil found there: an M2 of a *Mammuthus cf. throgontherii*. (Le Tensorer et al., 2015) The still small number of specimens recovered to date is suggestive of a rich and probably more varied fauna than found in the other sites. Concerning camelids, the most striking item is a tibia (AF-178) measuring ca. 650 mm (*C. dromedarius* averages 449.8 mm; *C. bactrianus* 442.7 mm; these and further comparative data are from (Martini 2011) and (Martini, in prep) indicating the presence of a gigantic camel species in the early Pleistocene. Less impressive but more unexpected are two scaphoidea, found in proximity but showing a degree of difference consistent with two separate species: AF-229 would fit in size to the mentioned tibia, AF-230 is not larger than that of a modern dromedary. Therefore, the limited fossil record from Aïn al Fil strongly hints at the coexistence of two species of camels, one of them being much larger than the living ones.

The lower strata from Hummal (layers 15 to 23) are dated between 1200 and 1400 Ka. This is a larger site which includes 23 known layers (Le Tensorer et al. 2011). It was excavated from 1997 to 2010 and has yielded abundant artifacts, as well as ca. 7000 macrofaunal remains. Some of the camelids found in the lower layers show a large size, although not as large as the Aïn al Fil giant camel. One rare complete metacarpal (E10948, layer 15) is 410 mm long (*C. dromedarius* averages 348.8 mm; *C. bactrianus* 323.2 mm) and is slenderer than in both modern species (distal breadth across the condyles: 106 mm; *C. dromedarius* 92.2 mm; *C. bactrianus* 96.4 mm. This breadth divided by the length: 25.9%; *C. dromedarius* 26.5%; *C. bactrianus* 29.9% mm). Another remarkable specimen is an atlas (E 10561, layer 19) which is more massive than in a dromedary (slightly larger than in a Bactrian camel), but with a small cranial articular concavity, suggestive of an animal with a relatively small head.

The best preserved camel fossil from the El Kowm basin is a cranium from Nadaouiyeh Aïn Askar. This site is known for its impressive richness in Acheulean technology, but has also yielded ca. 14000 fossil specimens (Jagher 2011). Most of the camelid material is still unstudied. The cranium was recovered in 1994 from level 7 which is dated at 450 Ka. It is dorsoventrally compressed, but almost complete. It shows an interesting mosaic of characters found either in *C. dromedarius* or *C. bactrianus* together with others that are unique, in particular around the orbit and in the dentition. A detailed description of this specimen and comparison with other fossil species are forthcoming (Martini, in prep.).

The upper part of Hummal (layers 5 to 12, dated 350 to 50 Ka) is divided among three Middle Paleolithic cultures: the Yabroudian, the Hummalian and the Mousterian. Overall the camelid material looks closer and closer to the recent species, both in shape and dimensions. However, the unexpected appearance of another giant form which is strictly limited to the Mousterian sublayers (layer 5) does not fit in the general trend of size reduction. Neither younger nor older samples indicate the presence of this species. It was close in size to the Aïn al Fil giant form; however, the morphology of the distal tibia (an informative character in camel diagnosis) is radically different. Like the latter, it coexisted with normal-sized or even small camels which might be close to the ancestry of both modern species (Martini et al., in prep.). It also coexisted with advanced species of our own genus: either *Homo neanderthalensis* or *H. sapiens* (Le Tensorer et al. 2011). Several measurements and proportions help define this species and show it was not an allometrically scaled dromedary or Bactrian camel. Several skeletal parts are about 130% larger than in modern camels; as a very rough estimate, it might have weighted twice as much, or about 1000 Kg. In total, 31 well-defined specimens and possibly 51 others have been excavated between 2005 and 2009. They have

been found in 6 to 7 different layers and represent therefore a temporally sustained population. Unfortunately, as of 2010 almost all specimens were stored in the Tell Arida research center, El Kowm, Syria, and in light of the current political situation, they are not accessible for further study.

A formal description of the giant Mousterian camel is still awaiting comparison with other large fossil camels (Martini, in prep.). The available information suggests that this population does not correspond to any described species. *Paracamelus* and *Camelus sivalensis* can be ruled out, because they are characterized by the absence of P_3 (present in the El Kowm form) and are not known after 2.0 Ma (Geraads 2014).

The North African, Middle Pleistocene *Camelus thomasi* was based on a normal-sized cranium which is incompatible with the large mandibulae from El Kowm. However, the name *C. thomasi* has been assigned to some unassociated large-sized postcranial elements form the same layers (Pomel 1893) and also from other sites in North Africa and in the Middle East (Gautier 1966; Grigson 1983; Peters 1998), but the latter identification are all questionable (Geraads 2014). Since the El Kowm sample implies the coexistence of a normal-sized and a giant form, it is conceivable that the El Kowm and *C. thomasi* small-sized material could be included in this species, while the large-sized material could represent a different species.

The other African species is *Camelus grattardi*, from the Member G of the Shungura Formation in Ethiopia (Gentry and Gentry 1969; Geraads 2014; Harris et al. 2010). It is dated at 2.2 Ma, therefore is substantially older than the Mousterian sample from El Kowm. Although there is little material that can be directly compared between the samples, *C. grattardi* represents a species within the size range of modern camels, not a giant form; hence this name does not come into question.

The most likely assignment of the Mousterian giant camel could be to the Russian and Asian species *C. knoblochi*, to which it is similar in size and age (Nehring 1901; Titov 2008). However, there are several indications pointing at a specific difference. Ecologically, the habitat in which *C. knoblochi* is found (temperate and cold steppe) and the habitat of the El Kowm basin (dry, hot steppe and desert) are exploited today by separate camel species with different adaptation. Since Old World camelids have had a long prior evolution, it is likely that a similar situation was already present in the middle Pleistocene. Morphologically, it is difficult to find differences between the El Kowm sample and published material of *C. knoblochi*. The clearest might be that found in metapodial condyles measurements. However, the North African sample assigned to *C. thomasi* includes postcranial material (Pomel 1893) that differs markedly from the Russian species (Titov

2008). The Syrian material can be expected to be closer to the Algerian sample, than to the Russian one. Evidently, none of these arguments are compelling; therefore a direct comparison is certainly needed before the Mousterian giant camel from the El Kowm basin can be considered a new species.

Conclusion

In summary, the El Kowm region is unique in the Middle East for its richness in fossil sites and abundant camelid material, stretching from the Early to the Late Pleistocene. The complete sample includes at least five distinct species; this total exceeds the number of described fossil *Camelus* species. Of special interest are a trend in size reduction over time, and the coexistence of a normal-sized and a giant-sized form in two distinct levels. Such diversity is surprising in a family that is usually considered ecologically homogeneous. While the study of the El Kowm sample will fill important gaps in the knowledge of fossil Camelidae, disentangling camelid evolution will lead to important advances in understanding environmental change and migration events in the Pleistocene of the Middle East.

Acknowledgements

Financial support for the excavations in Syria and the participation to the 2014 UISPP congress in Burgos was provided by the Swiss National Foundation.

References

DRIESCH, A. V. D., and H. OBERMAIER. 2007. The hunt for wild dromedaries during the 3rd and 2nd millennia BC on the United Arab Emirates coast. Camel bone finds from the excavations at Al Sufouh 2, Dubai, UAE. Pp. 133-167 in Skeletal Series and their Socio-economic Context (J. Grupe and J. Peters, eds.). Leidorf, Rahden.

FALCONER, H., and C. MURCHISON. 1868. Palaeontological memoirs and notes of the late Hugh Falconer. Robert Hardwicke, London. 1 - Fauna Antiqua Sivalensis.

FERANEC, R. S. 2003. Stable isotopes, hypsodonty, and the paleodiet of *Hemiauchenia* (Mammalia: Camelidae): a morphological specialization creating ecological generalization. Paleobiology 29:230-242.

GAUTIER, A. 1966. *Camelus thomasi* from the Northern Sudan and its bearing on the relationship *C. thomasi* - *C. bactrianus*. Journal of Paleontology 40:1368-1372.

GENTRY, A. W., and A. GENTRY. 1969. Fossil Camels in Kenya and Tanzania. Nature 222.

GERAADS, D. 2014. *Camelus grattardi*, sp. nov., a new camel from the Shungura Formation, Omo Valley, Ethiopia, and the relationships of African fossil Camelidae (Mammalia). Journal of Vertebrate Paleontology 34:1481-1485.

GRIGSON, C. 1983. A very large camel from the upper Pleistocene of the Negev Desert. Journal of Archaeological Science 10:311-316.

HARE, J. 2008. *Camelus ferus*in IUCN 2013. IUCN Red List of Threatened Species. Version 2013.1.

HARRIS, J. M., D. GERAADS, and N. SOLOUNIAS. 2010. Camelidae. Pp. 815-820 in Cenozoic Mammals of Africa (L. Werdelin and W. J. Sanders, eds.). University of California Press, London.

HARRISON, J. A. 1985. Giant Camels from the Cenozoic of North America. Smithsonian Contributions to Paleobiology 57.

HONEY, J. J., J. A. HARRISON, D. R. PROTHERO, and M. S. STEVENS. 1998. Camelidae. Pp. 439-462 in Evolution of Tertiary Mammals of North America: Terrestrial Carnivores, Ungulates, and Ungulatelike Mammals (C. M. Janis, K. Scott and L. L. Jacobs, eds.). Cambridge University Press, Cambridge.

JAGHER, R. 2011. Nadaouiyeh Aïn Askar - Acheulean variability in the Central Syrian Desertin The Lower and Middle Palaeolithc in the Middle East and Neighbouring Regions (J. M. Le Tensorer, R. Jagher and M. Otte, eds.). Etudes et Recherches Archéologiques de l'Université de Liège (ERAUL), Liège.

JAGHER, R., and J.-M. LE TENSORER. 2011. El Kowm, a key area for the palaeolithic of the Levant in Central Syriain The Lower and Middle Palaeolithc in the Middle East and Neighbouring Regions (J. M. Le Tensorer, R. Jagher and M. Otte, eds.). Etudes et Recherches Archéologiques de l'Université de Liège (ERAUL), Liège.

KINNE, J., N. A. WANI, U. WERNERY, J. PETERS, and C. KNOSPE. 2010. Is there a two-humped stage in the embryonic development of the dromedary? Anatomia, histologia, embryologia 39:479-80.

KÖHLER-ROLLEFSON, I. U. 1989. Zoological analysis of camel skeletons. Pp. 142-164 in Pella of the Decapolis. Vol. 2, Final Report on the College of Wooster Excavations in Area IX, the Civic Complex, 1979-1985 (R. H. Smith and L. P. Day, eds.). The College of Wooster, Wooster.

KÖHLER-ROLLEFSON, I. U. 1991. *Camelus dromedarius*. Mammalian species 375:1-8.

KOSTOPOULOS, D. S., and S. SEN. 1999. Late Pliocene (Villafranchian) mammals from Sarikol Tepe, Ankara, Turkey. Mitteilungen der Bayerischen Staatssammlung für Paläontologie und Historische Geologie 39:165-202.

LE TENSORER, J.-M., V. VON FALKENSTEIN, H. LE TENSORER, and S. MUHESEN. 2011. Hummal: A very long Paleolithic sequence in the steppe of Central Syria - Considerations on Lower Paleolithic and the beginning of Middle Paleolithicin The Lower and Middle Palaeolithc in the Middle East and Neighbouring Regions (J. M. Le Tensorer, R. Jagher and M. Otte, eds.). Etudes et Recherches Archéologiques de l'Université de Liège (ERAUL), Liège.

LESBRE, F.-X. 1903. Recherches anatomiques sur les Camélidés. Pp. 1-196 in Archives du Muséum d'Histoire Naturelle de Lyon (H. Georg, ed.), Lyon.

LIKIUS, A., M. BRUNET, D. GERAADS, and P. VIGNAUD. 2003. Le plus vieux Camelidae (Mammalia, Artiodactyla) d'Afrique: limite Mio-Pliocène, Tchad. Bulletin de la Société Géologique de France 174:187-193.

LOGVYNENKO, V. M. 2001. *Paracamelus minor* (Camelidae, Tylopoda) - a new camelid species from the Middle Pliocene of Ukraine. Vestnik zoologii 35:39-42.

MARTINI, P. 2011.A metrical analysis of the morphological variation in extant and fossil camels. Master's thesis, University of Zürich, Zürich.

MASON, I. L. 1984. Origin, Evolution and distribution of domestic camels. Pp. 16-35 in The Camelid: An all-purpose animal. Proceedings of the Khartoum Workshop on Camels, December 1979 (W. R. Cockrill, ed.). Scandinavian Institute of African Studies, Uppsala.

MORALES, J., D. SORIA, and E. AGUIRRE. 1980. Camelido finimioceno en Venta del Moro. Primera cita para Europa Occidental. Estudios Geológicos 36:139-142.

NEHRING, A. 1901. Mittheilung über einen fossilen Kamel-Schädel (*Camelus Knoblochi*) von Sarepta an der Wolga. Sitzungsbericht der Gesellschaft Naturforschende Freunde 5.

NOWAK, R. M. 1999. Walker's Mammals of the World. The Johns Hopkins University Press, Baltimore1-1936.

PETERS, J. 1998. *Camelus thomasi* Pomel, 1893, a possible ancestor of the one-humped camel? Zeitschrift für Säugetierkunde 63:372-376.

PETERS, J., and A. V. D. DRIESCH. 1997. The two-humped camel (*Camelus bactrianus*): new light on its distribution, management and medical treatment in the past. Journal of Zoology 242:651-679.

PICKFORD, M., J. MORALES, and D. SORIA. 1995. Fossil camels from the Upper Miocene of Europe: implications for biogeography and faunal change. Geobios 28:641-650.

POMEL, A. 1893. Caméliens et Cervidés. Paléontologie monographies.

POTTS, D. T. 2004. Camel hybridization and the role of *Camelus bactrianus* in the ancient Near East. Journal of the Economic and Social History of the Orient 47:143-165.

REYNAUD SAVIOZ, N. 2011. The faunal remains from Nadaouiyeh Aïn Askar (Syria). Preliminary indications of animal acquisition in an Acheulean site.in The Lower and Middle Palaeolithc in the Middle East and Neighbouring Regions (J. M. Le Tensorer, R. Jagher and M. Otte, eds.). Etudes et Recherches Archéologiques de l'Université de Liège (ERAUL), Liège.

RICHTER, D., T. C. HAUCK, D. WOJTCZAK, J. M. LE TENSORER, and S. MUHESEN. 2011. Chronometric age estimates for the site of Hummal (El Kowm, Syria)in The Lower and Middle Palaeolithc in the Middle East and Neighbouring Regions (J. M. Le Tensorer, R. Jagher and M. Otte, eds.). Etudes et Recherches Archéologiques de l'Université de Liège (ERAUL), Liège.

RYBCZYNSKI, N., J. C. GOSSE, C. R. HARINGTON, R. A. WOGELIUS, A. J. HIDY, and M. BUCKLEY. 2013. Mid-Pliocene warm-period deposits in the High Arctic yield insight into camel evolution. Nature communications 4:1550.

SEMPREBON, G. M., and F. RIVALS. 2010. Trends in the paleodietary habits of fossil camels from the Tertiary and Quaternary of North America. Palaeogeography, Palaeoclimatology, Palaeoecology 295:131-145.

SEN, S. 2010. Camelids do not occur in the late Miocene mammal locality of Çobanpinar, Turkey. Russian Journal of Theriology 9:87-91.

SPASSOV, N., and T. STOYTCHEV. 2004. The dromedary domestication problem: 3000 BC rock art evidence for the existence of wild One-humped camel in Central Arabia. Historia naturalis bulgarica 16:151-158.

STANLEY, H. F., M. KADWELL, and J. C. WHEELER. 1994. Molecular Evolution of the Family Camelidae: A Mitochondrial DNA Study. Proceedings. Biological sciences / The Royal Society 256:1-6.

STEIGER, C. 1990.Vergleichend morphologische Untersuchungen an Einzelknochen des postkranialen Skeletts der Altweltkamele. Ph.D. dissertation, Ludwig-Maximilians-Universität München, München.

TITOV, V. V. 2003. Paracamelus from the Late Pliocene of the Black Sea region. Pp. 17-24 in Advances in Vertebrate Paleontology: Hen to Panta (A. Petculescu and E. Stiuca, eds.), Bucharest.

TITOV, V. V. 2008. Habitat conditions for *Camelus knoblochi* and factors in its extinction. Quaternary International 179:120-125.

TITOV, V. V., and V. N. LOGVYNENKO. 2006. Early *Paracamelus* (Mammalia, Tylopoda) in Eastern Europe. Acta zoologica cracoviensia 49A:163-178.

VAN DER MADE, J., J. MORALES, S. SEN, and F. ASLAN. 2002. The first camel from the upper Miocene of Turkey and the dispersal of the camels into the Old World. Comptes Rendus Palevol 1:117-122.

VISLOBOKOVA, I. A. 2008. Main stages in evolution of Artiodactyla communities from the Pliocene-Early Middle Pleistocene of northern Eurasia: Part 2. Paleontological Journal 42:414-424.

WAPNISH, P. 1984. The dromedary and Bactrian camel in Levantine historical settings: The evidence from Tell Jemmeh. Pp. 171-200 in Animals and Archaeology: 3. Early Herders and their Flocks (J. Clutton-Brock and C. Grigson, eds.). British Archaeological Reports, International Series, Oxford.

WEBB, S. D., and J. A. MEACHEN. 2004. On the origin of lamine Camelidae including a new genus from the Late Miocene of the high plains. Bulletin of Carnegie Museum of Natural History 36:349-362.

WHEELER, J. C. 2012. South American camelids - past, present and future. Journal of Camelid Science 5:1-24.

Figures

This chapter does not include figures in its published version.

Chapter 4

A new species from Nadaouiyeh Aïn Askar (Syria) contributes to the diversity of Pleistocene Camelidae

Pietro Martini, Loïc Costeur, Reto Jagher, Jean-Marie Le Tensorer

Manuscript in preparation

Abstract

The family Camelidae (Mammalia, Artiodactyla) has a long and well known history in North America, but his record in the Old World is poor. In the El Kowm Basin, central Syria, several fossil assemblages rich in camelid remains form a long sequence, covering a time span from the Olduvai subchron to the late Pleistocene (1.8 Ma to 50 Ka), that has the potential to drastically improve our understanding of camel evolution. We describe the camelid fossils from the site Nadaouiyeh Aïn Askar, the largest temporally continuous assemblage from the El Kowm Basin, and define the new species *Camelus roris*, which is diagnosed on a well preserved cranium. Abundant specimens of mandibular, dental and postcranial elements show that there was only one dominant species from 500 Ka to 200 Ka, but isolated specimens demonstrate the sporadic presence of a second camelid form. We discuss the known fossil *Camelus* species and conclude that it is still premature to speculate about their relationships.

Keywords: *Camelus*, Camelidae, Artiodactyla, Middle East, Syria, new species

Introduction

The family Camelidae has its origins and a long and diverse history in North America, but a much meager record in Eurasia and Africa. It is first known in the middle Eocene (Uintan NALMA, ~45 Ma) and shows cursorial adaptations and microwear patterns that are suggestive of an early occupation of open habitats (Semprebon and Rivals 2010). It reached its maximal diversity in the Miocene, when at least 13 genera and 20 species coexisted in North America (Honey et al. 1998;

Semprebon and Rivals 2010). Dispersal into Eurasia only occurred in the Late Miocene (tribe Camelini), and the family reached South America (tribe Lamini) in the Pliocene (Scherer 2013; Webb and Meachen 2004). Its dominant role in North American faunas ended with local extinction at the Pleistocene-Holocene transition. Extant species of Camelini include the domesticated Bactrian camel (*Camelus bactrianus*, LINNAEUS 1758) and dromedary (*Camelus dromedarius*, LINNAEUS 1758); the wild camel (*Camelus ferus*, PRZEWALSKI 1883) is usually considered a subspecies of the former, but is genetically distinct (Burger 2016).

In the Old World, species referred to the genus *Paracamelus* are known since the latest Miocene MN13 (Pickford et al. 1995; Van der Made et al. 2002). Some eastern European sites containing camelids have been assigned to MN12 (Titov and Logvynenko 2006), but such an early age is debatable (Sen 2010). The relationships of *Paracamelus* to the American Camelini are unclear; it might descend from a late form of *Procamelus* or early *Megacamelus* (Pickford et al. 1995), be related to *Megatylopus* (Titov and Logvynenko 2006) or to none of the known genera (Rybczynski et al. 2013). Several species of large to small size are known from the late Miocene to the early Pleistocene (Havesson 1954); *Paracamelus* has been identified in China (Wang et al. 2013; Zdansky 1926), Spain (Morales et al. 1980; Pickford et al. 1995; Van der Made et al. 2002), Chad (Likius et al. 2003) and tentatively in Alaska (Harington 2011; Rybczynski et al. 2013), but the largest number of both species and remains are known from several localities in Eastern Europe and Central Asia (Havesson 1954; Kostopoulos and Sen 1999; Kozhamkulova 1986; Sen 2010; Titov 2003; Titov and Logvynenko 2006; Van der Made and Morales 1999; Vislobokova 2008).

Paracamelus is widely supposed to be ancestral to *Camelus*; however, in spite of the numerous Miocene and Pliocene species, the origins of *Camelus* have seldom been discussed (Pickford et al. 1995), the Pleistocene fossil record is overall scarce (Harris et al. 2010) and no evolutionary scenario discussing all described fossil species has been advanced yet (Geraads 2014).

"Camelus" sivalensis FALCONER & CAUTLEY 1836 is known from the Tatrot and Pinjor Formations of the Siwalik Group, Indian subcontinent, which correspond to Late Pliocene and Early Pleistocene (Gaur et al. 1984; Nanda 2008, 1978). It has recently been reassigned to *Paracamelus* (Alçiçek et al. 2013), but without an explicit justification. Its diagnosis is based on dental and mandibular characters (Colbert 1935b; Falconer and Murchison 1868; Matthew 1929; Nanda 1978).

The same authors named also *Camelus antiquus* FALCONER & CAUTLEY 1836 from the same formation, and considered it perhaps "closely allied to the Lama" (Falconer and Murchison 1868). Others have suggested it might be related to *Paracamelus alutensis* (Kostopoulos and Sen 1999), without stating the motivation. In fact, this species does not appear to be distinct from *"C." sivalensis*, since the differences are based on characters prone to variation in camelids; therefore, it has been synonymized with the latter (Colbert 1935b; Matthew 1929).

Camelus grattardi GERAADS 2014 was described from fragmentary material collected in the 1970s in the lower Member G, Shungura Formation, Omo Valley, Ethiopia (ca. 2.2 Ma) (Geraads 2014; Grattard et al. 1976; Howell et al. 1969).

Camelus knoblochi NEHRING 1901 (Nehring suggests the authorship should be referred to BRANDT, but is not aware of a previous publication (Nehring 1901)) is a very large and massive Middle Pleistocene species, that survived but became rare in the Late Pleistocene. Its distribution stretches from the Pontic region to northern China. Recently, it was listed in 38 localities excluding China; known material include 10 partial or fragmentary crania, 9 mandibles and postcranial skeletons (Titov 2008). However, material published in English is extremely scanty, and Western authors often dismiss this species spending only few generic words about it. It is considered closely related to Bactrian camels, with which it can be confused (Geraads 2014).

Camelus thomasi POMEL 1893 was described from Tighennif (or Ternifine, formerly also known as Palikao), a site in Algeria that current biostratigraphic considerations place it in the late

Early Pleistocene, possibly in the Jaramillo subchron at 1.06-0.90 Ma (Geraads 2016). The holotype is a fragmentary left maxilla, with parts of zygomatic, palatine, M^1, M^2 and an associated M^3; the original description also includes a large-sized metatarsale. Description of a larger sample, including a complete cranium and several postcrania, is forthcoming (Martini and Geraads, 2018)

A fauna from the southern Nefud desert has been briefly described (Thomas et al. 1998) and dated to the late Middle Pleistocene (Scerri et al. 2014; Stimpson et al. 2016). It is suggestive of a dry steppe habitat. This sample includes only a camelid maxilla (JMI 50) that is left unidentified to the specific level, but differs from *C. thomasi* and *C. dromedarius* in its palatine foramen found at the level of M^1 (Thomas et al. 1998).

The richest Middle East fossil camel assemblages discovered are those from the sites in the El Kowm Basin, Syria, which are presently known only through preliminary studies (Martini 2011; Martini et al. 2015). The four main sites of Nadaouiyeh Aïn Askar, Hummal, Umm el Tlel, and Aïn al Fil have provided abundant faunal material, dominated by camelids, equids, gazelles and other bovids (Griggo 2004; Reynaud Savioz 2011). The composite sequence reaches from older than 1.8 Ma to 50 Ka (Jagher et al. 2015; Le Tensorer et al. 2011; Le Tensorer et al. 2015). Our initial results have indicated that the local fauna contained an unexpected diversity of camel species, recording the coexistence of two different-sized species both in the oldest and in the youngest layers, and a dynamic change in morphology and size between these extremes (Martini et al. 2015). Hence, the ongoing analysis of the combined samples from El Kowm will give an overview of regional camel evolution with a clarity that is unmatched in the Old World.

In this contribution we undertake the systematic study of the El Kowm camelids and describe the samples from the locality of Nadaouiyeh Aïn Askar. We name a new camel species, *Camelus roris* sp. nov., which is based on a complete cranium and 95 additional specimens of dentition,

cranial and postcranial elements; it is therefore one of the most completely known Old World fossil camelid. Within the El Kowm record, Nadaouiyeh Aïn Askar has yielded the largest assemblage of fossils forming a temporally continuous sequence; its description is a fundamental step to understand the past diversity and the evolution of the genus *Camelus*.

Geological and stratigraphic setting

The village of El Kowm lies close to the geographical center of Syria, in the middle of a 10-km wide basin where several artesian springs dot the otherwise arid steppe, attracting animals as well as early humans (Jagher et al. 2015; Jagher and Le Tensorer 2011). Anthropic presence is continuously traced since the Olduvai subchron in the Lower Pleistocene (Le Tensorer et al. 2015), with a high density of Paleolithic sites that preserve both lithic artefacts and fossilized remains of the accompanying large fauna, most of them remains of hunting activity . Excavations have always had an archaeological focus; they started with the first recognition in 1966 (Buccellati and Buccellati 1967), continued with an overview of Neolithic sites in 1978 (Cauvin et al. 1979) and took on with a systematic survey of Paleolithic deposits in 1980 (Besançon et al. 1981) which recorded 72 locations over an area of 150 km^2 (the list was later extended to 143 sites) (Jagher et al. 2015).

The site of Nadaouiyeh Aïn Askar (henceforth Nadaouiyeh) was recognized early among the most promising in the El Kowm Basin (Jagher 2011, 2016). Regular fieldwork started in 1989 under the joint organization of the Universities of Basel and Damascus, and lasted until 2003 (Jagher and Le Tensorer 2011); afterwards the focus of excavations shifted to the nearby sites of Hummal (open since 1997) and Aïn al Fil (starting in 2008) until 2010. In 2011, the political unrest in Syria forced an ongoing interruption of fieldworks. Nadaouiyeh has yielded a rich and variable Upper Acheulean industry, including 12415 hand axes and bifacial tools (Jagher 2016).

Nadaouiyeh was formed at the intersection of two faults in the bedrock, creating a karstic system and allowed artesian ground water to spring at the surface (Jagher 2011). The combination of additional faulting, internal sedimentation and repeated cave collapses brought about a very complex stratigraphy. The 32 archaeological layers of Nadaouiyeh are grouped into seven main archaeological units by their stratigraphic position (Table 1). Six of these units, labeled Unit A to Unit F, have provided in situ camelid material that was included in this study. Additional fossils were recovered from the filling of Doline 3 (Dol.3), consisting of reworked deposits that were originally intermediate between Unit A and Unit B.

Absolute dating has proven difficult in the El Kowm Basin (Jagher and Le Tensorer 2011) and several attempts in Nadaouiyeh have been unsuccessful to date (Jagher 2016). The seven units have been dated indirectly, based on climatologic markers and archaeological correlation with other Middle Paleolithic (Acheulean) sites in the Levant (Jagher 2011). While the following dating can still be considered provisional, it provides an adequate context from a paleontological point of view.

The oldest archaeological material, from secondary deposits, might possibly be between 700 and 1000 Ka old, but the first camel remains are found in Unit F, which is considered approximately 550 Ka old. The following units C, D and E are temporally contiguous, covering the span between 550 and 450 Ka. There is a hiatus before Unit B, whose extension is estimated from 430 to possibly 350 Ka. Another stratigraphic hiatus after Unit B is biologically bridged by the reworked material in Doline 3 (hereafter considered as Unit A/B), dating between 350 and 200 Ka. This time span should also include the “Black Hummal” reworked sediments, named for the Hummalian technology they contain. The youngest remains in situ form Unit A, which can be placed at an age of about 150 Ka and bear a later Lower Paleolithic technology. The fossils included in this study can therefore be robustly bracketed between 150 and 550 Ka, corresponding to the middle and later parts of the Middle Pleistocene (Jagher 2011, 2016).

The ecological, taphonomical and archaeozoological setting of the faunal remain containing camelids in Nadaouiyeh have been identified by preliminary studies (Reynaud Savioz 2011; Reynaud Savioz and Morel 2005). The entire fauna is considered of anthropogenic origins, with extensive and destructive butchering exploitation, including bone smashing. Although the aerial weathering of the specimens has been overall minimal, the poor degree of fossilization and the geological movements have fragmented the fossils to a high degree. Therefore, besides the abundant and easily recognized gazelle remains, a large majority of the osteological material (including camelids) is left unidentified or organized only by size class.

The most abundant faunal elements are Camelidae, Bovidae and Equidae. Camelids have not yet been identified to species level. Bovids are divided in three size classes that have been identified as *Bos primigenius*, *Oryx cf. leucoryx* and *Gazella subgutturosa*, respectively (Reynaud Savioz 2011). The latter two species still survive in the Middle East and are typical representative of arid steppe fauna. Another possible identification for the supposed *Bos primigenius* remains might be the closely related *Pelorovis oldowayensis*, known from ‘Ubeidiya (Belmaker 2010; Geraads 1986; Martínez-Navarro et al. 2012) and probably present at Hummal as well, based on dental material (M. Belmaker, personal communication, 2012). Equids seem to be divided in three size groups that are tentatively referred to *Equus africanus*, *E. hemionus* and *E. ferus*; the remains have not been compared to fossil taxa yet. Other rare or occasional species include Rhinocerotidae (cf. *Stephanorhinus hemitoechus*), Elephantidae, Suidae, Hyaenidae (coproliths), large Felidae (*Panthera sp.*), small Canidae (cf. *Vulpes sp.*), micromammals, birds and abundant tortoises.

The frequency of each taxon fluctuates between units, also because of human hunting behavior, but forest and mountain species are entirely absent (leaving the identification of Suidae and large Bovidae open), and the overall composition is stable over the sequence; as a whole, the fauna of Nadaouiyeh is indicative of a treeless, arid steppe (Reynaud Savioz 2011).

Material and methods

The site of Nadaouiyeh has yielded a total of 463 identified camel remains, and 2908 unidentified specimens which belong to a size class compatible with camels (Reynaud Savioz 2011). Of the identified remains, the specimens too fragmentary or too poorly preserved were discarded, resulting in a selected sample of 126 morphologically informative specimens. The selected sample is listed in Table 2 and includes a complete cranium, mandibles, upper and lower dentition and postcranial material. The material described in this study is stored at IPNA. Remains from Nadaouiyeh Aïn Askar are identified by the prefix Nad-1.

Measurements were taken with a slide gauge calliper and rounded to the next 0.5 mm. As we observed that the metric difference between the right and left side of the same camel individual can be as great as 1-2 mm, even for small bones or dentition (Martini et al. 2017), we consider unnecessary to use a greater precision such as 0.1 mm.

We compared the fossil material with published data on both extant species, *C. bactrianus* and *C. dromedarius* (Martini et al. 2017), complemented with further observations on cranium (NMB 10390 for *C. bactrianus*, NMB 2128 for *C. dromedarius*) and on distal phalanx (unpublished data). Data on *C. thomasi* were obtained from the Tighennif sample, housed at the MNHN in Paris (Martini and Geraads, 2018). Data on other fossil *Camelus* and *Paracamelus* species are based on the literature.

Most of the postcranial differences are not qualitative, but rather depend on proportions that are easier to visualize metrically than on the specimens. Important metrical characters are illustrated using bivariate scatterplots. We do not apply statistical methods because the number of specimens for each element is very limited.

Institutional abbreviations

NMB, Naturhistorisches Museum Basel

MNHN, Museum National d'Histoire Naturelle, Paris

IPNA, Institut für Prähistorische und Naturwissenschaftliche Archäologie (Institute for Prehistorical and Scientific Archeology), University of Basel

Systematic Paleontology

Order ARTIODACTYLA Owen, 1848

Family CAMELIDAE Gray, 1821

Genus *Camelus* Linnaeus, 1758

Camelus roris nov. sp.

Etymology: from Latin *ros, roris* meaning "Camel of the morning dew". In reference to the name of the locality Nadaouiyeh, which means "Place of the morning dew".

Holotype: cranium Nad-1 F14-671, stored at IPNA (Fig 1A-D).

Paratype: maxilla Nad-1 A16-45 and M^3 Nad-1 A16-39 (Fig 2A).

Type locality: Nadaouiyeh Aïn Askar, El Kowm Basin, central Syria.

Type layer: Layer 7, at the base of Unit B.

Age: Middle Pleistocene. Based on archaeological comparisons of the Middle Eastern Acheulean technologies, the type layer (at the base of Unit B) is estimated at about 430 Ka. The referred material originates from Units A, A/B, B, C, D, E, and F, which cover the time span between 150 and 550 Ka as shown in Table 1 (Jagher 2011; Reynaud Savioz 2011).

Referred material: 93 additional specimens from Nadaouiyeh listed in Table 2 (the table includes other camelid specimens as well). The complete measurements are given in Table 3.

Diagnosis

A moderately large *Camelus* species, close in size to the extant Bactrian camel (*Camelus bactrianus*), with large P^4, large M^1, narrow distal lobe of M^2, small M^3; M^1 is at least ¾ as long as M^3; broad forehead; long, convex, bulging maxilla; facial crest present; narrow palate; palatine foramina at the level of M^1 (middle); deep, dorsally convex supraorbital notch; strong, massive superciliar arch; orbital rim massive and caudally constricted (on the zygomatic process of the frontal); shallow postorbital constriction, in caudal position (distant from the orbits); narrow braincase; temporal crest convex, occipital crests straight and blunt, a distinct bend in between; glenoid fossa with a well-developed anteromedial lip; anterior lip of occipital condyles clearly constricted. Mandibular corpus massive (pachyostotic). M_2 comparatively narrow and long. Calcaneus slender, with thick plantar border, plantar positioning of the sustentaculum, distally prominent cuboid facet. Articular facet of III metatarsale narrow; articular facet of IV metatarsale wide; metapodial condyles deep and narrow.

Differs from *Paracamelus* (including *"Camelus" sivalensis*) in the reduction of the upper premolar row; reduction of molar styles; the orbits are completely above the dentition; the facial part of the cranium is not elongated. Further differs from *P. gigas, P. aguirrei* and "*C." sivalensis* in its smaller size. Differs from *P. alutensis* and *P. alexejevi* in its less advanced choanas (at the level of M^3 rather than M^2) and presence of facial crest. Differs from *P. alutensis* in its larger size.

Differs from *C. grattardi* in the proportions of the dentition (M^1 not as wide, M^3 smaller).

Differs from *C. thomasi* in its smaller postcranial size; the proportions of the dentition (M^1 is longer, compared to M^3); caudal position of palatine foramina (at the level of M^1 instead of P^4); narrower braincase; and occipital condyles not enlarged caudally.

Differs from *C. knoblochi* in its smaller size; more rostral position of palatine foramina (at the level of M^1 instead of M^2-M^3); orbits low over the dentition; presence of maxillar crest; dorsally

concave supraorbital notch; highest point of the orbital rim in the rostral half; convex temporal crest; different proportions of the dentition (large M^1, narrow distal lobe of M^2, small M^3), presence of caudal nasal spine; glenoid fossa with developed anteromedial lip; and relatively larger condyles.

Differs from extant species *C. bactrianus* and *C. dromedarius* in its bulging preorbital region; shallower postorbital constriction; dorsally concave supraorbital notch; different proportions of the dentition (large P^4, large M^1, narrow distal lobe of M^2, small M^3); convex temporal crest, separated from the occipital crest by a distinct bend.

Further differs from *C. bactrianus* in the lower position of the orbit; conformation of the orbit (highest point in the cranial half, zygomatic process of the frontal constricted in the middle); narrower braincase; narrower palate; presence of a caudal nasal spine (uncommon in *C. bactrianus*); presence of a anteromedial lip of the glenoid fossa (uncommon in *C. bactrianus*)

Further differs from *C. dromedarius* in its larger size; presence of a facial crest; massive orbital rim; suture of the zygomatic arch close to the orbit; caudal position of palatine foramina; anterior lip of occipital condyles constricted (uncommon in *C. dromedarius*)

Description

Cranium

The cranium Nad-1 F14-671 closely resembles that of an extant camel (Fig. 1A-C). It is closer in size to an average Bactrian camel, hence larger than a dromedary (Martini et al. 2017). It is relatively complete, but is missing the anterior part of the rostrum and both zygomatic arches behind the orbits, and it has important damages to the dentition and to the basicranium. The cranium is dorsoventrally compressed, but barely deformed in other directions. The basicranium is bent ventrally relatively to the palate, so that the occipital condyles are now aligned with the dentition. The specimen measures 407 mm on the frontal aspect and 395 mm on the ventral aspect.

The rostrum is broken at the level of the alveoli of P^1. The incisivi, the dorsal part of the maxillae, and the nasals are missing; the nasal cavity is filled with coarse sediment. The infraorbital foramen is far from the orbits and overlies P^4. The region of the maxilla between the infraorbital foramen and the orbita is long, laterally convex and bulging. The anterior border of the orbit overlies the middle of M^2. The placement of the orbit over the dentition is low. Under the orbit there is a well-developed maxillar crest.

The forehead is broad and flat; in dorsal view, it has the shape of a rhombus or a kite, with straight rather than concave sides. This form is due to the reduced constriction at the basis of the rostrum, and the caudal position of the postorbital constriction. Only the left supraorbital foramen and the medial suture are discernible on the cracked surface. A round and medially symmetric line of break is present where the caudal suture of the nasals is found, between the supraorbital notches. However, in modern camel this suture has a V-shape, and therefore the structure is interpreted as just another crack.

The left orbit is complete, but slightly crushed (Fig. 1D). The right orbit is basally incomplete, and dorsoventrally completely crushed; its caudal part is represented by an intact separate fragment, which includes the basis of the zygomatic arch. The supraorbital notch is deep and dorsally convex. The orbital rim is higher in its rostral half. The superciliar arch is thick, massive and bulging; caudally, it is prolonged by the zygomatic process of the frontal which shows a constriction in its middle. The ventral part of the orbital rim is thick, of constant width but becoming abruptly narrower caudally on the temporal process of the zygomatic. The suture of the zygomatic arch reaches close to the orbit, and in this region the arch itself is thick. Both zygomatic arches are broken behind the orbits.

The postcranial constriction is distant from the orbits. In dorsal view, the anterior medial border of the temporal fossa (the posterior lateral border of the frontal) is straight and oblique. The

postcranial constriction is shallow, while the braincase is comparatively narrow (Fig. 3A). The parietals have mostly collapsed towards the cerebral cavity, but remained in place without exposing the cavity. The sagittal crest is low. The lateral part of the temporal squama is slightly convex, with a blunt temporal crest. The latter is separated from the straight occipital crest by a distinct bend. The central occipital region is missing.

The palate is narrow and shows a longitudinal medial crack. The right half of the palate is ventrally deformed, and between P^1 and M^2 it is displaced about 10 mm below the left half. The preserved part of the rostrum is arched dorsally; the deformation of the right palate cause this arching to appear more prominent than it was in life. The palatine foramina are found in a posterior placement (Fig. 3B), at the level of the middle of M^1. The palatine suture has a double parabolic shape and reaches to the mesial lobe of M^2. The rostral border of the choana appears to be pointed but with a small nasal spine.

The dentition is heavily damaged. It preserved the alveoli or parts of P^3 to M^3; the occlusal surface is completely missing from all of the cheek teeth. The caniniform P^1 are about to erupt: the left alveolus is already open in the alveolar border, but the preserved right tooth can be seen still deep in the maxilla. On the left side, parts of the threefold roots of P^3 and the root of P^4 are preserved, while on the right side the corresponding alveoles are found empty and partially filled with sediment. The roots of P^4 indicate a large size (Fig. 4A). M^1 is also large (Fig 4B-C); it is formed by two subequal lobes which are mesiodistally short, transversally broad. The left side preserved parts of the roots, showing its proportions; on the right side a fragment of M^1 for a height of about 25 mm is still present, but is heavily damaged and difficult to describe morphologically. M^2 and M^3 are subequally long; the width of the lobes decreases regularly, from M^1 to M^3 distal (Fig. 4C-D). The right M^2 is also partially preserved to a height of about 25 mm, while the left M^2 and both M^3 are broken close to the level of the alveoles. In all molars, the labial styles have the

same development as in modern camels: parastyle and mesostyle (mesial and central styles) are robust; the metastyle (distal style) is weak. The ribs are inconspicuous.

The pterygoid wings and the basisphenoid are not preserved. The glenoid fossa bears a large and prominent medial lip; the lateral parts of both fossae are broken. No peculiar character could be identified in the tympanic and petrosal region, in large part because this region is heavily damaged and filled with hard sediment. The paracondylar processes and the tympanic bullae are broken as well. The anterior lip of the occipital condyles shows a clear constriction. The mastoid foramina are broad and deep.

The low sagittal crest and small caniniform P^1 suggest that this individual was a female. The degree of dental wear cannot be judged because the teeth are too damaged, but the M^3 are fully erupted, while the P^1 is about to erupt; in extant *Camelus* species, this corresponds to an age approaching 7 years (Köhler-Rollefson 1989; Lesbre 1903).

Maxilla

Nad-1 A16-45 is a fragmentary left maxilla including the dental series P^4-M^2, to which the M^3 Nad-1 A16-39 can be fitted perfectly (Fig. 2A). The maxillar bone is highly damaged and not informative. The dentition is in advanced wear; M^1 has reduced enamel islets. P^4 is slightly damaged on the occlusal surface but is broken off and dislodged from its root. It is large and semicircular, with developed anterior style but imperceptible rib and posterior style. M^1 is mesiolabially broken; the mesial enamel islet (anterior fossa) is completely effaced, the distal one is very narrow although still long. The parastyle is not preserved; the mesostyle is well-developed; the distal rib and metastyle are absent. This is the widest molar and is also relatively long; both lobes are subequal and twice as wide as long, giving the tooth an almost square shape. M^2 is complete and has an intact occlusal surface, with a low but sharp relief. Parastyle and mesostyle are developed but less prominent than in M^1; however, both ribs and the metastyle are more pronounced than in that

tooth. This is the longest molar, and is overall wide; the mesial lobe is as broad as M^1, but the distal lobe is distinctly narrower, although of the same mesiodistal length. The M^3 has been recorded as a separate specimen, with the number Nad-1 A16-39; the preserved bone and sediment show that it belongs to this maxilla. The tooth is as well preserved as the M2; all three labial styles are developed, and the ribs are noticeable. The mesial lobe is close in size to the distal lobe of M2; the distal lobe is much narrower. Overall, this is the smallest molar. The labial walls of both lobes are almost parallel to each other.

Upper dentition

A16-46 is a damaged right M^2 in advanced wear, which shows similar measurements as its equivalent A16-39; both have a wide occlusal surface with a 5 mm narrower distal lobe. The parastyle is well developed, the other styles are broken.

A16-38 is a well-preserved left M^3. Its morphology, size and proportions are similar to the equivalent tooth in the maxilla A16-45, but it is slightly large. The parastyle and mesostyle are strongly developed, the metastyle and the ribs are pronounced as well, and the distal lobe is narrower than the mesial lobe. Surprisingly, this specimen bears a pillar (outer enamel fold) on the distolingual surface of the medial lobe, adjacent to the distal lobe. We interpret this lingual fold as an individual variation, not as a diagnostic character.

Mandibula

Three fragmentary mandibles, all from Doline 3 (Unit A/B), share a low but very massive corpus (Fig. 2C-D). Nad-1 A16-8 preserves M_2, roots of M_1 and the distal root of P_4 (Fig. 2G). The labial side is cracked, hence it is unclear if a mental foramen is present in this fragment. M_1 appears large and wide. M_2 has excellent preservation: its subequal lobes are longer than broad, with weakly defined styles and ribs. It shows moderate wear. In Nad-1 A16-27 only the roots of M_3 and the

distal root of M_2 are present; M_3 has moderate length and is quite narrow (Fig. 3F). Nad-1 A16-36 bears important damages on the lingual side (Fig. 3E). M_1 is only represented by root fragments, while M_3 and M_2 are perfectly preserved. The dentition is in full but not advanced wear. The lingual styles are very weak, the central ones almost absent. The occlusal profile is rounded to sharp. M_2 is of average length and is rather narrow. M_3 is rather short and of average width. No mental foramen is visible in the latter two specimens.

Lower dentition

All isolated teeth are from Doline 3 (Unit A/B). The sample includes 8 caniniform teeth. They can tentatively be identified at their position and sex, but are taxonomically not diagnostic.

Nad-1 A16-18 is a P_4 in initial wear. Its measurements show that it is long and narrow, but the reduced wear complicates a direct comparison to extant species (Fig. 4E).

Five isolated M_2 (Nad-1 A16-19, Nad-1 A16-20, Nad-1 A16-34, Nad-1 A16-43 and Nad-1 A16-44) show a modestly developed mesostylid, but metastylid, entostylid and ribs are very weak to absent. Apically, the distal lobe is longer than the mesial lobe, while closer to the roots the difference is small. All M_2 are relatively long with a narrow occlusal surface (Fig. 4F).

M_3 is represented by three isolated molars (Nad-1 A16-21, Nad-1 A16-41 and Nad-1 A16-42). The mesial lobe is larger than the central lobe; the mesostylid is developed, but ribs and other lingual stylids are absent. The distal lobe (hypoconulid) has an oblique lingual wall and a prominent distal stylid. Size and proportion of the M_3 are average.

Humerus

Only the distal part of the humerus is known from a large left fragment (Nad-1 G11-700), preserving almost half of the diaphysis, with a length of 209 mm along the medial side (Fig. 5E-G).

The medial epicondyle is damaged. The diaphysis has a distinctly greater inclination than in extant camels. The olecranon fossa is wide, but not very long. The muscular attachment fossa (for the lateral digit extensor) on the lateral side of the trochlea is long (Fig. 5F). The trochlea itself is relatively narrow, with a broad medial part, narrow lateral part and deep axial groove. The combination of size and inclination of the shaft is peculiar, but not highly diagnostic. Two additional distal fragments do not add further details.

Radioulnare

The morphology of the radioulnare is represented by three proximal fragments and four distal fragments, all of which are damaged or weathered. The proximal specimens indicate that the anconeus process is short, while the olecranon is thin; the proximal articular surface is very similar as in extant camels, but the articular fovea appears narrower. In the four distal fragments, the whole distal region is narrow, compared to the articular surface (Fig. 6D); this indicates reduced medial and lateral styloid processi. The medial condyle is narrower than the lateral one; its dorsal lip appears little developed. The medial dorsal ridge is relatively high, while the axial ridge is reduced (Fig. 6C). We notice that the variability of the distal region tends to be high, the relative measurement poorly reliable, and we have to regard these observations as tentative. However, as all specimens are quite similar, we assign them to the same species.

Carpalia

Several carpalia are present in the sample: four scaphoidea, four lunata, two triquetra, one hamatum and two trapezoidea are assigned to *Camelus roris*.

The scaphoidea are of average size, narrow and tall, especially in the dorsal region (Fig. 10B). The palmar distal facet (for the trapezoideum) is small, while the palmar lateral facet (for the lunatum) is elongated (Fig. 10A).

The lunata are moderately large, but do not have remarkable morphological characters.

The triquetra have relatively long proximal and distal facets.

The hamatum is quite small and low in the dorsal region. The proximal facet is narrow but the palmar region is massive and broad, with a dorsally shifted capitatum facet, causing the medial notch to be shallow.

The trapezoideum has a rather narrow distal facet.

Metacarpale

There are three proximal fragments of metacarpale, but neither morphology nor their measurements allow characterizing them compared to modern camel species. Six fragmentary condyles have a narrow shape, and as a group show very little metric variation (Fig. 7).

Femur

The femur is represented by six isolated femoral heads, a proximal fragment and two distal fragments. The heads show a diameter variation comparable to that of extant species, with a rather large average size. The largest head in the sample belongs to Nad-1 F18-11, a proximal fragment preserving also the neck and a part of the greater trochanter; interestingly, these features are even more massive than the head, suggesting an overall robust femur. This is the case also for the distal fragment Nad-1 E18-111 (Fig. 5C), which is large and has a particularly wide cranial trochlea, but condyles close to each other, forming a proportionally narrow distal articulation (Fig. 6B).

Patella

The three specimens of patella vary in the thickness of the proximal region, but are very close in shape and other measurements . They are deep and large and their articular facet is broader proximally than distally (Fig. 6F).

Tarsalia

The sample includes eight astragali, five calcanei, two cuboidea, one naviculare and one intermediolateral cuneiform.

The astragali are similar to each other, showing low metric variation; however, they are also very similar to extant camel species (Fig. 9B-D). They are relatively slender, have average size, a narrow calcaneal surface (Fig. 10C) and a small lateral condyle of the distal trochlea (articular surface for the cuboid), compared to the medial part (articular surface for the navicular; Fig. 10D). The length of the proximal lateral lip is intermediate.

The four calcanei are rather large and share several distinctive characters (Fig. 9F-I). The general shape is slender. The tuber is elongated and not particularly massive. The plantar border is thick but plantarly barely prominent (Fig. 11A). The sustentaculum is placed plantarly (Fig. 11B). The short cuboid facet is distally prominent, with a noticeably large distance between its distal tip and the malleolar condyle (or fibular trochlea).

In both cuboideum specimens the dorsal region is low and the proximal astragalar facet is broad (Fig. 11C). The latter character is in contrast with the narrow cuboid articular surface of the astragali (Fig. 10D).

The only naviculare is wide and large, but rather short. It has a tall palmar part and a deep and narrow articular concavity (Fig. 11D). The dorsolateral distal facet is proportionally small, while the palmar distal facet is relatively large.

The intermediolateral cuneiforme is narrow, low and deep, especially the proximal facet.

Metatarsale

Five proximal fragments of metatarsale are overall rather broad. The proximoplantar process (termed pygmaios in Giraffidae (Ríos et al. 2016)) is rather narrow and elongated (Fig. 8B). The facet of the III metatarsale (medial) is narrow, while that of the IV metatarsale (lateral) is broad; these two characters combined show a small metric variation and tightly unite all five specimens (Fig. 8A). The distal metatarsale (Fig. 5D) is represented by three fragments. The measurements of the condyles are all close to each other, indicating deep and narrow proportions (Fig. 7).

Proximal phalanx

The posterior proximal phalanx is well represented, with four complete specimens similar to each other (Fig. 9J-K and 9M-N): they share a narrow articular surface and deep condyles (Fig. 8D), with condyle lips of intermediate length (Fig. 8C). A single distal fragment of anterior proximal phalanx shares this morphology and is assigned to the same species (Fig. 9L).

Intermediate phalanx

The sample includes two complete specimens and two distal fragments of intermediate phalanx. The proximal articulation is wide, with a prominent volar region, so that the facet is tilted dorsally. The proximal surface for ligament attachment, on the sides of the diaphysis, extends further distally, reaching close to the condyle. The condyle is relatively narrow, with rather short abaxial lips.

Distal phalanx

Four specimens of distal phalanx have an overall triangular shape, less rounded than in extant species. The height is low, the abaxial side is long and the apex points toward the axial side.

Comparison

The holotype cranium and paratype maxilla share some dental proportions that we consider diagnostic for *Camelus roris*: P^4 is large (Fig. 4A), M^1 is large (Fig. 4B), M^2 is characterized by its distal lobe narrower than the mesial lobe (Fig. 4D), and M^3 is small, in particular when compared to M^1 (Fig. 4C). The ratio of the alveolar length of M^1 to that or M^3 is 75% or more in both specimens, while in extant *Camelus* species and *C. thomasi* it is included between 50% and 70%; only in one *C. dromedarius* it is above this interval.

It is not possible to compare our data with those from the literature, because the latter do not specify if the measurements are taken on the occlusal surface or at the alveolar level, and the difference is important in the case of M^1. Published upper dentition measurements indicate that, compared with *Camelus roris*, the species *C. knoblochi, Paracamelus gigas* and "*Camelus" sivalensis* are much larger (Gaur et al. 1984; Titov 2008; Zdansky 1926), *P. alexejevi* is of similar size (Logvynenko 2000), and *P. alutensis* is smaller (Kostopoulos and Sen 1999).

The inferior dentition assigned to *Camelus roris* has similar proportions as the upper dentition: P_4 and M_1 are long (Fig. 4E), M_2 is longer than the average in extant species (Fig. 4F, and M_3 is rather short. P4 appears narrow (but the single specimen is almost unworn; Fig. 4E), M1 is wide, M_2 is narrow, included within the variation of *C. dromedarius* but outside that of *C. bactrianus*(Fig. 4F), and M3 is overall small but not especially narrow.

Camelus bactrianus

The cranium Nad-1 F14-671 is close in size to *C. bactrianus*. Its preorbital and infraorbital region is bulging, while in *C. bactrianus* it is shallowly concave. The position of the orbit is lower, but a maxillar crest is present in both species. The supraorbital notch is dorsally convex and deeper than in modern camels, where it is consistently concave dorsally. The orbit has its highest point in the rostral part, caudal to it there is a broad superciliar arch, the zygomatic process of the frontal is less vertical and constricted in the middle, then the ventral part of the rim becomes abruptly wider; while in *C. bactrianus*, the highest point of the orbit is in the caudal part, where the superciliar arch is constricted at the dorsal basis of the zygomatic process of the frontal, but caudally and ventrally the rim of the orbit has a constant mediolateral width. Both species share a thick zygomatic arch, whose suture reaches close to the orbit. The postorbital constriction is less deep and more distant from the orbit; the anterior medial border of the temporal fossa (the posterior lateral border of the frontal) is not as concave as in *C. bactrianus.* The dorsal outline of the forehead has the shape of a rhombus with straight sides, while in *C. bactrianus* the sides are concave. The braincase is narrower. The temporal squama is laterally convex, and the occipital crest is straight with a blunt border; there is a distinct bend between the temporal and occipital crest. In *C. bactrianus* both crests are straight or only gently concave, and there is no clear transition between the two. The palate is narrower than in *C. bactrianus*, but in both species the palatine foramina are found the middle of M^1. The upper dentition of *Camelus roris* differs from that of both extant species: M^1 is longer and wider, while M^3 and the distal lobe of M^2 are reduced in size. The choana bears a caudal nasal spine, and the glenoid fossa has a strong medial lip: both characters are uncommon in *C. bactrianus*. Mandibles assigned to *Camelus roris* have a thicker corpus than the average *C. bactrianus*, varying from Nad-1 A16-27 which falls within this extant species' variation, to the strongly pachyostotic Nad-1 A16-8. The known lower dentition include a P_4 that, although barely in wear, is as long as the largest *C. bactrianus* but much narrower; the only M_1 is larger in all

dimensions; M_2 is comparably long but narrower, especially at the occlusal level; M_3 is on average shorter. The distal fragment of humerus Nad-1 G11-700 is larger than most *C. bactrianus* specimens, with a longer distal lateral attachment fossa (73 mm; in *C. bactrianus* NMB 10390 = 63 mm) and a greater inclination of the diaphysis. The radioulnare differs in having a thin olecranon, a short anconeus, a narrow proximal articular fovea (of the radius), a medial distal condyle narrower than the lateral one, large medial dorsal crest and small medial axial crest (the results for the radioulnare are tentative). The scaphoideum is narrower and dorsally taller, with a smaller palmar distal facet and longer palmar lateral facet. The hamatum is dorsally lower and palmarly more massive. No difference was noticed in the lunatum, triquetrum and trapezoideum. The proximal articulation of the metacarpale is similar, but the condyles are narrower. The head of the femur has a similar variation in diameter as in *C. bactrianus*, but the distal trochlea is wider. The patella is larger and has a greater maximal thickness. No difference is found in the fibula. The astragalus has a narrow calcaneal facet and on average a more prominent lateral part of the proximal trochlea. The calcaneus is more slender, with an elongate tuber, a thick plantar border, a plantarly placed sustentaculum, and a distally prominent cuboid facet. The cuboideum is dorsally low and has a broader proximal lateral facet. In the naviculare, the dorsolateral distal facet is relatively small, while the palmar distal facet is large. The proximal articulation of the metatarsale has a narrow and long plantar process; the distal condyles are deep and narrow. The articulation of the posterior proximal phalanx is narrow; the condyles of both anterior and posterior proximal phalanx are narrow and deep, with longer lips than in *C. bactrianus*. The intermediate phalanx is straight rather than axially curved, with an articular facet facing slightly dorsally and a shorter condyle whose lips have the same length. The distal phalanx is low and less rounded, with a longer abaxial side and an apex pointing axially rather than abaxially.

Camelus dromedarius

Compared to *C. dromedarius*, the cranium Nad-1 F14-671 has an overall larger size and is strikingly more massive: in particular, its elongate, bulging preorbital region and shallow, caudal postorbital constriction contrast vividly with the short, concave preorbital region and the postorbital constriction deep and close to the orbits in *C. dromedarius*. Hence, the frontal outline of the latter species appears almost shaped like a cross. The placement of the orbit is similarly low, but Nad-1 F14-671 has a maxillar crest. The supraorbital notch is dorsally convex, not concave as in extant camel species. The conformation of the orbits closely matches that in *C. dromedarius*, but the orbital rim differs in being much thicker and more massive. Unlike *C. dromedarius*, the zygomatic arch is thick and its suture reaches near to the orbit. The temporal squama is convex, while the occipital crest is relatively straight; the opposite situation is true in *C. dromedarius*, but in either case a distinct bend separates the two crests. The palatine foramina are found at the level of the middle of M^1, which is a more caudal position than in *C. dromedarius*, where they are almost always rostral to the contact point of P^4-M^1 (in one specimen, at the level of the anterior part of M^1). The cheek tooth row is longer. Other dental differences are the same as for *C. bactrianus*, whose upper dentition cannot be diagnosed from that of *C. dromedarius* (Martini et al. 2017). The shape of the choana and of the glenoid fossa is the same. The anterior lip of the condyles has a deep constriction, which is uncommon in *C. dromedarius*. The mandibula is much thicker than in *C. dromedarius*. The barely worn P_4 is longer but narrow; M_1 is larger; P_4 andare poorly known; M_2 is equally broad at the occlusal surface but broader at the alveolar level; M_3 does not show differences. The humerus Nad-1 G11-700 is larger, with a greater inclination of the shaft; the distal lateral attachment fossa is longer but the difference is less apparent than with *C. bactrianus*. The radioulnare has a narrower proximal fovea, broad distal articular surface compared to the distal width, smaller dorsal lip of the medial condyle and small axial dorsal crest (this description of the radioulnare are tentative). The scaphoideum is on average narrower, proximally deeper than

distally, dorsally high and has a combination of small palmar distal facet and long palmar lateral facet. The lunatum is larger, and its proximal facet is dorsally narrow. The hamatum is dorsally low and palmarly massive, with a small medial notch. The triquetrum and trapezoideum do not differ. The femur, including the caput, is larger; the distal articulation has similar proportions. The patella is larger, with articular facet proximally broader than distally; the opposite is true in *C. dromedarius*. No difference is found in the fibula. In the astragalus, the lateral part of the proximal trochlea is less prominent and the distal trochlea is medially larger, laterally narrower. The calcaneus is morphologically similar but larger. The cuboideum is similar. The naviculare is larger, relatively taller and broader but shorter and with a small dorsolateral distal facet. The proximal metatarsale and the distal condyles of both metacarpale and metatarsale are similar in *C. dromedarius*. Both anterior and posterior proximal phalanges have a narrow, deep condyle with shorter lips, but do not differ in the proximal articular surface. The intermediate phalanx has a dorsally tilted, large articular facet and a narrow, deep condyle. The distal phalanx is lower and less rounded.

Camelus knoblochi

The *C. knoblochi* cranium ROMK (no number) from Razdorskaya, Rostov Region, Russia (Titov 2008) is larger than Nad-1 F14-671 and differs in lacking a maxillar crest. The orbits have a dorsally concave supraorbital notch and the highest point of the border in the caudal half, unlike Nad-1 F14-671, they are also placed higher above the alveolar border. The frontal outline is comparable to the Nadaouiyeh cranium in showing a shallower constriction of the preorbital and postorbital regions than extant camels; the postorbital constriction is also distant from the orbits. The zygomatic arch appears relatively thinner. The temporal crest is rather straight. The palate appears wider than modern camels or Nad-1 F14-671, with palatine foramina placed at a level between M^2 and M^3; in all other *Camelus* crania, they are placed anterior to the middle of M^2. The choana has an ogival outline, without a caudal nasal spine. The glenoid fossa has a rectangular

shape, without a well-developed anteromedial lip. The condyles are small. The morphology and proportions of the upper dentition appear close to those of extant camel species, and unlike *Camelus roris*; M^1 is small and clearly not wider than the other molars, the lobes of M^2 and M^3 are subequal in size, and M^3 is large. Moreover, this northern camel is much larger. Additional published measurements (Titov 2008) indicate that in *C. knoblochi* the mandibula is taller than *C. roris,* narrower at the level of M_1, and rather similar in width at the level of M_3. The lower dentition include: large P_4, M_1 wide but not very long, M_2 and M_3 very large, proportionally broad and well beyond the size of extant camels or of *C. roris*. The metapodia of *C. knoblochi* are much larger than any found in Nadaouiyeh.

Camelus thomasi

Camelus thomasi is represented by the cranium TER-1689 from Tighennif, Algeria (Martini and Geraads 2018). In dorsal view, the preorbital constriction is shallower and the postorbital constriction is close to the orbit, unlike in Nad-1 F14-671; these characters give it a frontal outline with shallow concave sides, like in *C. bactrianus*. The postorbital constriction is deformed, but nevertheless appears wider than in Nad-1 F14-671; the braincase is also wider. The orbits are in a low position, similar to Nad-1 F14-671, but due to damage they cannot be compared in detail. The two fossil crania share the presence of a maxillar crest. In the Tighennif form, the occipital condyles are rostrally narrow, with a shallow constriction, but caudally very wide. The palatine foramina are found at the level of P^4, as in *C. dromedarius* and unlike Nad-1 F14-671. The upper dentition bears strong labial styles and similarly to *C. roris,* M^1 is wide and M^2 has a narrower distal lobe; however, *C. thomasi* differs in its shorter M^1, with lower ratio of alveolar length to M^3. The mandibular and postcranial sample from Tighennif shows a larger size than extant species or *C. roris* (Martini and Geraads 2018). Both forms have a pachyostotic mandible, but more so in the Tighennif camel. The lower dentition is similar; only M_2 is distinctly broader and on average shorter in *C. thomasi*. In the latter, the calcaneus has larger size, a wider but shorter tuber, the sustentaculum is more plantarly

placed and the plantar border is narrower. The astragalus is also larger in *C. thomasi*, but the morphology and proportion do not appear to differ. Both species have narrow and deep metapodial condyles. The proximoplantar process of the metatarsus (pygmaios) is long and narrow in *C. roris*, short and broad in *C. thomasi*. The condyles of proximal phalanges have lips that are subequal in the latter, while in C. roris and extant species the abaxial lip is clearly longer.

A few Pleistocene camel remains of very large size have been assigned to *Camelus thomasi*, such as three fossil specimens found at the Late Middle palaeolithic site of Far'ah II, Negev Desert, Israel (dated to 50 Ka) (Grigson 1983) or the partial skeleton from Site 1040, near the boundary between Egypt and Nubia (Gautier 1966). The recent description of the Tighennif sample (Martini and Geraads 2018) indicates that these specimens largely exceed the size of *C. thomasi*; as *Camelus roris* is even smaller, these specimens can be excluded.

The unidentified camelid maxilla JMI 50 from the Nefud desert is said to differ from *C. thomasi* and *C. dromedarius* in its palatine foramen found at the level of M^1 (Thomas et al. 1998). In this character it corresponds much better to Nad-1 F14-671. This late Middle Pleistocene faunal assemblage presents a strong similarity to the faunas found in Nadaouiyeh (also dated to the Middle Pleistocene) and other sites in the El Kowm Basin (Reynaud Savioz 2011), which is geographically and ecologically close to the Nefud desert. Therefore, the two sites are likely to share the same camel species, but unfortunately this maxilla is the only camelid specimen (Stimpson et al. 2016) and it is described as too poorly preserved for a convincing identification.

Camelus grattardi

Camelus grattardi is known from the maxilla Omo 75S-70-956 with P^4-M^2, which is completed with the M^3 Omo 75-69-2222, and additional dental and postcranial material. The most important diagnostic characters are the reduced P^4 and enlarged M^1; the size difference between

them is not encountered in any other Old World camelid (Geraads 2014). In Nad-1 F14-671, P^4 is large, M^1 is enlarged to a lesser extent, M^3 and the distal lobe of M^2 are reduced.

The distal left humerus Nad-1 G11-700 can be compared with the right specimen L1-68-78 assigned to *Camelus grattardi*. While the former has a diaphysis which is strongly inclined, the long axis of this bone in *C. grattardi* is almost perpendicular to the distal articulation (Geraads 2014); the distal articulation is also more symmetrical, while in Nad-1 G11-700 and extant species the medial trochlea is larger than the lateral capitulum.

Camelus sivalensis

The diagnosis of *"Camelus" sivalensis* rests mainly on dental and mandibular characters and is not clear-cut (Colbert 1935b; Matthew 1929; Nanda 2008). The original description and pictures of the cranium (Falconer and Murchison 1868) are poorly detailed. Additional material (Colbert 1935b; Gaur et al. 1984; Nanda 2008) indicates that both upper and lower premolar row are as developed as in *Paracamelus*, and unlike later *Camelus*; while the reduction of distal molars is distinctive for *C. roris*. The molar styles are strongly developed. All dental measurements indicate a larger animal than *C. roris*. The mandibula has a long, narrow symphysis closely resembling those in *Paracamelus*, which are correlated to an elongated facial part of the cranium. Postcranial descriptions of *"C." sivalensis* are very limited, as it is said to be similar to extant camels (Colbert 1935a; Falconer and Murchison 1868). The metacarpale is 479 mm long (Falconer and Murchison 1868), largely exceeding the extant species, *C. thomasi* and even *C. knoblochi*; however, the breadths of condyle and proximal metatarsalia (Grigson 1983) are very close to those of extant species and of the Nadaouiyeh sample.

Paracamelus

The genus *Paracamelus* is diagnosed from *Camelus* based on plesiomorphic traits (Geraads 2014; Harris et al. 2010); all the following differences are also valid with respect to *Camelus roris*. The main character of *Paracamelus* is the greater development of the facial part of the cranium and in particular of the premolar row: P^3 and P^4 are larger, P_3 is present in adults, and dP_2 is present in immatures, there is a large diastema between the cheek teeth and the caniniform anterior dentition, the symphysis is elongated, the rostral border of the orbit is found above M^3 and the caudal border is more posterior than the dentition (Havesson 1954; Titov 2003). In *Camelus roris*, P^4 is clearly smaller than M^1, the caniniform P^1 is rather close to the cheek teeth row, the orbit extends from above M^2 to above M^3 and the cranium is overall broad. Additionally, *Paracamelus* has more developed molar styles and lacks a maxillar crest. The Late Miocene *Paracamelus* species (*P. aguirrei* and *P. gigas*) are significantly larger than all younger camelid species, including *Camelus roris*. Only *Camelus knoblochi* can be compared in size with the early *Paracamelus*. Pliocene species (*P. praebactrianus* and *P. alexejevi*) are close in size to extant *Camelus*, and the Early Pleistocene *P. alutensis* is even smaller than *C. dromedarius*. Interestingly, *P. alutensis* shares with *C. roris* a reduction of the distal lobe of M^3 (Kostopoulos and Sen 1999). Postcranial differences, especially of the metapodia, that are sometimes included in the diagnosis of *Paracamelus* (Likius et al. 2003; Teilhard de Chardin and Trassaert 1937) are not considered valid (Geraads 2014).

Additional specimens from Nadaouiyeh

Camelus cf. roris

Maxilla

Nad-1 A16-35 is a fragmentary left maxilla, bearing M^2 and M^3 in initial wear; M^3 still has separate cusps, and the occlusal relief is high and sharp (Fig. 2B). Little of the maxillar bone is preserved, while the dentition is cracked but complete. In both teeth, parastyles and mesostyles are well expressed, while ribs and metastyles are weak. M2 is narrow, with both lobes similar in width; the distal lobe of M3 is narrower than the mesial lobe.

Nad-1 A16-37 is another fragmentary left maxilla, bearing M^2 and M^3 with a greater degree of wear than Nad-1 A16-35 (Fig. 2C). The maxillar bone is very fragmentary and poorly preserved. M^2 is complete, while M^3 has a damaged occlusal surface; however, its cusps are already fused. The occlusal relief has a middle height and is rather rounded. The parastyles and mesostyles are well expressed; ribs are weak, metastyles are broken in both teeth. Like in A16-35, both lobes of M^2 are similarly narrow, while M^3 becomes narrower distally.

The two formerly described specimens of maxilla are similar to each other in the proportions of the lobes and development of styles; Nad-1 A16-37 is comparable to the maxilla Nad-1 A16-45, but this specimen and the cranium Nad-1 F14-671 have asymmetric M^2 lobes, unlike Nad-1 A16-35 and Nad-1 A16-37. The latter two do not preserve M^1, and M^3 alone is not diagnostic. Therefore, it is not possible to definitely assign these specimens to *Camelus roris*. However, it is conceivable that the variation of this species includes the described proportions of the M^2; both individuals are younger than Nad-1 A16-45, which might explain the difference (although the cranium Nad-1 F14-671 is young too). On the other hand, if there was a second camel species coexisting with Nad-1

A16-45, it is unlikely that it would be so similar in size and development of labial styles. We conclude that these two fragments of maxilla can be assigned to *Camelus cf. roris*.

Mandibula

Nad-1 H13-703 (layer 8a, Unit D) is a relatively complete mandibula, preserving the ramus almost undamaged and part of the corpus until the alveoli of M_2, but no dentition except the roots of M_3 (Fig. 2D). It is comparable in size to *C. bactrianus*, but more massive and stout. The short coronoid process is strongly slanted backwards, forming a very open angle with the sloping alveolar ridge. Its outline is subtriangular, thick and broad at the basis but narrowing and curving gently toward the rounded apex. This shape is distinct from *C. dromedarius* (short, straight, thin and with a squared tip), *C. bactrianus*, *C. sivalensis* (both long, hook-shaped) and *C. thomasi* (bent backwards, twisted laterally and wider at the top). The cranial condylar notch is narrow. The condyle is slightly deformed and rather narrow, like in *C. dromedarius*, but with a large caudal lip and a clear lateral slope as in *C. bactrianus*. Its neck is thick. The caudal condylar notch is tall, deep and wide. The angular process is missing. On the mesial side of the ramus, the mandibular foramen is small. Most importantly, the preserved posterior part of the corpus is massive and tall: the alveolar ridge forms a relatively steep slope with respect to the ventral side, but a wide angle with the ascending ramus.

This specimen differs from the mandibles found in Doline 3 by its height distal to M_3. However, they share similar proportion of M_3 and massiveness. Other camel species, like *C. bactrianus* and *C. thomasi* (and possibly *C. sivalensis*) also have an important variation in posterior corpus height (Colbert 1935a; Martini and Geraads 2018; Martini et al. 2017); hence, this character does not definitely preclude the assignment of Nad-1 H13-703 to the same species as that found in Doline 3. It is considered *Camelus cf. roris*.

Anterior dentition

Eight specimen from Doline 3 are identified as caniniform dentition; of these, five are considered to be P_1, two are true C (one male and one female), and one is identified as a male I3. The caniniform dentition is very variable in morphology and size according to both age and sex; on the other hand, no taxonomic diagnostic trait could be identified, leading to their assignment to *Camelus cf. roris.*

"Black Hummal" short bones

The "Black Hummal" reworked sediments) has yielded only six specimens. Two of them differ morphologically from the sample as described above. The scaphoideum Nad-1 SP7-43.4 is small, short and dorsally low (instead of dorsally tall). It also shows a narrow distal dorsal facet (for the capitatum), but agrees with the other Nadaouiyeh specimens in having a small palmar distal facet (for the trapezoideum) and an elongated palmar lateral facet (for the lunatum). The hamatum Nad-1 SP7-43.5, is small, low in the palmar region (instead of low in the dorsal region) and has elongated facets. The other specimens from this layer (triquetrum, intermediolateral cuneiforme, femur head and distal fragment of astragalus) cannot be separated from other corresponding elements, but all share small size. This suggests that all the specimen belong to the same juvenile individual, which might also explain the morphological differences. Lacking strong diagnostic traits in either direction, we assign the whole "Black Hummal" sample to *Camelus cf. roris*.

Camelus sp.

Mandibula

Nad-1 F16-1282 is a small fragment of mandibular corpus, preserving alveoli and three broken roots that are tentatively identified as the two roots of M_1 with the mesial root of P_4, right side. The corpus is not massive; ventrally it is broken. The space between two of the roots is elevated and ossified, which can happen between the roots of the same molar when heavily worn (especially in M_1), but not between the roots of different teeth. Considering these two roots as belonging to the same molar, its alveolar length is of 26 mm, which is reasonable as M_1 but would be very short as M_2. However, the three roots are similar in breadth (presumed P_4 = 17 mm, presumed M_1 mesial = 16.5 mm, presumed M_1 mesial = 15 mm) while in modern species there is an increase in width from P_4 to M_2 mesial. On the other hand, the width of the roots in M_2 and M_3 is constant but much larger than in this fossil specimen. Hence, we tentatively interpret this fragment as the roots of P_4 mesial and roots of M_1, in an older individual of a rather small camel form, characterized by enlarged P_4. The narrowness of the corpus and the small size of presumed M1 are important differences between this specimen and all other mandibles known in Nadaouiyeh, that don't allow the assignment of Nad-1 F16-1282 to the same species as Nad-1 A16-8 and others. It is considered *Camelus sp*.

Scapula

Nad-1 E15-71 is a left scapula preserving the complete glenoid fossa, with slightly damaged edges and missing coracoid process; about two-thirds of the spine, with missing acromion; a small part of the supraspinatous fossa and a more substantial portion of the infraspinatous fossa (Fig. 5B). This specimen appears very similar to a massive *C. bactrianus*, with thicker caudal border and spine. Height and inclination of the spine seem the same as in that species. The neck is deep. The glenoid fossa is craniocaudally elongated; otherwise the distal articulation is similar to extant species.

Nad-1 H14-755 is a mostly complete scapula: only the cranial proximal region is broken, while the caudal proximal angle is preserved (Fig. 5A). The surface is completely cracked and in some spots broken. The caudal border appears slightly deformed in lateral direction, while the spine is likely deformed caudally. In the distal part, the internal spongeous bone has collapsed causing further damage to the surface, but the edges remained stable. It also appears that the distal articulation has undergone a lateral twist relatively to the proximal region. The medial face is flat, without sign of deformation. The overall size is small. The spine is not straight as in extant camels, but rather curved towards the caudal side. It is high and distinctly bent over the infraspinatous fossa. The acromion is short, reaching to less than half the distance to the glenoid fossa. The distal lateral twist causes the coracoid process to be in a more lateral position relatively to the proximal region. The glenoid fossa is large. The coracoid process is slender and proximally retracted. The cranial border (scapular notch) is rather concave, and has the same thickness as in extant camels. The caudal border is thin and raised laterally; however it is very long. In extant camels the caudal border can be as long as the spine and is usually shorter, but in this specimen it is clearly longer. The caudal proximal angle is acute, measuring about 80°, implying a straight dorsal border and a very blunt cranial angle; in contrast, in extant camels the caudal angle is obtuse and the dorsal border is rounded.

As the two complete scapulae are very different from each other, and there is no way to assign either to the postcranium of *Camelus roris*, both are considered *Camelus sp*.

Nad-1 D17-294 is the distal articulation of a right scapula, preserving part of the articular fossa and part of the coracoid process. Although it is highly fragmentary, the surface is well preserved. The coracoid process is large. This fragment is not distinctive, thus is assigned to *Camelus sp*.

Tibia

The tibia is represented only by three heavily damaged distal fragments. All of them are relatively wide, and the cochlea of Nad-1 SP31-2.1 shows a deep medial fossa but rather short axial and lateral fossae. As the preservation is too poor to add any other measurements or observations, we assign all tibiae to *Camelus sp*.

Fibula

In *Camelus*, the fibula is reduced to the lateral malleolus. The sample includes three specimens: the best preserved specimen has morphology and proportions very similar to both extant camel species, another is small and narrow as in a juvenile, and the third is a large dorsal fragment. They do not resemble each other closely, and none shows any distinctive characters; therefore they cannot be considered diagnostic and are assigned to *Camelus sp*.

Proximal phalanx

Two specimens of anterior proximal phalanx are complete in the proximal part, but the distal region is damaged or missing and cannot be easily compared to the complete and diagnostic posterior phalanx. In Nad-1 F18-227 the proximal articulation is dorsopalmarly short, with an almost subrectangular shape. Nad-1 G16-1350 is very massive; the plantar furrow extends further and deeper onto the round proximal articulation surface. As the two specimens are rather different, they are both assigned to *Camelus sp*.

Stratigraphic association

Table 4 shows and compares the repartition of the material across the stratigraphic units of Nadaouiyeh. A number of skeletal elements of *Camelus roris* are distinctive and diagnosable from both extant species on the basis of multiple characters and proportions. The five richest units share several diagnostic elements, which can be assigned to *Camelus roris*. The other two, Unit A and Unit F (the youngest and the oldest, respectively) have each yielded a small number of fossils, which are poorly informative but morphologically compatible with specimens from other parts of the stratigraphy. The only elements represented by multiple specimens showing differences beyond intraspecific variation are the scapula (in units B and C) and the mandibula (a fragment found in Unit D).

Discussion

The Middle Pleistocene locality of Nadaouiyeh Aïn Askar, El Kowm Basin, Syria has yielded a cranium and abundant mandibular, dental and postcranial remains of a new camel species, here named *Camelus roris*. Its size is comparable to the extant Bactrian camel (*C. bactrianus*), which is slightly larger than the dromedary (*C. dromedarius*) but smaller than the extinct *C. thomasi, C. knoblochi*, "*Camelus*" *sivalensis* and most species of *Paracamelus*. The new Syrian camel differs from *Paracamelus* in the reduction of the premolar rows, common to other *Camelus*; it differs from the latter in the relatively large size of the anterior remaining teeth (P4 and M1) and small size of the posterior (M3 and distal lobe of M2), proportions well marked in the upper dentition but apparently present also in the mandible.

The sample is divided into seven stratigraphic units, covering the period between 500 Ka and 200 Ka. As we have found that two different camel species can occur in the same fossil association (Martini et al. 2015), the moderately deep sequence of Nadaouiyeh might include more than one species. Comparing the distribution of diagnostic skeletal elements across the units (table 3), it

appears that most of the material is found over more than one unit, consistently showing the same morphology and linking the type material of *Camelus roris* to all parts of the sequence. Although each element is represented by only few specimens, we have not noticed any trend in size or morphology. Hence, the large majority of the camelid fossils can be assigned to the same species.

However, a very limited number of specimens suggest that other camel forms have occasionally entered the site. Two anterior proximal phalanges (Nad-1 F18-227 and Nad-1 G16-1350) are unlike each other in the articular surface, but the difference is not strong. A fragment of mandible (Nad-1 F16-1282, Unit D) is of difficult interpretation; we suggest that it might represent an older individual of a rather small camel form, characterized by a large P_4. We are cautious in drawing conclusions from this specimen; however it is very different from the other mandibles, which are larger, pachyostotic and with P_4 as reduced as in extant species. A compelling indication of the presence of a second species is the widely divergent anatomy of two complete scapulae, Nad-1 E15-71 (layer 7, basis of Unit B) and Nad-1 H14-755 (layer 8.1b, Unit C). The former is massive and similar to *C. bactrianus*, while the former is thin and morphologically very distinctive; they do not appear to be compatible with the variation of a single species. They are separated by a temporal hiatus likely shorter than 50 Ka.

This evidence suggests that during the Middle Pleistocene (at least) two different camel species coexisted in the Middle East. Considering that the remaining postcranial material demonstrates morphological continuity before and after the layers where the two scapulae are found, it follows that at the site of Nadaouiyeh Aïn Askar there was only one dominant camel form, but the sporadical presence or incursion of a second species occurred at least once.

The relationships of Quaternary *Camelus* species appear complex, with five well-known species (*C. bactrianus, C. dromedarius, C. knoblochi, C. roris* and *C. thomasi*) exhibiting a mosaic-

like distribution of cranial characters, such as dental proportions, position of palatine foramina, presence of maxillary crest, conformation of the orbit, and shape of the coronoid processes. Other traits such as overall proportions, size and presence of a maxillar crest, might be functional and therefore less useful for a phylogenetic reconstruction. *C. grattardi* is known only by a maxilla with peculiar dentition (Geraads 2014) and is presently even harder to put in an evolutionary context. The Pliocene or earliest Pleistocene "*Camelus*" *sivalensis* appears closer to the genus *Paracamelus* in the elongated face and unreduced premolar row; unfortunately it is poorly described and lacks a differential diagnosis from other *Camelus* and *Paracamelus* species (Colbert 1935a; Matthew 1929). The latter genus is supposedly ancestral to the extant camels, and is defined on plesiomorphic characters (Geraads 2014); however, the younger species such as *P. alexejevi* and *P. alutensis* seem too derived to be directly related to *Camelus*, while the older such as *P. gigas* or *P. aguirrei* are remote in time and morphology, and cannot be the immediate origin of the *Camelus* diversity. Pending the detailed description of the complete camelid collection from El Kowm, we refrain from proposing a phylogenetic hypothesis. We note that *C. dromedarius* is smaller than all other species, except for *P. alutensis* (Titov 2003) and the small camel from Mousterian layers in Hummal (Martini et al. 2015); this seems to be a derived condition, which can explain why *C. bactrianus* was often suggested to be closer to some fossil species (Gautier 1966; Geraads 2014; Kostopoulos and Athanassiou 2005). As we discussed, all extinct camels appear to share at least some diagnostic features with *C. dromedarius* and not with *C. bactrianus*; hence, we consider it incorrect to speculate on relationships based on superficial similarities, as it was done until now.

Conclusion

The middle-sized *Camelus roris* sp. nov. from the Middle Pleistocene locality of Nadaouiyeh Aïn Askar, El Kowm Basin, Syria, is known from a well-preserved cranium and additional material including dentition, mandibles and postcranium. A few elements indicate the occasional presence of a second camelid species, but the largest majority of the recovered material can be referred to

Camelus roris that is now one of the most completely known Old World fossil camelids. While the description of a new species is already a significant improvement in the poorly known record of Eurasian Camelidae, the ongoing study of other assemblages within the El Kowm Basin will shed light over a larger and dynamic diversity, covering almost two million years of their presently obscure evolution.

Acknowledgements

We are thankful to the useful comments by Bastien Mennecart and Denis Geraads; to Inna Popko for help with Russian and Ukrainian literature; to all the museum curators that allowed access to the comparative material in their care (listed in Martini &al 2017, to whom we add Denis Geraads, Museum National d'Histoire Naturelle, Paris); and to the Syrian team of collaborators, coordinated by Ahmed Taha, without whom the El Kowm excavations would not have been possible. This study is part of P. Martini's doctoral thesis, which is supported by the Swiss National Foundation, the Isaac Dreyfus-Bernheim Stiftung, and the Freiwillige Akademische Gesellschaft Basel.

References

ALÇIÇEK, M. C., S. MAYDA, and V. V. TITOV. 2013. Lower Pleistocene stratigraphy of the Burdur Basin of SW Anatolia. Comptes Rendus Palevol 12:1-11.

BELMAKER, M. 2010. Early Pleistocene Faunal Connections Between Africa and Eurasia: An Ecological Perspective. Pp. 183-205 in Out of Africa I: the First Hominin Colonization (J. G. Fleagle, J. J. Shea, F. E. Grine, A. L. Baden and R. E. Leakey, eds.). Springer.

BESANÇON, J., L. COPELAND, F. HOURS, S. MUHESEN, and P. SANLANVILLE. 1981. Le Paléolithique d'El Kowm. Rapport préliminaire. Paléorient 7:33-55.

BUCCELLATI, G., and M. K. BUCCELLATI. 1967. Archaeological Survey of the Palmyrene and the Jebel Bishri.

BURGER, P. A. 2016. The history of Old World camelids in the light of molecular genetics. Tropical animal health and production.

CAUVIN, J., M.-C. CAUVIN, and D. STORDEUR. 1979. Recherches préhistoriques à El Kowm (Syrie).

COLBERT, E. H. 1935a. Siwalik Mammals in the American Museum of Natural History. Transactions of the American Philosophical Society, New Series 26:i-x+1-401.

COLBERT, E. H. 1935b. Siwalik Mammals in the American Museum of Natural History. Transactions of the American Philosophical Society, New Series 26:1-401.

FALCONER, H., and C. MURCHISON. 1868. Palaeontological memoirs and notes of the late Hugh Falconer. Robert Hardwicke, London. 1 - Fauna Antiqua Sivalensis.

GAUR, R., P. RAGHAVAN, and S. R. K. CHOPRA. 1984. On the remains of *Camelus sivalensis* (Artiodactyla, Camelidae) from Pinjor Formation of Upper Siwaliks. Indian Journal of Earth Sciences 11:158-165.

GAUTIER, A. 1966. *Camelus thomasi* from the Northern Sudan and its bearing on the relationship *C. thomasi* - *C. bactrianus*. Journal of Paleontology 40:1368-1372.

GERAADS, D. 1986. Les ruminants du pleistocene d'Oubeidiyeh (Israel). Mémoires et Travaux du Centre de Recherches français de Jérusalem 5:143-181.

GERAADS, D. 2014. *Camelus grattardi*, sp. nov., a new camel from the Shungura Formation, Omo Valley, Ethiopia, and the relationships of African fossil Camelidae (Mammalia). Journal of Vertebrate Paleontology 34:1481-1485.

GERAADS, D. 2016. Pleistocene Carnivora (Mammalia) from Tighennif (Ternifine), Algeria. Geobios 49:445-458.

GRATTARD, J.-L., F. C. HOWELL, and Y. COPPENS. 1976. Remains of *Camelus* from the Shungura Formation, lower Omo Valley. Pp. 268–274 in Earliest Man and Environments in the Lake Rudolf Basin. (Y. Coppens, F. C. Howell, G. L. Isaac and R. E. Leakey, eds.). University of Chicago Press, Chicago.

GRIGGO, C. 2004. Mousterian fauna from Dederiyeh Cave and comparisons with Fauna from Umm El Tlel and Douara Cave. Paléorient 30:149-162.

GRIGSON, C. 1983. A very large camel from the upper Pleistocene of the Negev Desert. Journal of Archaeological Science 10:311-316.

HARINGTON, C. R. 2011. Pleistocene vertebrates of the Yukon Territory. Quaternary Science Reviews 30:2341-2354.

HARRIS, J. M., D. GERAADS, and N. SOLOUNIAS. 2010. Camelidae. Pp. 815-820 in Cenozoic Mammals of Africa (L. Werdelin and W. J. Sanders, eds.). University of California Press, London.

HAVESSON, Y. I. 1954. Третичные Верблюды Восточного Полушария (Род *Paracamelus*) [Tertiary camels from the Eastern Hemisphere (Genus *Paracamelus*)]. Trudy Paleontologicheskovo Instituta, Akademiya Nauk SSSR 47:100-162.

HONEY, J. J., J. A. HARRISON, D. R. PROTHERO, and M. S. STEVENS. 1998. Camelidae. Pp. 439-462 in Evolution of Tertiary Mammals of North America: Terrestrial Carnivores, Ungulates, and Ungulatelike Mammals (C. M. Janis, K. Scott and L. L. Jacobs, eds.). Cambridge University Press, Cambridge.

HOWELL, F. C., L. S. FICHTER, and R. WOLFF. 1969. Fossil Camels in the Omo Beds, Southern Ethiopia. Nature 223:150-152.

JAGHER, R. 2011. Nadaouiyeh Aïn Askar - Acheulean variability in the Central Syrian Desertin The Lower and Middle Palaeolithc in the Middle East and Neighbouring Regions (J. M. Le Tensorer, R. Jagher and M. Otte, eds.). Etudes et Recherches Archéologiques de l'Université de Liège (ERAUL), Liège.

JAGHER, R. 2016. Nadaouiyeh Aïn Askar, an example of Upper Acheulean variability in the Levant. Quaternary International 411:44-58.

JAGHER, R., H. EL SUEDE, and J. M. LE TENSORER. 2015. El Kowm Oasis, human settlement in the Syrian Desert during the Pleistocene. L'Anthropologie 119:542-580.

JAGHER, R., and J.-M. LE TENSORER. 2011. El Kowm, a key area for the palaeolithic of the Levant in Central Syriain The Lower and Middle Palaeolithc in the Middle East and Neighbouring Regions (J. M. Le Tensorer, R. Jagher and M. Otte, eds.). Etudes et Recherches Archéologiques de l'Université de Liège (ERAUL), Liège.

KÖHLER-ROLLEFSON, I. U. 1989. Zoological analysis of camel skeletons. Pp. 142-164 in Pella of the Decapolis. Vol. 2, Final Report on the College of Wooster Excavations in Area IX, the Civic Complex, 1979-1985 (R. H. Smith and L. P. Day, eds.). The College of Wooster, Wooster.

KOSTOPOULOS, D. S., and A. ATHANASSIOU. 2005. In the shadow of bovids: suids, cervids and giraffids from the plio-pleistocene of Greece. Pp. 179-190 in Les ongulés holarctiques du Pliocène et du Pléistocène (E. Crégut-Bonnoure, ed.). Maison de la géologie, Paris.

KOSTOPOULOS, D. S., and S. SEN. 1999. Late Pliocene (Villafranchian) mammals from Sarikol Tepe, Ankara, Turkey. Mitteilungen der Bayerischen Staatssammlung für Paläontologie und Historische Geologie 39:165-202.

KOZHAMKULOVA, B. S. 1986. The Late Cenozoic Two-Humped (Bactrian) Camels of Asia. Quartärpaläontologie 6:93-97.

LE TENSORER, J.-M., V. VON FALKENSTEIN, H. LE TENSORER, and S. MUHESEN. 2011. Hummal: A very long Paleolithic sequence in the steppe of Central Syria - Considerations on Lower Paleolithic and the beginning of Middle Paleolithicin The Lower and Middle Palaeolithc in

the Middle East and Neighbouring Regions (J. M. Le Tensorer, R. Jagher and M. Otte, eds.). Etudes et Recherches Archéologiques de l'Université de Liège (ERAUL), Liège.

LE TENSORER, J. M., H. LE TENSORER, P. MARTINI, V. VON FALKENSTEIN, P. SCHMID, and J. J. VILLALAIN. 2015. The Oldowan site Aïn al Fil (El Kowm, Syria) and the first humans of the Syrian Desert. L'Anthropologie 119:581-594.

LESBRE, F.-X. 1903. Recherches anatomiques sur les Camélidés. Pp. 1-196 in Archives du Muséum d'Histoire Naturelle de Lyon (H. Georg, ed.), Lyon.

LIKIUS, A., M. BRUNET, D. GERAADS, and P. VIGNAUD. 2003. Le plus vieux Camelidae (Mammalia, Artiodactyla) d'Afrique: limite Mio-Pliocène, Tchad. Bulletin de la Société Géologique de France 174:187-193.

LOGVYNENKO, V. M. 2000. Верблюды (Camelidae, Tylopoda) плиоцепа и эоплейстоцена Украины [The Camels (Camelidae, Tylopoda) from the Pliocene and Eopleistocene of Ukraine]. Vestnik zoologii Supplement N° 14:120-127.

MARTÍNEZ-NAVARRO, B., M. BELMAKER, and O. BAR-YOSEF. 2012. The Bovid assemblage (Bovidae, Mammalia) from the Early Pleistocene site of 'Ubeidiya, Israel: Biochronological and paleoecological implications for the fossil and lithic bearing strata. Quaternary International 267:78-97.

MARTINI, P. 2011.A metrical analysis of the morphological variation in extant and fossil camels. Master's thesis, University of Zürich, Zürich.

MARTINI, P., L. COSTEUR, J.-M. LE TENSORER, and P. SCHMID. 2015. Pleistocene camelids from the Syrian Desert: The diversity in El Kowm. L'Anthropologie 119:687-693.

MARTINI, P., and D. GERAADS. 2018. *Camelus thomasi* Pomel, 1893, from the Pleistocene type-locality Tighennif (Algeria): Comparisons with modern *Camelus*. Geodiversitas 40:115-134

MARTINI, P., P. SCHMID, and L. COSTEUR. 2017. Comparative Morphometry of Bactrian Camel and Dromedary. Journal of Mammalian Evolution.

MATTHEW, W. D. 1929. Critical Observations Upon Siwalik Mammals. Bulletin American Museum of Natural History 56:437-560.

MORALES, J., D. SORIA, and E. AGUIRRE. 1980. Camelido finimioceno en Venta del Moro. Primera cita para Europa Occidental. Estudios Geológicos 36:139-142.

NANDA, A. C. 1978. Occurrence of *Camelus sivalensis* Falconer and Cautley from the Tatrot Formation of Ambala, India. Journal of the Geological Society of India 19:160-164.

NANDA, A. C. 2008. Comments on the Pinjor Mammalian Fauna of the Siwalik Group in relation to the post-Siwalik faunas of Peninsular India and Indo-Gangetic Plain. Quaternary International 192:6-13.

NEHRING, A. 1901. Mittheilung über einen fossilen Kamel-Schädel (*Camelus Knoblochi*) von Sarepta an der Wolga. Sitzungsbericht der Gesellschaft Naturforschende Freunde 5.

PICKFORD, M., J. MORALES, and D. SORIA. 1995. Fossil camels from the Upper Miocene of Europe: implications for biogeography and faunal change. Geobios 28:641-650.

REYNAUD SAVIOZ, N. 2011. The faunal remains from Nadaouiyeh Aïn Askar (Syria). Preliminary indications of animal acquisition in an Acheulean site.in The Lower and Middle Palaeolithc in the Middle East and Neighbouring Regions (J. M. Le Tensorer, R. Jagher and M. Otte, eds.). Etudes et Recherches Archéologiques de l'Université de Liège (ERAUL), Liège.

REYNAUD SAVIOZ, N., and P. MOREL. 2005. La faune de Nadaouiyeh Aïn Askar (Syrie centrale, Pléistocène moyen) : aperçu et perspectives. Revue de Paléobiologie, Genève 10:31-35.

RÍOS, M., M. DANOWITZ, and N. SOLOUNIAS. 2016. First comprehensive morphological analysis on the metapodials of Giraffidae. Palaeontologia electronica 19.3.50A:1-39.

RYBCZYNSKI, N., J. C. GOSSE, C. R. HARINGTON, R. A. WOGELIUS, A. J. HIDY, and M. BUCKLEY. 2013. Mid-Pliocene warm-period deposits in the High Arctic yield insight into camel evolution. Nature communications 4:1550.

SCERRI, E. M. L., et al. 2014. Middle to Late Pleistocene human habitation in the western Nefud Desert, Saudi Arabia. Quaternary International.

SCHERER, C. S. 2013. The Camelidae (Mammalia, Artiodactyla) from the Quaternary of South America: Cladistic and Biogeographic Hypotheses. Journal of Mammalian Evolution 20:45-56.

SEMPREBON, G. M., and F. RIVALS. 2010. Trends in the paleodietary habits of fossil camels from the Tertiary and Quaternary of North America. Palaeogeography, Palaeoclimatology, Palaeoecology 295:131-145.

SEN, S. 2010. Camelids do not occur in the late Miocene mammal locality of Çobanpinar, Turkey. Russian Journal of Theriology 9:87-91.

STIMPSON, C. M., et al. 2016. Middle Pleistocene vertebrate fossils from the Nefud Desert, Saudi Arabia: Implications for biogeography and palaeoecology. Quaternary Science Reviews 143:13-36.

TEILHARD DE CHARDIN, P., and M. TRASSAERT. 1937. The Pliocene Camelidae, Giraffidae and Cervidae of South Eastern Shansi. Palaeontologia Sinica 102:1-56, pl. I-VI.

THOMAS, H., et al. 1998. Découverte des premières faunes pléistocènes de la pénisule Arabique dans le désert du Nafoud (Arabie Saoudite). Comptes rendus de l'Académie des Sciences de Paris 326:145-152.

TITOV, V. V. 2003. Paracamelus from the Late Pliocene of the Black Sea region. Pp. 17-24 in Advances in Vertebrate Paleontology: Hen to Panta (A. Petculescu and E. Stiuca, eds.), Bucharest.

TITOV, V. V. 2008. Habitat conditions for *Camelus knoblochi* and factors in its extinction. Quaternary International 179:120-125.

TITOV, V. V., and V. N. LOGVYNENKO. 2006. Early *Paracamelus* (Mammalia, Tylopoda) in Eastern Europe. Acta zoologica cracoviensia 49A:163-178.

VAN DER MADE, J., and J. MORALES. 1999. Family Camelidae. Pp. 221-224 in The Miocene Land Mammals of Europe (G. E. Rössner and K. Heissig, eds.). Verlag Dr. Friedrich Pfeil, München.

VAN DER MADE, J., J. MORALES, S. SEN, and F. ASLAN. 2002. The first camel from the upper Miocene of Turkey and the dispersal of the camels into the Old World. Comptes Rendus Palevol 1:117-122.

VISLOBOKOVA, I. A. 2008. Main stages in evolution of Artiodactyla communities from the Pliocene-Early Middle Pleistocene of northern Eurasia: Part 2. Paleontological Journal 42:414-424.

WANG, X., L. J. FLYNN, and M. FORTELIUS. 2013. Fossil Mammals of Asia - Neogene biostratigraphy and chronology. Columbia University Press, New York.

WEBB, S. D., and J. A. MEACHEN. 2004. On the origin of lamine Camelidae including a new genus from the Late Miocene of the high plains. Bulletin of Carnegie Museum of Natural History 36:349-362.

ZDANSKY, O. 1926. Paracamelus gigas, Schlosser. Palaeontologia Sinica 2:1-44, 4 tables.

Figures

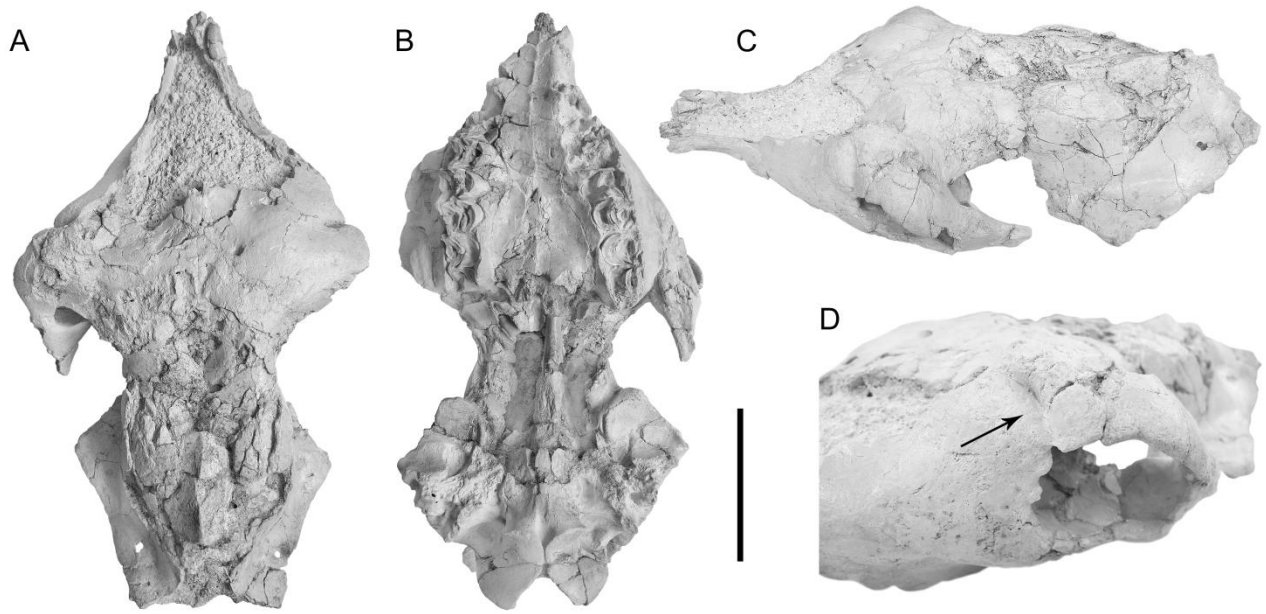

FIGURE 1. Cranium Nad F14-671 (*Camelus roris*, holotype). A, frontal view; B, basal view; C, latero-frontal view; D, detail of the orbit, with arrow pointing to the supraorbital notch. Scale bare equals 10 cm.

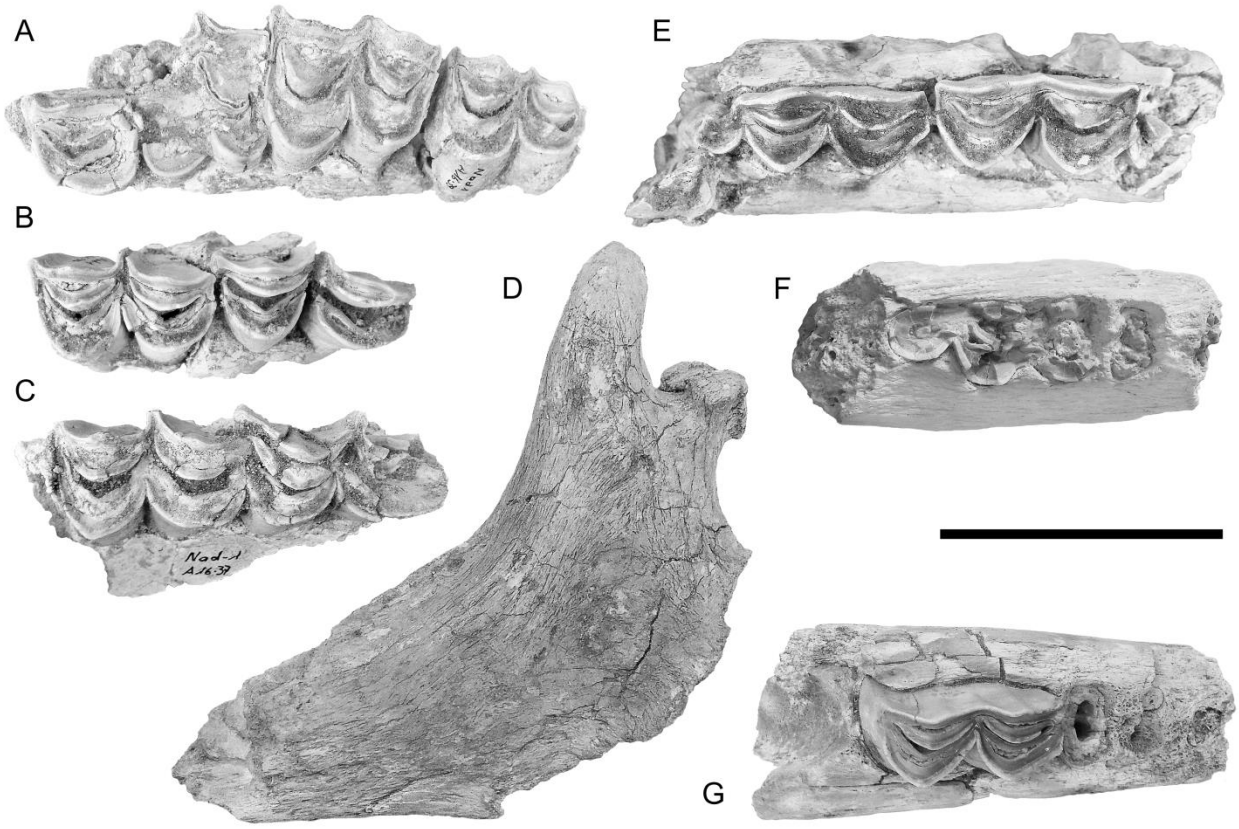

FIGURE 2. Upper dentition and mandibles. All figures in occlusal view except D. A, left maxilla Nad A16-45 with P1-M2, and corresponding M3 Nad A16-39 (*Camelus roris*, paratype); B, left maxilla Nad A16-35 with M2-M3 (*C.* cf. *roris*); C, left maxilla Nad A16-37 with M2-M3 (*C.* cf. *roris*); D, left mandible Nad H13-703 in lateral view (*C.* cf. *roris*); E, right mandible Nad A16-36 with m2-m3 (*C. roris*); F, right mandible Nad A16-27 with m3 (*C. roris*); G, right mandible Nad A16-8 with m2 (*C. roris*). Scale bare equals 5 cm.

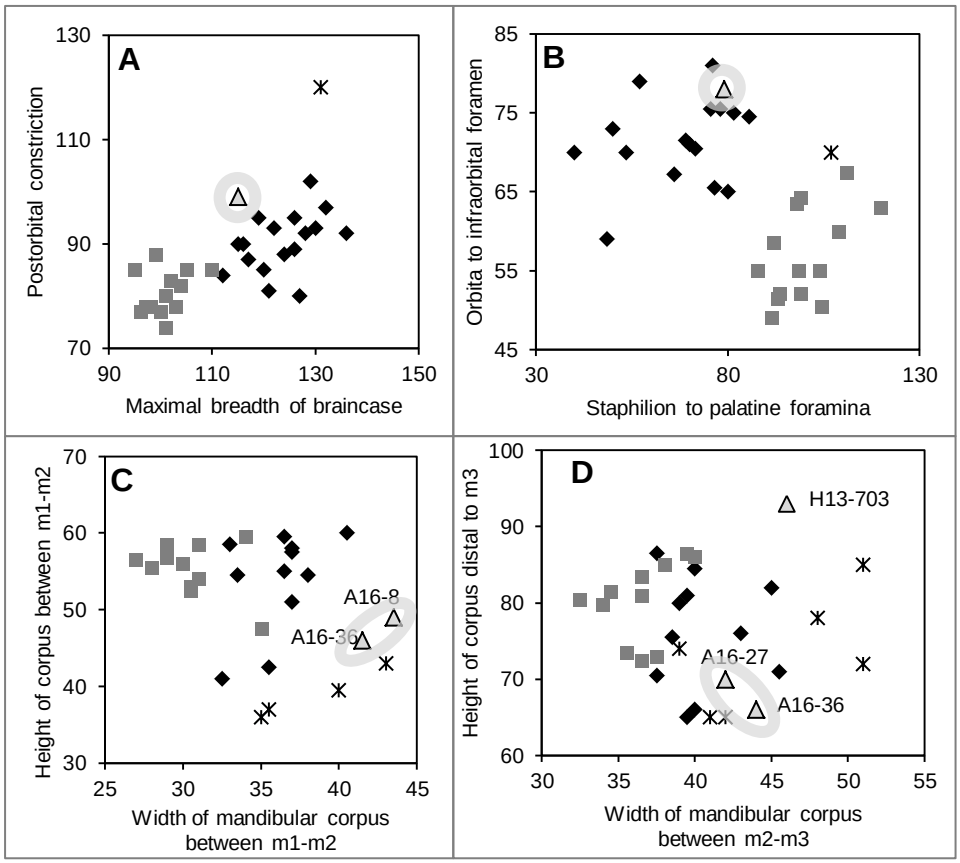

FIGURE 3. Plots of cranial and mandibular measurements (in mm). Diamonds: *Camelus bactrianus*, squares: *C. dromedarius* (measurements from Martini et al. 2017), asterisks: *C. thomasi* (from Martini and Geraads, in press), triangles: *C. roris* and *C.* cf. *roris*. A, width of postorbital constriction vs. maximal breadth of braincase; B, length from orbita to infraorbital foramen vs. length from staphilion (posterior margin of palate) to palatine foramina; C, height vs. width of mandibular corpus between m1 and m2; D, height of mandibular corpus distal to m3 vs. width between m2 and m3.

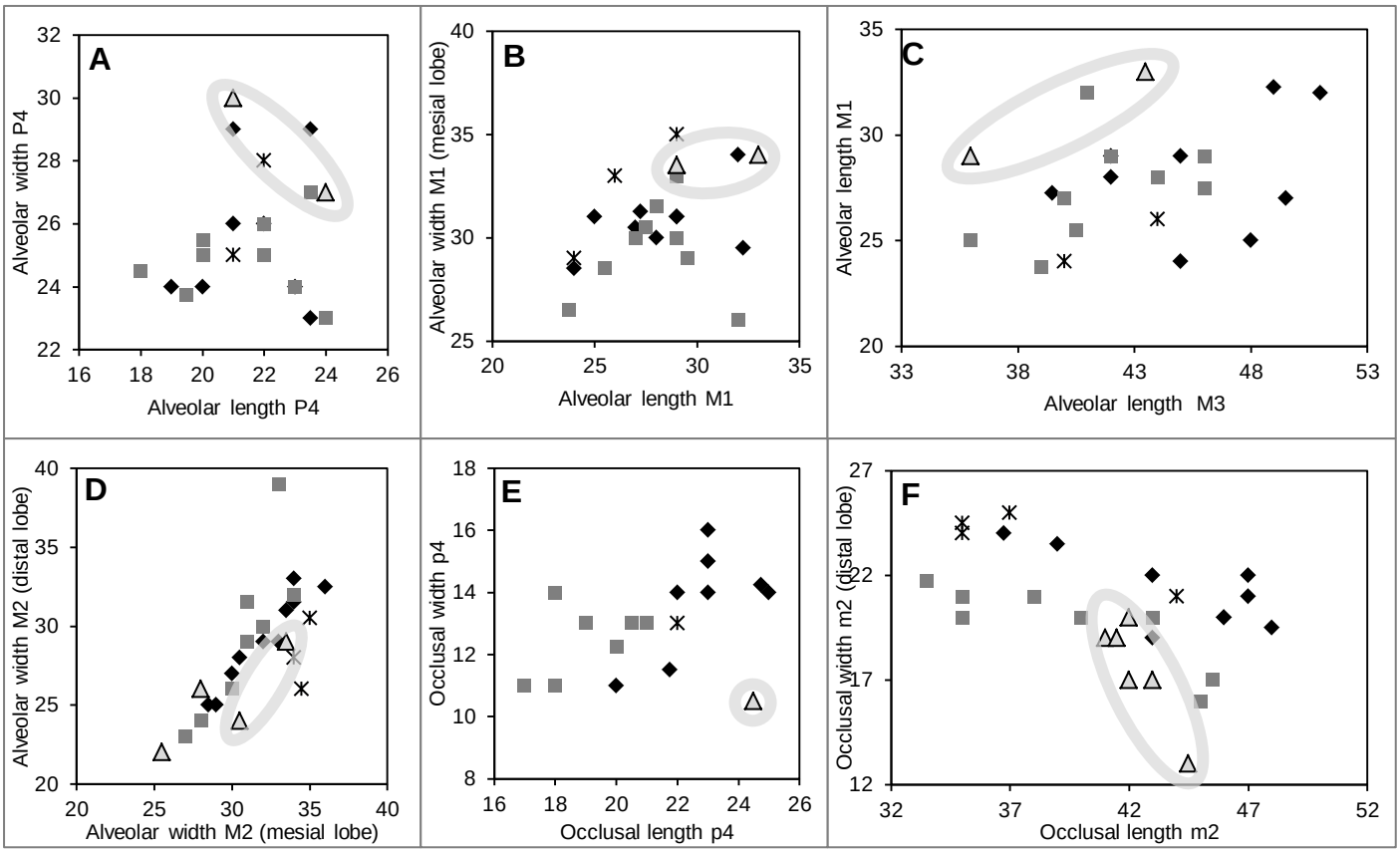

FIGURE 4. Plots of dental measurements (in mm). Diamonds: *Camelus bactrianus*, squares: *C. dromedarius* (measurements from Martini et al. 2017), asterisks: *C. thomasi* (from Martini and Geraads, 2018), triangles: *C. roris* and *C.* cf. *roris*. A, alveolar width vs. length of P4; B, alveolar width vs. length of M1 (greatest width is at the medial lobe); C, alveolar length of m1 vs. length of m3; D, alveolar distal width vs mesial width of M2; E, occlusal width vs length of p4; F, occlusal width vs length of m2 (greatest width is at the distal lobe).

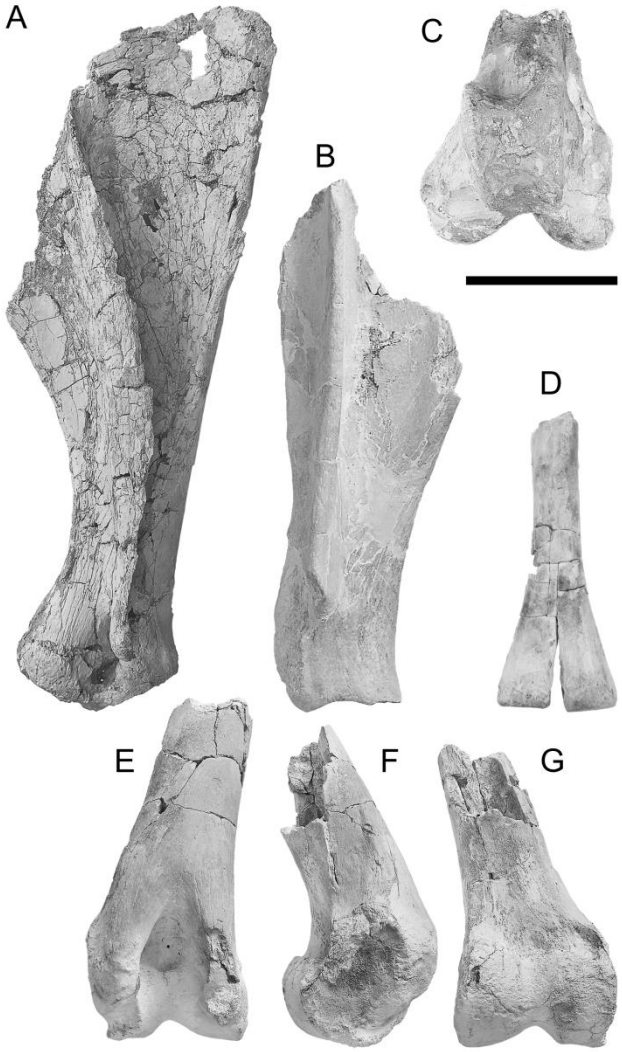

FIGURE 5. Long bones. A, left scapula Nad H14-755 (*Camelus sp*.); B, left scapula Nad E15-71 (*Camelus sp*. different from Nad H14-755); C, distal right femur Nad E18-111 (*C. roris*); D, distal left metatarsale Nad SP7-X (*C. roris*); E-G, distal left humerus Nad G11-700 (*C. roris*): E, palmar (caudal) view; F, lateral view; G, palmar (cranial) view. Scale bar equals 10 cm.

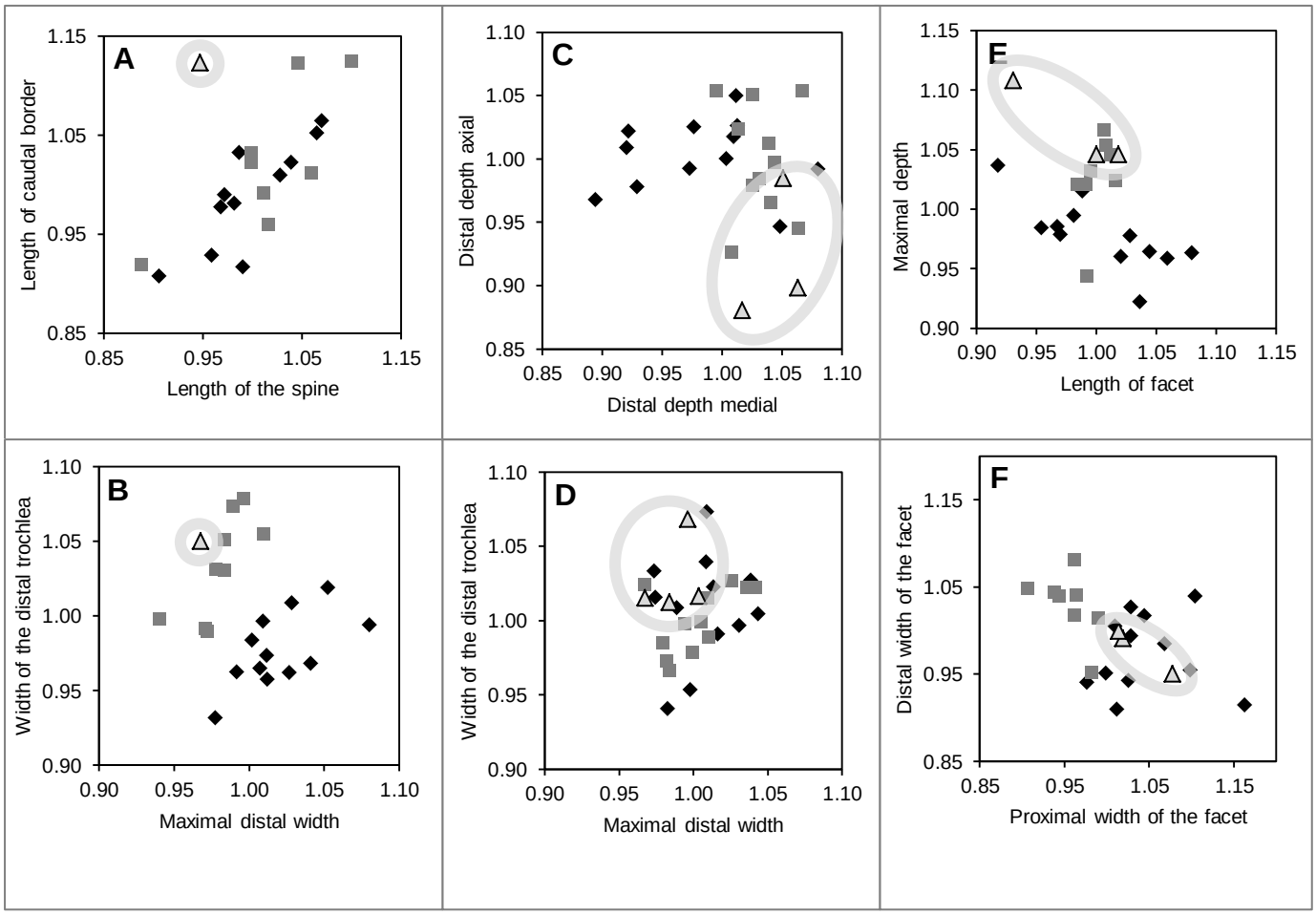

FIGURE 6. Plots of long bone measurements (harmonic scores). Diamonds: *Camelus bactrianus*, squares*: C. dromedarius* (measurements from Martini et al. 2017), triangles: *C. roris* and *C.* sp. from Nadaouiyeh. A, scapula, length of caudal border vs. length of the spine; B, femur, width of the distal trochlea vs maximal distal width; C, radioulnare, axial depth vs medial depth of the distal articulation; D, radioulnare, width of the distal trochlea vs maximal distal width (compare with B); E, patella, maximal depth vs length of articular facet; F, patella, distal vs proximal width of the facet.

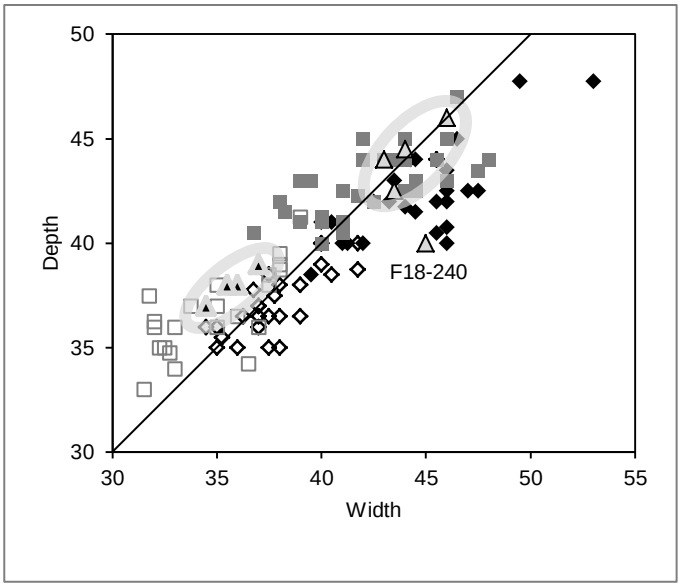

FIGURE 7. Plots of metapodial condyles measurements (mm). All diamonds: *Camelus bactrianus*, all squares: *C. dromedarius* (measurements from Martini et al. 2017), all triangles: *C. roris*. Filled diamonds, filled squares, and grey triangles: metacarpal condyles. Empty squares, empty triangles, and black-filled triangles: metatarsal condyles. Specimen Nad F18-240 is abnormally deformed.

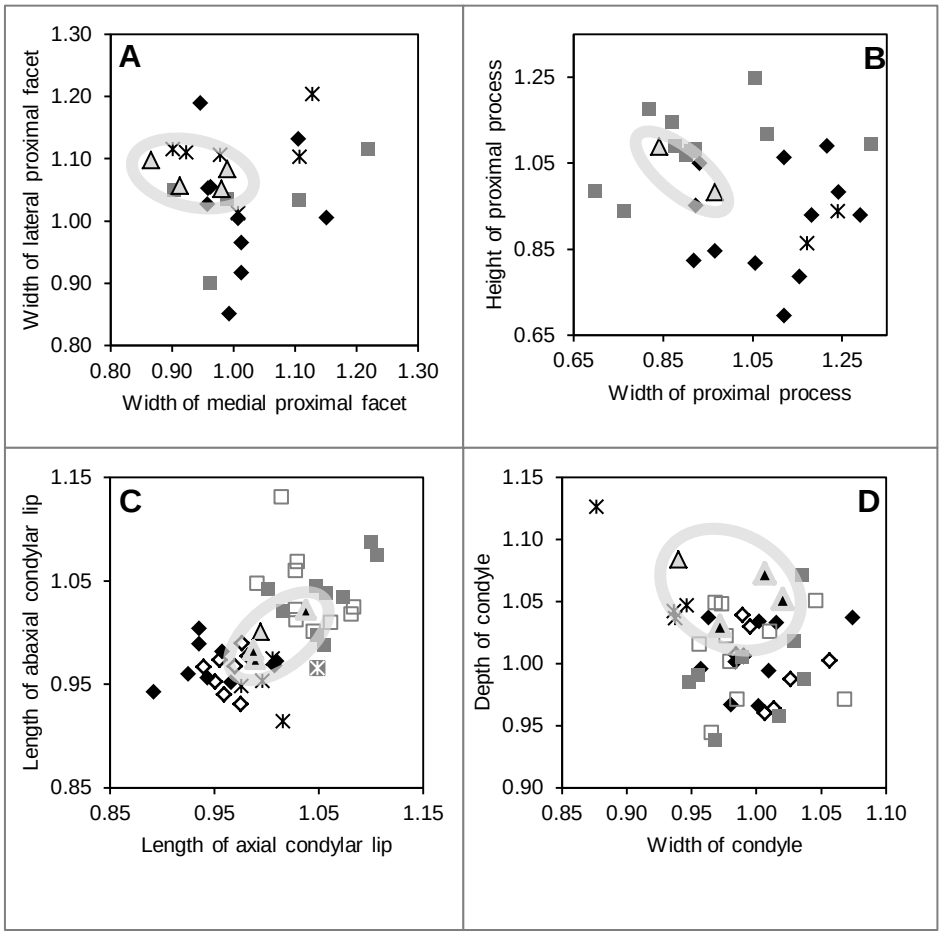

FIGURE 8. (Caption on next page)

FIGURE 8 (on previous page). Plots of metatarsal and phalangeal measurements (harmonic scores). All diamonds: *Camelus bactrianus*, all squares: *C. dromedarius* (measurements from Martini et al. 2017), all asterisks: *C. thomasi* (from Martini and Geraads, in press), all triangles: *C. roris*. Filled diamonds, filled squares, black asterisks, and grey triangles: anterior phalanges. Empty squares, empty triangles, white asterisks, and black-filled triangles: posterior phalanges. A, metatarsale, width of lateral vs. medial facet of the proximal articulation; B, metatarsale, length vs. width of the proximal triangular process; C, proximal phalanx, length of abaxial vs axial condylar lip; D, proximal phalanx, depth vs width of the condyle.

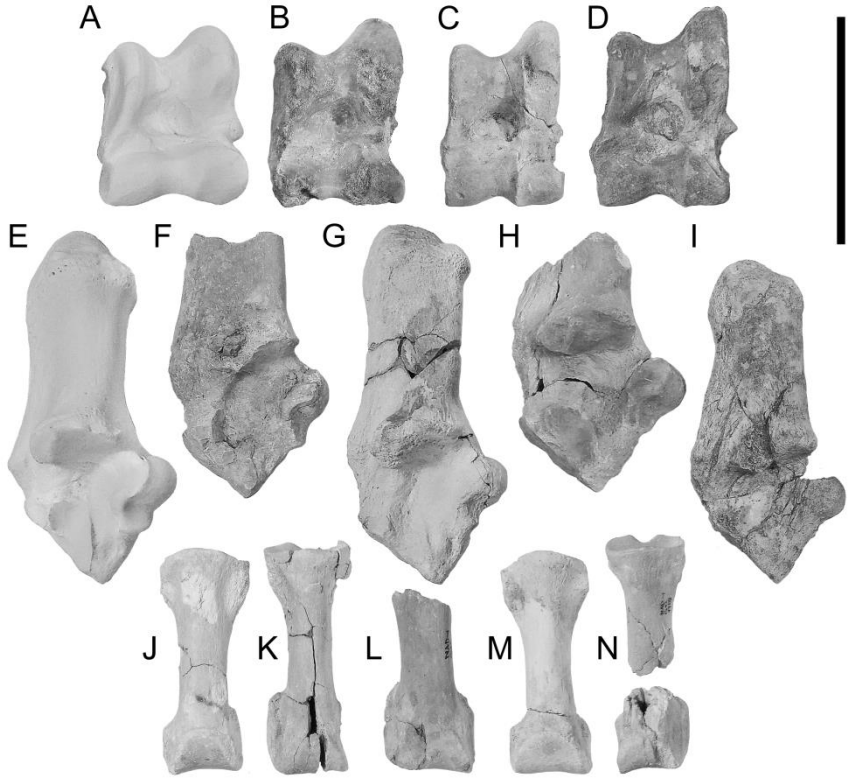

FIGURE 9. Short bones. A-D, astragali; E-I, calcanei; J-M proximal phalanges. A, E *Camelus bactrianus* (NMB 10390, shown for comparison); all others *C. roris*. Right specimens B, C, H, I are mirrored. B, Nad E14-85; C, Nad G12-1781; D, Nad G12-2019; F, Nad H13-117; G, Nad H13-984; H, Nad F12-148; I, Nad H14-1279; J, Nad F14-290 (posterior); K, Nad J12-55 (posterior); L, G12-1961 (anterior); M, Nad F12-145 (posterior); N, G12-1758 (posterior). Scale bar equals 5 cm.

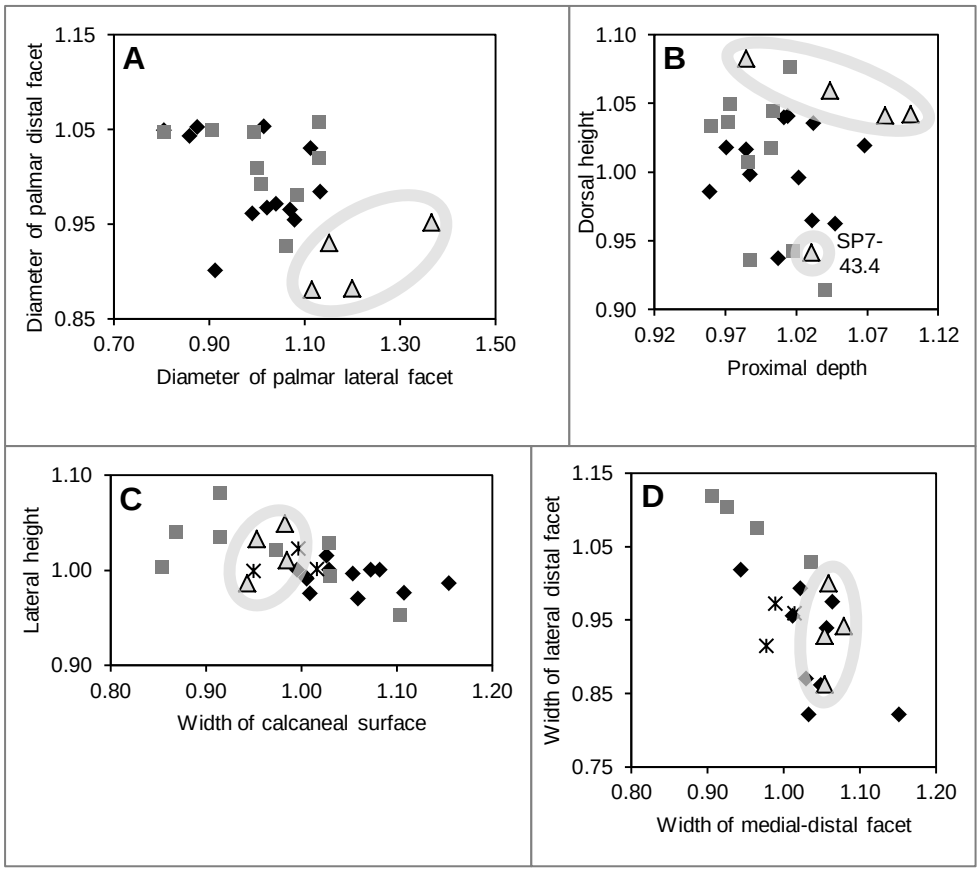

FIGURE 10. Plots of scaphoideum and astragalus measurements (harmonic scores). Diamonds: *Camelus bactrianus*, squares: *C. dromedarius* (measurements from Martini et al. 2017), asterisks: *C. thomasi* (from Martini and Geraads, in press), triangles: *C. roris* and *C.* cf. *roris*. A, scaphoideum, greatest diameter of palmar distal facet (for the trapezoideum) vs greatest diameter of palmar lateral facet (for the lunatum); B, scaphoideum, dorsal height vs. proximal depth (specimen SP7-43.4 belongs to the "Black Hummal assemblage"); C, astragalus, lateral height vs width of calcaneal surface; D, astragalus, width of lateral vs medial facets of distal trochlea (for the cuboid and the navicular, respectively).

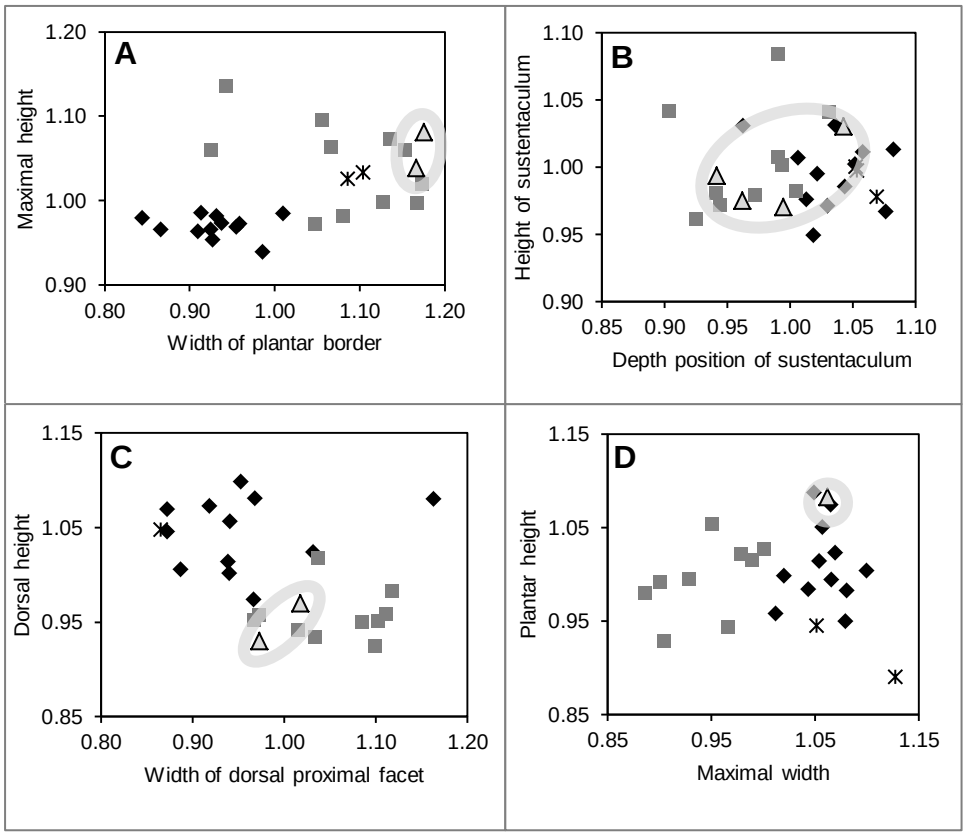

FIGURE 11. Plots of calcaneus, cuboideum and naviculare measurements (harmonic scores). Diamonds: *Camelus bactrianus*, squares: *C. dromedarius* (measurements from Martini et al. 2017), asterisks: *C. thomasi* (from Martini and Geraads, in press), triangles: *C. roris*. A, calcaneus, maximal height vs. width of the plantar border; B, calcaneus, height of the sustentaculum from the distal end vs. depth of the sustentaculum from the plantar border; C, cuboideum, dorsal height vs. width of dorsal proximal facet (for the astragalus); D, naviculare, plantar height vs. maximal width.

Tables

TABLE 1. Simplified stratigraphy of Nadaouiyeh (Jagher 2011; Reynaud Savioz 2011)

Unit	Layers	Age (Ka)	Notes
A	1, 2	150	Poor in camelid fossils
A/B	BH	200-350	"Black Hummal"; reworked sediments, close to 200 Ka
	Dol.3		Reworked sediments found between A and B
B	5, 5-90, 6	350-430	
	6.4, 7		Base of Unit B
C	8.1	450-475	
D	8, 8a, 8b, 8c, 8d	480-530	
E	9	540	
F	93-1	550	Poor in camelid fossils

TABLE 2. List of specimens included in this study. The total of 126 specimens is assigned to *Camelus roris* (95 specimens), *Camelus* cf. *roris* (17 specimens) or *Camelus* sp. (14 specimens). Holotype and paratype are marked with (*).

Label	Unit	Layer	Element	Side	Description	Species
F14-671	B	7	Cranium		Complete, damaged; & P3-M3 (broken)	*C. roris* *
A16-35	A/B	Dol.3	Maxilla	sin	& M2-M3, initial wear	*C. cf. roris*
A16-37	A/B	Dol.3	Maxilla	sin	& M2-M3 intermediate wear	*C. cf. roris*
A16-45	A/B	Dol.3	Maxilla	sin	& P4-M2 (includes M3 A16-39), advanced wear	*C. roris* *
A16-27	A/B	Dol.3	Mandibula	dex	& m2 (roots), m3 (roots)	*C. roris*
A16-8	A/B	Dol.3	Mandibula	dex	& p4 (roots), m1 (roots), m2	*C. roris*
A16-36	A/B	Dol.3	Mandibula	dex	& m1 (roots), m2-m3	*C. roris*
H13-703	D	8a	Mandibula	sin	& m2 (alveoles), m3 (roots)	*C. cf. roris*
F16-1282	D	8b	Mandibula	dex?	& p4? (roots), m1? (roots)	*C. sp.*
A16-10	A/B	Dol.3	Dens ant	sin	Caniniform I3 superior, male, worn	*C. cf. roris*
A16-11	A/B	Dol.3	Dens ant		Canine, male	*C. cf. roris*
A16-12	A/B	Dol.3	Dens ant		Canine, female	*C. cf. roris*
A16-13	A/B	Dol.3	Dens ant	sin?	Caniniform p1, female	*C. cf. roris*
A16-14	A/B	Dol.3	Dens ant		Caniniform p1	*C. cf. roris*
A16-15	A/B	Dol.3	Dens ant	sin	Caniniform p1, female	*C. cf. roris*
A16-16	A/B	Dol.3	Dens ant	dex	Caniniform p1, female? Very small	*C. cf. roris*
A16-17	A/B	Dol.3	Dens ant		Caniniform p1, female? Very small	*C. cf. roris*
A16-18	A/B	Dol.3	Dens inf	dex	p4, initial wear	*C. roris*
A16-19	A/B	Dol.3	Dens inf	sin	m2, initial wear	*C. roris*
A16-20	A/B	Dol.3	Dens inf	dex	m2, unworn	*C. roris*
A16-21	A/B	Dol.3	Dens inf	dex	m3, intermediate wear & fragment os	*C. roris*
A16-34	A/B	Dol.3	Dens inf	dex	m2, intermediate wear	*C. roris*
A16-41	A/B	Dol.3	Dens inf	sin	m3, intermediate wear	*C. roris*
A16-42	A/B	Dol.3	Dens inf	dex	m3, unworn	*C. roris*
A16-43	A/B	Dol.3	Dens inf	dex	m2, initial wear	*C. roris*
A16-44	A/B	Dol.3	Dens inf	sin	m2, initial wear	*C. roris*
A16-38	A/B	Dol.3	Dens sup	sin	M3, intermediate wear	*C. roris*
A16-39	A/B	Dol.3	Dens sup	sin	M3 (part of A16-45)	*C. roris*
A16-46	A/B	Dol.3	Dens sup	dex	M2 & fragment os	*C. roris*
E15-71	B	7	Scapula	sin	Proximally incomplete	*C. sp.*
D17-294	B	6b	Scapula	dex	Fragment distal	*C. sp.*
H14-755	C	8.1b	Scapula	sin		*C. sp.*
G15-209	D	8a	Humerus	dex	Fragment distal medial	*C. sp.*

G11-700	D	8c	Humerus	sin	Large fragment distal	*C. roris*
F18-265	F	93-1	Humerus	sin	Fragment distal medial	*C. sp.*
F13-261	A	1	Radioulnare	dex	Anconeus process	*C. roris*
H11-55	A	1	Radioulnare	sin	Fragment distal	*C. roris*
F14-701	C	8.1	Radioulnare	dex	Fragment proximal	*C. roris*
F11-51	C	8.1a	Radioulnare	dex	Fragment distal	*C. roris*
H14-1122	C	8.1b	Radioulnare	dex	Fragment distal	*C. roris*
G16-1323	D	8a	Radioulnare	dex	Fragment proximal	*C. roris*
H12-732	D	8b	Radioulnare	sin	Fragment distal	*C. roris*
SP7-43.3	A/B	BH	Carpalia	dex	Triquetrum	*C. cf. roris*
SP7-43.4	A/B	BH	Carpalia	sin	Scaphoideum	*C. cf. roris*
SP7-43.5	A/B	BH	Carpalia	dex	Hamatum	*C. cf. roris*
A16-23	A/B	Dol.3	Carpalia	sin	Scaphoideum	*C. roris*
A16-26	A/B	Dol.3	Carpalia	dex	Scaphoideum	*C. roris*
A16-31	A/B	Dol.3	Carpalia	sin	Triquetrum (very small)	*C. roris*
A16-32	A/B	Dol.3	Carpalia	dex	Lunatum, fragment dorsal (very small)	*C. roris*
A16-4	A/B	Dol.3	Carpalia	sin	Scaphoideum	*C. roris*
A16-6	A/B	Dol.3	Carpalia	sin	Trapezoideum	*C. roris*
D17-71	B	5-90	Carpalia	sin	Scaphoideum	*C. roris*
H14-1090	C	8.1b	Carpalia	sin	Lunatum	*C. roris*
E18-109	D	8	Carpalia	sin	Lunatum	*C. roris*
F16-204	D	8a	Carpalia	sin	Triquetrum	*C. roris*
G11-493	D	8b	Carpalia	dex	Hamatum	*C. roris*
E13-97	D	8d	Carpalia	sin	Lunatum	*C. roris*
E15-728	E	9	Carpalia	?	Trapezoideum	*C. roris*
A16-22	A/B	Dol.3	Metacarpale		Condyle	*C. roris*
A16-30	A/B	Dol.3	Metacarpale		Condyle	*C. roris*
A16-5	A/B	Dol.3	Metacarpale		Condyle	*C. roris*
G14-452	C	8.1b	Metacarpale		Fragment distal right	*C. roris*
J14-181	C	8.1b	Metacarpale		Fragment proximal	*C. roris*
G16-1237	D	8a	Metacarpale		Fragment distal right	*C. roris*
H13-494	D	8b	Metacarpale		Fragment proximal	*C. roris*
G16-671	D	8b/c	Metacarpale	sin	Fragment proximal lateral	*C. roris*
F18-240	F	93-1	Metacarpale		Epiphysis distal left	*C. roris*
SP7-43.1	A/B	BH	Femur		Caput	*C. cf. roris*
A16-1	A/B	Dol.3	Femur		Caput	*C. roris*
A16-2	A/B	Dol.3	Femur		Caput	*C. roris*
A16-3	A/B	Dol.3	Femur		Caput	*C. roris*
F18-11	C	8.1	Femur	dex	Fragment proximal	*C. roris*
G11-584	D	8c	Femur		Caput	*C. roris*
G12-2003	D	8c	Femur		Caput	*C. roris*
F14-1371	D	8d	Femur	dex?	Fragment distal (trochlea)	*C. roris*
E15-727	E	9	Femur		Caput	*C. roris*
E18-111	F	93-1	Femur	dex	Fragment distal	*C. roris*
P50-A-41	B	(?)	Patella	sin		*C. roris*
F12-116	D	8	Patella	dex		*C. roris*
F12-244	E	9	Patella	dex		*C. roris*
SP31-2.1	A/B	Dol.3	Tibia	sin	Fragment distal	*C. sp.*
Nad83-1	B	6	Tibia	dex	Fragment distal	*C. sp.*
D17-105	B	5-90	Tibia	dex	Fragment distal	*C. sp.*
G14-993	D	8b	Fibula	dex	Fragmentary	*C. sp.*
E18b-112	F	93-1	Fibula	dex		*C. sp.*
F18-225	F	93-1	Fibula	sin		*C. sp.*
SP7-43.2	A/B	BH	Tarsalia	sin	Astragalus, fragment distal	*C. cf. roris*
SP7-43.6	A/B	BH	Tarsalia	dex?	Cuneiforme intermediolateral	*C. cf. roris*
A16-24	A/B	Dol.3	Tarsalia	sin	Cuboideum (very small)	*C. roris*
A16-25	A/B	Dol.3	Tarsalia	dex	Cuboideum	*C. roris*
A16-28	A/B	Dol.3	Tarsalia	dex	Naviculare	*C. roris*
A16-29	A/B	Dol.3	Tarsalia	dex	Intermediolateral cuneiform (very small)	*C. roris*
A16-33	A/B	Dol.3	Tarsalia	sin	Astragalus (very small)	*C. roris*
SP7-51	A/B	Dol.3	Tarsalia	sin	Astragalus	*C. roris*
E14-85	B	5b	Tarsalia	dex	Astragalus	*C. roris*

H13-117	C	8.1	Tarsalia	sin	Calcaneus	*C. roris*
H13-984	C	8.1b	Tarsalia	sin	Calcaneus	*C. roris*
F12-148	D	8	Tarsalia	dex	Calcaneus	*C. roris*
E15-399	D	8	Tarsalia	sin	Astragalus	*C. roris*
E17-115	D	8	Tarsalia	sin	Astragalus	*C. roris*
H14-1279	D	8a	Tarsalia	dex	Calcaneus	*C. roris*
G12-2019	D	8c	Tarsalia	sin	Astragalus	*C. roris*
G12-1781	E	9	Tarsalia	dex	Astragalus	*C. roris*
SP7-X	(?)	(?)	Metatarsale	sin	Fragment distal	*C. roris*
H15-135	C	8.1b	Metatarsale	sin	Fragment proximal	*C. roris*
F15-498	D	8a	Metatarsale	dex	Fragment proximal	*C. roris*
F17-2	D	8a	Metatarsale		Fragment distal (juvenile?)	*C. roris*
G16-1	D	8a	Metatarsale	dex	Fragment proximal	*C. roris*
G16-1273	D	8a	Metatarsale	dex	Fragment proximal	*C. roris*
F16-1607	D	8b	Metatarsale	sin?	Fragment distal (medial?)	*C. roris*
G12-1747	E	9	Metatarsale	dex	Fragment proximal	*C. roris*
G16-1350	D	8a	Phalanx I ant		Fragment proximal	*C. sp.*
G12-1961	E	9	Phalanx I ant		Fragment distal	*C. roris*
F18-227	F	93-1	Phalanx I ant		Fragmentary	*C. sp.*
F14-290	B	5b	Phalanx I post			*C. roris*
J12-55	C	8.1	Phalanx I post			*C. roris*
F12-145	D	8	Phalanx I post			*C. roris*
G12-1758	E	9	Phalanx I post			*C. roris*
A16-7	A/B	Dol.3	Phalanx II		Fragment distal	*C. roris*
E14-78	B	5b	Phalanx II			*C. roris*
SP7-20	B	5b	Phalanx II			*C. roris*
G13-1307	D	8c	Phalanx II		Fragment distal	*C. roris*
G14-484	D	8a	Phalanx III			*C. roris*
G13-1607	D	8c	Phalanx III			*C. roris*
H13-1354	D	8c	Phalanx III			*C. roris*
G12-1738	E	9	Phalanx III			*C. roris*

TABLE 3. Measurements of *Camelus* remains from Nadaouiyeh. Details on the specimens are given in Table 2. ~ indicates approximated measurements; § indicates measurements that might be either mesial or lateral.

	CRANIUM	F14-671 cranium 7	A16-45 sin Dol.3
C6	Length of foramen magnum (opisthion to basion)	43	
C8	Basicranial length (basion to staphilion)	174 ~	
C14	Cheek length (predentale to orbita)	125 ~	
C15	Infraorbital length (infraorbital foramen to orbita)	78	
C18	Orbital length (maximal horizontal diameter)	60 ~	
C21	Minimal breadth of the frontal orbital process	19	
C22	Distance from zygomatic process of temporal to orbita	20.5	
C25	Position of palatine foramina (from staphylion)	79	
C33	Cheek tooth length (P3-M3, included; buccal side)	162 ~	
C34	Molar row length (M1-M3, included; buccal side)	117 ~	103 ~
C45	Maximal diameter of condyle	58.5	
C46	Breadth of glenoid fossa (maximal)	56 ~	
C47	Length of glenoid fossa (to postglenoid foramen)	33	
C52	Breadth between infraorbital foramina (lateral border)	101	
C53	Maximal biorbital breadth (between lateral borders)	240 ~	
C54	Minimal biorbital breadth (between medial borders)	187	
C56	Breadth of postorbital constriction (minimal)	99	
C57	Breadth of the braincase (maximal)	115	
C58	Breadth between squamotemporal foramina	116	
C71	Breadth between mastoid processes	157 ~	
C73	Maximal bicondylar breadth	84	
C74	Minimal bicondylar breadth	45	
C75	Breadth of foramen magnum (between condyles)	31	
C76	Breadth between mastoid foramina	65	

	MANDIBULA	A16-8 dex Dol.3	A16-27 dex Dol.3	A16-36 dex Dol.3	H13-703 sin 8a
M13	Length from m3 distal to angular process				110 ~
M14	Length from m3 distal to condylar process				119
M15	Thickness of the corpus measured between m1 and m2	43.5		41.5 ~	
M16	Thickness of the corpus measured between m2 and m3	47	42 ~	44 ~	46 ~
M17	Breadth of the condylus				40
M18	Height of the condylus				33.5
M20	Height of the corpus between m1 and m2	49		46	
M21	Height of the corpus distal to m3		70 ~	66 ~	93
M22	Height of the ramus from coronoid process to ventral border				205 ~
M23	Height of the ramus from rostral notch to ventral border				155 ~
M24	Height of the ramus from condylar process to ventral border				175 ~
M25	Height of the ramus from caudal notch to ventral border				125 ~

	UPPER DENTITION	F14-671 cranium 7	A16-45/39 sin Dol.3	A16-35 sin Dol.3	A16-37 sin Dol.3	A16-46 dex Dol.3	A16-38 sin Dol.3
Ds11	Alveolar length of P4	24 ~	21 ~				
Ds12	Alveolar breadth of P4	27 ~	30 ~				
Ds13	Occlusal length of P4		24				
Ds14	Occlusal breadth of P4		22				
Ds15	Alveolar length of M1	33 ~	29 ~				
Ds16	Alveolar breadth of mesial lobe of M1	34 ~	33.5				
Ds17	Alveolar breadth of distal lobe of M1	35	35				
Ds18	Occlusal length of M1		34 ~				
Ds19	Occlusal length of mesial lobe of M1		18 ~				
Ds20	Occlusal length of distal lobe of M1		16				
Ds21	Occlusal breadth of mesial lobe of M1						
Ds22	Occlusal breadth of distal lobe of M1		31				
Ds23	Alveolar length of M2	39.5	33	36 ~	32.5		
Ds24	Alveolar breadth of mesial lobe of M2	30.5	33.5	25.5 ~	28		
Ds25	Alveolar breadth of distal lobe of M2	24	29	22 ~	26		
Ds26	Occlusal length of M2		41	41	43	44 ~	

Ds27	Occlusal length of mesial lobe of M2		20	20	20	23								
Ds28	Occlusal length of distal lobe of M2		21	22	23	24 ~								
Ds29	Occlusal breadth of mesial lobe of M2		31	22	23	32								
Ds30	Occlusal breadth of distal lobe of M2		26	18.5	20	27								
Ds31	Alveolar length of M3	43.5	36 ~	44	44		39							
Ds32	Alveolar breadth of mesial lobe of M3	23.5 ~	33	23	26.5		30							
Ds33	Alveolar breadth of distal lobe of M3	20 ~	24	20 ~	19 ~		26							
Ds34	Occlusal length of M3		37.5	47			41							
Ds35	Occlusal length of mesial lobe of M3		19.5	22	26 ~		21							
Ds36	Occlusal length of distal lobe of M3		18.5	27			22							
Ds37	Occlusal breadth of mesial lobe of M3		25	17	19.5 ~		24							
Ds38	Occlusal breadth of distal lobe of M3		17.5	16			19							

	LOWER DENTITION	**A16-18 dex Dol.3**	**F16-1282 dex 8b**	**A16-8 dex Dol.3**	**A16-19 sin Dol.3**	**A16-34 dex Dol.3**	**A16-43 dex Dol.3**	**A16-44 sin Dol.3**	**A16-36 dex Dol.3**	**A16-27 dex Dol.3**	**H13-703 sin 8a**	**A16-21 dex Dol.3**	**A16-41 sin Dol.3**	**A16-42 dex Dol.3**
Di8	Alveolar length of P4													
Di9	Alveolar breadth of P4		17											
Di10	Occlusal length of P4	24.5												
Di11	Occlusal breadth of P4	10.5												
Di12	Alveolar length of M1		26	29										
Di13	Alveolar breadth of mesial lobe of M1		16.5											
Di14	Alveolar breadth of distal lobe of M1		15	23										
Di20	Alveolar length of M2			41					37.5					
Di21	Alveolar breadth of mesial lobe of M2			23					22					
Di22	Alveolar breadth of distal lobe of M2			22.5					22					
Di23	Occlusal length of M2			41	42	42	43	44.5	41.5					
Di24	Occlusal length of mesial lobe of M2			20 ~	19	20	20	22	21					
Di25	Occlusal length of distal lobe of M2			21	23.5	21	23	24	21					
Di26	Occlusal breadth of mesial lobe of M2			18	17.5	20	17.5	14	20					
Di27	Occlusal breadth of distal lobe of M2			19	17	20	17	13	19					
Di28	Alveolar length of M3								48.5	52	54 ~			
Di29	Alveolar breadth of mesial lobe of M3								20	21	21.5 ~			
Di30	Alveolar breadth of central lobe of M3								19	21	22 ~			
Di31	Alveolar breadth of distal lobe of M3								10	13	13			
Di32	Occlusal length of M3								47			51	52	53.5
Di33	Occlusal length of mesial lobe of M3								19.5			20	21	
Di34	Occlusal length of central lobe of M3								19			17	17.5	
Di35	Occlusal length of distal lobe of M3								9.5			13	14	
Di36	Occlusal breadth of mesial lobe of M3								17.5			19.5	18	
Di37	Occlusal breadth of central lobe of M3								17			20	19	
Di38	Occlusal breadth of distal lobe of M3								8.5			11	9.5	

	SCAPULA	**D17-294 dex 6b**	**H14-755 sin 8.1**	**E15-71 sin 7**
sc1	Cranial length (cranial angle to glenoid fossa)		350 ~	
sc2	Length of the spine (dorsal border to acromion)		365 ~	
sc3	Caudal length (caudal angle to glenoid fossa)		404	
sc4	Dorsal depth (cranial to caudal angle)		230 ~	
sc5	Depth of the supraspinatous fossa (cranial angle to spina)		100 ~	
sc6	Depth of the infraspinatous fossa (caudal angle to spina)		135 ~	
sc7	Depth of the neck		71	78.5
sc8	Maximal distal depth		107	
sc9	Acromion to glenoid fossa		92	
sc10	Acromion to coracoid		75	
sc11	Depth of the glenoid fossa	69	69	71 ~
sc12	Breadth of the glenoid fossa		66	63

	HUMERUS	**G15-209 dex 8a**	**G11-700 sin 8c**	**F18-265 sin 93-1**
hu12	Maximal diameter, at the nutritional foramen		65 ~	
hu13	Minimal diameter, at the nutritional foramen		57 ~	
hu14	Distal medial depth (medial epicondyle to trochlea)	80 ~		
hu15	Distal axial depth (trochlear groove)		43	37.5
hu16	Distal lateral depth (lateral epicondyle to capitulum)		90	
hu17	Distal breadth (trochlea to capitulum)		87.5	
hu18	Distal breadth of the trochlea (to trochlear groove)		46	
hu19	Distal breadth of the capitulum (to trochlear groove)		42	
hu20	Depth of the trochlea (medial)	60	71	66
hu21	Depth of the capitulum (lateral)		65	
hu22	Height of the olecranon fossa		40	
hu23	Breadth of the olecranon fossa		35 ~	

	RADIOULNARE	**F13-261 dex 1**	**E15-211.1 ? 5b**	**F14-701 dex 8.1**	**G16-1323 dex 8a**	**H11-55 sin 1**	**F11-51 dex 8.1a**	**H14-1122 dex 8.1b**	**H14-1188 dex 8.1b**	**H12-732 sin 8b**
ru5	Maximal breadth of the olecranon		45 ~							

ru6	Minimal breadth of the olecranon	22									
ru8	Length of the trochlear notch (anconeus to coronoid process)				44						
ru9	Breadth of the trochlear notch			81 ~	80 ~						
ru10	Breadth of the medial radial articular facet			42 ~	38 ~						
ru11	Breadth of the lateral radial articular facet			45 ~	41						
ru12	Depth of the lateral radial articular facet			42 ~	43 ~						
ru13	Depth of the coronoid process				85						
ru14	Proximal breadth of the radius			89 ~	94 ~						
ru17	Distal medial depth (transversal crest included)						54	53	49 ~	61	
ru18	Distal axial depth (transversal crest included)						54	49 ~		55	
ru19	Distal lateral depth (ulnar articular surface)					25	26	28		30	
ru20	Maximal distal breadth					88 ~	95 ~	98		110	
ru21	Breadth of the distal articular surface					80.5	85	86		95 ~	
ru22	Depth of the distal medial (radial) articular surface					39 ~	44	45	41 ~	49	
ru23	Depth of the distal axial (radial) articular surface						36 ~	37		41	
ru24	Depth of the convex (palmar) part of the distal medial (radial) articular surface					31 ~	36	38	31 ~	40	
ru25	Breadth of the distal medial (radial) articular surface						31 ~	29		34 ~	
ru26	Breadth of the distal axial (radial) articular surface)						17 ~	21		20	
ru27	Breadth of the distal lateral (ulnar) articular surface)						37 ~	35		40	

	METACARPALE	**J14-181 sin 8.1b**	**H13-494 sin 8b**	**G16-671 sin 8bc**	**A16-5 condyle Dol.3**	**A16-22 condyle Dol.3**	**A16-30 condyle Dol.3**	**G14-452 condyle 8.1b**	**G16-1237 condyle 8a**	**F18-240 condyle 93-1**	
mp3	Medial depth of the proximal articulation	51	48 ~								
mp4	Lateral depth of the proximal articulation	49	45	51							
mp5	Breadth of the proximal articulation	76	75								
mp6	Breadth of the medial proximal facet	32	32.5								
mp7	Breadth of the lateral proximal facet	30	28	32.5							
mp8	Depth of the proximal articulation	49	42								
mp9	Depth of the medial proximal facet	47	42								
mp13	Depth of the medial condyle				46 § ~	43 § ~	47 §	44 §	43.5 §	45 §	
mp14	Depth of the lateral condyle				46 § ~	43 § ~	47 §	44 §	43.5 §	45 §	
mp15	Breadth of the medial condyle				46 §	44 §		44.5 §	42.5 §	40 § ~	
mp16	Breadth of the lateral condyle				46 §	44 §		44.5 §	42.5 §	40 § ~	

	FEMUR	**F18-11 dex 8.1**	**F14-1371 dex? 8d**	**E18-111 dex 93-1**	**G11-584 caput N 8c**	**G12-2003 caput N 8c**	**A16-1 caput N dol.3**	**A16-2 caput N dol.3**	**A16-3 caput N dol.3**	**SP7-43.1 caput N bh**	**E15-727 caput N 9**
fe5	Depth (diameter) of the head	61			60	56	58.5	54	59	51	59
fe6	Proximal breadth (head to greater trochanter)	125 ~									
fe7	Minimal depth proximal (depth of the neck)	39 ~									
fe8	Minimal breadth proximal (breadth of the neck)	58									
fe11	Distal medial depth (medial condyle to trochlea)			128 ~							
fe12	Breadth of medial condyle			43 ~							
fe13	Depth of the trochlea (groove to intercondylar fossa			87							
fe14	Distal cranial breadth (breadth of the trochlea)		48	52							
fe15	Distal lateral depth (lateral condyle to trochlea)			121							
fe16	Breadth of lateral condyle			55							
fe17	Distal maximal breadth (condyle to condyle)			115							
fe18	Length of medial condyle			64							
fe19	Length of lateral condyle			68							

	PATELLA	**F12-116 dex 8**	**F12-244 dex 9**	**P50-A41 sin ?**
pa1	Maximal length	90	90	
pa2	Length of the articular surface	85	78 ~	87 ~
pa3	Maximal depth	47	50	49
pa4	Maximal breadth	45	47	46
pa5	Proximal breadth of the articular surface	39	39	43
pa6	Distal breadth of the articular surface	37	37.5	37

	TIBIA	**SP31-2.1 sin Dol.3**	**D17-105 dex 5-90**	**Nad83-1 dex 6**
ti12	Minimal depth of the diaphysis			32 ~
ti14	Depth of the medial fossa of the cochlea (maximal)	47	38 ~	
ti15	Depth of the axial fossa of the cochlea (maximal)	44	38 ~	
ti16	Depth of the lateral fossa of the cochlea	37	31 ~	
ti17	Dorsal breadth of the cochlea	82	83	
ti18	Palmar depth of the cochlea	90 ~		92

	A16-9	**H11-103**	**H15-135**	**F15-498**	**G16-1**	**G16-1273**	**G12-1747**	**F16-1607**	**SP7-x**	**F17-2**

	METATARSALE	?	sin	sin	dex	dex	dex	dex	sin?	sin	condyle
		Dol.3	8.1	8.1b	8a	8a	8a	9	8b	?	8a
mp18	Length of the triangular process				25			26 ~			
mp19	Breadth of the triangular process				22	23	19	18			
mp20	Depth of the medioplantar proximal facet				14.5	14		15			
mp21	Depth of the medial proximal facet		32.5		30	32 ~	32	32			
mp22	Depth of the lateral proximal facet			37	44.5	41	39	37			
mp5	Breadth of the proximal articulation			64 ~	65.5	64 ~	66				
mp6	Breadth of the medial proximal facet		23	21	19	22 ~	19	20			
mp7	Breadth of the lateral proximal facet			21.5	23	23	21 ~				
mp8	Depth of the proximal articulation				54	51.5	49	48 ~			
mp11	Minimal depth of the diaphysis	21.5							23.5	22.5	
mp12	Minimal breadth of the diaphysis									33	
mp13	Depth of the medial condyle								39	38	37 §
mp14	Depth of the lateral condyle									38	37 §
mp15	Breadth of the medial condyle								37	36	34.5 §
mp16	Breadth of the lateral condyle									35.5	34.5 §
mp17	Maximal distal breadth									80	

	ANTERIOR PROXIMAL PHALANX	G16-1350	G12-1961	F18-227
		8a	9	93-1
pp1	Length of the axial side			108
pp3	Proximal depth (articular surface)	40		35 ~
pp4	Proximal breath (articular surface)	48		47 ~
pp5	Depth of the diaphysis		19	21 ~
pp6	Breadth of the diaphysis		21	24 ~
pp7	Depth of the condyle		27.5	27 ~
pp8	Breadth of the condyle		38.5	
pp9	Length of the axial lip of the condyle		33	
pp10	Length of the abaxial lip of the condyle		36	37

	POSTERIOR PROXIMAL PHALANX	F14-290	J12-55	F12-145	G12-1758
		5b	8.1	8	9
pp1	Length of the axial side	95		95	
pp2	Length of the abaxial side	92.5	93	92.5	
pp3	Proximal depth (articular surface)	32	29.5	32	28.5
pp4	Proximal breath (articular surface)	39	37	39	34
pp5	Depth of the diaphysis	18	15.5	18	
pp6	Breadth of the diaphysis	20	17.5	20.5	
pp7	Depth of the condyle	24	24	25.5	22
pp8	Breadth of the condyle	35		37	33
pp9	Length of the axial lip of the condyle	29	29 ~	29.5	26
pp10	Length of the abaxial lip of the condyle	32	32		29

	INTERMEDIATE PHALANX	A16-7	E14-78	SP7-20	G13-1307
		Dol.3	5b	5b	8c
ip1	Length of the axial side		54	54.5	
ip2	Length of the abaxial side		56	59	
ip3	Length of the plantar side		64	63.5	
ip4	Proximal depth (maximal)		29	27	
ip5	Proximal breath (articular surface)		34.5	33	
ip6	Minimal breadth of the diaphysis	27	27.5	28	25
ip7	Depth of the condyle	16.5	17	16	16
ip8	Breadth of the condyle	35.5	36	37	33
ip9	Length of the axial lip of the condyle	26	28	26.5	26.5 §
ip10	Length of the abaxial lip of the condyle	28	27.5	29	26.5 §

	DISTAL PHALANX *(unpublished data; not included in Martini et al. 2017)*	G14-484	G13-1607	H13-1354	G12-1738
		8a	8c	8c	9
dp1	Maximal length	29	29	25	27
dp2	Maximal breadth	29	25.5	22.5	21.5
dp3	Maximal height	20.5	20	19.5	19
dp4	Height of the axial side	23	22.5	22	21
dp5	Height of the abaxial side	24	24	24	21.5
dp6	Length of the axial side	26	24.5	22	24
dp7	Length of the abaxial side	29	29	24.5	25
dp8	Dorsal length	28.5	27	25.5	26
dp9	Distance from the facet to the axial lateral foramen	8.5	9	7	8
dp10	Distance from the facet to the abaxial lateral foramen		9	7.5	7

	SCAPHOIDEUM	A16-4 sin	A16-23 sin	A16-26 dex	D17-71 sin	SP7-43.4 sin
		Dol-3	Dol-3	Dol-3	5-90	BH
Ks1	Height dorsal	39	37	40	36	31
Ks2	Height in the middle	28.5	27	30	27	25
Ks3	Height palmar	33	31	36	32 ~	30 ~
Ks4	Depth maximal	53	52	61	51	47
Ks5	Depth proximal	47	51	56	47	45
Ks6	Breadth of proximal facet, dorsal		30.5	32	29	28
Ks7	Breadth of proximal facet, palmar	27		28.5	26	26.5
Ks8	Total depth of distal facets	40	38 ~	43	40 ~	36.5
Ks9	Depth of dorsal distal facet	23	23 ~	26 ~	21	22

Ks10	Breadth of dorsal distal facet	26.5	27	28 ~	24	22
Ks11	Breadth of palmar distal facet	19	18 ~	21	18 ~	17 ~
Ks12	Maximal diameter of palmar distal facet	23.5	22	24	21 ~	22 ~
Ks13	Length of lateral (palmar) facet	17.5 ~	18 ~		16 ~	19
Ks14	Lateral (palmar) facet to lateral dorsal distal corner	35	35 ~		33	33 ~

	LUNATUM	**A16-32 dex Dol-3**	**H14-1090 sin 8.1b**	**E18-109 sin 8**	**E13-97 sin 8d**
Kl1	Height maximal	37	44	44	44.5
Kl2	Lateral depth of the proximal facet	33	37	34 ~	43
Kl3	Medial depth of the proximal facet	27	31.5	30 ~	30
Kl4	Dorsal breadth of the proximal facet	23	26	25 ~	31
Kl5	Minimal breadth of the proximal facet	15 ~	19		23
Kl6	Maximal diagonal		55 ~		60.5
Kl7	Depth of the distal facet		46 ~		53.5
Kl8	Dorsal breadth of the distal facet	19.5	19	22 ~	27.5
Kl9	Minimal breadth (in the middle) of the distal facet		16	18	20
Kl10	Distance from distal lateral tip, to distal dorsomedial tip				37
Kl11	Distance from distal lateral tip, to distal palmar tip				39
Kl12	Distance from distal dorsolateral, to the central eminence of the distal facet		25 ~	25.5 ~	29

	TRIQUETRUM	**A16-31 sin Dol-3**	**F16-204 sin 8a**	**SP7-43.3 sin BH**
Kq1	Dorsal maximal height	39	44	38
Kq2	Dorsal height, between tips of both facets	25	27	21
Kq3	Height in the middle	28.5	30	27
Kq4	Palmar height	34.5	35.5 ~	32.5
Kq5	Depth of proximal facet	47	53	46
Kq6	Breadth of proximal facet	29.5	34	28
Kq7	Depth of distal facet	37.5	44	37
Kq8	Breadth of distal facet	21	25.5	21

	TRAPEZOIDEUM	**A16-6 sin Dol-3**	**E15-728 ? 9**
Kt1	Maximal height	27	32
Kt2	Maximal diagonal	31.5	
Kt3	Maximal diameter of the distal facet	25	28
Kt4	Breadth of the proximal facet	20.5	
Kt5	Minimal diameter of the distal facet	16	19

	HAMATUM	**G11-493 dex 8b**	**SP7-43.5 dex BH**
Kh1	Height of the dorsal region	23	21.5
Kh2	Height of the palmar region	28	22
Kh3	Maximal diameter (including the hamulus)		46.5
Kh4	Depth of the proximal facet	44	39.5
Kh5	Depth of the distal facet	40	36
Kh6	Maximal breadth (from medial notch)	36	28
Kh7	Breadth of the proximal facet (in palmar region)	24.5	21
Kh8	Breadth of the distal facet	30	26
Kh9	Diagonal of the palmar medial facet	15	

	FIBULA	**G14-993 dex 8b**	**E18b-112 dex 93-1**	**F18-225 sin 93-1**
fi1	Height dorsal	33 ~	31	23
fi2	Height in the middle (height of the process)		30	25
fi3	Height plantar		20 ~	17.5 ~
fi4	Maximal depth		41 ~	39.5
fi5	Depth of the proximal facet		37 ~	37
fi6	Depth of the distal facet		31	31
fi7	Dorsal breadth of the proximal facet	27	26	23.5
fi8	Plantar breadth of the proximal facet		19 ~	15
fi9	Breadth of the distal facet		18	18
fi10	Depth of the medial (astragalus) facet		33	32

	ASTRAGALUS	**A16-33 sin Dol-3**	**SP7-52 sin Dol-3**	**E14-85 dex 5b**	**E15-399 sin 8**	**E17-115 sin 8**	**G12-2019 sin 8c**	**G12-1781 dex 9**
Ta1	Height of the lateral side	70 ~	75	78			79 ~	75.25
Ta2	Height axial	55	59	59.5	61		61.5	58.5
Ta3	Height of the medial side	63	69 ~	68.5	72 ~		72	68
Ta4	Proximal depth of the lateral side	30 ~	32.5	32			33	30.5
Ta5	Distal depth of the lateral side	22	24 ~	24	26.5	31	27	23
Ta6	Middle depth of the lateral side	33	37	36.5	38	42	39.5	35
Ta7	Proximal breadth	42	42 ~	46 ~			46	44
Ta8	Breadth of the calcaneal surface	28 ~		30	33	33	31	28.5
Ta9	Breadth at the lateral (calcaneal)		55		55 ~	62	60	51

	process							
Ta10	Distal breadth	46		50 ~		58 ~	52	47.5
Ta11	Greater maximal diameter (dorsolateral-distomedial)	81 ~		88 ~			93 ~	85.5
Ta12	Lesser maximal diameter (dorsomedial-distolateral)	71	76	79	81		82	76.5
Ta13	Minimal depth of the proximal trochlea (groove)	22	21 ~	23			24.5	22
Ta14	Breadth of the medial part of the distal trochlea	31		32.5 ~			35	32
Ta15	Breadth of the lateral part of the distal trochlea	17		18			18	19
Ta16	Medial depth of the distal trochlea	22		25 ~		31 ~	28	26
Ta17	Axial depth of the distal trochlea (groove)	16	17	16.5	19	20	20	18
Ta18	Lateral depth of the distal trochlea	22	24	23	27	33	28	24
Ta19	Height of the calcalneal surface	49		48 ~			56	43 ~
	CALCANEUS	**E14-80.1 dex 5b**	**H13-117 sin 8.1**	**H13-984 sin 8.1b**	**F12-148 dex 8**	**H14-1279 dex 8a**		
Tc1	Maximal height (greatest length)			154		140		
Tc2	Depth of the tubercle			51		42		
Tc3	Maximal breadth of the tubercle			44				
Tc4	Minimal breadth of the tubercle		21.5	22		21		
Tc5	Depth medial (plantar border to substentaculum)		64 ~	60	65	58		
Tc6	Breadth of the substentaculum		45 ~	45	49	34 ~		
Tc7	Medial distal height		73 ~	74	77	67 ~		
Tc8	Depth lateral (plantar border to fibular trochlea)		71	70	73	53		
Tc9	Height of the fibular trochlea	28	36	33	34 ~	29 ~		
Tc10	Breadth of the fibular trochlea	18.5	21	19	22	16		
Tc11	Distal lateral height (fibular trochlea to distal facet)		64	60	63	53.5		
Tc12	Breadth of the plantar border		22	25	25	22		
Tc13	Height of the distal (cuboid) facet		41	44	45	41		
Tc14	Breadth of the distal (cuboid) facet		25	22	26			
	CUBOIDEUM	**A16-24 sin Dol.3**	**A16-25 dex Dol.3**					
Tq1	Dorsal height	31	36					
Tq2	Medial height (proximal process to centrodistal medial facet)		33					
Tq3	Plantar diagonal (proximal process to plantar tuberosity)		55					
Tq4	Proximal depth (proximal dorsal border to plantar tuberosity)		69.5					
Tq5	Distal depth (distal dorsal border to plantar tuberosity)		65					
Tq6	Lateral depth (proximal dorsolateral border to plantar tuberosity)		61					
Tq7	From the plantar border of the proximal facet, to the dorsal border of the distal facet	52	60					
Tq8	From the dorsal border of the proximal facet, to the plantar border of the distal facet	49	57.5					
Tq9	Depth of the proximal facet	48	57					
Tq10	Depth of the distal facet	37	44					
Tq11	Length of the lateral groove (laterodorsal border of the proximal facet to distal facet)	39.5	45.5					
Tq12	Length of the plantar tubercle (centrodistal medial facet to plantar tuberosity)		42					
Tq13	Proximal breadth (centrodistal medial facet to lateral border of proximal facet)	43.5	50					
Tq14	Distal breadth (centrodistal medial facet to lateral border of distal facet)	39	50					
Tq15	Maximal diagonal breadth (proximal process to lateral border of distal facet)		57.5					
Tq16	Breadth of the main proximal facet	33	41.5					
Tq17	Breadth of the distal facet	24	32					
Tq18	Breadth of the dorsal proximal facet	19	22					
	NAVICULARE	**A16-28 dex Dol.3**						
Tn1	Dorsal height	24 ~						
Tn2	Lateral height	16.5						
Tn3	Plantar height	39						
Tn4	Maximal depth	53 ~						
Tn5	Maximal breadth	38						
Tn6	Depth of the distal dorsal and lateral facet	45						
Tn7	Depth of the distal dorsal facet	35.5						
Tn8	Depth of the distal plantar facet	16						
Tn9	Breadth of the distal dorsal facet	22						
	INTERMEDIOLATERAL CUNEIFORME (ECTOMESOCUNEIFORME)	**A16-29 dex Dol.3**	**SP7-43.6 dex? BH**					

TI1	Maximal breadth	33	30
TI2	Proximal breadth	18	18
TI3	Proximal depth	34.5	
TI4	Diameter of the plantar lateral facet	12.5	
TI5	Diameter of the dorsal lateral facet	15	
TI6	Lateral depth	28.5	
TI7	Lateral height	16	
TI8	Breadth of distal facet	21	20
TI9	Depth of distal facet	31	28

TABLE 4. Stratigraphic distribution of each skeletal element. For each unit, the approximate dating (in Ka) is given. Holotype and paratype are indicate in bold and with (*). Elements present only with uncertain attribution (assigned to *Camelus* cf. *roris* or *C.* sp.) are indicated in brackets. Elements that might represent a different species (assigned to *Camelus* sp.) are indicated in bold and with (?). See Table 2 for details on specimens.

Unit A (150 Ka) N=2	Unit A/B (200-350 Ka) N=52	Unit B (350-430 Ka) N=10	Unit C (450-475 Ka) N=12	Unit D (480-530 Ka) N=34	Unit E (540 Ka) N=8	Unit F (550 Ka) N=6
	Maxilla*					
	M^2 / M^3			(Mandibula)		
	Mandibula			**Mandibula?**		
	P_4 / M_2 / M_3					
	C / I^3 / P_1					
		Scapula?	**Scapula?**			
				Humerus		(Humerus)
Radioulnare			Radioulnare	Radioulnare		
	Scaphoideum	Scaphoideum				
	Lunatum		Lunatum	Lunatum		
	Triquetrum			Triquetrum		
	(Hamatum)			Hamatum		
	Trapezoideum				Trapezoideum	
	(Femur)		Femur	(Femur)	(Femur)	(Femur)
		Patella		Patella	Patella	
	(Tibia)	(Tibia)				
				(Fibula)		(Fibula)
	Astragalus	Astragalus		Astragalus	Astragalus	
			Calcaneus	Calcaneus		
	Cuboideum					
	Naviculare					
	Cuneiforme					
	Metacarpale		Metacarpale	Metacarpale		Metacarpale
			Metatarsale	Metatarsale	Metatarsale	
		Phalanx I	Phalanx I	Phalanx I	Phalanx I	(Phalanx I)
	Phalanx II	Phalanx II		Phalanx II		
				Phalanx III	Phalanx III	

Chapter 5
A giant and a small camel lived side by side in the Late Pleistocene of Syria

Pietro Martini, Loïc Costeur, Jean-Marie Le Tensorer, Peter Schmid

Manuscript in preparation

Abstract

The paleontological record of African and Eurasian Camelidae is poorly known and even less well understood. Three fossil species of the extant genus *Camelus* have long been known only through fragments and ancient incomplete descriptions. In the El Kowm Basin, central Syria, a 1.8 Ma long stratigraphic sequence rich in camelid remains is revealing an unexpected number of different species, succeeding each other over time. In this report we focus on the Late Pleistocene layer 5 from the site of Hummal, characterized by its rich Mousterian industry and by the compresence of two camel forms. We describe the new species *Camelus concordiae*, an animal smaller than extant dromedaries, and *Camelus moreli*, a giant camel rivalling the largest known Eurasian forms. Both species are known through abundant cranial and postcranial material and show several unique morphological traits, adding significantly to the knowledge on the Old World Camelidae. Other camel fossils from Israel, Jordan and Syria might be assigned to either of these species, but none are known in the terminal Late Pleistocene and Holocene; this suggests that the ancestor of domestic dromedaries is not to be found in the Levant.

Introduction

The evolution of Old World Camelidae is not well understood. This family appears in Eurasia in the late Miocene (MN13, late Turolian) and dispersed rapidly throughout the arid belt, extending from China to Eastern Europe and to northern Africa (Honey et al. 1998; Pickford et al. 1995; Van der Made et al. 2002). By the Miocene and Pliocene all species are classified into the genus *Paracamelus*; the extant genus *Camelus* is known from the Early Pleistocene (Geraads 2014). It differs from *Paracamelus* in derived traits such as reduction of premolars, reduction of molar styles and shortening of the rostrum (Geraads 2014; Harris et al. 2010; Havesson 1954; Kostopoulos and Sen 1999; Likius et al. 2003). The diversity and evolution of *Paracamelus* in the territories of the former USSR have been discussed by Havesson (1954), but subsequent works have shed doubts over the characters he used to reciprocally define the species (Kostopoulos and Sen 1999;

Topachevsky 1956), and there is no up-to-date review of this genus. Further, most of the literature on *Paracamelus* has been published in Russian, Ukrainian or other languages (Havesson 1954; Logvynenko 2000; Topachevsky 1956), but very little in English, and this genus has largely escaped the attention of Western scholars (Geraads 2014; Harrison 1985; Howell et al. 1969; Titov and Logvynenko 2006).

Concerning the genus *Camelus*, the fossil species are fragmentary or known solely through 19th century summary publications (Falconer and Murchison 1868; Nehring 1901; Pomel 1893). Even the extant camels are surprisingly understudied; until recently it was not even clear if they represented separate species, or domesticated forms of the same wild ancestor. Only recently was the interest in camel evolution renewed, with a thorough morphometric comparison of the skeleton in extant species (Martini et al. 2017), two descriptions of unpublished African material (Geraads 2014; Martini and Geraads 2018) and the discovery of a deep sequence rich in camel bones in Syria (Martini et al. 2015).

Until recently, four extinct species of *Camelus* had been described. *C. sivalensis* FALCONER & CAUTLEY 1836 (Falconer and Murchison 1868) has been described from the Siwalik Hills of Pakistan and India, in the Tatrot and Pinjor formation (Gaur et al. 1984; Nanda 2008, 1978) and was often considered ancestral to later species; however, it shows all the diagnostic (although primitive) traits of *Paracamelus*, and should be properly reevaluated and referred to that genus. From the same region, the name *C. antiquus* FALCONER & CAUTLEY 1836 has been proposed, but later synonymized with *C. sivalensis* (Colbert 1935a; Matthew 1929).

C. thomasi POMEL 1893 has been identified in the middle Pleistocene of Tighennif, Algeria (Pomel 1893). Younger materials from other parts of Africa and from the Near East have been referred to this species (Gautier 1966; Grigson 1983), but later most of these attributions have been dismissed (Harris et al. 2010). Different authors have considered this form closer to either the Bactrian (Gautier 1966) or the Arabian camel (Peters 1998). We recently described a larger sample from Tighennif, including a complete cranium, and showed that *C. thomasi* is not directly related to either extant species (Martini and Geraads 2018).

C. knoblochi NEHRING 1901 has been found at a number of localities in the former USSR (middle and late Pleistocene), but as for *Paracamelus* very limited information are available (Nehring 1901; Titov 2008). Its massiveness has been put in relation with *C. bactrianus*.

Finally, the Eastern African *C. grattardi* GERAADS 2014 is known only from very fragmentary material (Geraads 2014); current excavations will provide more information about this species (John Rowan, personal communication 2017).

The basin of El Kowm, Syria, represents a uniquely rich window into the study of camel evolution. This region lies halfway between the oasis of Palmyra and the valley of the Euphrates, in the geographical center of Syria (Jagher et al. 2015; Jagher and Le Tensorer 2011). Several Paleolithic sites are known within few kilometers. They mainly consist of ancient artesian wells, which attracted fauna and human hunters from the surrounding arid steppe. The faunal accumulation is dominated in every layer by camel remains. The lithic associations include several cultures from Lower Paleolithic (Oldowan) to Middle Paleolithic (Mousterian), covering the last 1.8 million years (Le Tensorer et al. 2015). This makes the El Kowm basin the longest sequence containing camel fossils in the Old World and offers a unique opportunity to study the diversity of this family in the Pleistocene of the Middle East, at the crossroad of three continents.

In our previous studies on the Camelidae from the El Kowm Basin, we have provisionally outlined the changes within the camel remains over the whole sequence (Martini et al. 2015) and described the species *Camelus roris*, based on the Middle Pleistocene assemblage of Nadaouiyeh Aïn Askar (Martini et al. in preparation). This species is close in size to a Bactrian camel, and it is characterized by relatively large P4 and M1, but reduced M2 and M3. *Camelus roris* became thus the fifth fossil species currently accepted for this genus.

Here we describe the late Middle Pleistocene-early Late Pleistocene remains associated with the Mousterian industry in the site of Hummal, El Kowm Basin. The site has provided abundant remains of two coexisting camel species: the smallest was formerly considered *C. dromedarius*, but we illustrate several cranial, mandibular, dental and postcranial differences that allow us to diagnose a separate species, here called *Camelus concordiae*. The second form represents a giant camel, comparable to the largest known Old World forms, which is named *Camelus moreli* based on mandibular, dental, and postcranial remains. The addition of three new and well-distinct camelid species underlines the importance of the El Kowm Basin for understanding the evolution of this family during the Pleistocene.

Geological and stratigraphic setting

The El Kowm Basin is found in the heart of Syria, and unlike most Levantine sites, it lies outside of the Mediterranean climate. It is characterized by a cluster of oasis in an otherwise arid

steppe that since the Early Pleistocene attracted both animals and their Paleolithic hunters. Four main sites have been excavated with a focus on archeological inquiry, but as many as 143 locations are known within ~10 km of the El Kowm village (Jagher et al. 2015; Jagher and Le Tensorer 2011).

The smallest excavated site is termed Aïn al Fil and records one of the earliest human presences outside of Africa, dated to the Olduvai subchron (~1.8 Ma) (Le Tensorer et al. 2015). The largest site is Hummal, which includes two sequences separates by a hiatus: the lowest levels (15-23) represent the late Early Pleistocene, the upper layers (5-12) the late Middle and early Late Pleistocene (Hauck 2015; Le Tensorer et al. 2011; Richter et al. 2011; Wegmüller 2015; Wojtczak 2015). Extensive investigations have also taken place in Nadaouiyeh Aïn Askar, where an incredibly rich Middle Pleistocene Acheulean industry was associated with a *Homo erectus* parietal; this site conveniently fits in the temporal gap in Hummal (Jagher 2011, 2016; Schmid 2015; Schmid et al. 1997). Finally, Umm el Tlel covers the second half of the late Pleistocene and includes a Mousterian industry of unclear relationships with Hummal (Griggo 2004; Hauck 2015, 2011). Although absolute dating is difficult in El Kowm, the fine archeological subdivisions provide a crude but adequate temporal background for a paleontological study.

The faunal association is constant in all parts of the combined sequence: camelids are dominant, together with gazelle and equids of several species. Frequent are also antelopes (such as *Oryx*), large bovines (*Bos* or *Pelorovis*) and rhinoceroses (*Stephanorhinus*); occasionally, carnivores (canids, hyaenids, large felids), proboscideans, suids, ostrich and tortoises. Human activity is responsible for a large part of the assemblage, and probably for relative frequency of different animals. The fauna does not contain forest or mountain species and consistently indicates a treeless steppe (Jagher et al. 2015; Reynaud Savioz 2011; Reynaud Savioz and Morel 2005).

In this report, we focus on layers associated with Mousterian technology in Hummal. More than 30 sublevels are collected in unit 5 (subunits a-h), which exceeds four meters of depth. They are exposed in the section West and South of the Hummal well; additionally, reworked sands containing the same industries originate from the same sedimentary rocks. Preliminary TL results place the layer 5g (basal in the sequence) within OIS5 (98-128 Ka) while the upper parts of the complex are certainly older than 36 Ka. In the Levant, Mousterian cultures are known until ~50 Ka. Other models have given somewhat different estimates (Hauck 2015). Therefore, the age of remains here can be considered the first half of the Late Pleistocene, and maybe approximated at 100-50 Ka.

Material and methods

The initial and provisional identification of fossils from Hummal has identified 394 camelid specimens from the Mousterian layers. Our study includes data on 170 confirmed camelid specimens, which are listed in Table 1; measurements are listed in Table 2. Preliminary observation suggested that in the El Kowm Basin *Camelus moreli* is found only in the Mousterian layers of Hummal, while *C. concordiae* might be present elsewhere. We restrict this study to the Mousterian layers of Hummal, and will describe the other camel assemblages in a forthcoming report.

The Mousterian industry is found in more than 30 sublevels of Unit 5, from the *in situ* sections West and South and a deposit of reworked sands. Remains of both species here described are found in at least 20 sublevels, in both sections and in sands. We do not attempt a finer stratigraphic subdivision within the Mousterian assemblage.

A part of the sample (64 confirmed specimens; one specimen not located) is currently preserved at the IPNA in Basel and could be studied in detail. Unfortunately, the largest part of the Hummal assemblage (106 confirmed, 223 other specimens) is housed at the Tell Arida Research Center, El Kowm, Syria. Due to the ongoing conflicts in Syria, the location has been inaccessible since 2011, which is prior to the start of our study. Nevertheless, we have been able to integrate the available data on the material preserved at Tell Arida: postcranial measurements (Martini 2011), dental and mandibular measurements (taken in 2007) and photographs. Casts of some of the most relevant specimens, including the holotype of *C. moreli*, are also preserved at IPNA and NMB.

All our measurements have been taken with a slide gauge caliper and rounded to the next 0.5 mm. As we found that the difference between the right and left side of the same individual can be as great as 1-2 mm, even for small bones or dentition, we consider unnecessary to use a greater precision, such as 0.1 mm.

We compared the fossil material with published data on both extant species, *C. bactrianus* and *C. dromedarius* (Martini et al. 2017), with *C. thomasi* from MNHN in Paris (Martini & Geraads, 2018) and with the new *Camelus* species from the nearby Middle Pleistocene site of Nadaouiyeh Aïn Askar (Martini et al., in preparation). Data on other fossil *Camelus* and *Paracamelus* species are based on the literature.

Most of the postcranial differences are not qualitative, but rather depend on proportions that are easier to visualize metrically than on the specimens. Important metrical characters are illustrated

using bivariate scatterplots. We also show scatterplots of data transformed to Harmonic Scores (HS), according to Martini et al. (2017); this is a transformation that scales each measurements to a baseline average (here, mean value of both extant *Camelus* species), and corrects each scaled measurement by removing an estimation of size which is approximated by the harmonic average of all its scaled measurements. The result is an index that shows the relative importance of each measurement, allowing the comparison of proportions in specimens of different size. Patterns that can be seen in scatterplots of raw measurements can be visualized better in scatterplots of HS, therefore we chose to show the latter, when appropriate.

The number of specimens for most of the elements is very limited; therefore we do not apply any statistical test.

Institutional abbreviations

NMB, Naturhistorisches Museum Basel

MNHN, Museum National d'Histoire Naturelle, Paris

IPNA, Institut für Prähistorische und Naturwissenschaftliche Archäologie (Institute for Prehistorical and Scientific Archeology), University of Basel

Systematic Paleontology

Order ARTIODACTYLA Owen, 1848

Family CAMELIDAE Gray, 1821

Subfamily CAMELINAE Gray, 1821

Tribe CAMELINI Gray, 1821

Genus *Camelus* Linnaeus, 1758

Species Camelus moreli nov. sp.

Etymology: dedicated to the memory of Philippe Morel, former archeologist and paleontologist of the Syro-Swiss mission in El Kowm, who died by accident in 1998.

Holotype: fragmentary mandibular symphysis Hu W-3467.2 with left and right p1 and right p4 (Fig. 1). Housed at Tell Arida Research Center, El Kowm, Syria.

Type locality: Hummal, El Kowm Basin.

Type layer: layer 5B III, sector South

Distribution: Hummal, El Kowm Basin (Sectors South and West, layers 5a to 5d in the Mousterian cultural horizon)

Age: early Late Pleistocene (approximately 100 Ka to 50 Ka)

Referred specimens: Left mandibula, fragment with m2, Hu S-2683.2 (Fig. 2); left m3 Hu C26-12 (Fig. 7); lumbar vertebra (L1-L4) Hu A32-29; lumbar vertebra (L2-L4) Hu W-2175; lumbar vertebra (L1-L2) Hu W-2565; lumbar series (L1 to L7) Hu S-8409, Hu S-8415, Hu S-8416, Hu S-8417, Hu S-8418, Hu S-8419, Hu S-8420; radioulnare, proximal fragments Hu SM-10, Hu W-1387, and Hu W-749 (Fig. 3); scaphoidea Hu A32-A.02, Hu PS00-18 and Hu W-3430; hamata Hu C26-3, Hu S-8100, and Hu W-3653; capitatum Hu W-3429; capites femoris Hu SM00-1 and Hu W-1472; femur, mediodistal fragment Hu W-724; tibia, distal fragments Hu C35-26, Hu PS00-3, and Hu W-229 (Fig. 4); fibulae (malleolar bones) Hu D28-6.1, Hu W-1040, Hu W-2028.3, and Hu W-2028.4; metacarpale, distal fragment Hu D35-2 (Fig. 3) and condyle Hu P12-8; articulated partial left tarsus Hu W-2029 (including metatarsale, proximal fragment Hu W-2029.1; cuboideum, Hu W-2029.2; naviculare, Hu W-2029.3; medial cuneiforme, Hu W-2029.4; and intermediolateral cuneiforme, Hu W-2029.5; Fig. 5); metatarsale, proximal fragment Hu PS00-11; distal phalanx Hu W-3440.

Tentatively referred specimens: Uncertain identification: radioulnare, proximal fragment Hu W-2222. Provisional identification that could not be verified: 33 additional specimens housed in Tell Arida, including both known and additional elements (petrosum, incisive, sacrum, scapula, humerus, and triquetrum).

Diagnosis

A very large *Camelus* species, lacking p3, with pachyostotic mandibula; short, upturned symphysis without a distinct rostral constriction; p1 much closer to c than to p4; massive lumbar vertebrae with narrow articular processes; low and broad hamatum; wide, short metacarpal condyles; tibial cochlea with enlarged dorsolateral prominence, and rather deep central and lateral fossae; fibula deep, with narrow proximal facet and wide distal facet; dorsally low cuboideum with

narrow proximodorsal facet and deep proximal articular region; naviculare narrow with tall plantar region; short, wide, low and rounded distal phalanx.

Differs from all *Camelus* and *Paracamelus* species (except *C. knoblochi*, *P. gigas* and *P. aguirrei*) in larger size.

Differs from *C. dromedarius* in the shorter and upward turned symphysis without a constriction; pachyostotic mandible; lower and broader hamatum; broader distal metacarpale with massive diaphysis and wide, short condyles; tibial cochlea with enlarged dorsolateral prominence and deeper lateral fossa; fibula with wider distal facet, low dorsal part and overall dorsoplantar depth; cuboideum with narrower proximodorsal facet, and deeper proximal articular region; naviculare with taller plantar part; distal phalanx shorter, lower and wider

Differs from *C. bactrianus* in the position of p1, much closer to c than to p3 (rather than equidistant from them), and symphysis without a clear constriction; pachyostotic mandible; lower and broader hamatum; massive metacarpal diaphysis; tibial cochlea with enlarged dorsolateral prominence and deeper central fossa; fibula with narrow proximal facet, low dorsal part and overall dorsoplantar depth; cuboideum with lower dorsal region, narrower proximodorsal facet, and deeper proximal articular region; naviculare narrower; distal phalanx shorter, lower and wider.

Differs from *C. roris* in more pachyostotic mandible; less distintictive scaphoideum shape; lower and broader hamatum; cuboideum with narrower proximodorsal facet and deeper proximal facets; narrow naviculare; wider, shorter metapodial condyles; shorter, wider, rounder distal phalanx.

Differs from *C. thomasi* in presence of p1, immediately caudal to the anterior mental foramen; narrower distal metacarpale and narrower, deeper condyles; deeper, narrower fibula; cuboid with taller dorsal aspect and deeper proximal facets; naviculare narrower and taller.

Differs from *C. grattardi* in narrower molars.

Differs from *C. knoblochi* in much longer p4, longer m2 (and supposedly m1), shorter m3, narrower metacarpal condyles, and different climatic requirement (subtropical instead of boreal).

Differs from *Paracamelus* species (including *"C." sivalensis*) in shortened rostral mandible, absence of p3, and reduction of molar styles.

Description

The holotype Hu W-3467.2 is a fragmentary mandibular symphysis (Fig. 1). The right side is broken distal to p4, which is damaged but complete; the left side is broken immediately distal to the caudal border of the symphysis. Both caniniform p1 are preserved, while the rostral alveolar border is damaged and neither canines nor incisives are present at all. However, the preserved alveoles of the incisors indicate that the symphysis could not have extended much more rostrally. The surface is poorly preserved. The mandibula is very massive and deep. The symphysis is short and ends a short distance caudal to p1, which itself is closer to the canine than to the cheek tooth row. In lateral view, between p4 and p1 the inferior border is straight and parallel to the superior border. There is a distinct bend under p1 and the tip of the symphysis rostral to p1 is turned strongly upwards. The rostral mental foramen is placed immediately in front of p1. The symphysis ends a short distance caudally to p1. There appears to be no widening of the symphysis rostral to p1, unlike in extant camels. Considering the damages to the anterior alveolar border, it is possible that a weak constriction was present, but certainly not as clear as in extant camels. The p1 are of moderate size, which might correspond to either sex; but the alveoles for the canines are large and imply an adult male individual. The p4 is large (Fig. 13a) and divided into two unequal parts; the distal lobe is wider but shorter than the mesial lobe, which is subtriangular and less symmetrical than the other. The occlusal surface is in advanced wear, and valleys have been obliterated.

Hu S-2683.2 is a fragment of left mandible, bearing only a damaged molar (Fig. 2). Like the holotype, the corpus is very massive (Fig. 11b). The ventral border shows a strong rostral tapering. The molar is much larger than in extant camels; by comparison of its estimated measurements it is considered an m2 (Fig. 13c).

The left m3 Hu C26-12 was measured as a complete specimen, but the mesial lobe has subsequently been broken and lost (Fig. 7). It is in advanced wear, with flat occlusal relief. Its huge size is apparent, but in morphology and proportions does not appear to differ from other camel species (Fig. 13d). The labial wall of the distal lobe (hypoconulid) is oblique; the styles are very weak and ribs completely missing.

The lumbar vertebrae include three isolated specimens (Hu A32-29, Hu W-2175, Hu W-2565; all within L1 and L4) and a complete series of seven elements, preserved in position (Hu S8409, Hu S8415, Hu S8416, Hu S8417, Hu S8418, Hu S8419, Hu S8420). They are characterized by very massive, tall bodies, contrasting with rather small articular processes. The arch and spinal processes are too fragmentary to give information on the presence of humps.

The proximal radioulnare fragments (Hu SM-10, Hu W-1387, and Hu W-749) are of large to very large size, but are poorly preserved and do not show differences from the modern species (Fig. 3).

Three of the seven carpal bones are known. Three specimens represent the scaphoideum: Hu PS00-18 and Hu W-3430 are large dorsal fragments, Hu A32-A.02 is complete and is characterized by average height and narrow proximal facet, but otherwise its proportions are similar to those of extant species (Fig. 17a, 17b). The hamatum occurs three times as well (Hu C26-3, Hu S-8100, and Hu W-3653) and is low and broad; the combination of proximal aspect width and palmar height strongly set this element apart from other camel forms (Fig. 17c). The single capitatum specimen, Hu W-3429, has a very large size but otherwise is not peculiar.

The metacarpale is represented by a massive distal fragment (Hu D35-2, Fig. 3); it has an average overall width, while the diaphysis is relatively thick. However, both proportions are within the variation of both extant species (Fig. 14). The condyles are broad and shallow (Fig. 15).

The isolated condyle Hu P12-8 is identified as a metacarpale by virtue of its large size; however, it is smaller than the condyles in Hu D35-2 and might represent either size variation within the species, or be in fact a metatarsale instead (Fig. 15). Unlike the other metacarpale specimen, the condyles show intermediate proportions.

Two femoral heads (Hu SM00-1 and Hu W-1472) and a medial condyle (Hu W-724) are too fragmentary to illustrate the morphology of the femur, but all three pieces are distinctly larger than any modern camel specimen.

The distal cochlea of the tibia (fragments Hu C35-26, Hu PS00-3, and Hu W-229) shows large to very large size and a unique morphological distinction (shared only with *C. concordiae*) (Fig. 4). On the lateral side of the distal tibia, two prominences separated by a gully form the lateral fossa of the cochlea, that articulates with the fibula (reduced to a malleolar bone). In camels (extant species, as well as other fossils from El Kowm Basin), the two halves of the fossa have a similar size, but the plantar one is more prominent. In *C. moreli*, the dorsal half and the dorsolateral prominence are enlarged. Consequently, the dorsal width of the cochlea results almost as great as the plantar width (Fig 16a), while in other camels the plantar width is considerably larger. Another relevant character is that the central and the lateral fossa are rather deep (Fig. 16b).

The fibula identified as *C. moreli* include three large (Hu W-1040, Hu W-2028.3, and Hu W-2028.4) and one very small (Hu D28-6.1) specimens; the latter shares the same proportions, hence

is interpreted as a juvenile of the same form. All are dorsoplantarly deep, with a low dorsal part, a narrow proximal facet, and a rather wide distal facet (Fig. 18).

The specimen Hu W-2029 consists of an articulated left tarsus of large size (Fig. 5). It is composed by four tarsalia of the distal row and the proximal metatarsale. The cuboideum (Hu W-2029.2) is dorsally low, has a narrow proximodorsal facet (for the astragalus) and a deep proximal articular region (facets for astragalus and calcaneus, together; Fig 20a). The naviculare (Hu W-2029.3) has an average dorsal height, but is taller in the plantar region and overall narrow (Fig. 20b). The two cuneiformes (Hu W-2029.4 and Hu W-2029.5) cannot be measured, and do not appear peculiar.

Two proximal fragments of metatarsale (Hu W-2029.1 and Hu PS00-11) are poorly preserved, and do not seem to differ from extant species.

The distal phalanx Hu W-3440 is very broad, low and short on both sides.

Comparison

The large size immediately separates *Camelus moreli* from both extant camel species; compared to the average in *C. bactrianus*, the largest of the two, several measurements can be more than 30% higher, such as proximal breadth of the radius (+34.0%), distal breadth of the metacarpale (+39.3%), dorsal breadth of the tibial cochlea (+36.1%); proportionally, the largest measurement is the minimal depth of the metacarpal diaphysis (+49.5%) (see SOM). The Mousterian giant camel is also larger than the African *C. grattardi* and *C. thomasi*, the Indian *"C." sivalensis* and the Eurasian *Paracamelus alutensis*, *P. alexejevi* and *P. praebactrianus*. It is close in size to the largest Eurasian camels, such as *Camelus knoblochi*, *Paracamelus gigas* and *P. aguirrei*. Within the El Kowm camelid fauna, *C. moreli* is larger than the described species *C. roris* from the Middle Pleistocene and *C. concordiae* that lived at the same time. Ongoing studies indicate that all other Middle Pleistocene and late Early Pleistocene camels from Hummal are smaller, but the middle Early Pleistocene (ca. 1.8 Ma) site of Aïn al Fil has yielded a few remains of a similar-sized, although distinct species.

Camelus moreli also differs from both extant species in several morphological traits. In dromedaries, the tip of the symphysis is almost parallel to the corpus and there is no distinct bend; in Bactrian camel, the morphology is intermediate with a weaker upward bending than in the holotype Hu W-3467.2. The symphysis is much longer in *C. dromedarius*; in *C. bactrianus* the

symphysis is shorter, but the p1 is placed halfway between p3 and the canine. Extant species show a transversal constriction of the symphysis between p3 and c; this is apparently not the case in *C. moreli*, and even accounting for the damage only a slight constriction is possible. The lumbar vertebrae have narrow articular processes in comparison to the massive bodies. In both extant species the hamatum is significantly narrower and taller, and in dromedaries it is even taller. The distal metacarpale is relatively broader than in dromedaries, and the diaphysis is antero-posteriorly thicker; however, in proportion the only specimen is not outside the variation of extant species. Its condyles are broad and short, similar to *C. bactrianus* but differing from *C. dromedarius*. The tibial cochlea is a good diagnostic element (Martini et al. 2017) and in *C. moreli* it is characterized by a large dorsolateral prominence, causing the dorsal side of the cochlea to be as wide as the plantar side. In extant camels the dorsolateral prominence is small, and the dorsal side is visibly narrower than the plantar side. The lateral and central fossae of *C. moreli* are rather deep; in *C. dromedarius* the lateral fossa is short and the central fossa is deep, in *C. bactrianus* the opposite is true (the differences are clearer in the lateral fossa). The fibula differs from *C. bactrianus* in its narrow proximal facet; from *C. dromedarius* in its wider distal facet; and from both in its low dorsal part and overall dorsoplantar depth. The dorsal side of the cuboideum is lower than in *C. bactrianus*, and the proximodorsal facet is deeper and narrower than both extant species, more so compared to *C. dromedarius*. The naviculare is narrower than in *C. bactrianus* and its plantar part is taller than *C. dromedarius*. The distal phalanx is shorter, lower and wider than in extant species.

Historically, Bactrian camels and dromedaries were crossed to produce a larger and stronger animal, that was appreciated for work and pack duties (Köhler-Rollefson 1991; Potts 2004). Published measurements from archeological finds (Köhler-Rollefson 1989; Uerpmann 1999) indicate that hybrids were indeed at the upper limit of purebred camels' variation. However, they were still smaller than *C. moreli*.

Within the El Kowm camelid fauna, no species is similar to *C. moreli*. All other camel forms are smaller; the only exception is a poorly represented species from Aïn al Fil (1.8 Ma), but a complete tibia and a scaphoid can be compared to the Mousterian large camel and show completely different proportions. Two species have been described so far: the coeval *C. concordiae* (see below) and *C. roris* from the Middle Pleistocene (Acheulean horizon) of Nadaouiyeh Aïn Askar (Martini et al., in preparation). Not many known elements of *C. roris* can be compared with *C. moreli*. The mandibula is similarly massive, but no symphysis is known in Nadaouiyeh. The metacarpal condyles are narrower and deeper. The scaphoideum is narrow and tall, with a characteristic small palmar distal facet and an elongated palmar lateral facet; in the one assigned to the large Mousterian

form, the proportions are closer to the standard shape of extant species. On the contrary, the hamatum has an average shape in Nadaouiyeh, with a rather narrow proximal facet, while in *C. moreli* it is proximally very wide and palmarly low. The cuboideum differs in that the proximodorsal facet (for the astragalus) is wide in *C. roris*, narrow in the large Mousterian camel; in the latter, the proximal articular region is very deep. In both species the naviculare has a tall plantar region, but it is overall narrower in *C. moreli*. The distal phalanx is shorter, wider and rounder than in *C. roris*. The m3, the proximal radioulnare, and the head of the femur differ significantly in size but not in morphology.

The Maghreb species *C. thomasi* is characterized by the strongly pachyostotic body of the mandibles (Martini & Geraads, 2018); the two fragmentary mandibles of *C. moreli* shows equally massive proportions and it is appropriate to define them pachyostotic as well. In *C. thomasi* p1 is thought to be absent or have a very anterior placement; in fact, the anterior mental foramen is visible in two specimens, but the p1 is not. In *C. moreli*, the well-developed p1 is found immediately caudal to the anterior mental foramen; however, in extant camels this tooth is prone to be missing or lost, so this might be due to individual variation. The m3 differs only in size. The diaphysis of the metacarpale is similarly robust, but the distal articulation is narrower and the condyles are narrower and deeper in *C. thomasi*. The fibula is deeper and narrower. The cuboid has a similarly narrow proximodorsal (astragalar) facet, but the dorsal aspect is taller and the proximal articular surface is shorter. The naviculare is low and wide, with proportions that are the opposite than in *C. moreli*.

The Eastern African species *C. grattardi* is only known though a distal humerus and the upper dentition, and is characterized by average size, reduced P4 and very wide molars (Geraads 2014). Although element that can be directly compared with *C. moreli* are missing, in the latter species m3 is not wider than in extant camels, and we expect the lower dentition to show the same proportions that are unlike *C. grattardi*.

The Eurasian species *C. knoblochi* is the only Middle to Late Pleistocene very large camel and is comparable in size to *C. moreli*. Unfortunately, few descriptions and depictions of this species are available: Nehring (1901) described the cranium and Titov (2008) depicted it, adding some dental, mandibular and metapodial measurements. However, the mandibula and the postcranium are largely unpublished or only in Russian sources that are difficult to access. Therefore, only few measurements of mandibula, lower dentition and distal metacarpale (Titov 2008) could be compared between *C. knoblochi* and *C. moreli*. The mandible of *C. knoblochi*

appears similar to that of *C. bactrianus*: at the level of m1 it is tall, but not especially broad, contrasting with the much lower but wider bodies in *C. moreli* but also *C. thomasi* and *C. roris*. The lower cheek teeth are wide, but with an impressive trend of (relative) elongation towards the back: the p4 compares in length with the smallest *C. dromedarius*, m1 with the average in extant species, m2 with the largest *C. bactrianus* and m3 is much longer than any other *Camelus* known. In *C. moreli* only p4, m2 and m3 are known (one specimen each from different individuals); they are much larger than extant camels, but do not differ in proportions, so that p4 is much longer than in *C. knoblochi*, m2 is somewhat longer and m3 is distinctly shorter. The p4 and m3 are also somewhat narrower. Further, the distal metacarpale is close in size and proportions, but the condyles are narrower in *C. moreli*. Another evident difference is found in the ecological distribution of the two species: *C. knoblochi* is found only in central and northern Eurasia, and in the late Pleistocene it was restricted to Asia east of the Ural Mountains. Its southernmost reported occurences are Leninakan, Lakhuti (Middle Pleistocene) and Samarkand (Late Pleistocene) (Titov 2008). In these regions it was part of the *Mammuthus primigenius-Coelodontha antiquitatis* fauna; an association that is very different from that found in the El Kowm Basin during all of the Pleistocene, dominated by camelids, equids and bovids that can be referred to subtropical genera such as *Oryx* and *Gazella*. Extant camels show strong ecological adaptations, coupled with limited tolerance for climates outside of their natural range, and a small overlap in distribution (Köhler-Rollefson 1991; Manefield and Tinson 1996; Mason 1984).

Paracamelus is differentiated from *Camelus* by several primitive traits; the latter genus shows reduction of all premolars and absence of p3, shortening of the rostral part of both cranium and mandibula, and reduction of molar styles and ribs. *C. moreli* fully corresponds to the diagnosis of *Camelus* in all these characters. *"Camelus" sivalensis*, on the other hand, shares all these traits with *Paracamelus* species.

Species Camelus concordiae nov. sp.

Etymology: genitive of Latin *concordia*, as a wish and encouragement for peace and prosperity in the war-torn regions of Syria and the Middle East.

Holotype: right mandibula Hu C27-1, preserving parts of the ramus and p4-m3 in advanced stage of wear (Fig. 6). Housed at IPNA, Basel, Switzerland.

Type locality: Hummal, El Kowm Basin.

Type layer: Mousterian sands, reworked sands originally part of layer complex 5

Distribution: Hummal, El Kowm Basin (Sectors South and West, layers 5a to 5d in the Mousterian cultural horizon)

Age: early Late Pleistocene (approximately 100 Ka to 50 Ka)

Referred specimens: see SOM for the complete list of specimens, that comprise 6 maxillae (Fig. 8), 17 mandibles (including the holotype; Fig. 9, 10), 25 isolated posterior teeth, and 40 postcranial elements including radioulnare (fragment olecranon), scaphoideum, triquetrum, pisiforme, hamatum, trapezoideum, femur (caput and distal fragment), tibia (distal fragment) tibia, fibula, cuboideum, naviculare, metacarpale (fragments), metatarsale (fragments), and phalanx proximal anterior and posterior.

Three specimens (mandibula Hu E31-C01; mandibula Hu P15-sable.1; cuboideum Hu C31-16) were found in reworked sediments, containing both Mousterian (layer 5) and Hummalian (layers 6 and 7) industries; they correspond morphologically to elements indisputably from the Mousterian horizon and are included in this study.

Tentatively referred specimens: Uncertain identification (see text for explanation): incisors, Hu B27-B04.1 and Hu P15-sable2; humerus, distal fragments Hu A32-2, Hu A32-30, Hu S-8030, Hu S-8178, and Hu S-8765; radioulnare, proximal fragments Hu A32-1 and Hu S-8398; capitata Hu A32-A.01, Hu W-3451.3, and Hu ZZ31-B.04; intermediolateral cuneiform Hu W-4101. Provisional identification that could not be verified: 190 additional specimens housed in Tell Arida that were not recorded as “giant camel” (= *C. moreli*), including both known and additional elements (petrosum, anterior dentition, axis fragment, pelvis fragment, diverse vertebrae, scapula, humerus, radioulnare, patella fragment, astragalus, calcaneus, phalanx media).

Diagnosis

A small *Camelus* species, lacking p3, with low, robust corpus and low, caudally inclined mandibular ramus; slender, straight, triangular coronoid process; posterior position of caudal mental foramen; V-shaped choana; palatine foramina at the level of P4; infraorbital foramen at the level of P3-P4; overall short dentition and narrow m2; scaphoideum with short proximal facet and narrow trapezoideum facet; pisiforme with short tuber and small facet; tibial cochlea with enlarged dorsolateral prominence, and rather short central and lateral fossae; fibula with wide proximal facet

and narrow distal facet; dorsally low cuboideum with wide proximodorsal facet; naviculare deep, wide and low; short proximal phalanx, with wide diaphysis and long condylar lips.

Slightly smaller than *C. dromedarius*; larger than *P. alutensis*; much smaller than all other Camelini.

Differs from *C. dromedarius* in mandibular corpus tapering, more robust; lower, caudally inclined ramus; coronoid process with wider basis; narrow, pointed choana; infraorbital foramen at the level of P3-P4 (instead of P4-M1); narrow m2; wider M3/m3; proximally shorter scaphoideum; smaller articular facet of pisiforme; deeper hamatum; tibial cochlea with larger dorsolateral prominence and shorter central fossa; proximally wider fibula; wider, lower naviculare; shorter, stouter proximal phalanx.

Differs from *C. bactrianus* in mandibular corpus posteriorly taller and thicker; caudal mental foramen more posterior; lower, caudally inclined ramus; coronoid process shorter, straight, with wider basis; palatine foramina at the level of P4 (instead of M1 or M2); infraorbital foramen at the level of P3-P4 (instead of P4-M1); shorter upper dentition; shorter p1, narrower m1 and m2, shorter m3; proximally shorter scaphoideum; pisiform lower, with shorter tuber; taller trapezoideum; tibial cochlea with larger dorsolateral prominence and shorter lateral fossa; distally narrower fibula; dorsally lower cuboid with wider proximodorsal facet; deeper, lower naviculare; shorter proximal phalanx with longer condylar lips.

Differs from *C. moreli* in slenderer mandibular corpus; wider, proximally shorter scaphoideum; taller, narrower hamatum; tibial cochlea with shorter central and lateral fossae; shorter fibula, with wider proximal and narrower distal facet; cuboid with wider proximodorsal facet; wider and lower naviculare.

Differs from *C. roris* in slenderer mandibular corpus and ramus; straight coronoid process; palatine foramina at the level of P4 (instead of M1); infraorbital foramen at the level of P3-P4 (instead of P4-M1); shorter upper dentition and narrower P4 and M1; shorter p4 and m2; proximally shorter scaphoideum; tibial cochlea with larger dorsolateral prominence; shorter and taller naviculare; proximal phalanx with wider, shallower condyle and longer condylar lips.

Differs from *C. thomasi* in slenderer mandibular corpus; presence of caudal mandibular foramen; lower ramus; thinner, straight, apically narrow coronoid process; infraorbital foramen at the level of P3-P4 (instead of P4-M1); shorter M3; narrow m2; tibial cochlea with larger

dorsolateral prominence; taller trapezoideum; dorsally lower cuboideum with wider proximodorsal facet; longer naviculare; shorter proximal phalanx with longer condylar lips.

Differs from *C. grattardi* in narrower dentition.

Differs from *C. knoblochi* in anteriorly wider, posteriorly taller mandibular corpus; palatine foramina at the level of P4 (instead of M2-M3); infraorbital foramen at the level of P3-P4 (instead of P4-M1); more pointed shape of choana; narrower dentition, with shorter P4 and shorter posterior molar.

Differs from *Paracamelus* species (including *"C." sivalensis*) in absence of p3, reduction of p4, and reduction of molar styles.

Description

The holotype Hu C27-1 is a broken right mandible (Fig. 6). The ramus preserves the coronoid process except its tip, but is broken at the level of the incisura between coronoid process and condyle. The dentition includes p4-m1 in good condition. The corpus is broken before the symphysis; neither p1 nor the rostral mental foramen are visible. The overall size is less than in *C. dromedarius*. The dentition is in very advanced wear, with all occlusal features erased from p4 to even m2, indicating a very old individual.

The ramus is sufficiently complete to show that it was relatively low. The corpus is shallow, but quite robust. The caudal mental foramen is placed under the mesial lobe of m2. The p4 is subtriangular, with the anterior stylid curving inwards and forming a slight concavity on the lingual side. The m1 is occlusally damaged. All molars show weak stylids and lack of ribs. In spite of the heavy wear, m2 and m3 shows rounded cusps on the lingual side, while labially they have a flattened profile.

As many as 16 additional mandibles are securely assigned to *C. concordiae* (Fig. 9, 10). The sample includes individuals in different stages of tooth wear, allowing the reconstruction of the metric variation across the population. They all share small size with the holotype, and many specimens are relatively complete, confirming and expanding all its distinctive characters. The ramus is posteriorly inclined, and it is always low: the angular process is placed barely higher than the occlusal surface of the dentition. The coronoid process has a narrow triangular shape, wider at the basis than at the tip, and it is straight. The condyle is never well preserved. The caudal mental foramen can be found from under the distal lobe of m1 to under the mesial lobe of m2. The corpus

is tapering, being as tall as extant species posteriorly but distinctly lower anteriorly. There is no instance of p3. The symphysis is never preserved, but in specimen Hu SM-27 its posterior edge is found immediately caudal to the alveoles of p1, at a short distance from p4.

Six instances of fragmentary maxillae are known (Fig. 8). The palatine foramina are found next to P4. The anterior edge of the choana appears to be triangular and pointed. In one specimen (Hu P15-1), the infraorbital foramen is found above the mesial border of P4. It is impossible to judge precisely the height of the orbit above the dentition, but it does appear neither noticeably low, nor high.

All upper and lower cheek teeth (P3-M3, p4-m4) are known, in several stages of wear. In shape and structure they do not appear to differ from extant camels, being especially similar to *C. dromedarius*. All upper teeth are on average small and rather short, but not narrow (Fig. 12a-d). In the lower dentition, p4 is quite small; m1 has a similar size as extant camels; m2 is narrow and shorter; m3 is also shorter but comparatively broad (Fig. 13a-d).

Hu SM-11 is the corpus a second or third lumbar vertebra: it is small, narrow and relatively tall.

Hu ZZ31-M1a is a fragmentary olecranon process of the radioulnare that can be referred to *C. concordiae* because of its small size.

Two femoral heads have a quite large size. Another fragment represents the medial distal condyle; it is small, narrow and deep.

The carpal bones are well represented, with all elements being known except for lunatum and capitatum. The scaphoideum has a short proximal but a long distal aspect, a narrow palmodistal facet (for the trapezoideum) and a wide, rather tall dorsal region (Fig. 17a, 17b). The triquetrum is small but tall, with a narrow distal facet. The pisiforme is very small, overall deep but low, and has quite short tuber and a small articular facet. The trapezoideum has larger than average size, and is tall. Finally, the hamatum is small to average-sized and has a deep proximal facet, but cannot otherwise be separated from extant camels (Fig. 17c).

A proximal and a distal fragment of metacarpale have rather large, but not gigantic size. The condyle has an intermediate shape (Fig. 15).

Three distal tibiae, showing small to average size, have a peculiar morphology that is very close to *C. moreli*: both species uniquely share an enlarged dorsolateral prominence of the cochlea (Fig. 16a). A group of small specimens can, however, be morphometrically be distinguished from *C. moreli* by the relatively small depth of the central and lateral fossa (Fig. 16b), and they are identified as *C. concordiae*.

The fibula has average size and a relatively short proximal process; the proximal facet is wide and the distal facet is narrow (Fig. 18).

Among the tarsalia, only two elements are known, but each with five quite complete specimens. The cuboideum has average size, with a low dorsal region, a wide proximodorsal facet (for the astragalus), and wide distal facet (Fig. 20a). The naviculare is small, overall and especially plantarly low, deep and wider than the average extant camel; the distal facet is deep (Fig. 20b).

A proximal and two distal fragments of metatarsale have average size and proportions.

The proximal phalanx is represented by a complete anterior specimen, a complete but damaged anterior specimen, and three fragmentary specimens. They have an average to slightly large size. The diaphysis is wide and the condyle is characterized by long lips. The anterior specimens have both proximal articulation and distal condyle rather narrow and deep, while in the posterior specimens these regions are rather short.

Comparison

Cranially, *Camelus concordiae* is the smallest known species of *Camelus*. Among Old World Camelidae, only the Early Pleistocene *Paracamelus alutensis* is smaller. In comparing the dentition, we found that m2 is the tooth with the most regular shape in *Camelus*: its measurements across different good-sized samples (*C. dromedarius, C. bactrianus, C. thomasi, C. roris* and *C. concordiae*) show that for each species, the occlusal length and width are strictly correlated to each other and to the amount of wear: unworn m2 are long and narrow, heavily used teeth are short and broad. Each species has different minima and maxima, and different regression lines.

C. concordiae is generally similar to a small *C. dromedarius*, but there are several consistent differences. The mandibles and the dentition are always smaller; however, some postcranial elements show a similar or even slightly larger size. The mandible is more robust and is lower anteriorly, but has a similar height in the posterior region, indicating a tapering shape. The caudal mental foramen is found at the same position in both species. The ramus is posteriorly slanted and

proportionally lower. The coronoid process has a wider basis and more pointed apex, giving an overall more triangular shape. The symphysis seems shorter. The choana has a triangular, pointed shape that is seldom The infraorbital foramen has a more rostral position: it is found at a level between P3 and P4, while in *C. dromedarius* it is between P4 and M1. Measurements of the upper dentition (P3-M3) overlap those of the smallest *C. dromedarius*, with a similar width but remaining below the average length of the extant species. The P3 is especially short. The M3 is wider than in *C. dromedarius* at a similar length. In the lower dentition, p4 and m1 fit well with the variation of the latter. Regarding m2, *C. concordiae* has a ~2 mm lower minimal, maximal and average length than *C. dromedarius*, but is narrower: at a given length, its width is ~2 mm smaller. In contrast, m3 is shorter but relatively wider.

The postcranium is generally of a similar or smaller size as in *C. dromedarius*, but some elements (such as the femoral head, the metapodia and the anterior proximal phalanx) are larger. The scaphoideum is proximally shorter and dorsally wider, the pisiforme has a smaller (narrower and shorter) articular facet, and the hamatum is somewhat deeper. Other proportions of these and of the remaining carpalia are within the variation of *C. dromedarius*. The distal tibia has a larger dorsolateral prominence, and a shorter central fossa. The fibula has a broader proximal facet. The cuboid has on average a wider distal facet. The naviculare is broader, with a lower plantar region. The proximal phalanges are shorter and stouter.

Compared with *C. bactrianus*, *C. concordiae* is clearly smaller. The corpus has similar proportions, being robust but shallow; in proportion, it is somewhat taller and thicker posteriorly. The mental foramen is found in a more caudal position than possible in *C. bactrianus*. The ramus is lower and more inclined posteriorly; the coronoid process is shorter, straight instead of curved, and with a declining width toward the apex. The palatine foramina are in a more rostral position: in *C. bactrianus* they are found next to m1 or even m2. The infraorbital foramina are more rostral as well: in the extant species, they are sometimes found above the middle of P4, but usually above the contact line of P4 and M1. The upper dentition is smaller, with minimal overlap in length; the width is proportionally similar. The p4 is shorter as well, while m1 fully overlaps in length but appears on average narrower. The m2 is on average shorter, although the length mostly overlaps, but at any given length it is ~5 mm narrower. The m3 is shorter, without overlap in length but an important overlap in width.

The postcranium is usually smaller, but can have a similar size (femoral head, metapodia, anterior proximal phalanx). The scaphoideum is proximally shorter, palmarly narrower and dorsally

wider and taller than *C. bactrianus*. The triquetrum is palmarly taller. The pisiforme has a short, rounded tuber and is overall lower. The trapezoideum is taller. The hamatum has a deeper proximal facet. The distal tibia differs in the larger dorsolateral prominence, and in the shorter lateral fossa. The fibula has a narrower distal facet. The cuboid is dorsally lower and has a wider proximodorsal (astragalar) facet. The naviculare is deeper but has a lower plantar region. The proximal phalanx is shorter, with a narrower proximal articulation, a stouter diaphysis, and significantly longer condylar lips.

Compared to *Camelus moreli*, which is found in the same assemblage as *C. concordiae*, the main difference is in size. Although camels can have an important sexual dimorphism, the disparity between both Mousterian species is huge and too large to be accommodated in the same species. Ontogeny is also unable to explain this difference, because several small-sized mandibles, including the holotype, have an advanced wear indicating adult and even senile individuals. However, there are also several specimens of average size that are difficult to assign to either species, and some elements that show morphological differences as well as intriguing similarities. In both species, the mandible is quite robust, although more so in the giant form; the symphysis is (or appears to be) short in both. Measurements of the lower dentition in *C. moreli* are almost twice as much as small *C. concordiae*; otherwise no difference is apparent. The lumbar vertebra is also much smaller, but has a similarly tall corpus. In *C. concordiae,* the scaphoideum is proximally shorter and overall wider. The hamatum is palmarly taller and both proximal and distal facets are narrower. The distal tibia is very similar; these two species are the only forms in which the cochlea has an enlarged dorsolateral prominence; the only consistent morphological difference between the largest and the smallest specimens is that the latter have a (slightly) shorter central and lateral fossa of the tibia. The fibula is overall shorter, with a wider proximal facet and a somehow narrower distal facet. The cuboid has a wider proximodorsal (astragalar) facet, and a shorter proximal articular region. The naviculare is wider and lower.

Camelus roris, from the Middle Pleistocene of Nadaouiyeh Aïn Askar, has the size of a *C. bactrianus,* and is larger than *C. concordiae*. The Nadaouiyeh species has a more massive mandibular corpus and a taller, robust, posteriorly inclined ramus as well. The coronoid process is subtriangular as well, but it is curved posteriorly and much thicker. The palatine foramina, found at the middle of M1, are more posterior. The infraorbital foramen is also more posterior: it is found above the middle of P4. All upper cheek teeth are longer; P4 and M1 are also wider, M2 is wider with a partial overlap, and M3 overlaps in width. The p4 is longer, with a similar width. The lower m1 is unknown in *C. roris*. The m2 is longer, with a small overlap; at the same length it is on

average ~1 mm wider than *C. concordiae*, but in *C. roris* species the regression is steeper, indicating that the tooth has a wider basis and narrow top (occlusal surface) which can be described as more pyramidal than pillar-like shape. The m3 is longer on average, but there is complete overlap of measurements between the two species. The femoral head have a similar diameter. In *C. concordiae*, the scaphoideum is proximally shorter and dorsally wider. The triquetrum is overall shorter and palmarly taller. The trapezoideum and the hamatum are slightly taller as well. The few, fragmentary metapodia do not show differences. The distal tibia is poorly represented in Nadaouiyeh, but it lacks an enlargement of the dorsolateral prominence. The cuboideum has similar proportions. The naviculare is equally wide, but shorter and taller. The proximal phalanx is similar and can best be distinguished by the deeper, narrower condyle with shorter lips in *C. roris*.

The North African *C. thomasi* has a pachyostotic mandible, whose corpus is more robust than *C. concordiae*. The corpus is also proportionally lower, but in both species it is relatively taller in the posterior region and rostrally tapering. The caudal mental foramen is not present in *C. thomasi*. The ramus is taller, but the angular process can be placed very low. The coronoid process is much thicker, with a widened apex and a slight caudal bending, completely different from the thin, straight, gently tapering process in *C. concordiae*. In the Algerian species, the infraorbital foramen is found in a more posterior position, above the contact line of P4 and M1. The palatine foramina are similarly placed next to P4 or even P3. The anterior edge of the choana has a triangular shape in both. The upper dentition is close in size; *C. thomasi* is dentally only slightly large, except for the clearly longer M3. The lower cheek teeth are all somewhat longer and overlap in width, except m2 which at any given length is 5-6 mm wider; m3 overlaps in dimension with the largest specimen of *C. concordiae*. The distal tibia is not well represented; estimated measurements suggest a shorter medial fossa, longer lateral fossa, and a dorsolateral prominence even smaller than in extant camel species. The trapezoideum is much lower. The metapodia do not show clear differences. The fibula is rather similar. The cuboideum has a taller dorsal region, but a narrower proximodorsal (astragalar) facet. The naviculare is even lower and wider, but shorter. The proximal phalanx is longer, with a similarly deep and narrow condyle but with shorter lips, especially the abaxial one.

Camelus grattardi is principally known for its upper dentition; the available measurements indicate that all cheek teeth are larger and relatively wider than in *C. concordiae*.

The mandible of *Camelus knoblochi* is not known in detail, but available measurements (Titov 2008) indicate that while large, the mandible is relatively gracile: anteriorly it is narrower than in *C. concordiae*, posteriorly it is equally robust but lower. Published photographs of the

cranium show that the infraorbital foramen is in a more posterior position, above P4-M1 like in extant species. The palatine foramina are much more posterior, being found next to the contact line of M3 and M3. The anterior edge of the choana is ogival, more rounded than in *C. concordiae*. All upper and lower cheek teeth are relatively wide; in the upper dentition, P4 is long and the molar series goes from relatively short M1 to long M3; in the lower dentition, the relative elongation starts already from p4 to m3. In contrast, all cheek teeth in *C. concordiae* are uniformly rather short, and m2 is narrow. Descriptions of the postcranium in *C. knoblochi* are insufficient for a detailed comparison.

Species of *Paracamelus* and *"C." sivalensis* differ from *C. concordiae* in the same way as from *C. moreli*: absence of p3, shortening of the rostral mandibula, reduction of molar styles and ribs. Moreover, the small Syrian camel also possesses a small P4, indicating reduction of the upper premolars as well.

Additional specimens

The anterior dentition does not show specific characters; two incisors of small size are referred to *C. cf. concordiae.*

The upper right molar Hu CD28-F04 is unique among Mousterian dentition. It is longer than all *C. concordiae* upper molars, closer in dimension to an average *C. dromedarius* (Fig. 12d); there is a distinct distal slant, the distal lobe is conspicuously longer and narrower than the mesial lobe, and the styles are well-developed, especially the mesostyle. The strong asymmetry suggests that the specimen is an M3, but its size does not fit with either Mousterian species, and its morphology differs from any other known camel species: no molar shows a longer distal than medial lobe. It cannot be determined at a specific level.

Three tooth fragments and a fragmentary thoracal vertebra are unidentified.

Five distal fragment of humerus are all incomplete and in poor conditions. They vary in size from small to large, but not beyond the variation seen in extant camels. They don't appear to differ in shape either. As there is no obvious separation in two morphological groups, all specimens are tentatively assigned to *Camelus cf. concordiae*. Six highly fragmentary specimens are unidentified.

The proximal radioulnare is not diagnostic; we assigned three very large specimens to *C. moreli* and a small one to *C. concordiae* only based on size. However, there are other specimens of intermediate size. The distal fragment Hu W-2222 is quite large and we assign it to *Camelus cf.*

moreli. The proximal radius Hu A32-1 and the fragment of olecranon Hu S-8398 are of average size and for this reason are tentatively assigned to *Camelus cf. concordiae*. One fragmentary specimen is unidentified.

The hamatum Hu W-3451.2 is too fragmentary for positive identification.

Three specimen of capitatum have average size and no morphological peculiarity, and are assigned to *Camelus cf. concordiae*.

A fragmentary patella is unidentified.

The distal tibia Hu S-12442 differs from both Mousterian species in lacking an enlarged dorsolateral prominence; further, its central fossa is short and its lateral fossa is long, while both are long in *C. moreli* and both are short in *C. concordiae*. It contrasts with the diagnosis of both species, and presently cannot be assigned to either known form. Another distal tibia (Hu W-3629) has a small size, but is too fragmentary for identification.

The astragalus Hu SM-18 is short, with wide calcaneal surface and narrow proximal trochlea. The astragalus Hu ZZ33-8 is very elongated, with a narrow calcaneal surface (Fig. 19a, 19b). Other measurements are similar and indicate a rather large size, but the differences are significant and suggest interspecific distinction. However, it is not possible to associate neither specimen with *C. moreli* or *C. concordiae*, therefore they are assigned to *Camelus sp*. An additional distal fragment is also unidentified.

Four specimens of calcaneus have been studied, but two appear to be immatures and two are weathered fragments of the tuber, hence they remain unidentified.

One intermediolateral cuneiforme is fragmentary, but on the basis of its small size is assigned to *Camelus cf. concordiae*.

Two fragment of metapodia and one distal fragment of phalanx are unidentified.

In addition to the sample described thus far, which includes 170 analyzed specimens, the Mousterian layers of Hummal have yielded 223 other specimens located in Tell Arida that could not be studied either directly or indirectly. 33 specimens were provisionally identified as “giant camel” and we refer them to *Camelus ?moreli*, while 190 were simply identified as “camel” and we refer them to *Camelus ?concordiae*.

Discussion

We have described two new species of *Camelus*, which differ in size from each other and from most other species of the same genus; *C. moreli* is gigantic, while *C. concordiae* is small. Extant camel species are domesticated animals with several breeds and accordingly a wide range of mass. Dromedaries usually weight 400-600 kg (Köhler-Rollefson 1991) to a maximum of 650 kg (Kadim et al. 2008); Bactrian camels are more massive. Walker's Mammals of the World indicates 300-690 kg for both species combined (Nowak 1999). For hybrid camels an average of 650 kg and a maximum of 900 kg is reported (Potts 2004). *Camelus moreli* was significantly larger than all of them; therefore, its average weight must have been much greater than 650 kg, approaching and likely exceeding 1000 kg. *Camelus concordiae* has consistently small cranial and dental size, but the dimension of some postcranial bones (femoral head, trapezoideum, metapodia, and proximal phalanx) can be even larger than in *C. dromedarius*. The mentioned remains are too small to belong to *C. moreli* and seem to indicate that even the smaller species was able to reach important sizes. We suggest that *C. concordiae* had a little head and was on average less heavy than *C. dromedarius*, but some individuals (maybe males) might occasionally be just as large, and suggest a body weight range of 300-600 kg.

The mandibular symphysis of *C. moreli* suggests an overall short facial part of the cranium. In general, the limb bones (metacarpale, fibula, cuboideum, naviculare) appear to be more developed in sagittal than in transversal dimensions. This might be suggestive of a different weight distribution, with less need for lateral stability. The small articular processes of the lumbar vertebrae point to a reduced strength of the dorsal spine. A possible, but at this point highly speculative, explanation is that *C. moreli* might not have had any humps, thus bearing a lesser weight and reducing the need for lateral stability and a strong spine. Unfortunately, the postcranial bones do not offer many clues to reconstruct the appearance of *C. concordiae*, but the caudally inclined ramus of the mandible might indicate a lower, more elongated head. Only the discovery of more complete remains might shed light on the proportions of both species.

The fossil described here are from layer 5 in Hummal, a thick complex containing Mousterian industry. Small-sized camels are found also in older Middle Pleistocene layers, and forthcoming studies will show if they can be included within *C. concordiae*. In contrast, *C. moreli* is not known elsewhere in the El Kowm Basin. Giant camels have not been reported from the late Mousterian of Umm el Tlel, another site in this basin; there is only a small camel species, which has been considered *C. dromedarius* (Griggo 2004) but might in fact be *C. concordiae*. In Early Pleistocene

layers from Hummal some relatively large camels are found, but none that can be considered giant. In the nearby site Aïn al Fil, we identified a tibia, a metacarpal condyle and a scaphoideum of a similar size as *C. moreli*; however, the tibia and scaphoideum show a completely different morphology and certainly represent a different species. Interestingly, the occurrence of a second, smaller camel form is indicated by a single scaphoideum of small size and very different shape. Therefore, at Aïn al Fil we find coexistence of two different-sized camels as in the Mousterian layers of Hummal. Coexistence of a large and a small camel is also reported from the Pontic region, in the Khapry faunal unit (early Early Pleistocene); in this case, *Paracamelus gigas* and *P. alutensis*, respectively, are present (Alçiçek et al. 2013).

Elsewhere in the Levant, camel fossils are rare. Outside of this region, a relevant discovery was Site 1040 in Sudan, where a large-sized skeleton was interpreted as *Camelus thomasi* by Gautier (1966). In fact, there is no reason to assign the Sudan specimen to *C. thomasi* (Martini and Geraads, 2018); no morphological comparison was performed, the size clearly exceeds the material from the type locality of Tighennif, and the dating is tentative. The skeleton was found on top of a terrace, where loose association with early Upper Paleolithic artifacts suggested an age of 22 Ka. However, the fossilization is not advanced, and remains of modern caravan dromedaries are often found in the region (Gautier 1966). Hence, a possibility to consider is that Site 1040 represents simply a hybrid between the extant camel species, which are large and were historically appreciated as pack animals. This specimen needs reliable dating and accurate description before its relevance to camelid evolution can be stated.

Following the Sudan determination, Grigson (1983) assigned to *C. thomasi* some remains of large size (naviculare, proximal metatarsale, and metacarpal condyle) from Far'ah II, in the Negev Desert, dated to about 50 Ka. These fossils are as large as the giant camel from the coeval layers in Hummal; the metapodia are morphologically not diagnostic, but the illustration shows that the naviculare is narrower than in *C. dromedarius*. Therefore, we refer the Far'ah large camel to *Camelus moreli*.

Other Levantine camel fossils are fragmentary and scarce, but never show gigantic size and are commonly assigned to *C. dromedarius*. A surface find from Dugit Beach, See of Galilee, is a left M1 or M2 which is shorter, but not narrower, than the average *C. dromedarius* (Huig de Groot, personal communication, 2017). Other Early and Middle Pleistocene remains are known from 'Ubeidiyah (Israel) and Latamne (Syria); Late Pleistocene ones from Sabha, Emireh, Tabun C, Qafzeh, (Israel), Douara (Syria), and Azraq (Jordan) (Grigson 1983; Payne and Garrard 1983).

None is known from the terminal Late Pleistocene and prehistoric Holocene, represented by many Upper Paleolithic and Natufian archeological sites. These remains are most common in the arid intern regions, but also present on the coast in mesic habitat and woodland faunal association; thus they differ from extant desert adapted *C. dromedarius*, and possibly belong to a different species (Payne and Garrard 1983). The abundant material of Hummal shows that indeed a different species lived in the Late Pleistocene of the Levant; and the measurements of the Dugit Beach specimen agree with this determination. Hence, we propose that all the Late Pleistocene small camelid from Syria, Israel and Jordan should be referred to *C. concordiae*.

Camelus concordiae and *C. dromedarius* are similar in size and many morphological details, although the differences are consistent with a species-level difference. In this study, we did not attempt at a phylogenetic reconstruction because of the lack of data in several species; however, we suggest that among known *Camelus* species, they have the greatest resemblance. The closeness in time (Late Pleistocene, respectively Holocene) and space (Levant, respectively southern Arabic Peninsula) with the putative wild ancestor of *C. dromedarius* support this suggestion. Over the evolutionary relationship of extant camels with fossil species has been much speculated and little consensus exists. Archeological fossil associations from Oman and the United Arabian Emirates are thought to represent remains of ancient wild dromedaries (Beech et al. 2009; Curci et al. 2014; Driesch et al. 2008; Driesch and Obermaier 2007; Spassov and Stoytchev 2004); they equal in size modern, domesticated animals. Other domesticated animals descend from a wild form that was larger, and the same has been suggested to be true for the dromedary (Curci et al. 2014; Driesch and Obermaier 2007; Grigson 2012). It is therefore surprising to find that a near relative was somewhat smaller than domesticated camels, reinforcing the idea that a direct descent of *C. dromedarius* from *C. concordiae* should be excluded.

Conclusions

The site of Hummal has yielded abundant material of two new species of *Camelus* characterized by different sizes: *C. moreli* was gigantic, while *C. concordiae* was small. The forms two coexisted during the Late Pleistocene of Syria and the Levant, in a subtropical steppe environment that was probably less arid than the habitat of extant camels. Both species are known through abundant cranial and postcranial specimens that show many unique morphological traits. This study is part of a recent renewal of interest in the evolution of camelids, and new discoveries have shown that their diversity has been underestimated and that relationships to the extant species have been suggested carelessly. Future work will review the whole sample from El Kowm and shed

light on the turnover within this family during the Pleistocene of the Middle East. Here, we refrained from attempting at conducting a phylogenetic reconstruction, but we argue that *Camelus concordiae* is the species morphologically, geographically and stratigraphically closest to the supposed wild ancestor of domestic dromedaries. *Camelus moreli* is less completely known, and its relation with other camels is more obscure, but it appears to share important similarities with *C. concordiae* itself. Both new species add critical data to the diversity of this family, but still leave us without any answer in the search for the ancestral camel, evolutionarily the most elusive of domestic animals.

Acknowledgements

We thank Chloé Lecompte for sharing measurements on the Tell Arida fossils, Bastien Mennecart for fruitful discussions, Huig de Groot for offering information on the Dugit Beach specimen, Denis Geraads for access to the Tighennif collection and for providing Soviet literature, Inna Popko for help with Russian and Ukrainian translation, and Marisa and Pierre Harper for their hospitality. The Syro-Swiss research in El Kowm would not have been possible without the logistic support of the Tell Arida staff, led by Ahmed Taha, and all the participants to the excavations.

This study is part of P. Martini's doctoral thesis, which is supported by the Swiss National Foundation, the Isaac Dreyfus-Bernheim Stiftung, and the Freiwillige Akademische Gesellschaft Basel. These institutions and the Tell Arida Foundation have also funded excavations in El Kowm.

References

ALÇIÇEK, M. C., S. MAYDA, and V. V. TITOV. 2013. Lower Pleistocene stratigraphy of the Burdur Basin of SW Anatolia. Comptes Rendus Palevol 12:1-11.

BEECH, M., M. MASHKOUR, M. HUELS, and A. ZAZZO. 2009. Prehistoric camels in south-eastern Arabia: the discovery of a new site in Abu Dhabi's Western Region, United Arab Emirates. Proceedings of the Seminar for Arabian Studies 39:17-30.

BELMAKER, M. 2010. Early Pleistocene Faunal Connections Between Africa and Eurasia: An Ecological Perspective. Pp. 183-205 in Out of Africa I: the First Hominin Colonization (J. G. Fleagle, J. J. Shea, F. E. Grine, A. L. Baden and R. E. Leakey, eds.). Springer.

BESANÇON, J., L. COPELAND, F. HOURS, S. MUHESEN, and P. SANLANVILLE. 1981. Le Paléolithique d'El Kowm. Rapport préliminaire. Paléorient 7:33-55.

BUCCELLATI, G., and M. K. BUCCELLATI. 1967. Archaeological Survey of the Palmyrene and the Jebel Bishri.

BURGER, P. A. 2016. The history of Old World camelids in the light of molecular genetics. Tropical animal health and production.

CAUVIN, J., M.-C. CAUVIN, and D. STORDEUR. 1979. Recherches préhistoriques à El Kowm (Syrie).

COLBERT, E. H. 1935a. Siwalik Mammals in the American Museum of Natural History. Transactions of the American Philosophical Society, New Series 26:1-401.

COLBERT, E. H. 1935b. Siwalik Mammals in the American Museum of Natural History. Transactions of the American Philosophical Society, New Series 26:i-x+1-401.

CURCI, A., M. CARLETTI, and M. TOSI. 2014. The camel remains from site HD-6 (Ra's al-Hadd, Sultanate of Oman): an opportunity for a critical review of dromedary findings in eastern Arabia. Anthropozoologica 49:207-22.

DRIESCH, A. V. D., H. BRÜCKNER, H. OBERMAIER, and A. ZANDER. 2008. The hunt for wild dromedaries at the United Arab Emirates coast during the 3rd and 2nd millennia BC. Camel bones from the excavations at Al Sufouh 2, Dubai, UAE. Pp. 487-497 in Archaeozoology of the Near East VIII. Actes des huitièmes Rencontres internationales d'Archéozoologie de l'Asie du Sud-Ouest et des régions adjacentes. Maison de l'Orient et de la Méditerranée, Jean Pouilloux, Lyon.

DRIESCH, A. V. D., and H. OBERMAIER. 2007. The hunt for wild dromedaries during the 3rd and 2nd millennia BC on the United Arab Emirates coast. Camel bone finds from the excavations at Al Sufouh 2, Dubai, UAE. Pp. 133-167 in Skeletal Series and their Socio-economic Context (J. Grupe and J. Peters, eds.). Leidorf, Rahden.

FALCONER, H., and C. MURCHISON. 1868. Palaeontological memoirs and notes of the late Hugh Falconer. Robert Hardwicke, London. 1 - Fauna Antiqua Sivalensis.

GAUR, R., P. RAGHAVAN, and S. R. K. CHOPRA. 1984. On the remains of *Camelus sivalensis* (Artiodactyla, Camelidae) from Pinjor Formation of Upper Siwaliks. Indian Journal of Earth Sciences 11:158-165.

GAUTIER, A. 1966. *Camelus thomasi* from the Northern Sudan and its bearing on the relationship *C. thomasi* - *C. bactrianus*. Journal of Paleontology 40:1368-1372.

GERAADS, D. 1986. Les ruminants du pleistocene d'Oubeidiyeh (Israel). Mémoires et Travaux du Centre de Recherches français de Jérusalem 5:143-181.

GERAADS, D. 2014. *Camelus grattardi*, sp. nov., a new camel from the Shungura Formation, Omo Valley, Ethiopia, and the relationships of African fossil Camelidae (Mammalia). Journal of Vertebrate Paleontology 34:1481-1485.

GERAADS, D. 2016. Pleistocene Carnivora (Mammalia) from Tighennif (Ternifine), Algeria. Geobios 49:445-458.

GRATTARD, J.-L., F. C. HOWELL, and Y. COPPENS. 1976. Remains of *Camelus* from the Shungura Formation, lower Omo Valley. Pp. 268–274 in Earliest Man and Environments in the Lake Rudolf Basin. (Y. Coppens, F. C. Howell, G. L. Isaac and R. E. Leakey, eds.). University of Chicago Press, Chicago.

GRIGGO, C. 2004. Mousterian fauna from Dederiyeh Cave and comparisons with Fauna from Umm El Tlel and Douara Cave. Paléorient 30:149-162.

GRIGSON, C. 1983. A very large camel from the upper Pleistocene of the Negev Desert. Journal of Archaeological Science 10:311-316.

GRIGSON, C. 2012. Camels, copper and donkeys in the Early Iron Age of the southern Levant: Timna revisited. Levant 44:82-100.

HARINGTON, C. R. 2011. Pleistocene vertebrates of the Yukon Territory. Quaternary Science Reviews 30:2341-2354.

HARRIS, J. M., D. GERAADS, and N. SOLOUNIAS. 2010. Camelidae. Pp. 815-820 in Cenozoic Mammals of Africa (L. Werdelin and W. J. Sanders, eds.). University of California Press, London.

HARRISON, J. A. 1985. Giant Camels from the Cenozoic of North America. Smithsonian Contributions to Paleobiology 57.

HAUCK, T. C. 2011. Mousterian technology and settlement dynamics in the site of Hummal (Syria). Journal of Human Evolution 61:519-37.

HAUCK, T. C. 2015. Garden of Eden or Desert Exile: The Mousterian of Hummal in context. L'Anthropologie 119:659-675.

HAVESSON, Y. I. 1954. Третичные Верблюды Восточного Полушария (Род *Paracamelus*) [Tertiary camels from the Eastern Hemisphere (Genus *Paracamelus*)]. Trudy Paleontologicheskovo Instituta, Akademiya Nauk SSSR 47:100-162.

HONEY, J. J., J. A. HARRISON, D. R. PROTHERO, and M. S. STEVENS. 1998. Camelidae. Pp. 439-462 in Evolution of Tertiary Mammals of North America: Terrestrial Carnivores, Ungulates, and Ungulatelike Mammals (C. M. Janis, K. Scott and L. L. Jacobs, eds.). Cambridge University Press, Cambridge.

HOWELL, F. C., L. S. FICHTER, and R. WOLFF. 1969. Fossil Camels in the Omo Beds, Southern Ethiopia. Nature 223:150-152.

JAGHER, R. 2011. Nadaouiyeh Aïn Askar - Acheulean variability in the Central Syrian Desertin The Lower and Middle Palaeolithc in the Middle East and Neighbouring Regions (J. M. Le Tensorer, R. Jagher and M. Otte, eds.). Etudes et Recherches Archéologiques de l'Université de Liège (ERAUL), Liège.

JAGHER, R. 2016. Nadaouiyeh Aïn Askar, an example of Upper Acheulean variability in the Levant. Quaternary International 411:44-58.

JAGHER, R., H. EL SUEDE, and J. M. LE TENSORER. 2015. El Kowm Oasis, human settlement in the Syrian Desert during the Pleistocene. L'Anthropologie 119:542-580.

JAGHER, R., and J.-M. LE TENSORER. 2011. El Kowm, a key area for the palaeolithic of the Levant in Central Syriain The Lower and Middle Palaeolithc in the Middle East and Neighbouring Regions (J. M. Le Tensorer, R. Jagher and M. Otte, eds.). Etudes et Recherches Archéologiques de l'Université de Liège (ERAUL), Liège.

KADIM, I. T., O. MAHGOUB, and R. W. PURCHAS. 2008. A review of the growth, and of the carcass and meat quality characteristics of the one-humped camel (Camelus dromedaries). Meat science 80:555-69.

KÖHLER-ROLLEFSON, I. U. 1989. Zoological analysis of camel skeletons. Pp. 142-164 in Pella of the Decapolis. Vol. 2, Final Report on the College of Wooster Excavations in Area IX, the Civic Complex, 1979-1985 (R. H. Smith and L. P. Day, eds.). The College of Wooster, Wooster.

KÖHLER-ROLLEFSON, I. U. 1991. *Camelus dromedarius*. Mammalian species 375:1-8.

KOSTOPOULOS, D. S., and A. ATHANASSIOU. 2005. In the shadow of bovids: suids, cervids and giraffids from the plio-pleistocene of Greece. Pp. 179-190 in Les ongulés holarctiques du Pliocène et du Pléistocène (E. Crégut-Bonnoure, ed.). Maison de la géologie, Paris.

KOSTOPOULOS, D. S., and S. SEN. 1999. Late Pliocene (Villafranchian) mammals from Sarikol Tepe, Ankara, Turkey. Mitteilungen der Bayerischen Staatssammlung für Paläontologie und Historische Geologie 39:165-202.

KOZHAMKULOVA, B. S. 1986. The Late Cenozoic Two-Humped (Bactrian) Camels of Asia. Quartärpaläontologie 6:93-97.

LE TENSORER, J.-M., V. VON FALKENSTEIN, H. LE TENSORER, and S. MUHESEN. 2011. Hummal: A very long Paleolithic sequence in the steppe of Central Syria - Considerations on Lower Paleolithic and the beginning of Middle Paleolithicin The Lower and Middle Palaeolithc in the Middle East and Neighbouring Regions (J. M. Le Tensorer, R. Jagher and M. Otte, eds.). Etudes et Recherches Archéologiques de l'Université de Liège (ERAUL), Liège.

LE TENSORER, J. M., H. LE TENSORER, P. MARTINI, V. VON FALKENSTEIN, P. SCHMID, and J. J. VILLALAIN. 2015. The Oldowan site Aïn al Fil (El Kowm, Syria) and the first humans of the Syrian Desert. L'Anthropologie 119:581-594.

LESBRE, F.-X. 1903. Recherches anatomiques sur les Camélidés. Pp. 1-196 in Archives du Muséum d'Histoire Naturelle de Lyon (H. Georg, ed.), Lyon.

LIKIUS, A., M. BRUNET, D. GERAADS, and P. VIGNAUD. 2003. Le plus vieux Camelidae (Mammalia, Artiodactyla) d'Afrique: limite Mio-Pliocène, Tchad. Bulletin de la Société Géologique de France 174:187-193.

LOGVYNENKO, V. M. 2000. Верблюды (Camelidae, Tylopoda) плиоцепа и эоплейстоцена Украины [The Camels (Camelidae, Tylopoda) from the Pliocene and Eopleistocene of Ukraine]. Vestnik zoologii Supplement N° 14:120-127.

MANEFIELD, G. W., and A. H. TINSON. 1996. Camels: A Compendium. University of Sydney Post Graduate Foundation in Veterinary Science376.

MARTÍNEZ-NAVARRO, B., M. BELMAKER, and O. BAR-YOSEF. 2012. The Bovid assemblage (Bovidae, Mammalia) from the Early Pleistocene site of 'Ubeidiya, Israel: Biochronological and paleoecological implications for the fossil and lithic bearing strata. Quaternary International 267:78-97.

MARTINI, P. 2011.A metrical analysis of the morphological variation in extant and fossil camels. Master's thesis, University of Zürich, Zürich.

MARTINI, P., L. COSTEUR, J.-M. LE TENSORER, and P. SCHMID. 2015. Pleistocene camelids from the Syrian Desert: The diversity in El Kowm. L'Anthropologie 119:687-693.

MARTINI, P., and D. GERAADS. 2018. *Camelus thomasi* Pomel, 1893, from the Pleistocene type-locality Tighennif (Algeria): Comparisons with modern *Camelus*. Geodiversitas 40:115-134.

MARTINI, P., P. SCHMID, and L. COSTEUR. 2017. Comparative Morphometry of Bactrian Camel and Dromedary. Journal of Mammalian Evolution.

MASON, I. L. 1984. Origin, Evolution and distribution of domestic camels. Pp. 16-35 in The Camelid: An all-purpose animal. Proceedings of the Khartoum Workshop on Camels, December 1979 (W. R. Cockrill, ed.). Scandinavian Institute of African Studies, Uppsala.

MATTHEW, W. D. 1929. Critical Observations Upon Siwalik Mammals. Bulletin American Museum of Natural History 56:437-560.

MORALES, J., D. SORIA, and E. AGUIRRE. 1980. Camelido finimioceno en Venta del Moro. Primera cita para Europa Occidental. Estudios Geológicos 36:139-142.

NANDA, A. C. 1978. Occurrence of *Camelus sivalensis* Falconer and Cautley from the Tatrot Formation of Ambala, India. Journal of the Geological Society of India 19:160-164.

NANDA, A. C. 2008. Comments on the Pinjor Mammalian Fauna of the Siwalik Group in relation to the post-Siwalik faunas of Peninsular India and Indo-Gangetic Plain. Quaternary International 192:6-13.

NEHRING, A. 1901. Mittheilung über einen fossilen Kamel-Schädel (*Camelus Knoblochi*) von Sarepta an der Wolga. Sitzungsbericht der Gesellschaft Naturforschende Freunde 5.

NOWAK, R. M. 1999. Walker's Mammals of the World. The Johns Hopkins University Press, Baltimore1-1936.

PAYNE, S., and A. GARRARD. 1983. *Camelus* from the Upper Pleistocene of Mount Carmel, Israel. Journal of Archaeological Science 10.

PETERS, J. 1998. *Camelus thomasi* Pomel, 1893, a possible ancestor of the one-humped camel? Zeitschrift für Säugetierkunde 63:372-376.

PICKFORD, M., J. MORALES, and D. SORIA. 1995. Fossil camels from the Upper Miocene of Europe: implications for biogeography and faunal change. Geobios 28:641-650.

POMEL, A. 1893. Caméliens et Cervidés. Paléontologie monographies.

POTTS, D. T. 2004. Camel hybridization and the role of *Camelus bactrianus* in the ancient Near East. Journal of the Economic and Social History of the Orient 47:143-165.

REYNAUD SAVIOZ, N. 2011. The faunal remains from Nadaouiyeh Aïn Askar (Syria). Preliminary indications of animal acquisition in an Acheulean site.in The Lower and Middle Palaeolithc in the Middle East and Neighbouring Regions (J. M. Le Tensorer, R. Jagher and M. Otte, eds.). Etudes et Recherches Archéologiques de l'Université de Liège (ERAUL), Liège.

REYNAUD SAVIOZ, N., and P. MOREL. 2005. La faune de Nadaouiyeh Aïn Askar (Syrie centrale, Pléistocène moyen) : aperçu et perspectives. Revue de Paléobiologie, Genève 10:31-35.

RICHTER, D., T. C. HAUCK, D. WOJTCZAK, J. M. LE TENSORER, and S. MUHESEN. 2011. Chronometric age estimates for the site of Hummal (El Kowm, Syria)in The Lower and Middle Palaeolithc in the Middle East and Neighbouring Regions (J. M. Le Tensorer, R. Jagher and M. Otte, eds.). Etudes et Recherches Archéologiques de l'Université de Liège (ERAUL), Liège.

RÍOS, M., M. DANOWITZ, and N. SOLOUNIAS. 2016. First comprehensive morphological analysis on the metapodials of Giraffidae. Palaeontologia electronica 19.3.50A:1-39.

RYBCZYNSKI, N., J. C. GOSSE, C. R. HARINGTON, R. A. WOGELIUS, A. J. HIDY, and M. BUCKLEY. 2013. Mid-Pliocene warm-period deposits in the High Arctic yield insight into camel evolution. Nature communications 4:1550.

SCERRI, E. M. L., et al. 2014. Middle to Late Pleistocene human habitation in the western Nefud Desert, Saudi Arabia. Quaternary International.

SCHERER, C. S. 2013. The Camelidae (Mammalia, Artiodactyla) from the Quaternary of South America: Cladistic and Biogeographic Hypotheses. Journal of Mammalian Evolution 20:45-56.

SCHMID, P. 2015. Nadaouiyeh – A *Homo erectus* in Acheulean context. L'Anthropologie 119:694-705.

SCHMID, P., et al. 1997. Découvertes de restes humains dans les niveaux acheuléens de Nadaouiyeh Aïn Askar (El Kowm, Syrie Centrale). Paléorient 23:87-93.

SEMPREBON, G. M., and F. RIVALS. 2010. Trends in the paleodietary habits of fossil camels from the Tertiary and Quaternary of North America. Palaeogeography, Palaeoclimatology, Palaeoecology 295:131-145.

SEN, S. 2010. Camelids do not occur in the late Miocene mammal locality of Çobanpinar, Turkey. Russian Journal of Theriology 9:87-91.

SPASSOV, N., and T. STOYTCHEV. 2004. The dromedary domestication problem: 3000 BC rock art evidence for the existence of wild One-humped camel in Central Arabia. Historia naturalis bulgarica 16:151-158.

STIMPSON, C. M., et al. 2016. Middle Pleistocene vertebrate fossils from the Nefud Desert, Saudi Arabia: Implications for biogeography and palaeoecology. Quaternary Science Reviews 143:13-36.

TEILHARD DE CHARDIN, P., and M. TRASSAERT. 1937. The Pliocene Camelidae, Giraffidae and Cervidae of South Eastern Shansi. Palaeontologia Sinica 102:1-56, pl. I-VI.

THOMAS, H., et al. 1998. Découverte des premières faunes pléistocènes de la pénisule Arabique dans le désert du Nafoud (Arabie Saoudite). Comptes rendus de l'Académie des Sciences de Paris 326:145-152.

TITOV, V. V. 2003. Paracamelus from the Late Pliocene of the Black Sea region. Pp. 17-24 in Advances in Vertebrate Paleontology: Hen to Panta (A. Petculescu and E. Stiuca, eds.), Bucharest.

TITOV, V. V. 2008. Habitat conditions for *Camelus knoblochi* and factors in its extinction. Quaternary International 179:120-125.

TITOV, V. V., and V. N. LOGVYNENKO. 2006. Early *Paracamelus* (Mammalia, Tylopoda) in Eastern Europe. Acta zoologica cracoviensia 49A:163-178.

TOPACHEVSKY, V. A. 1956. Remains of small camel (Paracamelus alutensis) from the upper Pliocene of the south of Ukraine. Proc. Inst. Zool. Kiev 13:93-100.

UERPMANN, H.-P. 1999. Camel and horse skeletons from protohistoric graves at Mleiha in the Emirate of Sharjah (U.A.E.). Arabian archaeology and epigraphy 10:102-118.

VAN DER MADE, J., and J. MORALES. 1999. Family Camelidae. Pp. 221-224 in The Miocene Land Mammals of Europe (G. E. Rössner and K. Heissig, eds.). Verlag Dr. Friedrich Pfeil, München.

VAN DER MADE, J., J. MORALES, S. SEN, and F. ASLAN. 2002. The first camel from the upper Miocene of Turkey and the dispersal of the camels into the Old World. Comptes Rendus Palevol 1:117-122.

VISLOBOKOVA, I. A. 2008. Main stages in evolution of Artiodactyla communities from the Pliocene-Early Middle Pleistocene of northern Eurasia: Part 2. Paleontological Journal 42:414-424.

WANG, X., L. J. FLYNN, and M. FORTELIUS. 2013. Fossil Mammals of Asia - Neogene biostratigraphy and chronology. Columbia University Press, New York.

WEBB, S. D., and J. A. MEACHEN. 2004. On the origin of lamine Camelidae including a new genus from the Late Miocene of the high plains. Bulletin of Carnegie Museum of Natural History 36:349-362.

WEGMÜLLER, F. 2015. The Lower Palaeolithic assemblage of Layers 15–18 (Unit G) at Hummal. An exemplary case addressing the problems placing undated, archaic-looking stone tool assemblages in the Early and Lower Palaeolithic record by techno-typological classification. L'Anthropologie 119:595-609.

WOJTCZAK, D. 2015. Rethinking the Hummalian industry. L'Anthropologie 119:610-658.

ZDANSKY, O. 1926. Paracamelus gigas, Schlosser. Palaeontologia Sinica 2:1-44, 4 tables.

Figures

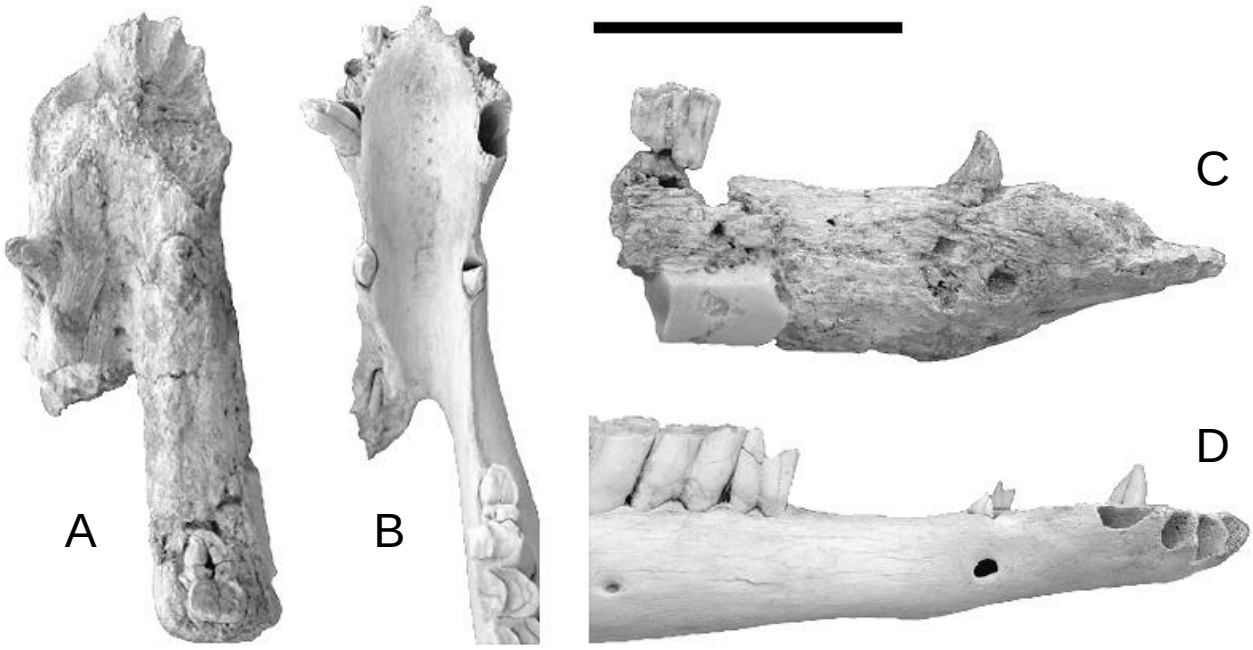

Fig. 1 Mandibular symphysis Hu W-3467.2 (*C. moreli*, holotype; A, C), compared to Recent *C. dromedarius* (B, D). **A**, **B** Occlusal view. **C**, **D** Lateral view. Scale bar equals 10 cm.

Fig. 2 Left mandibular fragment Hu S-2683.2 with m2 (*C. moreli*), occlusal view. Scale bar equals 5 cm.

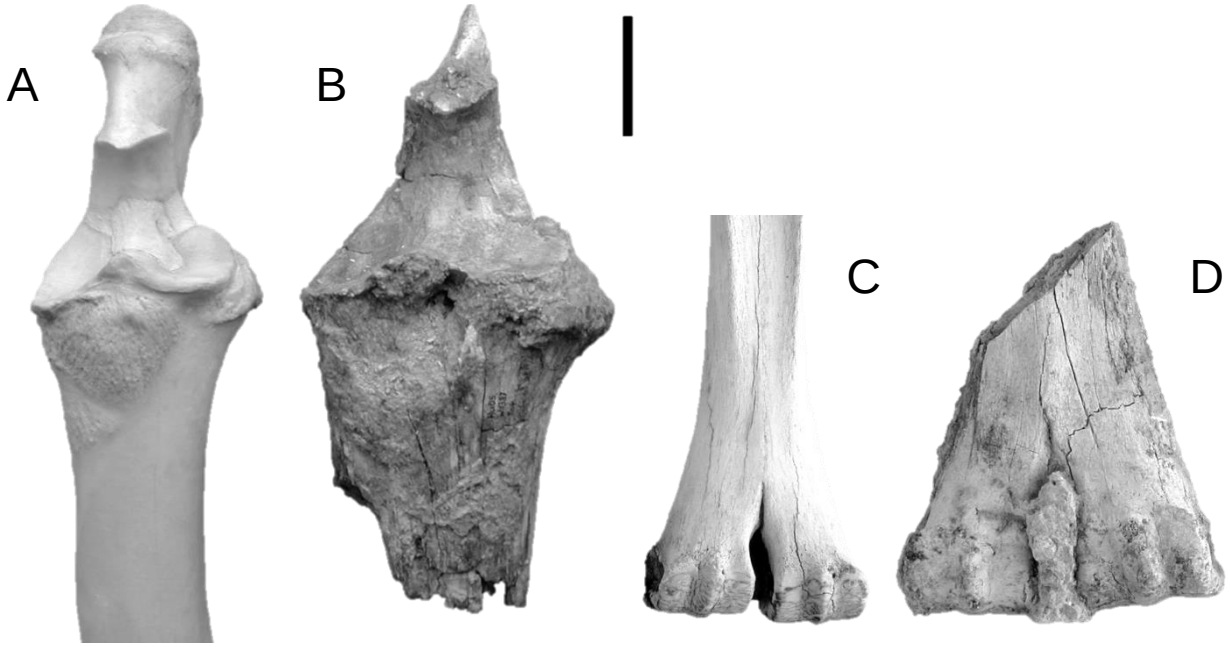

Fig. 3 Comparison of scapular limb bones. **A** Proximal fragment of left radioulnare, dorsal view (Recent *C. dromedarius*) **B** Hu W-1387 (*C. moreli*). **C** Distal metacarpale, palmar view (Recent *C. dromedarius*). **D** Hu D35-2 (*C. moreli*). Scale bar equals 5 cm.

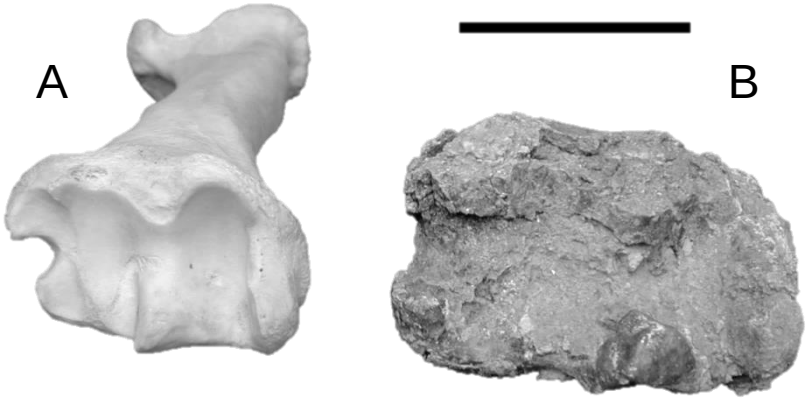

Fig. 4 Comparison of left distal tibia. **A** Recent *C. dromedarius*. **B** Hu C35-26 (*C. moreli*). Scale bar equals 5 cm.

Fig. 5 Comparison of partial articulated tarsus. **A** Recent *C. dromedarius*. **B** Hu W-2029 (*C. moreli*). Scale bar equals 5 cm.

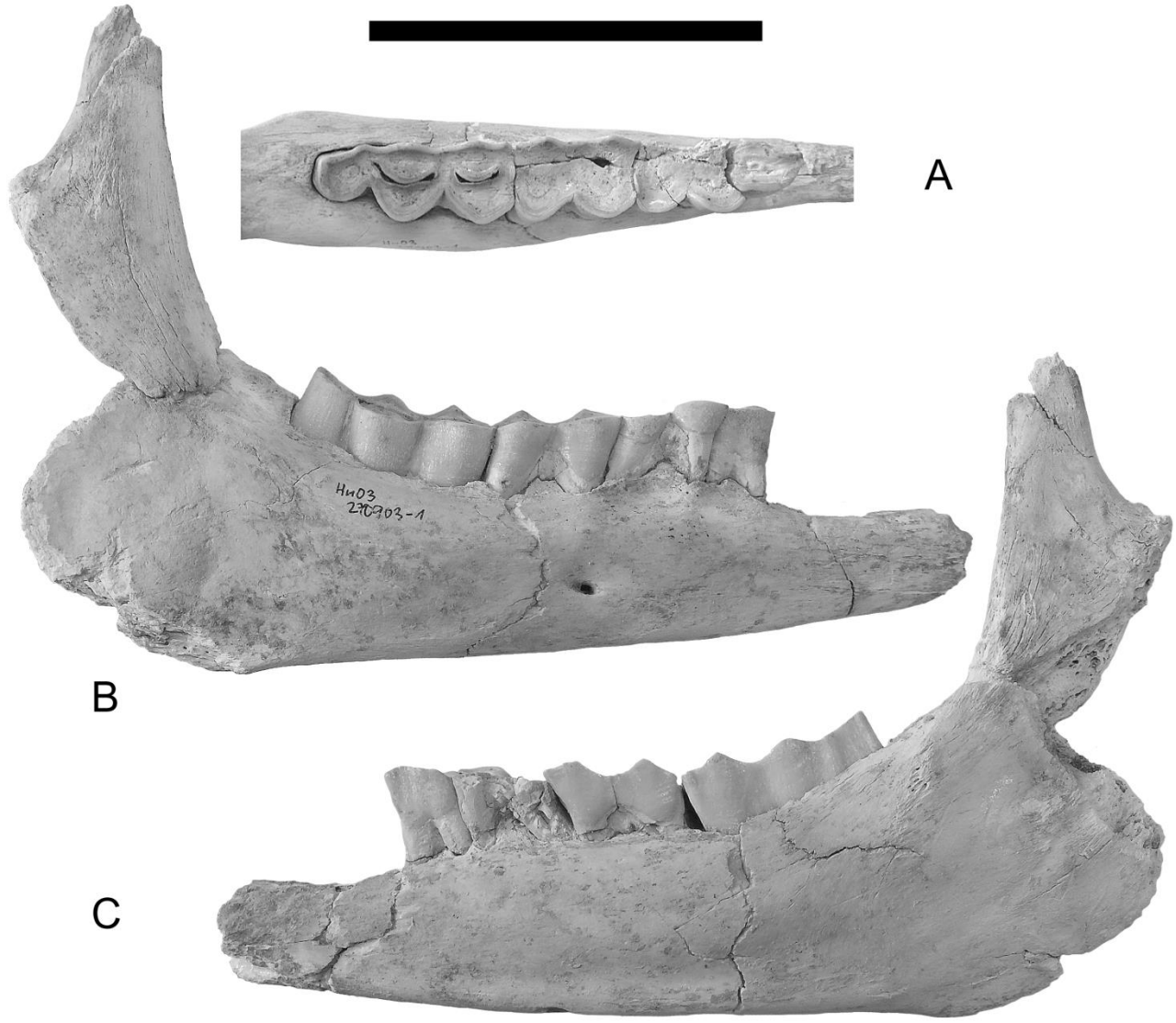

Fig. 6 Right hemimandibula Hu C27-1 (*Camelus concordiae*, holotype). **A** Occlusal view. **B** Labial view. **C** Lingual view. Scale bar equals 10 cm.

Fig. 7 Fragments of m3, both missing the mesial lobe. **A** Hu C26-12 (left m3, *C. moreli*). **B** Hu SM-25.3 (right m3, *C. concordiae*). Scale bar equals 5 cm.

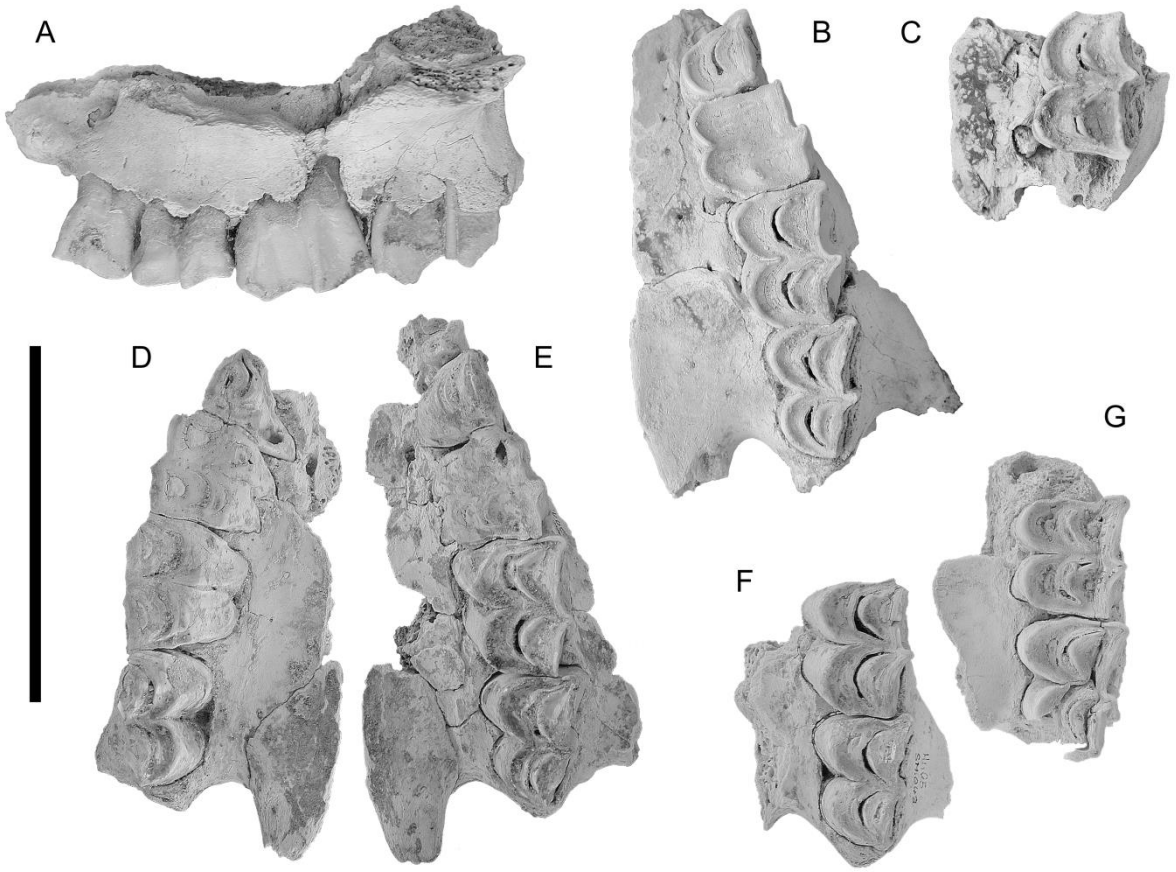

Fig. 8 Maxillae and upper dentition of *Camelus concordiae*. **A** Left maxilla Hu P15-1, lateral view. **B** Same as A, occlusal view. **C** Fragmentary left maxilla Hu P15-2 with M2, occlusal view. **D** Right maxilla Hu SM-41 occlusal view. **E** Same as D, left maxilla of the same individual. **F** Fragmentary left maxilla Hu SM-43, with M2 and M3, occlusal view. **G** Fragmentary left maxilla Hu SM-44, with M1 and M2, occlusal view. Scale bar equals 10 cm.

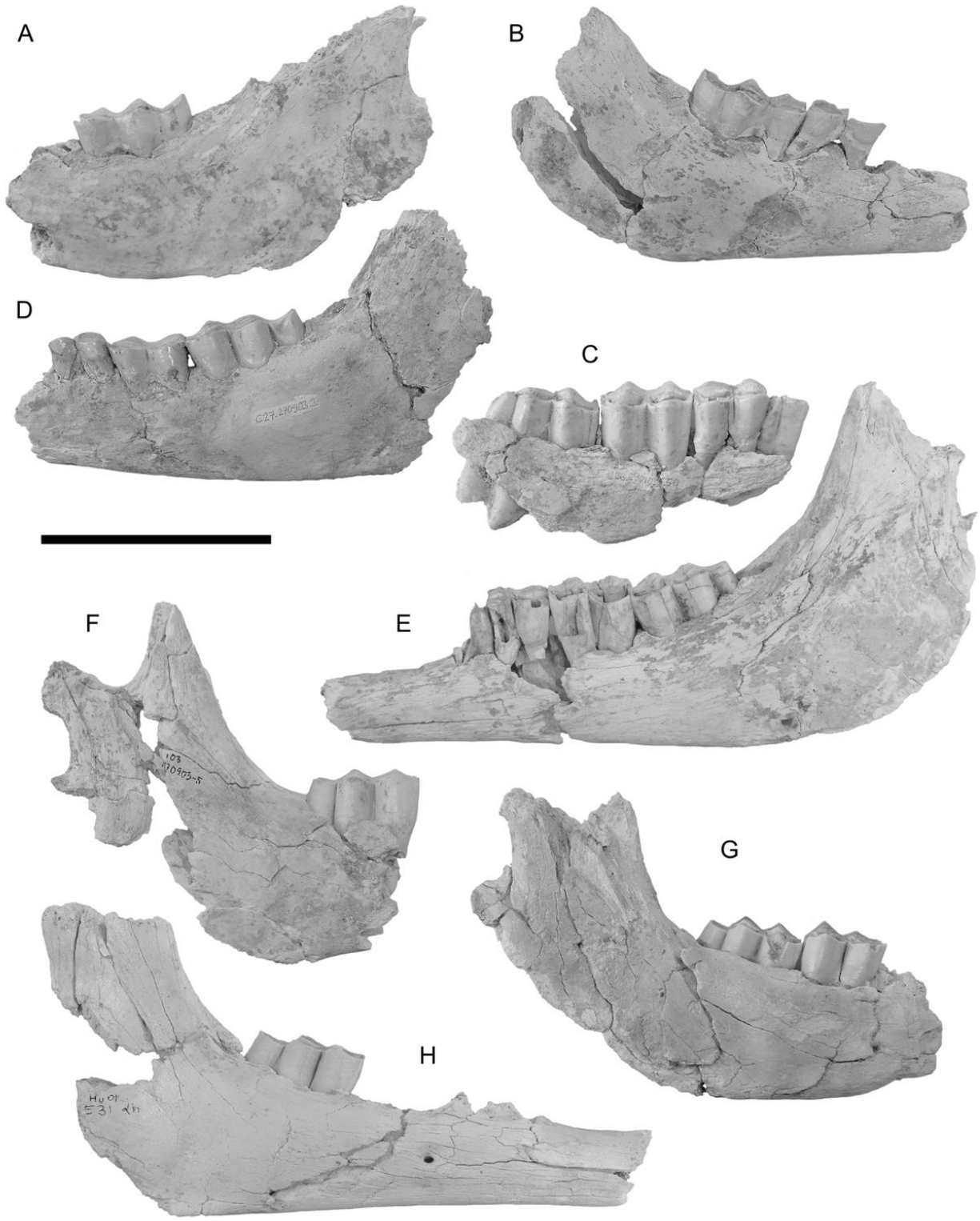

Fig. 9 Mandibles of *C. concordiae* in labial view. **A** Left hemimandible Hu B27-1a. **B** Right hemimandible Hu B27-1c. **C** Left hemimandible Hu C26-50. **D** Left hemimandible Hu C27-2 (likely same individual as the holotype Hu C27-1). **E** Left hemimandible Hu C27-3. **F** Right hemimandible Hu C27-5. **G** Right hemimandible Hu C28/29-19. **H** Right hemimandible Hu E31-C01. Scale bar equals 10 cm.

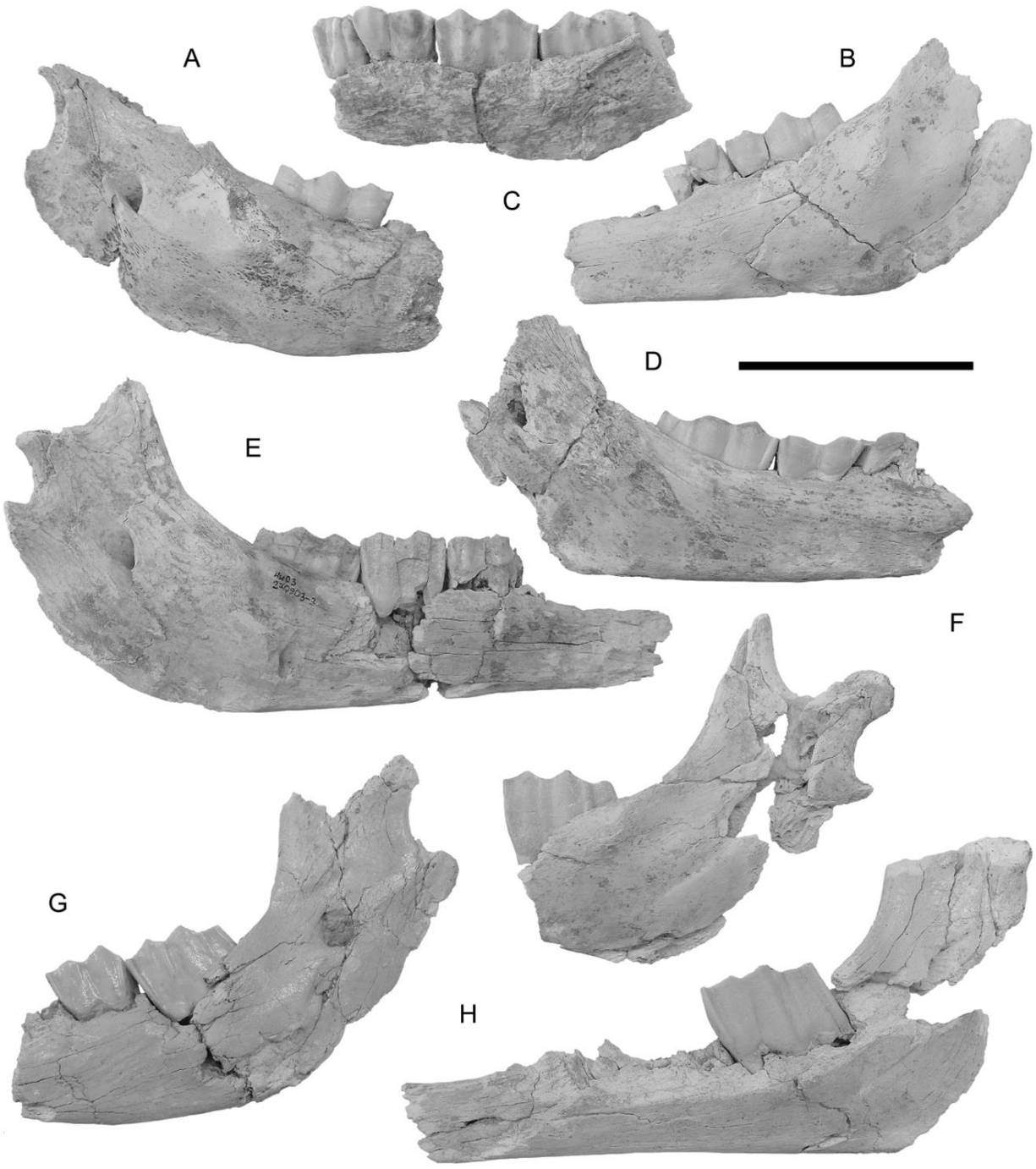

Fig. 10 Mandibles of *C. concordiae* in lingual view. **A** Left hemimandible Hu B27-1a. **B** Right hemimandible Hu B27-1c. **C** Right hemimandible Hu C26-50. **D** Right hemimandible Hu C28/29-19. **E** Left hemimandible Hu C27-3. **F** Right hemimandible Hu C27-5. **G** Left hemimandible Hu C27-2. **H** Right hemimandible Hu E31-C01. Scale bar equals 10 cm.

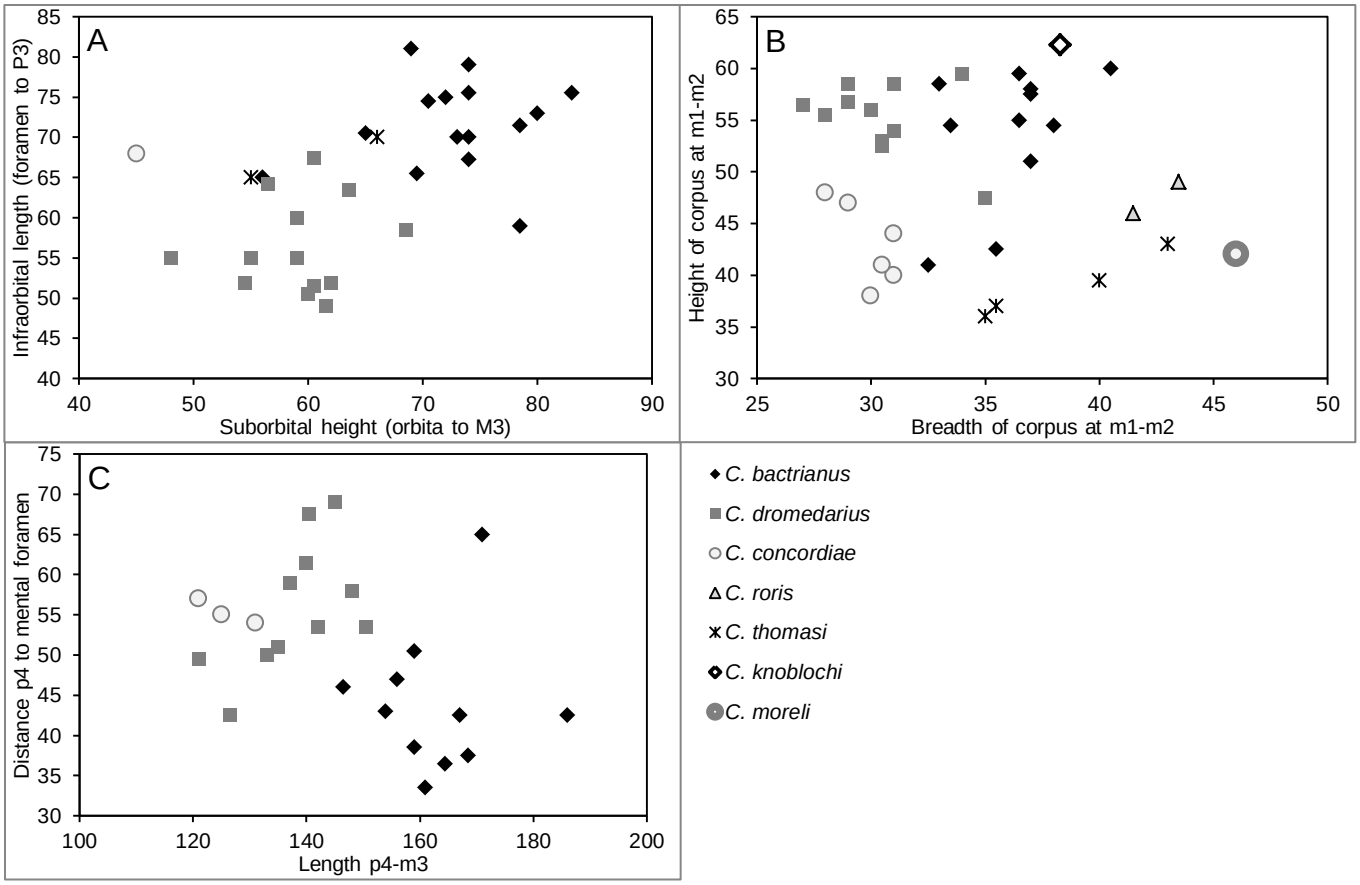

Fig. 11 Bivariate scatterplots of cranial and mandibular measurements in *Camelus* species (in mm). **A** Position of the orbit: suborbital height (distance from orbit to M3 distal) vs. infraorbital length (distance from infraorbital foramen to P4 mesial). **B** Proportions of the mandibular corpus between m1 and m2: breadth vs height. **C** Placement of the caudal mental foramen: length of the cheek tooth row (p4 to m3) vs. distance from p4 to the caudal mental foramen.

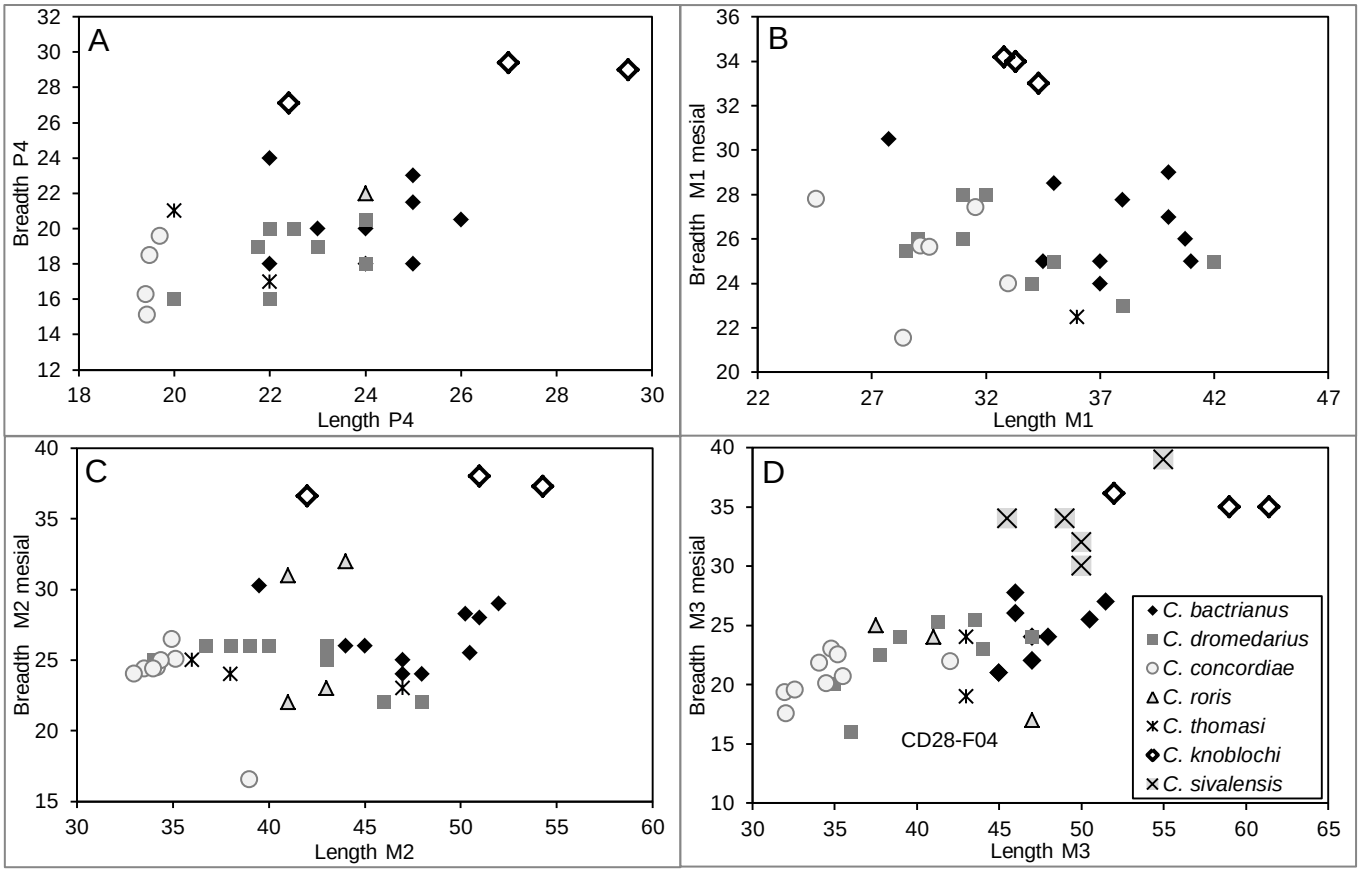

Fig. 12 Bivariate scatterplots of upper dentition measurements in *Camelus* species: occlusal length vs. occlusal breadth (measured on the mesial lobe). **A** Length and breadth of P4. **B** Length and breadth of M1. **C** Length and breadth of M2. **D** Length and breadth of M3.

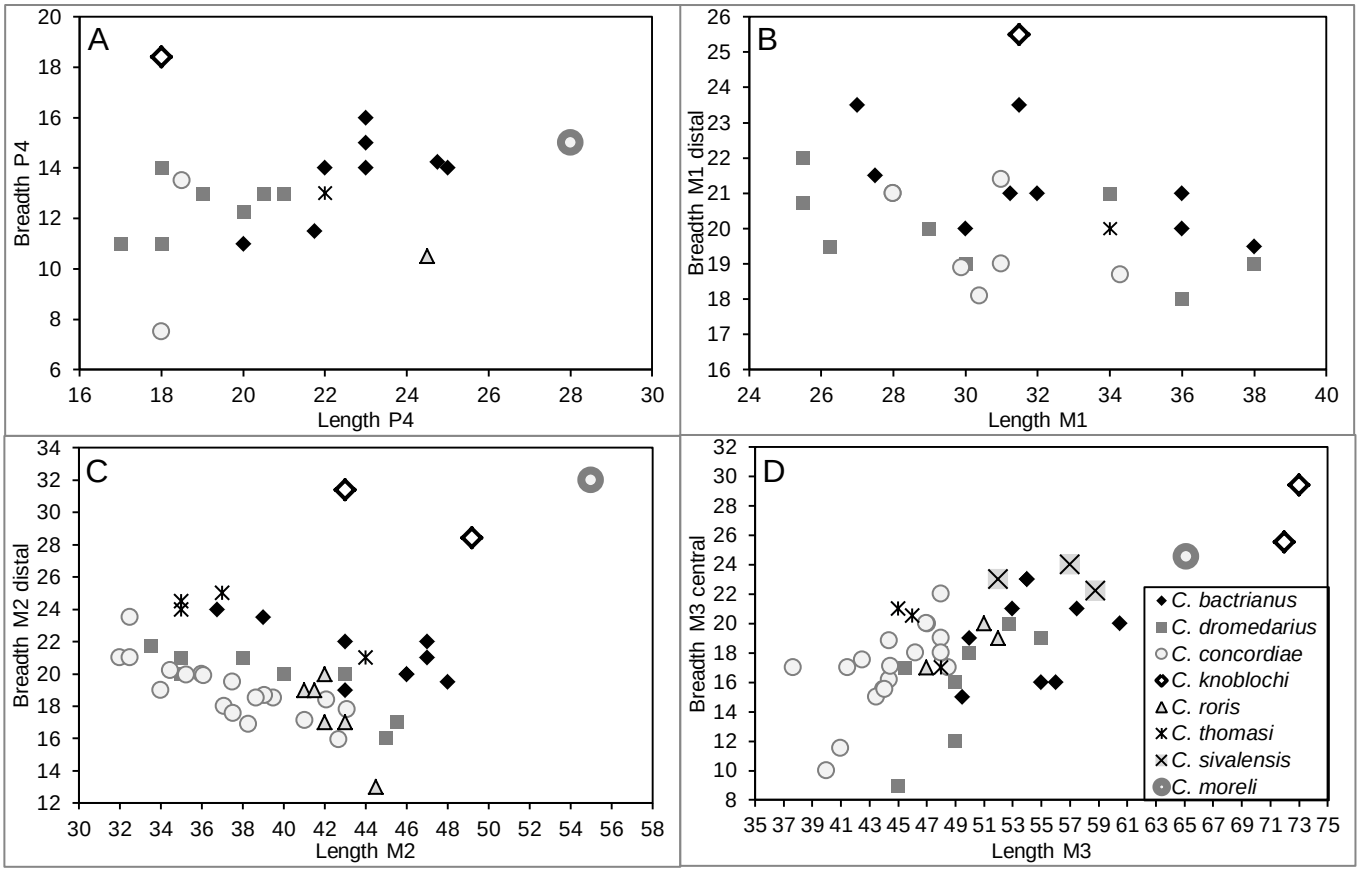

Fig. 13 Bivariate scatterplots of lower dentition measurements in *Camelus* species (in mm): occlusal length vs. occlusal breadth. **A** Length and breadth of p4. **B** Length and breadth of m1 (distal lobe). **C** Length and breadth of m2 (distal lobe). **D** Length and breadth of M3 (central lobe).

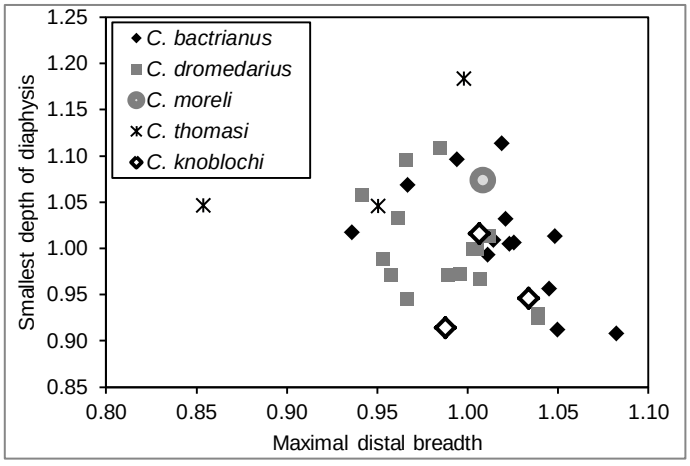

Fig. 14 Bivariate scatterplots of metacarpal measurements in *Camelus* species (harmonic scores): maximal distal breadth vs. smallest depth of the diaphysis.

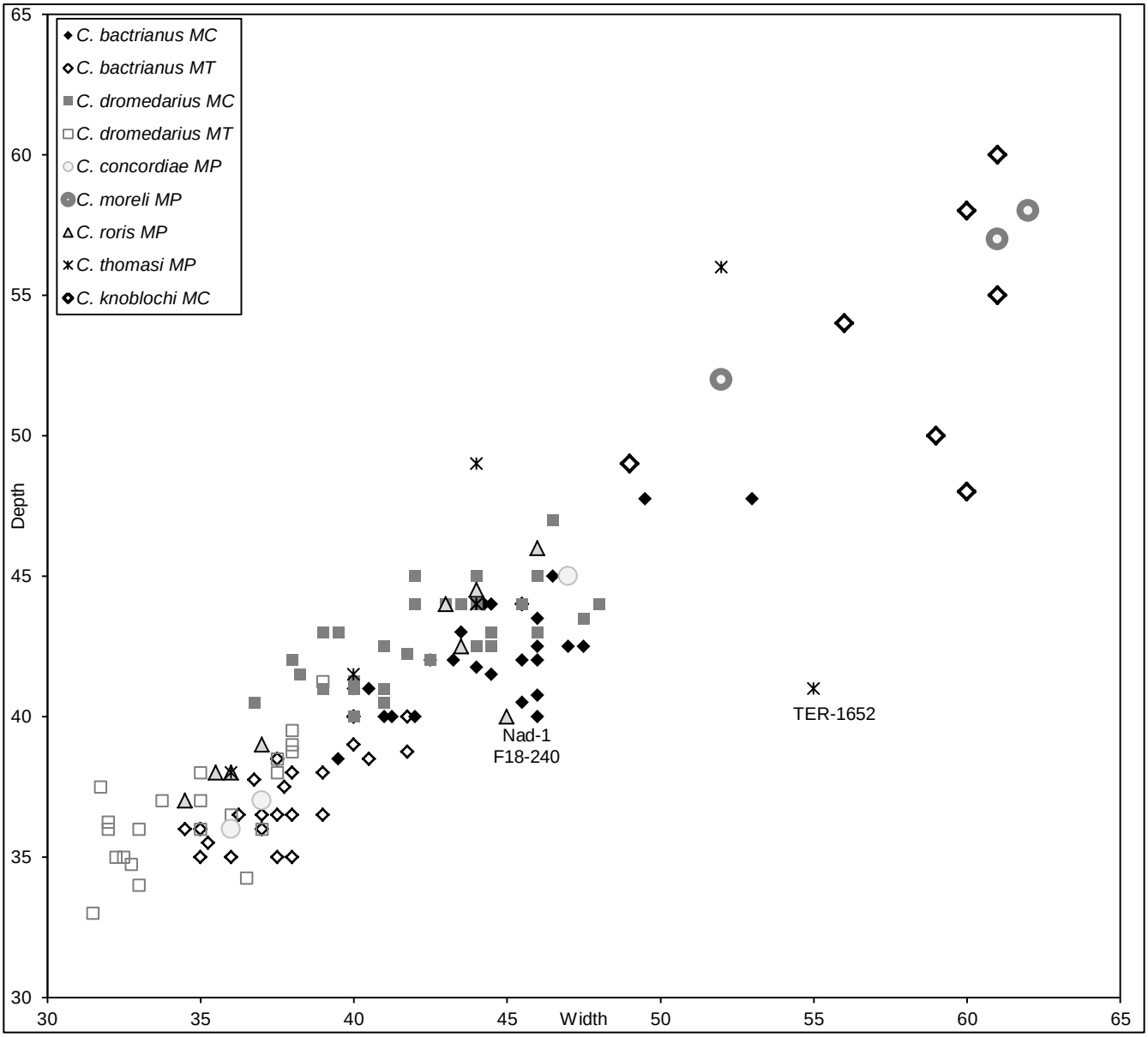

Fig. 15 Bivariate scatterplots of metapodial (MP) condyles measurements in *Camelus* species (in mm): width vs. depth. Metacarpal (MC) and metatarsal (MT) condyles are indicated separately for Recent species. Two labeled fossil specimens show abnormal proportions because of a deformation.

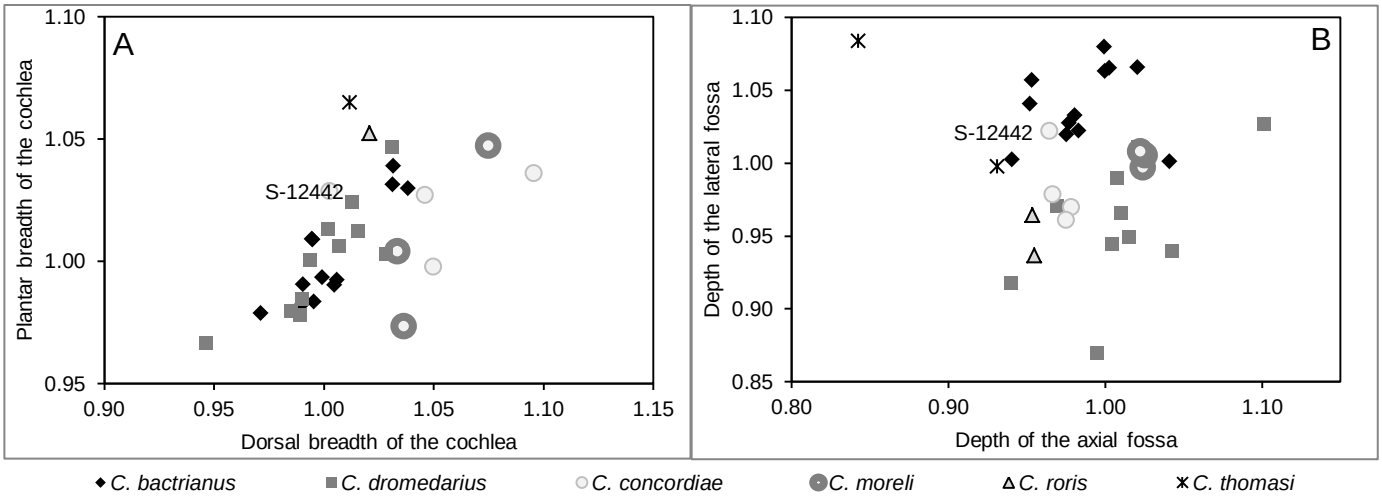

Fig. 16 Bivariate scatterplots of tibial measurements in *Camelus* species (harmonic scores). **A** Breadth proportions of the cochlea: dorsal vs. plantar. **B** Relative depth of articular fossae: axial fossa vs. lateral fossa.

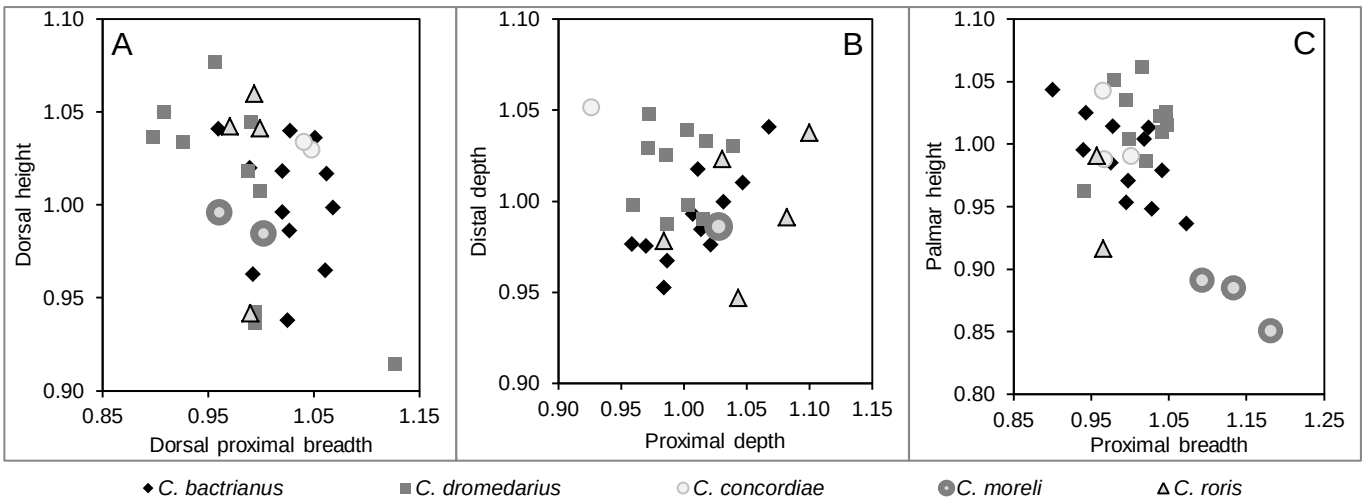

Fig. 17 Bivariate scatterplots of carpal bone measurements in *Camelus* species (harmonic scores). **A** Dorsal proportions of the scaphoideum: dorsal proximal breadth vs. dorsal height. **B** Depth proportions of the scaphoideum: proximal depth vs. distal depth. **C** Proportions of the hamatum: breadth of proximal facet vs. plantar height

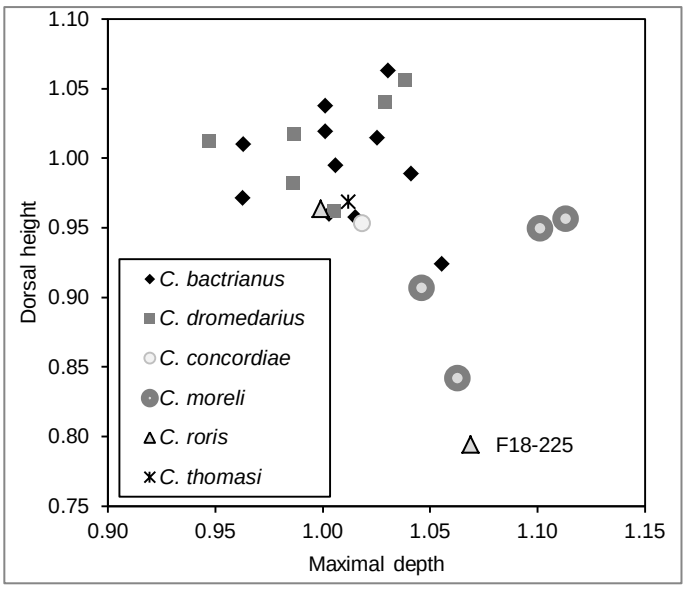

Fig. 18 Bivariate scatterplot of fibula measurements in *Camelus* species (harmonic scores): maximal depth vs. dorsal height.

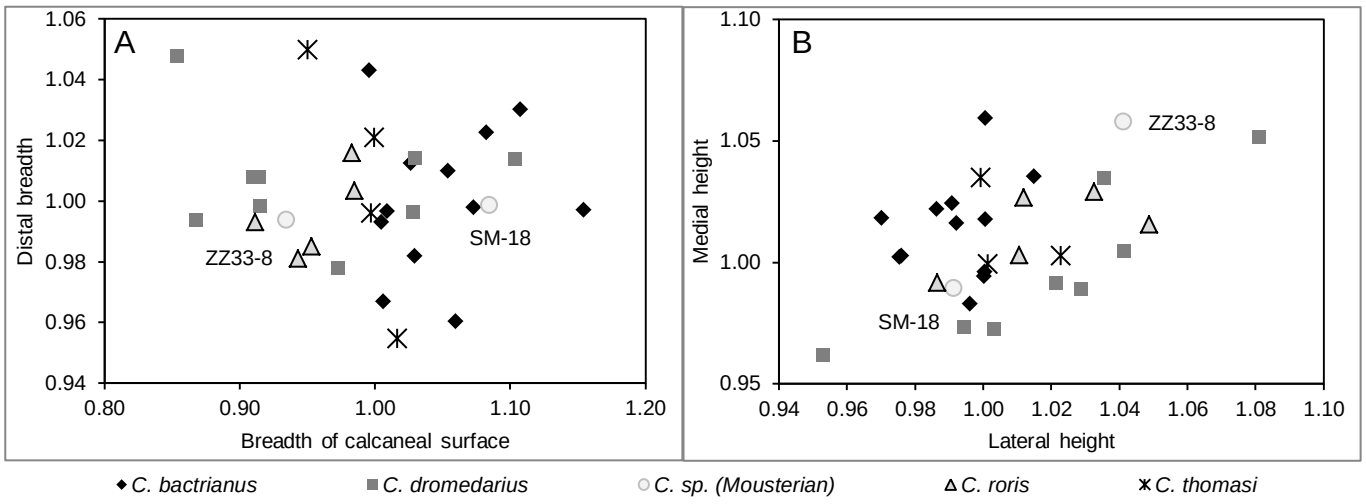

Fig. 19 Bivariate scatterplots of astragalus measurements in *Camelus* species (harmonic scores). **A** Breadth proportions: breadth of calcaneal surface vs. breadth of the distal trochlea. **B** Height proportions: lateral height vs. medial height.

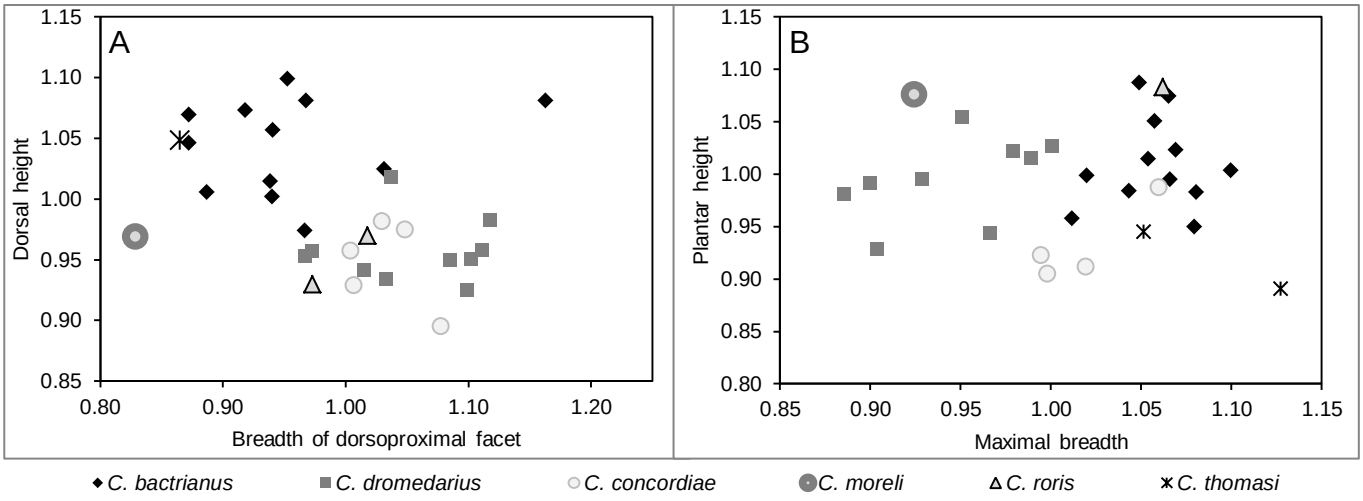

Fig. 20 Bivariate scatterplots of tarsal bones measurements in *Camelus* species (harmonic scores). **A** Dorsal proportions of the cuboideum: breadth of dorsoproximal facet (for the astragalus) vs. dorsal height. **B** Proportions of the naviculare: maximal breadth vs. plantar height.

Tables

Table 1 List of specimens included in this study. The total of 170 specimens is assigned to *Camelus moreli* (42 specimens), *Camelus* cf. *moreli* (1 specimen), *Camelus concordiae* (100), Camelus cf. concordiae (13) or *Camelus* sp. (14 specimens). Holotype and paratype are marked with (*). Former # indicates former inventory number, which might have been used in former reports; it is given for reference. Current # indicates the correct number according to our revision, which is used in this study. Layer "5x" indicates reworked Mousterian sands. "Housed" indicates most recent housing of the specimen, either Basel (IPNA) or El Kowm (Tell Arida Center).

Former #	Current #	Layer	Element	Side	Description	Housed	Species
P15-1	P15-1	5x	Maxilla	sin	& P4-M3	El Kowm	*C. concordiae*
P15-2	P15-2	5x	Maxilla	dex	Fragment & M2	El Kowm	*C. concordiae*
SM-41	SM-41	5x	Maxilla	both	Complete, sin & dex	El Kowm	*C. concordiae*
SM-42	SM-42	5x	Maxilla	sin	Fragment & M1	El Kowm	*C. concordiae*
SM-43	SM-43	5x	Maxilla	sin	Fragment & M2-3	El Kowm	*C. concordiae*
SM-44	SM-44	5x	Maxilla	sin	Fragment & M1-2	El Kowm	*C. concordiae*
B27-220104-1A	B27-1a	5x	Mandibula	sin	& m1-m3	Basel	*C. concordiae*
-220104-1	B27-1c	5x	Mandibula	dex	& m2-m3	Basel	*C. concordiae*
C26-200903-50	C26-50	5x	Mandibula	dex	& p4-m3	Basel	*C. concordiae*
C26-290903-51	C26-51	5a3-5x	Mandibula	dex	& m1-m3	El Kowm	*C. concordiae*
C27-270903-1	C27-1	5x	Mandibula	dex	& p4-m3	Basel	*C. concordiae* *
C27-270903-2	C27-2	5x	Mandibula	sin	& m1-m3	Basel	*C. concordiae*
C27-270903-3	C27-3	5x	Mandibula	sin	& m1-m3	Basel	*C. concordiae*
C27-270903-5	C27-5	5x	Mandibula	dex	& m3	Basel	*C. concordiae*
H34-19	C28/29-19	5x	Mandibula	dex	& m2-m3	Basel	*C. concordiae*
CD28-F01	CD28-F01	5x	Mandibula	sin		Basel	*C. concordiae*
E31-C01	E31-C01	5x-6x	Mandibula	dex	& m3	Basel	*C. concordiae*
sable-1	P15-sable.1	5x-6x	Mandibula	sin	& m3, fragment	Basel	*C. concordiae*
-2684	S-2683.2	5b3	Mandibula	sin	& M2	El Kowm	*C. moreli*
SM-23	SM-23	5x	Mandibula	sin	& M1-2	El Kowm	*C. concordiae*
SM-24	SM-24	5x	Mandibula	sin	& M3	El Kowm	*C. concordiae*

SM-27	SM-27	5x	Mandibula	dex	& P4, M1-2	El Kowm	*C. concordiae*
SM-28	SM-28	5x	Mandibula	dex	& P4, M2-3	El Kowm	*C. concordiae*
SM-30	SM-30	5x	Mandibula	sin	& M2 (juvenile)	El Kowm	*C. concordiae*
-3467.2	W-3467.2	5b3	Mandibula		Symphysis & P4	El Kowm	*C. moreli* *
AB28-D09.2	AB28-D09.2	5b4	Dens		Molar fragment	Basel	*C. sp.*
B28-17.04	B28-17.04	5x	Dens		Fragment unidentified	Basel	*C. sp.*
SM00-3	SM00-3	5x	Dens		Fragment unidentified	Basel	*C. sp.*
B27-B04.1	B27-B04.1	5x	Dens ant	sin	Incisive	Basel	*C. cf. concordiae*
sable-2	P15-sable.2	5x-6x	Dens ant	dex	Incisive	Basel	*C. cf. concordiae*
-	B27-2a	5x	Dens sup	dex	M2	Basel	*C. concordiae*
-	B27-3a	5x	Dens sup	dex?	M1, unworn	Basel	*C. concordiae*
C26-290903-16	C26-16	5x	Dens sup	dex	M3	El Kowm	*C. concordiae*
C26-100903-2	C26-2	5a3-5x	Dens sup		M3	El Kowm	*C. concordiae*
C27/28-C06	C27/28-C06	5x	Dens sup		P3, unworn	Basel	*C. concordiae*
CD28-F04	CD28-F04	5x	Dens sup	dex	M3	Basel	*C. sp.*
P15-3	P15-3	5x	Dens sup	sin	P4	El Kowm	*C. concordiae*
SM-45	SM-45.1	5x	Dens sup		M3	El Kowm	*C. concordiae*
SM-45	SM-45.2	5x	Dens sup		M3	El Kowm	*C. concordiae*
SM-45	SM-45.3	5x	Dens sup		M1	El Kowm	*C. concordiae*
SM-45	SM-45.4	5x	Dens sup		M3	El Kowm	*C. concordiae*
-	B26-9	5x	Dens inf	dex	m2	Basel	*C. concordiae*
P15-6	C26-12	5x	Dens inf	sin	m3, fragment	Basel	*C. moreli*
C26-290903-44.1	C26-44.1	5x	Dens inf	sin	m2	El Kowm	*C. concordiae*
C26-290903-44.2	C26-44.2	5x	Dens inf	sin	m3	El Kowm	*C. concordiae*
CD28-F05	CD28-F05	5x	Dens inf	dex	m3	Basel	*C. concordiae*
SM-25.1	SM-25.1	5x	Dens inf		m3	El Kowm	*C. concordiae*
SM-25.2	SM-25.2	5x	Dens inf		m3	El Kowm	*C. concordiae*
-	SM-25.3	5x	Dens inf	dex	m3, fragment	Basel	*C. concordiae*
SM-26.1	SM-26.1	5x	Dens inf	sin	m2	El Kowm	*C. concordiae*
SM-26.2	SM-26.2	5x	Dens inf	sin	m2	El Kowm	*C. concordiae*
SM-26.3	SM-26.3	5x	Dens inf	sin	m2	El Kowm	*C. concordiae*
SM-26.4	SM-26.4	5x	Dens inf	sin	m2	El Kowm	*C. concordiae*
SM-26.5	SM-26.5	5x	Dens inf	sin	m2	El Kowm	*C. concordiae*
-	SM-26.6	5x	Dens inf	sin	m2	Basel	*C. concordiae*
SM-26.6	SM-26.6	5x	Dens inf	sin	m2	El Kowm	*C. concordiae*
SM-29	SM-29	5x	Dens inf	dex	m2	El Kowm	*C. concordiae*
-8409	S-8409	5f1	Vertebra lumbar		Lumbar 1	El Kowm	*C. moreli*
-2565	W-2565	5b2	Vertebra lumbar		Lumbar 1-2	El Kowm	*C. moreli*
A32-29	A32-29	5b2	Vertebra lumbar		Lumbar 1-4, & cranial zygapophysis	Basel	*C. moreli*
-8415	S-8415	5f1	Vertebra lumbar		Lumbar 2	El Kowm	*C. moreli*
-	SM-11	5x	Vertebra lumbar		Lumbar 2-3	El Kowm	*C. concordiae*
-2175	W-2175	5b1	Vertebra lumbar		Lumbar 2-4	El Kowm	*C. moreli*
-8416	S-8416	5f1	Vertebra lumbar		Lumbar 3	El Kowm	*C. moreli*
-8417	S-8417	5f1	Vertebra lumbar		Lumbar 4	El Kowm	*C. moreli*
-8418	S-8418	5f1	Vertebra lumbar		Lumbar 5	El Kowm	*C. moreli*
-8419	S-8419	5f1	Vertebra lumbar		Lumbar 6	El Kowm	*C. moreli*
-8420	S-8420	5f1	Vertebra lumbar		Lumbar 7	El Kowm	*C. moreli*
P12/W-4	P12-4	5b	Vertebra thoracal		Fragment	Basel	*C. sp.*
A32-2	A32-2	5b1	Humerus	sin	Fragment distomedial	Basel	*C. cf. concordiae*
A32-3	A32-3	5b1	Humerus	sin	Fragment proximal diaphysis	Basel	*C. concordiae*
A32-30	A32-30	5b2	Humerus	sin	Fragment distal	Basel	*C. cf. concordiae*
C28-C10	C27/28-C10	5x	Humerus		Fragment distal	Basel	*C. concordiae*
C28-C11	C27/28-C11	5x	Humerus	sin	Fragment distal	Basel	*C. concordiae*
P12/W-5	P12-5	5b	Humerus	dex	Fragment distal	Basel	*C. concordiae*
P12/W-9	P12-9	5a	Humerus	dex	Small fragments, distal	Basel	*C. concordiae*
-8030	S-8030	5d2	Humerus	dex	Fragment distal	El Kowm	*C. cf. concordiae*
-8178	S-8178	5e	Humerus	sin	Fragment distal	El Kowm	*C. cf. concordiae*
S-8765	S-8765	5b1	Humerus	sin	Fragment distal	El Kowm	*C. cf. concordiae*
SM00-4	SM00-4	5x	Humerus		Fragments	Basel	*C. concordiae*
A32-1	A32-1	5b1	Radioulnare	dex?	Fragment proximal	Basel	*C. cf. concordiae*
C28-D05	C28-D05	5x	Radioulnare		Small fragments diaphysis	Basel	*C. concordiae*
-8398	S-8398	5e	Radioulnare	sin	Olecranon	El Kowm	*C. cf. concordiae*

SM-10	SM-10	5x	Radioulnare	sin	Fragment proximal	El Kowm	*C. moreli*
-1387	W-1387	5a4	Radioulnare		Fragment proximal	El Kowm	*C. moreli*
-2222	W-2222	5b3	Radioulnare	dex	Fragment proximal	El Kowm	*C. cf. moreli*
-749	W-749	5b1	Radioulnare	dex	Fragment proximal	El Kowm	*C. moreli*
ZZ31-ASond.M1	ZZ31-M1.A	5c2	Radioulnare	sin	Olecranon	Basel	*C. concordiae*
A32-A.01	A32-A.02	5b1-4	Scaphoideum	sin		El Kowm	*C. moreli*
P15-24.2	P15-24.2	5x	Scaphoideum	sin	Small	El Kowm	*C. concordiae*
PS00-18	PS00-18	5x	Scaphoideum	sin	Fragment dorsal	El Kowm	*C. moreli*
SS-7	SS-7	5x	Scaphoideum	sin		El Kowm	*C. concordiae*
-3430	W-3430	5b3	Scaphoideum	dex	Fragment	El Kowm	*C. moreli*
-	CD28-F08	5x	Triquetrum	sin?		Basel	*C. concordiae*
P15-24.1	P15-24.1	5x	Triquetrum	dex	Fragment	El Kowm	*C. concordiae*
-8181	S-8181	5e	Triquetrum	sin		El Kowm	*C. concordiae*
C28/29-D/04	C28/29-D04	5x	Pisiforme	dex		Basel	*C. concordiae*
C26-100903-3	C26-3	5a3-5x	Hamatum	sin		El Kowm	*C. moreli*
C28/29-D/01	C28/29-D01	5x	Hamatum	sin	Juvenile	Basel	*C. concordiae*
C28/29-D/02	C28/29-D02	5x	Hamatum	sin		Basel	*C. concordiae*
-8100	S-8100	5d5	Hamatum	sin		El Kowm	*C. moreli*
-3451.2	W-3451.2	5b3	Hamatum	dex	Fragment	El Kowm	*C. sp.*
-3653	W-3653	5b3	Hamatum	dex	Fragment	El Kowm	*C. moreli*
ZZ31-B.05	ZZ31-B.05	5c2	Hamatum	dex		El Kowm	*C. concordiae*
A32-A.01	A32-A.01	5b1-4	Capitatum	sin		El Kowm	*C. cf. concordiae*
-3429	W-3429	5b3	Capitatum	dex		El Kowm	*C. moreli*
-3451.3	W-3451.3	5b3	Capitatum	dex		El Kowm	*C. cf. concordiae*
ZZ31-B.04	ZZ31-B.04	5c2	Capitatum	dex		El Kowm	*C. cf. concordiae*
A32-C.01	A32-C.01	5b1-4	Trapezoideum	sin		El Kowm	*C. concordiae*
-3451.4	W-3451.4	5b3	Trapezoideum	dex		El Kowm	*C. concordiae*
B27-220104-1B	B27-1b	5x	Femur	dex	Caput femoris	Basel	*C. concordiae*
C27-D04	C27-D04	5x	Femur	dex	Distal fragment	Basel	*C. concordiae*
CD28-F14	CD28-F14	5x	Femur	dex	Caput femoris	Basel	*C. concordiae*
SM00-1	SM00-1	5x	Femur	?	Caput femoris	Basel	*C. moreli*
-1472	W-1472	5b3	Femur	sin	Caput femoris	El Kowm	*C. moreli*
N-724	W-724	5b1	Femur		Fragment medial condyle	El Kowm	*C. moreli*
B34-25	B34-25	5a3	Patella?			Basel	*C. concordiae*
A32-D	A32-D	5b1-4	Tibia	sin	Fragment distal	El Kowm	*C. concordiae*
C33-1	C33-1	5b5	Tibia	sin	Fragment distal	El Kowm	*C. concordiae*
C35-26	C35-26	5a3	Tibia	sin	Fragment distal	Basel	*C. moreli*
PS00-3	PS00-3	5x	Tibia	dex	Fragments	El Kowm	*C. moreli*
S-12442	S-12442	5b3	Tibia	dex	Fragment distal	El Kowm	*C. sp.*
-2028.1	W-2028.1	5a3	Tibia	dex	Fragment distal	El Kowm	*C. concordiae*
-229	W-229	5a4	Tibia	dex	Fragment distal	El Kowm	*C. moreli*
-3629	W-3629	5b3	Tibia	dex	Fragment distal	El Kowm	*C. sp.*
D28-6.1	D28-6.1	5x	Fibula	sin		El Kowm	*C. moreli*
-1040	W-1040	5b3	Fibula	dex		El Kowm	*C. moreli*
-2028.2	W-2028.2	5a3	Fibula	dex		El Kowm	*C. concordiae*
-2028.3	W-2028.3	5a3	Fibula	dex		El Kowm	*C. moreli*
-2028.4	W-2028.4	5a3	Fibula	sin	Fragment	El Kowm	*C. moreli*
CD28-F10	CD28-F10	5x	Astragalus	sin	Fragment distolateral	Basel	*C. concordiae*
SM-18	SM-18	5x	Astragalus	sin	Fragment	El Kowm	*C. sp.*
ZZ33-8	ZZ33-8	5b1	Astragalus	sin		Basel	*C. sp.*
B26-170903.04	B26-4	5x	Calcaneus	sin	Juvenile	Basel	*C. sp.*
C27/28-C12	C27/28-C12	5x	Calcaneus	sin	Fragment tuber	Basel	*C. sp.*
C27-290903-1	C27-1	5x	Calcaneus	dex		El Kowm	*C. sp.*
ZZ33-7	ZZ33-7	5b1	Calcaneus	sin	Fragment tuber, juvenile	Basel	*C. sp.*
C28/29-D/03	C28/29-D03	5x	Cuboideum	sin		Basel	*C. concordiae*
C31-14	C31-16	5h-6b	Cuboideum	dex		El Kowm	*C. concordiae*
CD28-F07	CD28-F07	5x	Cuboideum	sin		Basel	*C. concordiae*
SM-22	SM-22	5x	Cuboideum	dex		El Kowm	*C. concordiae*
-2029	W-2029.2	5b3	Cuboideum	sin	Articulated partial tarsus	El Kowm	*C. moreli*
ZZ33-6.3	ZZ33-6	5b1	Cuboideum	sin		Basel	*C. concordiae*
A32-B.03	A32-B.03	5b1-4	Naviculare	dex		El Kowm	*C. concordiae*
D28-6.2	D28-6.2	5x	Naviculare	dex	Fragment	El Kowm	*C. concordiae*

SM-20	SM-20	5x	Naviculare	sin		El Kowm	*C. concordiae*
-2029	W-2029.3	5b3	Naviculare	sin	Articulated partial tarsus	El Kowm	*C. moreli*
-4085	W-4085	5b5	Naviculare	sin		El Kowm	*C. concordiae*
ZZ33-5.2	ZZ33-5	5b1	Naviculare	sin		Basel	*C. concordiae*
-2029	W-2029.4	5b3	Cuneiforme medial	sin	Articulated partial tarsus	El Kowm	*C. moreli*
-2029	W-2029.5	5b3	Cuneiforme intermediolateral	sin	Articulated partial tarsus	El Kowm	*C. moreli*
-4101	W-4101	5b5	Cuneiforme intermediolateral	sin		El Kowm	*C. cf. concordiae*
D35-2	D35-2	5a3	Metacarpale	sin	Fragment distal	El Kowm	*C. moreli*
P12/W-8	P12-8	5b	Metacarpale		Condyle	Basel	*C. moreli*
-8098	S-8098	5d5	Metacarpale	?	Fragment distal	El Kowm	*C. concordiae*
ZZ31-B.03	ZZ31-B.03	5c2	Metacarpale	sin	Fragment proximal	El Kowm	*C. concordiae*
CD28-F12	CD28-F12	5x	Metatarsale		Fragment distal	Basel	*C. concordiae*
CD28-F13	CD28-F13	5x	Metatarsale		Fragment distal	Basel	*C. concordiae*
PS00-11	PS00-11	5x	Metatarsale	sin	Fragment proximolateral	El Kowm	*C. moreli*
-2029	W-2029.1	5b3	Metatarsale	sin	Proimal fragment, articulated partial tarsus	El Kowm	*C. moreli*
-4086.1	W-4086.1	5b5	Metatarsale	sin	Fragment proximal	El Kowm	*C. concordiae*
P12/W-7	P12-7	5b	Metapodium		Fragment	Basel	*C. concordiae*
ZZ39-9	ZZ33-9	5b2	Metapodium		Fragment	Basel	*C. concordiae*
S-12622	S-12622	5e	Phalanx I ant			El Kowm	*C. concordiae*
SM-6	SM-6	5x	Phalanx I ant		Fragment proximal	El Kowm	*C. concordiae*
C27/28-C13	C27/28-C13	5x	Phalanx I ant		Fragment condyle	Basel	*C. concordiae*
Db Grotte-1	grotte-1	5x	Phalanx I post		Fragment distal	Basel	*C. concordiae*
SK-Os-SK06.38	SK06-38	5h	Phalanx I post		Fragment proximal	El Kowm	*C. concordiae*
-2909.2	W-2909.2	5b2	Phalanx I post		Fragment condyle	El Kowm	*C. concordiae*
-3440	W-3440	5b3	Phalanx III			El Kowm	*C. moreli*

Table 2 Measurements of *Camelus* remains from Hummal, Mousterian layers. Details on the specimens are given in Table 1. ~ indicates approximated measurements; § indicates measurements that might be either mesial or lateral. CM = *Camelus moreli* (on black background); CC = *Camelus concordiae*. Measurements of W-3467.2 and S-2684.2 were estimated from pictures.

	MAXILLA	P15-1 sin CC	SM-41 dex CC
C33	Cheek tooth length (P3-M3, included)		123.57
C34	Molar row length (M1-M3, included)	91.03	92.92

	MANDIBULA	S-2684.2 sin CM	W-3467.2 syn CM	B27-1A dex CC	B27-1C dex CC	C26-51 dex CC	C27-1 dex CC	C27-2 sin CC	C27-3 sin CC	C27-5 dex CC	C28/29-19 dex CC	E31-C01 dex CC	SM-27 dex CC	SM-30 sin CC
M7	Length from p4 to m3 distal						121		125 ~			131	144.5	130.5
M15	Thickness of the corpus measured between m1 and m2 (* = between p4 and m1)	46 ~	36 * ~		30		31	30.5	29		28	31 ~		
M16	Thickness of the corpus measured between m2 and m3	48 ~		34	36 ~		38	38.5	38 ~		34	34 ~		
M19	Height of the corpus mesial to p4						35		37			39		
M20	Height of the corpus between m1 and m2	42 ~			38 ~		40	41	47 ~		48	44		
M21	Height of the corpus distal to m3 (** = between m2 and m3)	58 ** ~		68	71	70.4	67	66	70	69	68 ~	73 ~	68 ~	68
M22	Height of the ramus from coronoid process to ventral border													191 ~
M23	Height of the ramus from rostral notch to ventral border						130 ~		130 ~	125 ~				130.5
M24	Height of the ramus from condylar process to ventral border													137.5
M25	Height of the ramus from caudal notch to ventral border								100 ~		110 ~			

	(continued)	W-3467.2 syn CM	C26-51 dex CC	C27-1 dex CC	C27-3 sin CC	E31-C01 dex CC	SM-27 dex CC	SM-28 dex CC	SM-30 sin CC	C26-50 dex CC
M7	Length from p4 to m3 distal									130 ~
M8	Length from i1 to p4	159 ~								
M9	Symphyseal length: from i1 to the most caudal point of the symphysis (medial)	107 ~								
M11	Position of caudal mental foramen: from p4 mesial to caudal mental foramen			57	55	54				
M13	Length from m3 distal to angular process								85.3	
(N/A)	Diastema between p1-p4 (in extant camels calculated as M6 - M7 - Di3)	83.5	71					70 ~		
(N/A)	Length m1-m3 (in extant camels calculated as Di12 + Di20 + Di28)		112				120		112	
(N/A)	Distance from p1 mesial, to symphysis caudal (in extant camels = M6 + M9 - M4)	22 ~								

	UPPER DENTITION (P4-M1)	P15-1 CC	P15-3 CC	SM-41 sin CC	SM-41 dex CC	SM-42 CC	SM-44 CC	SM-45.3 CC
Ds11	Alveolar length of P4	16.35	18.79	18.24	17.65			
Ds13	Occlusal length of P4	19.7	19.43	19.4	19.48			
Ds14	Occlusal breadth of P4	19.57	15.11	16.28	18.48			
Ds15	Alveolar length of M1	21.26		23.07	23.37	31.16	24.1	22.03
Ds18	Occlusal length of M1	24.58		29.55	28.4	36.69	31.56	29.16
Ds21	Occlusal breadth (of mesial lobe) of M1	27.8		25.63	21.55		27.42	25.7

	UPPER DENTITION (M2)	B27-2A dex CC	P15-1 CC	P15-2 CC	SM-41 sin CC	SM-41 dex CC	SM-43 CC	SM-44 CC
Ds23	Alveolar length of M2		25.88	27.82	26.86	28.2	28.29	30.98
Ds26	Occlusal length of M2	39	33.55	34.21	34.42	34.02	35.17	34.96
Ds27	Occlusal length of mesial lobe of M2	20						
Ds28	Occlusal length of distal lobe of M2	23						
Ds29	Occlusal breadth (of mesial lobe) of M2	16.5	24.35	24.47	24.94	24.37	25.03	26.45
Ds30	Occlusal breadth of distal lobe of M2	15						

	UPPER DENTITION (M3)	C26-2 CC	C26-16 CC	P15-1 CC	SM-41 sin CC	SM-41 dex CC	SM-43 CC	SM-45.1 CC	SM-45.2 CC	SM-45.4 CC	CD28-F04 C. sp.
Ds31	Alveolar length of M3	34.97	30.83	34.48	34.74	34.9	36.16		27.41	31.27	
Ds34	Occlusal length of M3	32.06	32	35.22	35.54	32.62	34.51		34.84	34.1	42 §
Ds35	Occlusal length of mesial lobe of M3										20§
Ds36	Occlusal length of distal lobe of M3										23§
Ds37	Occlusal breadth (of mesial lobe) of M3	17.52	19.3	22.52	20.69	19.51	20.07	21.24	22.97	21.8	22§
Ds38	Occlusal breadth of distal lobe of M3										18§

	LOWER DENTITION (c, p1, p4)	W-3467.2 symph CM	C26-50 dex CC	C27-1 dex CC	C27-3 dex CC
Ds4	Alveolar breadth of c	>21			
Ds5	Alveolar length of p1	22 ~			
Ds6	Alveolar breadth of p1	11 ~			
Di8	Alveolar length of p4		18	18	19
Di9	Alveolar breadth of p4		12	10	12
Di10	Occlusal length of p4	28 ~	18	18.5	
Di11	Occlusal breadth of p4	15 ~	7.5	13.5	

	LOWER DENTITION (m1)	B27-1A dex CC	C26-50 dex CC	C27-1 dex CC	C27-2 sin CC	C27-3 dex CC	C28/29-19 dex CC	SM-23 CC	SM-27 CC	SM-30 CC
Di12	Alveolar length of m1		26	26		22 ~		23.7	28.2	23.3
Di13	Alveolar breadth of mesial lobe of m1		16	16		17.5				
Di14	Alveolar breadth of distal lobe of m1		19	18	17.5		18.5			
Di15	Occlusal length of m1	31	31	28		28 ~		30.4	34.3	29.9
Di16	Occlusal length of mesial lobe of m1		14.5	15						
Di17	Occlusal length of distal lobe of m1		16	13	13.5	15				
Di18	Occlusal breadth of mesial lobe of m1		18	20						
Di19	Occlusal breadth (of distal lobe) of m1	21.4	19	21	20.5	21		18.1	18.7	18.9

	LOWER DENTITION (m2)	S-2684.2 sin CM	B26-9 dex CC	B27-1C dex CC	C26-44.1 CC	C26-50 dex CC	C26-51 CC	C27-1 dex CC	C27-2 sin CC	C27-3 dex CC	C28/29-19 dex CC
Di20	Alveolar length of m2			32.5	27.93	36	31	30	28.5	31	30
Di21	Alveolar breadth of mesial lobe of m2			17		21		21	19.5	21 ~	21
Di22	Alveolar breadth of distal lobe of m2			19.5		21		22.5	22 ~	22	19
Di23	Occlusal length of m2	55 ~	47	32	34.47	39.5	36.1	32.5	32.5	36	34
Di24	Occlusal length of mesial lobe of m2	26 ~	23	16		20		16.5	16.5	17	16.5
Di25	Occlusal length of distal lobe of m2	30 ~	24	16		20		16	16	19	18
Di26	Occlusal breadth of mesial lobe of m2	32 ~				17		24	21	18.5 ~	19
Di27	Occlusal breadth (of distal lobe) of m2	32 ~		21 ~	20.21	18.5	19.9	23.5	21	20	19

	(continued)	SM-23 CC	SM-26.1 CC	SM-26.2 CC	SM-26.3 CC	SM-26.4 CC	SM-26.5 CC	SM-26.6 sin CC	SM-27 CC	SM-28 CC	SM-29 CC	SM-30 CC
Di20	Alveolar length of m2	35.8	35.55	30.47	36.63	35.65	32.23		39.2	38.6	34.66	34.9
Di21	Alveolar breadth of mesial lobe of m2											
Di22	Alveolar breadth of distal lobe of m2											
Di23	Occlusal length of m2	37.1	37.55	35.26	42.69	41.03	39.07	37.5	42.1	43.1	38.66	38.3
Di24	Occlusal length of mesial lobe of m2							18				
Di25	Occlusal length of distal lobe of m2							19.5				
Di26	Occlusal breadth of mesial lobe of m2							18				
Di27	Occlusal breadth (of distal lobe) of m2	18	17.57	19.93	15.95	17.12	18.68	19.5	18.4	17.8	18.51	16.9

	LOWER DENTITION (m3)	C26-12 sin CM	B27-1A dex CC	B27-1C dex CC	C26-44.2 CC	C26-50 dex CC	C26-51 CC	C27-1 dex CC	C27-2 sin CC	C27-3 dex CC	C27-5 dex CC
Di28	Alveolar length of m3	61.14	47	48.5	45.21	46.5	48.2	50	48	45	
Di29	Alveolar breadth of mesial lobe of m3		20	20.5		19		22	21 ~	20	
Di30	Alveolar breadth of central lobe of m3		19.5	20		17		21	20	20	
Di31	Alveolar breadth of distal lobe of m3		13	12		10		14	13	10	
Di32	Occlusal length of m3	65.15	47	47	46.24	40 ~	48.5	48	48	44	42.5
Di33	Occlusal length of mesial lobe of m3		17	16		20		18.5	18	17	18
Di34	Occlusal length of central lobe of m3	23.5	18	18.5		16		19	17	17	15.5
Di35	Occlusal length of distal lobe of m3	21	14	13		7		13	13.5	9	10
Di36	Occlusal breadth of mesial lobe of m3		21	21		13		23	19	17	18
Di37	Occlusal breadth of central lobe of m3	24.5	20	20	18.01	10	17	22	19	15.5	17.5
Di38	Occlusal breadth (of distal lobe) of m3	15	12	12		6		12	9	7.5	9

	(continued)	C28/29-19 dex CC	CD28-F05 dex CC	E31-C01 dex CC	SM-24 CC	SM-25.1 CC	SM-25.2 CC	SM-25.3 dex CC	SM-27 CC	SM-28 CC	SM-30 CC
Di28	Alveolar length of m3	45			46.2	43	43.38		47.6	47.3	44.6
Di29	Alveolar breadth of mesial lobe of m3	18 ~									
Di30	Alveolar breadth of central lobe of m3	18 ~									
Di31	Alveolar breadth of distal lobe of m3	10									
Di32	Occlusal length of m3	41.5	41	48	44.4	44.39	44.5		37.7	43.5	44.1
Di33	Occlusal length of mesial lobe of m3	18.5	19.5	19							
Di34	Occlusal length of central lobe of m3	15	16	16.5							
Di35	Occlusal length of distal lobe of m3	10	6	14.5				12			
Di36	Occlusal breadth of mesial lobe of m3		14	17							
Di37	Occlusal breadth of central lobe of m3	17	11.5	18	18.8	16.18	17.07	20	17 ~	15 ~	15.5
Di38	Occlusal breadth (of distal lobe) of m3	9	5	8.5				12			

	HUMERUS	A32-2 sin *CC (cf.)*	A32-30 sin *CC (cf.)*	S-8030 dex *CC (cf.)*	S-8178 sin *CC (cf.)*	S-8765 sin *CC (cf.)*
hu14	Distal medial depth (medial epicondyle to trochlea)	98	93	97	82	92
hu15	Distal axial depth (trochlear groove)	45		40.5	38	38.5
hu16	Distal lateral depth (lateral epicondyle to capitulum)			87	68	80
hu17	Distal breadth (trochlea to capitulum)			91	78	82

	RADIOULNARE	SM-10 sin CM	W-749 dex CM	W-1387 CM	W-2222 dex CM (cf.)	S-8398 sin CC (cf.)	ZZ31-M1.A sin CC
ru3	Length of the olecranon (to anconeus)					100	
ru4	Depth of the olecranon				74	66	61 ~
ru5	Maximal breadth of the olecranon				45.5	40	40
ru6	Minimal breadth of the olecranon						20 ~
ru7	Depth of the anconeus process					79	
ru8	Length of the trochlear notch (anconeus to coronoid process)			57			
ru9	Breadth of the trochlear notch	99	103	108			
ru14	Proximal breadth of the radius			125			

	METACARPALE	D35-02 sin CM	P12-8 CM	S-8098 CC	ZZ31-B.03 sin C. sp.
mp3	Medial depth of the proximal articulation				51
mp4	Lateral depth of the proximal articulation				47
mp5	Breadth of the proximal articulation				76.5
mp11	Minimal depth of the diaphysis	34			
mp13	Depth of the medial condyle	57		45	
mp14	Depth of the lateral condyle	58	52		
mp15	Breadth of the medial condyle	61		47	
mp16	Breadth of the lateral condyle	62	52	45	
mp17	Maximal distal breadth	134			

	FEMUR	SM00-1 CM	W-724 CM	W-1472 CM	C27-D04 dex CC	B27-1b CC	CD28-F14 CC
fe5	Depth (diameter) of the head	68		70		57.5	57
fe11	Distal medial depth (medial condyle to trochlea)				93		
fe12	Breadth of medial condyle		50		27		

	TIBIA	C35-26 sin CM	PS00-3 dex CM	W-229 dex CM (cf.)	W-2028.1 dex CC (cf.)	A32-D sin CC (cf.)	C33-1 sin CC (cf.)	S-12442 dex C sp.	W-3629 dex C sp.
ti14	Depth of the medial fossa of the cochlea (maximal)	60 ~	44	46	47	37	42.5	43	
ti15	Depth of the axial fossa of the cochlea (maximal)	63 ~	51.5	50	45.5	38	41.5	42	
ti16	Depth of the lateral fossa of the cochlea	51 ~	42	41	37.5	32	34	37	
ti17	Dorsal breadth of the cochlea	111	94	88	85	75	77.5	76	
ti18	Palmar depth of the cochlea	111 ~	97.5	91	86	75.5	81	83	79
ti19	Breadth of the medial fossa of the cochlea	37 ~							
ti20	Breadth of the axial fossa of the cochlea	29 ~							
ti21	Breadth of the lateral fossa of the cochlea	28 ~							

	METATARSALE	PS00-11 sin CM	W-2029.1 sin CM	CD28-F12 CC	CD28-F13 CC	W-4086.1 sin C. sp.
mp20	Depth of the medioplantar proximal facet	21				
mp21	Depth of the medial proximal facet	38.5				32.5
mp22	Depth of the lateral proximal facet		50			41
mp5	Breadth of the proximal articulation					67
mp14	Depth of the lateral condyle			36 ~	37 ~	
mp16	Breadth of the lateral condyle			36 ~	37 ~	

	ANTERIOR PROXIMAL PHALANX	C27/28-C13 CC	S-12622 CC	SM00-6 CC
pp1	Length of the axial side		106	
pp2	Length of the abaxial side		104	
pp3	Proximal depth (articular surface)		39	36 ~
pp4	Proximal breath (articular surface)		45	42 ~
pp5	Depth of the diaphysis		20	
pp6	Breadth of the diaphysis		24.5	
pp7	Depth of the condyle	27	27.5	
pp8	Breadth of the condyle	40 ~	42	
pp9	Length of the axial lip of the condyle		39	
pp10	Length of the abaxial lip of the condyle		40	

	POSTERIOR PROXIMAL PHALANX	W-2909.2 CC	SK06-38 CC
pp2	Length of the abaxial side	84	
pp3	Proximal depth (articular surface)	29	29.5
pp4	Proximal breath (articular surface)	38	36
pp5	Depth of the diaphysis	17.5	
pp6	Breadth of the diaphysis	21	
pp7	Depth of the condyle	21	
pp10	Length of the abaxial lip of the condyle	32	

	DISTAL PHALANX *(not included in Martini et al. 2017)*	W-3440 CM
dp1	Maximal length	29
dp2	Maximal breadth	31
dp3	Maximal height	23
dp4	Height of the axial side	25.5
dp5	Height of the abaxial side	29
dp6	Length of the axial side	25
dp7	Length of the abaxial side	28
dp8	Dorsal length	28.5
dp9	Distance from the facet to the axial lateral foramen	10

	SCAPHOIDEUM	A32-A.02 sin CM	PS00-18 sin CM	W-3430 dex CM	P15-24.2 sin CC	SS-7 sin CC
Ks1	Height dorsal	38	40	45	28	37
Ks2	Height in the middle	31			20	28
Ks3	Height palmar	34.5				
Ks4	Depth maximal	57				52
Ks5	Depth proximal	52				44
Ks6	Breadth of proximal facet, dorsal	31.5	35		24.5	32
Ks7	Breadth of proximal facet, palmar	27				29
Ks8	Total depth of distal facets	42				42
Ks9	Depth of dorsal distal facet	25 ~				24
Ks10	Breadth of dorsal distal facet	30	31		20	28
Ks11	Breadth of palmar distal facet	21				18
Ks12	Maximal diameter of palmar distal facet	26				24
Ks13	Length of lateral (palmar) facet	17.5				
Ks14	Lateral (palmar) facet to lateral dorsal distal corner	37 ~				36

	TRIQUETRUM	CD28-F08 sin CC	P15-24.1 dex CC	S-8181 sin CC
Kq1	Dorsal maximal height	40	33	
Kq2	Dorsal height, between tips of both facets	24	21	25
Kq3	Height in the middle	30	26	29
Kq4	Palmar height		33	38
Kq5	Depth of proximal facet		41	46
Kq6	Breadth of proximal facet	30 ~	25.5	31
Kq7	Depth of distal facet	39 ~	31	37.5
Kq8	Breadth of distal facet	20	20	22

	PISIFORME	C28/29-D04 dex CC
Kp1	Diameter of the tuberosity	45 ~
Kp2	Proximal depth	46 ~
Kp3	Maximal depth	48 ~
Kp4	Maximal height	38 ~
Kp5	Breadth of the articular facet	28 ~
Kp6	Height of the articular facet	22 ~

	TRAPEZOIDEUM	A32-C.01 sin CC	W-3451.4 dex CC
Kt1	Maximal height	30	29
Kt2	Maximal diagonal	32	
Kt3	Maximal diameter of the distal facet	25	23
Kt4	Breadth of the proximal facet	20.5	21
Kt5	Minimal diameter of the distal facet	15.5	18

	CAPITATUM	W-3429 dex CM	A32-A.01 sin C. sp.	W-3451.3 dex C. sp.	ZZ31-B.04 sin C. sp.
Kc1	Height of the palmar region	33	30	31	27.5
Kc2	Height of the dorsomedial region	27	23	24	21.5
Kc3	Maximal diameter		50	52.5	48
Kc4	Depth of the lateral part	46	41	44	39
Kc5	Depth of the proximal lateral ridge	41.5	36	39	34
Kc6	Depth of the distal facet	38	31		34
Kc7	Maximal breadth		41	44	37.5
Kc8	Breadth of the distal facet		39	40	36
Kc9	Maximal diagonal of the palmar proximal facet	18	20		15
Kc10	Diagonal of the palmar lateral facet	15.5	14	13	13

	HAMATUM	C26-3 sin CM	S-8100 sin CM	W-3653 dex CM	C28/29-D01 sin CC	C28/29-D02 sin CC	ZZ31-B.05 dex CC	W-3451.2 dex C. sp.
Kh1	Height of the dorsal region	26	32.5	32.5	23.5	27	27	28
Kh2	Height of the palmar region	27	31	31 ~	24	31	31	
Kh3	Maximal diameter (including the hamulus)		64.5		50 ~	60 ~	55	
Kh4	Depth of the proximal facet	53	58	55	41	52	49	
Kh5	Depth of the distal facet	46	51		34 ~	46	43	
Kh6	Maximal breadth (from medial notch)	33	43 ~		27.5	34.5	32.5	36
Kh7	Breadth of the proximal facet (in palmar region)	30	39	36	22 ~	27.5	26	
Kh8	Breadth of the distal facet	31.5	43		22 ~	34	32	
Kh9	Diagonal of the palmar medial facet					16	14.5	

	FIBULA	D28-6.1 sin CM	W-1040 dex CM	W-2028.3 dex CM	W-2028.4 sin CM	W-2028.2 dex CC
fi1	Height dorsal	25	35	36	36	33
fi2	Height in the middle (height of the process)	24	35.5	38.5	33	31
fi3	Height plantar	16	23.5	27		21.5
fi4	Maximal depth	37	52	58	53	45
fi5	Depth of the proximal facet	33	48	52	46	38
fi6	Depth of the distal facet	28.5	41	48.5	46	35
fi7	Dorsal breadth of the proximal facet	20.5	22			28
fi8	Plantar breadth of the proximal facet	11.5	17		20	19.5
fi9	Breadth of the distal facet	16	24	26	24	20
fi10	Depth of the medial (astragalus) facet	28	37	42	44	37

	ASTRAGALUS	ZZ33-8 sin C. sp.	SM-18 sin C. sp.
Ta1	Height of the lateral side	76 ~	73.5
Ta2	Height axial	56.5	58
Ta3	Height of the medial side	70 ~	66.5
Ta4	Proximal depth of the lateral side	31 ~	32
Ta5	Distal depth of the lateral side		24
Ta6	Middle depth of the lateral side	35 ~	35
Ta7	Proximal breadth	44 ~	42
Ta8	Breadth of the calcaneal surface	28 ~	33
Ta9	Breadth at the lateral (calcaneal) process	53	
Ta10	Distal breadth	48 ~	49
Ta11	Greater maximal diameter (dorsolateral-distomedial)	85 ~	83
Ta12	Lesser maximal diameter (dorsomedial-distolateral)	76 ~	75
Ta16	Medial depth of the distal trochlea	25	
Ta18	Lateral depth of the distal trochlea	22	

	CALCANEUS	B26-4 sin C. sp.	C27-1 dex C. sp.	C27/28-C12 sin C. sp.	ZZ33-7 sin C. sp.
Tc1	Maximal height (greatest length)	106			
Tc2	Depth of the tubercle				36
Tc3	Maximal breadth of the tubercle			32 ~	33.5 ~
Tc4	Minimal breadth of the tubercle	16.5			21
Tc5	Depth medial (plantar border to substentaculum)	48			
Tc6	Breadth of the substentaculum	34	37		
Tc7	Medial distal height	55	58		
Tc8	Depth lateral (plantar border to fibular trochlea)	53			
Tc9	Height of the fibular trochlea	26	26.5		
Tc10	Breadth of the fibular trochlea	16	15		
Tc11	Distal lateral height (fibular trochlea to distal facet)	46	46		
Tc12	Breadth of the plantar border	15			18 ~
Tc13	Height of the distal (cuboid) facet	36			
Tc14	Breadth of the distal (cuboid) facet	18			

	CUBOIDEUM	W-2029.2 sin CM	CD28-F07 sin CC	C28/29-D03 sin CC	C31-14 dex CC	SM-22 dex CC	ZZ33-6 sin CC
Tq1	Dorsal height	40 ~	35	30	31	27	31 ~
Tq2	Medial height (proximal process to centrodistal medial facet)				29	27	
Tq3	Plantar diagonal (proximal process to plantar tuberosity)		47		41.5	39	
Tq4	Proximal depth (proximal dorsal border to plantar tuberosity)		64		55	55.5	58 ~
Tq5	Distal depth (distal dorsal border to plantar tuberosity)		55		51	52	52 ~
Tq6	Lateral depth (proximal dorsolateral border to plantar tuberosity)		54		47	45	50 ~
Tq7	From the plantar border of the proximal facet, to the dorsal border of the distal facet	73 ~	55	54.5 ~	46 ~	51	
Tq8	From the dorsal border of the proximal facet, to the plantar border of the distal facet	65 ~	55	48	48	45	49
Tq9	Depth of the proximal facet	69 ~	54	47 ~	47	47	49 ~
Tq10	Depth of the distal facet	47 ~	38.5	39	37	38	35
Tq11	Length of the lateral groove (laterodorsal border of the proximal facet to distal facet)	49 ~	44	40.5	39	35	42
Tq12	Length of the plantar tubercle (centrodistal medial facet to plantar tuberosity)		37		35	34	
Tq13	Proximal breadth (centrodistal medial facet to lateral border of proximal facet)	52 ~	50	45	45	39	
Tq14	Distal breadth (centrodistal medial facet to lateral border of distal facet)		46.5	39	40.5	39.5	
Tq15	Maximal diagonal breadth (proximal process to lateral border of distal facet)	70 ~	52 ~		45	40.5	
Tq16	Breadth of the main proximal facet		38.5	33 ~	33	28	
Tq17	Breadth of the distal facet		30	25	24	24	26 ~
Tq18	Breadth of the dorsal proximal facet	20	22	19	19	19	19 ~

	NAVICULARE	W-2029.3 sin CM	A32-B.03 dex H 5b1-4	D28-6.2 dex H 5x	SM-20 sin H 5x	W-4085 sin H 5b5	ZZ33-5 sin H 5b1
Tn1	Dorsal height	26	18.5		18	19	17.5
Tn2	Lateral height		15.5	16.5	14	16	14.5
Tn3	Plantar height	44.5	30	27	26	30	28 ~
Tn4	Maximal depth		47	45	45	47	46
Tn5	Maximal breadth	38	32	30	28.5		30
Tn6	Depth of the distal dorsal and lateral facet	55	43	37	39.5	41	43
Tn7	Depth of the distal dorsal facet		35	34	30	34.5	34.5
Tn8	Depth of the distal plantar facet		12		12	10.5	13.5
Tn9	Breadth of the distal dorsal facet		16		19	19	19

	CUNEIFORME MEDIALE	W-2029.4 sin CM
Tm1	Maximal height	24
Tm2	Maximal breadth	26
Tm3	Maximal diameter	28.5
Tm4	Maximal diameter of the proximal facet	18
Tm5	Maximal diameter of the distal facet	22

	CUNEIFORME INTERMEDIOLATERALE	W-2029.5 sin CM	W-4101 sin C. sp.
Tl1	Maximal breadth		35
Tl2	Proximal breadth		19
Tl3	Proximal depth	40	36
Tl4	Diameter of the plantar lateral facet		
Tl5	Diameter of the dorsal lateral facet		16
Tl6	Lateral depth		
Tl7	Lateral height		18
Tl8	Breadth of distal facet		22.5
Tl9	Depth of distal facet	37	33

	LUMBAR VERTEBRAE	W-2565 L1-2 CM	A32-29 L1-4 CM	W-2175 L2-4 CM	S-8409 L1 CM	S-8415 L2 CM	S-8416 L3 CM	S-8417 L4 CM	S-8418 L5 CM	S-8419 L6 CM	S-8420 L7 CM	SM-11 L2-3 CC
lu1	Length of the body	85	92	81		77	81	78	81	74	69	61
lu2	Length of the arch	101				96.5	87			52	46.5	
lu3	Length between zygapophyses	118				115	106.5			108	103	
lu4	Dorsal length of the spine											
lu5	Cranial height of the spine											
lu6	Cranial height of arch and body	79	83		74	80				77	88	
lu7	Cranial height of the body	54	46	52	48	53	53	53	45	41	53	35
lu8	Cranial breadth of the body	70	60	66	70	70	70	68	76	72	77.5	42
lu9	Cranial breadth of the zygapophyses	34	45		30	35	41			63	61	
lu10	Caudal height of the spine											
lu11	Caudal height of arch and body	89				89				86	81	
lu12	Caudal height of the body	45		47	52	56	53	54	54	50	50	34
lu13	Caudal breadth of the body	69		70	72	70	66	77	83.5	76	65	46
lu14	Caudal breadth of the zygapophyses	31			30	31	36			75		

Chapter 6
The diversity of Camelidae in El Kowm and in the Levant

Pietro Martini, Loïc Costeur, Jean-Marie Le Tensorer

Manuscript in preparation

Abstract

Camelidae have been present in Eurasia and Africa for the last 6 million years, but our understanding of their diversity is fragmentary. There is no solid evolutionary framework for the origins of the extant genus *Camelus* and its evolution during the Pliocene and Pleistocene. The El Kowm Basin fossiliferous sequence (1.8 Ma-0.05 Ma) has yielded abundant camelid remains, and provides an opportunity to expand paleontological knowledge on this family. Previously, we have described three new species from this region: *Camelus roris* (Middle Pleistocene), *Camelus concordiae* and *Camelus moreli* (Late Pleistocene). The analysis of the complete combined sequence (all available and identified camelid specimens from the sites Aïn al Fil, Nadaouiyeh Aïn Askar, and Hummal) indicates that at least three other unnamed species were present in the Early Pleistocene, while the Middle Pleistocene diversity can best be explained by an overlap or alternation of the already described species. The Late Pleistocene sees the extinction of Camelidae in the Levant, which can be included in the worldwide Quaternary megafaunal extinction event.

Introduction

The El Kowm Basin, in the center of Syria, is rich in Pleistocene sites that have yielded a combined fossiliferous sequence spanning the last 1.8 Ma (Jagher et al. 2015; Jagher and Le Tensorer 2011). It contains a steppe fauna rich in Camelidae remains (Martini et al. 2015). This family of Artiodactyla originated in North America, and colonized the Eurasian continent in the late Turolian (MN13, late Miocene; approximately 6 Ma) (Colombero et al. 2014; Honey et al. 1998; Pickford et al. 1995; Vislobokova 2008a); unfortunately, its evolution in this continent is poorly understood (Kostopoulos and Sen 1999). Known fossil species are grouped in the paraphyletic genus *Paracamelus* SCHLOSSER 1903, identified from the late Miocene to the early Pleistocene (6-2 Ma) (Alçiçek et al. 2013; Havesson 1954; Kozhamkulova 1986; Titov and Logvynenko 2006; Vislobokova 2008b), and the extant genus *Camelus* LINNAEUS 1758, which appeared in the late Pliocene of eastern Africa (Harris 1987; Harris et al. 2010). However, many named species are

poorly described or based on fragmentary material. For this reason, we have previously argued that the camelid succession in the El Kowm Basin has the potential to shed light on the diversity and evolution of this family (Martini et al. 2015).

The origins of *Camelus* are to be found in the basal forms of *Paracamelus*, such as *P. aguirrei* MORALES 1984 (Morales et al. 1980; Titov and Logvynenko 2006). The most basal species is *Camelus sivalensis* FALCONER & CAUTLEY 1836 (Colbert 1935; Falconer and Murchison 1868; Matthew 1929), described from the Siwalik Hills of Pakistan and India (Tatrot and Pinjor Formations; Late Pliocene and Early Pleistocene). Equally ancient, but dentally much closer to extant camels, is the eastern African *Camelus grattardi* GERAADS 2014 from Ethiopia, Omo Valley, Shungura formation (early Pleistocene, 2.2) (Geraads 2014); other East African occurences of *Camelus*, extending to the Early Pliocene (Gentry and Gentry 1969; Grattard et al. 1976; Harris 1987; Harris et al. 2010; Howell et al. 1969), might belong to this species as well. These species were contemporary to the last *Paracamelus*, which include the small *P. alutensis* (STEFANESCU 1895) in the Black Sea Region and the very large *P. gigas* SCHLOSSER 1903 in Eastern Europe, central Asia and northern China. *Paracamelus alutensis* disappears close to 2.0 Ma, while *P. gigas* is recorded in China until 0.35 Ma (Alçiçek et al. 2013; Havesson 1954; Kozhamkulova 1986; Titov 2003; Vislobokova 2008a). In the late Early Pleistocene, the North African *Camelus thomasi* POMEL 1893 is known primarily in Tighennif, Algeria; most other instances of this species cannot be accepted (Harris et al. 2010; Martini and Geraads 2018). Fragmentary remains of camelids are known throughout the Pleistocene in North Africa and the Middle East (Grigson 1983; Payne and Garrard 1983; Stimpson et al. 2016; Thomas et al. 1998). The Middle and Late Pleistocene *Camelus knoblochi* NEHRING 1903 is known from cold-adapted faunas in Eastern Europe, central and northern Asia (Titov 2008).

In two previous studies, we have described three new species in the genus *Camelus* from the El Kowm Basin. *Camelus roris* is a middle-sized species from the Middle Pleistocene of the site Nadaouiyeh Aïn Askar (henceforth Nadaouiyeh) (Martini et al. in preparation-a), *Camelus concordiae* is small and coexisted with the gigantic *Camelus moreli* in the Late Pleistocene layers of the site Hummal (Martini et al. in preparation-b). Here we review the entire sequence of the three sites in the El Kowm Basin that were included in our study: Aïn al Fil, Hummal and Nadaouiyeh. We complete our description of Camelidae in this region by investigating the Early and Middle Pleistocene fossils from Hummal and Aïn al Fil. We discuss the diversity of this family in the composite sequence: covering the last 1.8 Ma, the sites of the El Kowm Basin represent an

unparalleled time depth among Pleistocene sites in the Middle East, and in general among Old World sites containing camelids.

We show that a minimum of six distinct species are represented in the three sites combined: two at Aïn al Fil, one in the lower section of Hummal, one at Nadaouiyeh, and two in the upper section of Hummal, in particular the Mousterian complex. As the total of fossil *Camelus* species elsewhere amounts to four allopatric species, none of which is present in the Middle East, the greatest share of the diversity within the genus is now known in the El Kowm Basin.

Stratigraphic setting

Aïn al Fil is a smaller site than Hummal and Nadaouiyeh, and is found 1 Km north-west of the former (Le Tensorer et al. 2015). It was discovered in 2003 and preliminary investigation were undertaken in 2008 and 2010. It includes a lithic assemblage more archaic than at 'Ubeidiya (Le Tensorer et al. 2015). The number of fossils collected is small, and so far only four belong to Camelidae; many more were left in the matrix for expected future excavation. The fossiliferous levels (K, I and L) correspond to the lower part of the sequence, to which an age slightly older than 1.8 Ma was assigned by paleomagnetism (the Olduvai subchron was identified in layer K) and biostratigraphy (presence of *Equus stenonis* cf. *senezensis* and a *Mammuthus* form transitional between *M. meridionalis* and *M. trogontherii*) (Le Tensorer et al. 2015).

The richest site included in this study is Hummal, whose stratigraphy is divided into seven archaeological units. In this study, we informally indicate the fossil assemblage of each unit by the name of the associated lithic industry.

The entire Hummal sequence is divided into two sections, separated by a large temporal hiatus. The lower section includes only Unit G (layers 15 to 23) and is characterized by an Oldowan industry (Lower Paleolithic) of difficult dating; it appears older than Gesher Benot Ya'akov (lower limit ~0.8 Ma) but younger than 'Ubeidiya (upper limit ~1.2 Ma) (Bar-Yosef and Belmaker 2011; Le Tensorer et al. 2011a; Le Tensorer et al. 2011b). Layer 17 has been referred to the Middle Pleistocene based on the presence of the rodent *Ellobius* (Maul et al. 2015), but to the Early Pleistocene (Matuyama chron) by paleomagnetism (Richter et al. 2011). Unfortunately, more detailed dating are still missing (Wegmüller 2015). The sample from Unit G is hereafter termed the "Oldowan assemblage".

The site of Nadaouiyeh Aïn Askar is situated 7 km north of Hummal and is subdivided into six Units, A to F, which are dated by archaeological correlation with a solid Levantine chronology (Jagher 2011, 2016; Reynaud Savioz 2011). Its central, continuous stratigraphy (B to E) is included between 0.5 Ma and 0.35 Ma; the basis of the immediately preceding Unit F extends toward the beginning of the Middle Pleistocene, while Unit A follows a hiatus and is dated to about 0.20-0.15 Ma, younger than the Yabrudian and Hummalian cultures of Hummal. Both Unit A and F have yielded only limited fossils. Reworked fossiliferous sands that originated between Unit A and B are deposited in "Doline 3", together with a small deposit containing lithic material of Hummalian industry. The camelid fauna of Nadaouiyeh has been described in a separate study (Martini et al. in preparation-a) in which the new species *Camelus roris* has been named.

The upper section of Hummal includes Unit A to F (Jagher et al. 2015; Le Tensorer et al. 2011a). Unit A (layers 1-3) includes Holocene historical and protohistorical sediments with scarce camelid remains too fragmentary for identification. Unit B (layer 4) is formed by Upper Pleistocene sediments that were not excavated extensively, and have not yielded any camelid fossils. Unit C (layer 5) is a massive complex, with a thickness of 4 m and more than 30 sublevels, characterized by Mousterian industry and rich in camelid fossils; they are described in a separate paper (Hauck 2011; Martini et al. in preparation-b). Unit D (layers 6-7) includes seven geological levels with Hummalian industry and a more modest assemblage of camelid remains. Unit E (layers 8-12) contains rare Yabroudian industry but a large number of fossils. Unit F (layers 13-14) is poor in both fossils and lithic remains, which are not identified with certainty but might be equivalent to the "Acheuleo-Tayacian" culture; layer 14 is sterile. Therefore, the camelid remains studied in this contribution originate from layers 6 to 13 and are divided into three stratigraphical and cultural horizons, hereafter termed the "Acheuleo-Tayacien assemblage", the "Yabroudian assemblage", and the "Hummalian assemblage".

The limited archaeological material of the "Acheuleo-Tayacien" layers has ambiguous affinities within the Middle Paleolithic; it can be compared to Tabun F, Umm Qatafa and perhaps Yabroud, but a more precise temporal correlation than middle or lower Middle Pleistocene is not possible. No direct dating of layer 13 was performed (Jagher et al. 2015).

The Yabroudian culture is known on the Levantine coast since 0.325 Ma, and the transition to the overlying Hummalian sequence is estimated at 0.25 Ma. The complex characterized by this industry belongs therefore to the later part of the Middle Pleistocene (Jagher et al. 2015).

The Hummalian industry is represented by two *in situ* layers (divided in seven geological levels) and a deposit of reworked sands, which includes artifacts corresponding to the earlier part of this cultural complex (Wojtczak and Ismail-Meyer 2017). This assemblage is as old as the terminal Middle Pleistocene, and is bracketed at 0.25-0.175 Ma (Jagher et al. 2015; Richter et al. 2011)

The three assemblages described here are only tentatively dated, but they form a temporal sequence which is constrained to the Middle Pleistocene. As two of the three stratigraphical units include only a small number of fossils, the assemblages are examined together under the label of "Upper Hummal I", taking care to discuss possible differences among them.

The thickest subdivision of the Hummal sequence is Unit C, formed by the layer complex 5 which amounts to almost half of the excavated depth of the site. Layer 5 was deposited during the existence of the Mousterian industry and is dated to the terminal Middle Pleistocene and early Late Pleistocene, approximately 0.15-0.045 Ma (Hauck 2011; Jagher et al. 2015; Le Tensorer et al. 2011a). In a previous study, we described the camelid remains from this complex and showed the coexistence of two new species, the giant *Camelus moreli* and the smaller but more abundant *Camelus concordiae* (Martini et al. in preparation-b). This unit is here labeled "Upper Hummal II", and the material herein contained is termed "Mousterian assemblage".

Materials and Methods

Aïn al Fil has yielded only four Camelidae specimens thus far. The Oldowan assemblage includes 429 identified camelid remains, of which 153 were analyzed. In the Acheuleo-Tayacien assemblage 22 camelid fossils were identified and 8 were examined. The Yabroudian assemblage counts 182 identified camelid specimens, as many as 61 could be studied. The Hummalian assemblage includes 47 identified specimens and 15 which were investigated. Finally, 13 specimens of unclear stratigraphic origins were investigated. Specimens were excluded when too fragmentary or too poorly preserved to be morphologically informative; those which were selected, in total 254, are listed in Table 1. The present work discusses but does not describe the samples from Nadaouiyeh (463 identified camelid remains, 126 studied) (Martini et al. in preparation-a), nor from the Mousterian assemblage of Hummal (394 identified and 170 studied camelid fossils) (Martini et al. in preparation-b). Remains from Aïn al Fil are indicated by the prefix AF; from Nadaouiyeh Aïn Askar, by the prefix Nad-1; and from Hummal, by the prefix Hu.

Part of the sample from Hummal is preserved at the IPNA in Basel and could be examined in detail. Unfortunately, the largest part of the material as well as the Aïn al Fil sample is stored at the

Tell Arida Research Center, El Kowm, Syria. The still ongoing unrest in Syria have made the location inaccessible since 2011, and the state of the collection is unknown. Only limited data on this material was available for the present study: postcranial measurements (Martini 2011), dental and mandibular measurements (taken in 2007 by Chloé Lecompte) and photographs.

Measurements have been taken with a slide gauge caliper, rounded to the next 0.5 mm (Martini et al. 2017). Greater precision (such as 0.1 mm) was deemed unnecessary, even for small bones and dentition. All measurements are presented in Table 2.

The fossil material was compared with published data on both extant species, *C. bactrianus* and *C. dromedarius* (Martini et al. 2017), with *C. thomasi* from the MNHN in Paris (Martini and Geraads 2018) and with the three already named species from El Kowm: *C. roris, C. moreli,* and *C. concordiae* (Martini et al. in preparation-a; Martini et al. in preparation-b). Data on other fossil species are based on the literature.

Most of the postcranial differences are not qualitative, but rather depend on proportions that are easier to visualize metrically than on the specimens. Important metrical characters are illustrated using bivariate scatterplots. We also show scatterplots of data transformed to Harmonic Scores (HS), according to Martini et al. (2017); this is a transformation that scales each measurements to a baseline average (we used the interspecific average of extant *Camelus*), and corrects each scaled measurement by removing an estimation of size, which is approximated by the harmonic average of all its scaled measurements. The result is an index that shows the relative importance of each measurement, allowing the comparison of proportions in specimens of different size. Scatterplots of HS are often able to visualize more clearly the same patterns that can be seen in scatterplots of raw measurements; hence, we chose to show the latter, when appropriate.

The number of specimens for most of the elements is very limited; therefore we do not apply any statistical test.

Institutional abbreviations

NMB, Naturhistorisches Museum Basel

MNHN, Museum National d'Histoire Naturelle, Paris

IPNA, Institut für Prähistorische und Naturwissenschaftliche Archäologie (Institute for Prehistorical and Scientific Archeology), University of Basel

Descriptions and comparisons

1. Aïn al Fil

Three specimens (tibia, scaphoideum, hamatum) from Aïn al Fil show a large size, comparable to *C. moreli*. The fourth specimen (scaphoideum) has a smaller size, close to *C. dromedarius*.

Camelus sp. "Aïn al Fil large"

The complete tibia AF.178 is very large and slender; its total length was estimated at 650 mm, but other measurements are less extreme. The proximal epiphysis has average width but is dorsoplantarly short, with a reduced lateral condyle. The diaphysis is also transversally wide (Fig. 10a). The distal cochlea is characterized by a very long medial fossa, short medial and lateral ones, and a small dorsolateral prominence (Fig. 10b, 10c, 10d).

Among extant species, *C. dromedarius* has longer and slenderer tibia than *C. bactrianus*; the only fossil preserving this complete element, *C. thomasi*, is comparable in slenderness to *C. dromedarius*, but specimen AF178 is much more elongated. Its estimated length (650 mm) is 44.5% greater than the average *C. dromedarius* (449.8 mm), and 21.5% more than in *C. thomasi* (535 mm). The proximal epiphysis is shorter than in extant species, with an intermediate relative breadth. The diaphysis is wider than in *C. dromedarius* and *C. thomasi*; its proportions are closer to *C. bactrianus* but wider and shallower than the average (Fig. 10a). The proportions of the cochlea are unique: the medial fossa is extremely long (Fig. 11c), the lateral and axial fossae are shorter than all but some *C. dromedarius* and the small unassigned specimen Nad-1 D17-105 (Nadaouiyeh, layer 5-90) (Fig. 11d). Moreover, the difference between the wider plantar breadth and narrower dorsal breadth (Fig. 11b) is greater than *C. dromedarius, C. bactrianus, C. moreli* and *C. concordiae*; it is similar to the unidentified Hu S-12442 from Hummal (Mousterian assemblage, layer 5b3), the wider but small E-9903 (Oldowan assemblage, layer 18), the wider Nad-1 SP31-2.1 (Nadaouiyeh, Dol.3) and *C. thomasi* TER-1649 (Tighennif). This specimen differs strongly from all named species, including the large *C. thomasi* and *C. moreli*. By its size and especially the proportion of the medial distal fossa it can also be diagnosed from unassigned Oldowan and Nadaouiyeh specimens.

The hamatum AF.221 is proximally wide, but less than in *C. moreli*; it differs from the latter in having a tall palmar and a low dorsal region (Fig.12c). The distal facet is rather deep and narrow. This specimen is larger than all the Oldowan ones, but otherwise similar. It is also larger than *C. dromedarius, C. concordiae, C. roris*, the Yabroudian assemblage and all but one *C. bactrianus*. Its proximal breadth is larger than in *C. roris, C. concordiae* and the Yabroudian assemblage. Its dorsal height is less than in *C. bactrianus* and less than average in all other forms.

The scaphoideum AF.229 is dorsally wide and palmarly narrow. The dorsodistal facet is short, but the palmodistal facet (for the trapezoideum) is narrow and elongated (Fig.11a), making the distal aspect deep. The narrowness of this facet, separates this specimen from *C. bactrianus* and *C. moreli*, and is at the lower edge of variation in *C. dromedarius* and *C. roris*, but can be compared to *C. concordiae* and Hu E32-27 (Oldowan assemblage, layer 18). The distal depth is greater than all *C. dromedarius, C. bactrianus, C. roris, C. moreli* and the Oldowan assemblage (Fig.11b). The proximal facet is dorsally wider than *C. roris, C. moreli*, the Oldowan assemblage, and all but one *C. dromedarius*, and palmarly it is narrower than *C. bactrianus*. The morphology can be generally compared with *C. concordiae* and the Yabroudian assemblage, which are however much smaller.

Camelus sp. "Aïn al Fil small"

A second scaphoideum, AF.230, completes the sample from Aïn al Fil. It is not only much smaller than AF.229, but also very different. The distal aspect is even deeper (Fig.11b), but the dorsodistal facet is long while the palmodistal one is short and wide (Fig.11a). The proximal aspect is short and narrow: its depth is at the lower edge of the variation in extant species, and shorter than in all fossils except *C. concordiae*, and its dorsal width of the proximal facet is less than in *C. bactrianus, C. roris, C. concordiae*, the Yabroudian and the Oldowan assemblage, and in AF.229; it is within the variation of *C. dromedarius* and close to *C. moreli*. In proportion, the distal aspect is significantly deeper than in any other studied specimen (Fig.11b). The dorsodistal facet (for the capitatum) is deeper than in all fossils and at the upper edge of the variation of extant species; it is also narrower than in *C. moreli* and *C. concordiae*. The palmodistal facet is wider and shorter than *C. dromedarius, C. moreli, C. concordiae* and AF.229; it is as wide as *C. bactrianus* but shorter than all but one specimen; it is wider but not shorter than *C. roris* and the Yabroudian assemblage; it is either wider or shorter than all Oldowan specimens (Fig.11a).

2. Lower Hummal (Oldowan assemblage)

Camelus sp. "Oldowan"

Only the mandibular fragment Hu K33-381 (layer 18) could be studied directly; in addition, good pictures of Hu E-9242 (layer 16) are described. Isolated dentition includes one specimen each of P4 (associated with the mandible Hu K33-381, layer 18), M3 (Hu K33-235, layer 17c), p4 (Hu K33-417, layer 18) m2 (Hu K33-218, layer 17c) and some fragments.

Hu K33-381 is a fragmentary right mandibula, preserving a part of the corpus with m2-m3 in decent conditions and the highly damaged distal lobe of m1 (Fig. 1). The corpus is heavily damaged on both sides and on the alveolar border rostral to m1, but its lateral face is flat, suggesting a thin shape. The caudal mental foramen cannot be located. Rostrally, the corpus extends until the beginning of the symphysis, which is a short distance from the dentition. The m2 is in advanced wear; the occlusal relief is flat in m2, but forms a low angle in m3.

Hu E-9242 is a left mandibula with almost complete ramus and corpus preserving p4-m3, but broken a short distance anterior to p4 (Fig. 2). The preservation is poor: the bone surface is completely cracked, although overall not very deformed. The dentition is also rather complete but highly damaged, with individual lobes separated and rostrally inclined; m3 is not in full wear, indicating an immature individual. The deformation prevents acceptable measurement. The corpus is robust, quite low; a caudal mental foramen is not visible. The ramus is tall, and forms an angle slightly more than 90° with the corpus. The angular process is broken off, the large condyle is placed high above the break point. The coronoid process is short, straight, slightly wider at the basis than at the tip, and rather thin. Dorsally it is only about twice as prominent as the condyle. This morphology differs clearly from *C. thomasi*, where the coronoid process is massive, bent caudally and apically enlarged; the Algerian species also has a deeper ramus and a less prominent condyle. The ramus preserved in one *C. cf. roris* specimen (Nad-1 H13-703, layer 8a) is also deeper and it is slanted caudally; the coronoid process is thick and slightly curved. The shape of the ramus is similar to that in *C. concordiae*, but in the latter species the ramus is low, not tall, and the overall size is less. In *C. bactrianus* the coronoid process is long and hook-shaped. The differences with *C. dromedarius* are less evident; this extant species has a lower ramus, but higher angular process, and the coronoid process forms a wider, rounder angle with the condyle.

The P4 Hu K33-381is small; it fits in size *C. concordiae*, the smallest *C. dromedarius* but also *C. thomasi*. The M3 Hu K33-235 is in advanced wear, with flat relief. The distal lobe is much narrower than the mesial lobe. There are three well-developed styles and no ribs. It is small: at the occlusal surface it is close in dimension with small *C. dromedarius* and *C. roris*, slightly larger than *C. concordiae*, and smaller than *C. thomasi* or *C. bactrianus*. Alveolarly, it is significantly smaller than *C. dromedarius, C. roris*, and *C. thomasi* (no alveolar data for *C. concordiae*). The p4 Hu K33-417 is large, comparable to big *C. bactrianus* and *C. roris*, smaller than *C. moreli*, and larger than *C. dromedarius, C. thomasi, C. concordiae* and the Yabroudian assemblage. It is longer but narrower than in *C. knoblochi* (Fig. 8a). The m2 Hu K33-381 is of average length but very wide, comparable to *C. thomasi* only; it is slightly wider than *C. bactrianus*, much smaller than *C. knoblochi* or *C. moreli*, and much wider than all other forms (Fig. 8b). Another m2 specimen, Hu K33-218, is much less worn and is accordingly longer, but also much narrower: it fits only within *C. roris* and the less worn *C. dromedarius* and *C. concordiae* (Fig. 8b). The difference in width between both specimens is similar to *C. roris* but greater than in all other species (Fig. 8c). The m3 is large, fitting with the widest *C. bactrianus* and even *C. sivalensis*; it is larger than *C. dromedarius, C. roris, C. concordiae*, the Yabroudian and the Hummalian assemblages; it is longer than *C. thomasi*, it is somewhat narrower, but much shorter than *C. moreli* and *C. knoblochi* (Fig. 8d).

For the peculiar atlas Hu E-10561 (layer 19) only measurements are available. The dorsal arch is damaged, especially on the left side. The distance between cranial and caudal foramina (alar foramina, respectively transversal foramina) is very large, while the distance between both crania is small (Fig. 7b). The ventral fossa is restricted. The cranial fovea is relatively small, while the caudal fovea is large. Due to the lack of both remain and publications, this specimen cannot be compared to other fossil forms, but it show important differences with both extant species: the position of the four dorsal foramina (Fig. 7b) and the size difference between cranial and caudal regions are unique , while the small ventral fossa is a diagnostic trait of *C. dromedarius* from *C. bactrianus*, where it is invariably much larger.

Three distal fragments of radioulnare (all layer 16) are all rather small; one specimen (Hu E-9396) has a relatively deep medial articular facet and small lateral facet, which is similar *to C. dromedarius, C. roris* and the Yabroudian assemblage, but differs from *C. bactrianus*.

The scaphoideum is always narrower proximally than in *C. bactrianus*; it also is distally wider than *C. roris* and most *C. bactrianus*, and differs from *C. roris* in the larger palmodistal facet

(for the trapezoideum) and smaller palmolateral facet (for the lunatum) (Fig. 11c). The lunatum has a long and narrow proximal facet; its proportions overlap with the Yabroudian assemblage but not with *C. dromedarius*, *C. bactrianus* or *C. roris*. The distal facet is also elongated and narrow. The triquetrum does not show peculiar traits. The pisiforme is represented only by a fragment of the articular facet, which is small and narrower than in *C. dromedarius*. As many as ten specimen of trapezoideum are known; as a group they are elongated and narrow (Fig. 12b), but remains from layer 15 are smaller than all others, with narrower proximal facet and wider distal facet . The capitatum is represented by two fragments and one specimen (Hu K33-195.1) which is fused with a trapezoideum (Fig. 4). It is low, unusually so in the dorsal region, but overall wide with a large and deep distal facet; however, the peculiar fusion requires caution in judging its proportions. Most specimens of hamatum are small, and two have average size; they differ from *C. bactrianus* in the low dorsal region, other proportions are very variable (Fig. 12c).

The complete metacarpale Hu E-10948 (layer 15) is large and elongated; its length of 410 mm is comparable to that in *C. thomasi, C. knoblochi* or *Paracamelus alexejevi*, but less than *P. gigas, C. sivalensis* and much greater than in other species. It is slenderer than *C. bactrianus* and *C. knoblochi* and more similar to *C. dromedarius*, *C. thomasi* or *Paracamelus*. The proximal articulation is as wide as in *C. bactrianus*. The condyles are larger than in almost all extant specimens. Measurements indicate that the medial condyle is wide, but the lateral one is narrow; such proportions are unusual and might indicate some deformation or measuring error. Other specimens of condyle yield contradictory results: Hu D31-25 (layer 16) is deep and narrow; Hu H33-11 (layer 18) is wide and short.

The tibia is represented by two distal fragments. Hu E-9903 (layer 18) is rather small; its diaphysis is narrower than in *C. bactrianus* and deeper than in *C. dromedarius*, but closer to the latter species and to *C. thomasi* (Fig. 10a). The cochlea has rather short medial fossa, rather long lateral fossa (Fig.10c), and great dorsal breadth. Hu E-11336 (layer 16) has average size and similar proportions of the fossae. They cluster with *C. concordiae*, *C. thomasi*, and close to *C. bactrianus*; they are the opposite than seen in the Aïn al Fil large camel; and the lateral fossa is longer than in *C. dromedarius* and *C. roris*. The large dorsal breadth of appears to indicate a large dorsolateral prominence, as in *C. concordiae* or *C. moreli*, although the plantar breadth is not available in the same specimen to confirm this suspicion.

The fibula shows an important variation, but all individuals are deeper than the average in extant camels. Except for one specimen, they are smaller than in *C. bactrianus*. On the other hand,

the astragalus is always large; the length of the lips in the proximal trochlea appears intermediate between *C. bactrianus* and *C. dromedarius* (Fig. 13b) and the distal trochlea is narrow (Fig. 13a). The calcaneus is morphologically more homogeneous: it has the same size as *C. bactrianus*, but is slenderer than in this species (Fig. 14a). Its slenderness is comparable to the smaller *C. roris* and *C. dromedarius*, and to the larger *C. thomasi*. The sustentaculum has a position intermediate between *C. bactrianus* or *C. thomasi* (closer to the fibular trochlea) and *C. dromedarius* or *C. roris* (closer to the plantar border); however, its placement is higher (more proximal) than the average of other species. The fibular trochlea is rather low and dorsally protruding, as in *C. bactrianus* but unlike *C. dromedarius*. The plantar border has intermediate width (Fig. 14a). The distal facet is shorter than in *C. bactrianus*. Two specimens of cuboideum differ from *C. bactrianus* and *C. moreli* in the wide dorsoproximal astragalar facet; the dorsal region has intermediate height (Fig. 14b). However, specimen Hu P57-3 (layer 16) is proximally narrow and distally wide, while specimen Hu E-10579.1 (layer 18) has opposite proportions, resulting in a difference greater than found within any other single species. The naviculare is rather small, with a tall plantar region similar to *C. roris* and *C. moreli* and unlike *C. thomasi*, *C. concordiae* and the Yabroudian assemblage (Fig. 14d). Its overall width and depth are intermediate, but with minimal overlap with the wider *C. bactrianus*, *C. roris* and *C. thomasi* and the more elongated *C. dromedarius*, *C. concordiae* and the Yabroudian assemblage (Fig. 14c). The distal facet is wider than in *C. dromedarius*. The intermediolateral cuneiforme is small but wide, with a deep distal facet.

The metatarsale is represented by two proximal fragments (Hu E-10485, layer 16; Hu K33-365, layer 18). The proximal articulation is dorsoplantarly shorter than extant camels, *C. roris* and *C. knoblochi*, while it is similar to *C. thomasi*. The proximal triangular process is rather wide and short, outside of the variation in *C. dromedarius* and within that of *C. bactrianus*; it is narrower than in *C. thomasi* and wider than in *C. roris*. The facets have average proportions. An isolated condyle (L31-198, 17) is deep and narrow.

Both anterior and posterior proximal phalanges can be large, but all specimens (in total 11) are short (Fig. 6). The proximal articulation is narrower than in *C. bactrianus*. The diaphysis is robust: the anterior phalanx is wider, the posterior is deeper than in *C. dromedarius*, but both overlap widely with *C. bactrianus*. The condyles are always narrower than the average of *C. dromedarius* and especially *C. bactrianus* (Fig. 9b); the anterior ones are also shallower than in *C. concordiae*, *C. roris* and *C. thomasi*. The condylar lips have a variable length, but they are always longer than in *C. bactrianus* (Fig. 9a). A single specimen has a short abaxial lip like in *C. thomasi*.

The intermediate phalanx is represented by seven specimens that have a deep proximal articulation and a narrow, thin diaphysis which is different from *C. dromedarius*. The condyles are variable in shape, but always narrower than in *C. dromedarius*. The condylar lips are symmetrical (Fig. 9c), and differ from *C. bactrianus* (where the abaxial lip is longer) and *C. dromedarius* (where the axial lip is shorter); there is a less clear separation from *C. roris* (where the lips are asymmetrical but intermediate in length between extant species).

All five specimens of distal phalanx differ from *C. bactrianus* and *C. dromedarius* in the low shape and long abaxial side (Fig. 9d, 9e); in this they resemble *C. roris* but are on average smaller and narrower.

3. Nadaouiyeh Aïn Askar

The camelid remains from Nadaouiyeh have been described in a previous report (Martini et al. in preparation-a). Most of the sample is included in the new species *Camelus roris*, while some other elements are tentatively assigned to this species or left unidentified. As the upper layers of Hummal suggest the coexistence of *C. roris* with the smaller *C. concordiae* (this study), we consider that the second could be found at Nadaouiyeh as well.

Camelus roris

This species is based on a rather complete cranium, a maxilla and 93 additional specimens from Nadaouiyeh that include mandibles, dentition, and abundant postcranial elements representing most of the paraxial skeleton. Its diagnosis rests on the large M1 and small M3, broad face and forehead, narrow palate, presence of maxillary crest, palatine foramina at the level of M1, dorsally convex supraorbital notch, pachyostotic mandible, and narrow, long m2. Its size is comparable to *C. bactrianus*, slightly larger than *C. dromedarius*.

Camelus cf. roris

Some of the elements found in Nadaouiyeh are considered similar to the type material, but with a degree of uncertainty that caused us to assign them to *Camelus* cf. *roris*. This material includes two maxillae with little worn dentition and different M2 proportions (Nad-1 A16-35 and Nad-1 A16-37, both Dol.3), which may be included in intraspecific variation, a mandibula (Nad-1

H13-703, layer 8a) which differs in the tall corpus at the level of m3, and several isolated anterior (caniniform) teeth that are not diagnostic. There is no reason to review the identification of this material yet.

The tibiae in Nadaouiyeh were considered too poorly preserved for reliable description. However, at least one specimen (Nad-1 D17-105, layer 5-90) shows a small dorsolateral prominence, which is a state opposite to what is found in *C. concordiae*. Having excluded the only known alternative species, it seems reasonable to refer all tibiae to *Camelus* cf. *roris*.

Camelus cf. *roris / concordiae*

The reworked sediments called "Black Hummalian" (referring to the industry included) have yielded six small specimens, which show some differences with the rest of the assemblage. However, they look similar to the partially coeval remains in the Hummalian and Yabroudian levels of Hummal, which also tend to be rather small. The latter are considered to represent a mix of two forms similar to *C. roris* and *C. concordiae*, respectively (this study), and we regard the "Black Hummal" sample with the same uncertainty.

Two specimens of scapula show deep morphological differences, including a different degree of thickness. They clearly belong to separate *Camelus* forms; considering the known species, the rather massive Nad-1 E15-71 might better correspond to *Camelus* cf. *roris* while the thinner Nad-1 H14-755 might tentatively be referred to *Camelus* cf. *concordiae*.

Camelus sp.

The small fragment of mandible Nad-1 F16-1282 was excluded from *C. roris* on the ground of small m1 and narrow corpus. The m1 might fit in the variation of *C. concordiae*, but the roots of p4 are larger than in this species, which also has a rather wide corpus. However, the "small" specimen Hu G23-1 from the Yabroudian levels of Hummal has a narrow corpus as well. It is not impossibile that Nad-1 F16-1282 belongs to *C. concordiae* like Hu G23-1, but it is not likely either. Hence, we do not refer this specimen to any known species.

Remaining elements insufficiently known include the fibula and two proximal phalanges.

4. Upper Hummal I (Yabroudian and Hummalian assemblages)

Camelus cf. *roris / concordiae*

Two small fragments of mandibular corpus (layer 11) have been studied directly (Fig. 3). Both are highly damaged. Hu G34-1 is a left mandibular corpus preserving m2 and fragments of roots of m1. The body is low and thin. The caudal mental foramen is not present, while the channel for the rostral foramen is visible; therefore, the caudal foramen might have been absent or caudal to m2. The m2 is broken, but it is clearly not very worn, suggesting a younger ager. This tooth is shorter than in *C. roris*, and for its length it is narrower than *C. dromedarius*, *C. thomasi* and *C. bactrianus*; however, its size corresponds to a young adult individual of *C. concordiae*. Hu G34-16 is a right mandibular ramus found close to Hu G34-1 (both layer 11), including roots of m1 mesial, p4 and a part of the corpus rostral to it. The remains of p4 suggest a small tooth. The corpus is pachyostotic: it seems comparable to *C. thomasi* or *C. roris* and is easily more massive than *C. bactrianus, C. dromedarius* and *C. concordiae*. Compared to Hu G34-1, it is almost twice as wide at the same level of m1 mesial (Fig. 3).

Two additional mandibles (Hu E-6114 and Hu E-6115; both layer 8a) are known through some measurements of the vertical ramus only (Fig. 7a). They appear to have a similar size as *C. dromedarius* and *C. cf. roris*, being larger than *C. concordiae*. They both have a complete dentition, which is similar to each other and to the fragmentary mandibles Hu E-9045 (layer 10c) and Hu G34-1 (aforementioned, layer 11): p4 is small and short, comparable to *C. concordiae* or to small *C. dromedarius*, but smaller than *C. bactrianus* and *C. roris* (Fig. 8a). The m1 has small to average size; it overlaps with the smallest *C. bactrianus, C. dromedarius* and *C. concordiae*. The m2 fits within the size distribution of *C. concordiae*, is slightly narrower than in *C. dromedarius*, significantly narrower than *C. bactrianus* and *C. thomasi*, and significantly shorter than *C. roris*(Fig. 8b, 8c). The m3 fits with large *C. concordiae*, is slightly wider than small *C. dromedarius*, is shorter than *C. bactrianus* and is comparable to *C. roris* and *C. thomasi* (Fig. 8d)

No superior dentition is available; an isolated m2 and an isolated m3 are available from the Hummalian sands. The m2 (Hu D29-2) is rather long and wide; it is intermediate between *C. dromedarius, C. bactrianus*, and *C. thomasi*; it is slightly wider, but compatible with *C. roris* and could even fit within the variation of the Oldowan assemblage. However, it is clearly different from *C. concordiae* and the previously mentioned specimens, all belonging to the Yabroudian

assemblage (Fig. 8b). The m3 (Hu D29-x1) is narrow and not very long; it is shorter than *C. bactrianus* and overlaps in length with *C. roris*, *C. thomasi*, large *C. concordiae*, small *C. dromedarius* and the Yabroudian assemblage. However, it is clearly narrower than *C. thomasi* and large *C. concordiae*, and somewhat narrower than the other forms as well (Fig. 8d).

All the long bones, metatarsals and phalanges of both Yabroudian and Hummalian assemblages are either smaller or very close to the average in extant *Camelus*. There are only non-informative fragments of scapula and humerus, and no metacarpal. The distal radioulnare in the Hummalian assemblage remind of *C. roris* in the high medial dorsal ridge and reduced axial dorsal ridge. It differs from the latter in the smaller size and enlarged lateral and medial tuberosities of the distal articulation. The lateral articular facet (for the triquetrum) is narrow and deep. A distal femur is also found in the Hummalian assemblage; it has a narrow medial condyle and a protruding dorsal trochlea of intermediate width. A distal tibia (Hu B30-34, layer 11a) has a very thick diaphysis and a shallow, rather wide cochlea; all articular fossae are short (Fig. 10b, 10c, 10d). The dorsolateral prominence is quite large, intermediate between *C. concordiae* (large) and extant *Camelus* (reduced); in other fossils such as *C. thomasi* and *C. cf. roris* it is even smaller. Overall this specimen is mostly similar to *C. concordiae*, less so to *C. dromedarius* and clearly distinct from *C. cf. roris* and *C. bactrianus*. The metatarsal shows a thick diaphysis and a narrow distal bifurcation; the condyles are asymmetric, one rather wide and the other narrow. The proximal phalanx is similar to *C. dromedarius*, *C. concordiae* and the Oldowan assemblage: intermediate length, wide diaphysis and narrow condyles with long lips (Fig. 9a, 9b). The latter character differs clearly from *C. bactrianus*, *C. thomasi* and *C. roris*. Like in *C. concordiae*, the proximal articulation is rather narrow in the anterior proximal phalanx but wider in the posterior one. The intermediate phalanx has a short proximal articulation in dorsovolar direction; the condyle is narrow and deep, with lips of intermediate length, resembling *C. roris* more than extant *Camelus* species (Fig. 9c).

All carpal and tarsal bones are represented (except the medial cuneiforme). The carpalia, fibula and astragalus are smaller than the average of extant species, the pisiforme is large, and the other tarsalia are close and sometimes above the average, but never large.

The scaphoideum is small; the proximal facet is dorsally wide and palmarly narrow, the distal aspect is deep, the distopalmar facet is narrow and the laterodistal facet is large; the latter two traits are diagnostic for *C. roris* (Fig. 11c), but it differs from this species in the variable dorsal height. The lunatum has a long proximal facet, like *C. roris* and the Oldowan assemblage; it is always longer and on average narrower than *C. bactrianus* and *C. dromedarius*. The triquetrum has a deep

proximal facet (Fig. 11d) and a deep, narrow distal facet, similar to *C. roris* and unlike extant species; it is neither similar nor clearly different from *C. concordiae*. The pisiforme has a short, rounded tuber and a wide articular facet (Fig. 12a); both traits are like in *C. dromedarius* and *C. concordiae*, but they differ strongly from *C. bactrianus*. The trapezoideum is deep, with a rather narrow distal facet (Fig. 12b); it resembles *C. concordiae, C. roris* and the Oldowan assemblage more than *C. thomasi* or the extant species. The capitatum is dorsally rather tall, differing from *C. bactrianus* and the Oldowan assemblage, but otherwise not distinctive. The palmar region of the hamatum is slightly lower than in *C. dromedarius* and *C. concordiae*, although not as low as in *C. moreli* (Fig. 12c). The proximal facet is narrow. One specimen (Hu B30-21.2, layer 11) is overall deep. This element is most similar to *C. roris*, but is not incompatible with *C. bactrianus* or *C. concordiae*.

The fibula has a narrow proximal and a wide distal facet; surprisingly, the greatest similarity is with *C. moreli*, and some resemblance is found with *C. bactrianus* and an unassigned specimen from Nadaouiyeh. The astragalus is present with two forms: they share a wide calcaneal surface (wider than in *C. roris* and *C. thomasi*) (Fig. 13a), and a thin distal trochlea (overlapping with the thinner *C. dromedarius* and Oldowan complex, but thinner than in *C. bactrianus* and *C. roris*). The astragalus Hu A28-2 (Hummalian sands) further has average size, overall elongated shape and narrow distal trochlea (Fig. 13a, 13b); its proportions do not allow assigning it to any named species, although some resemblance can be found with the Oldowan assemblage. The other specimens are small and are characterized by a long lateral and short medial lip of the proximal trochlea, like in *C. dromedarius* or *C. roris* but unlike *C. bactrianus*, and a wide distal trochlea (Fig. 13a, 13b); this group is overall similar to *C. dromedarius* and *C. sp.* from the Mousterian assemblage. The calcaneus is shorter than in *C. roris*, the Oldowan assemblage and most *C. dromedarius*; it is as short as *C. concordiae* and within the variation of *C. bactrianus* (Fig. 14a). The tuber is transversally wide, but sagittally short. The sustentaculum has a very plantar position, differing from *C. bactrianus* and *C. thomasi*. The fibular trochlea is placed lower than in *C. dromedarius* and *C. roris*, and less prominent than in *C. bactrianus* and the Oldowan assemblage; it is similar to *C. thomasi*. The plantar border is wide, unlike in *C. bactrianus* (Fig. 14a), and the distal facet has an average shape. The overall proportions are closer to *C. dromedarius*, *C. roris* or *C. concordiae* althought they are not identical to any of them. The cuboideum is similar to *C. dromedarius, C. roris, C. concordiae* and the Oldowan assemblage in the low dorsal height and wide dorsoproximal facet (for the astragalus); it is unlike *C. bactrianus, C. thomasi* and *C. moreli* (Fig. 14b). The naviculare is the lowest in the sample, showing the greatest difference from *C.*

bactrianus, C. roris and the Oldowan assemblage. It is also wider than *C. dromedarius* and *C. moreli*, deeper than *C. bactrianus* and *C. roris*, and both wider and deeper than the Oldowan assemblage. It resembles *C. concordiae* the most (Fig. 14c, 14d). The intermediolateral cuneiforme is unremarkable.

5. Upper Hummal II (Mousterian industry)

The camelid remains from the Mousterian layers of Hummal have been described in a previous report (Martini et al. in preparation-b). Most but not all specimens could be assigned to either *C. concordiae* or to *C. moreli*, both first described in this complex. We discuss the remaining sample in light of the new discoveries, especially in Yabroudian and Hummalian layers.

Camelus concordiae

This species is known through a good sample of mandibles, some maxillae, additional dentition and several postcranial elements, although less than for *C. roris*. Its main characters are the smallest craniodental size among known *Camelus* species, narrow m2, and palatine foramina at the level of P4; among the postcranial characters we mention the large dorsolateral prominence of the distal tibia. It is mostly similar to *C. dromedarius*, but differs in several diagnostic traits.

Camelus moreli

This giant Late Pleistocene camel is represented by scarce mandibular and postcranial material, but the known elements show a unique morphology, in addition to the remarkable size. It is defined by pachyostotic mandible with short, symphysis turned upwards and advanced position of p1; the most typical postcranial elements are the distal tibia with large dorsolateral prominence, the low and broad hamatum, and narrow but plantarly tall naviculare. It is as large as *Camelus knoblochi* and *Paracamelus gigas*, the largest known Eurasian camelids, but the former shows reduced p4-m1 and enlarged m3, while the latter retains p3 and has an elongated rostrum. The large form present in Aïn al Fil is also in the same size group, but has a radically distinct configuration of the distal tibia.

Camelus sp.

Several specimens with poor preservation or lack of diagnostic characters could not be referred with certainty to either known species; they were in part assigned to *C.* cf. *concordiae* or *C.* cf. *moreli* based on their smaller, respectively larger size.

The distal tibia Hu S-12442 (layer 5b3) was excluded from both species because of its small dorsolateral prominence, deep lateral fossa and short central fossa (Fig. 10b, 10c, 10d). In fact, its shape is identical to the extant *C. bactrianus*, which thus far is unknown as a fossil in El Kowm. The distal tibia of *C. roris* is known only by some poorly preserved and tentatively assigned specimens, hence this species cannot be excluded either. Until stronger evidence of *C. bactrianus* is found, we refrain to assign a single postcranial fragment to this extant species, hence we leave the identification of Hu S-12442 open.

Two astragali, with different morphology, could not be assigned to either species (Fig. 13a, 13b). The Hummalian and Yabroudian assemblages also have evidence of two different forms of astragalus, but they do not correspond to the Mousterian forms. The distinctions from each other are clear but not huge, and we suspect that further finds might bridge the gaps and indicate that they all belong within the variation of a single species. Presently, they are considered *Camelus sp*.

Discussion

1. Aïn al Fil

The three large specimens in Aïn al Fil testify to the presence of a large camel that cannot be compared to any other species known by the same elements (tibia, hamatum, scaphoideum); a fourth specimen, another scaphoideum, has a smaller size and a radically different morphology. Their respective proportions are sometimes at the opposite limits of variation in the total comparative sample, which include several species and dozens of individuals. It is strongly implied that they can neither be included in the same species, nor in any other known. They in particular differ from *C. thomasi* and all other fossils from El Kowm. The large species shows the least differences with the Oldowan assemblage of Hummal, which is also the temporally closest form. The Aïn al Fil fossils are larger and morphologically quite distinct, hence we considered them different; but this species might be closely related, or even ancestral to the Oldowan form.

Size and slenderness of the tibia are reminiscent of the large *Paracamelus* species, such as *P. gigas*; the pictures and measurements given by Zdansky (Zdansky 1926) indicate that the latter was

shorter with a wider proximal epiphysis, deeper lateral condyle, deeper distal cochlea with especially large lateral fossa, almost as long as the medial one. *P. alexejevi* (Havesson 1954) is significantly smaller than the camel in Aïn al Fil, has relatively deeper diaphysis, and the medial fossa of the cochlea is not enlarged. *P. aguirrei* is intermediate between these two forms (Morales 1984), but its tibia is not known. Other *Paracamelus* species are smaller. The largest *Camelus* species are *C. moreli*, which has cochlea with similar size but totally different conformation, and *C. knoblochi* whose tibia is much shorter but has similar-sized epiphysis, indicating greater robustness (Havesson 1954). Apparently, the Aïn al Fil tibia is longer than any known Old World camelid. Only large *P. gigas* would approach its length, but the morphological differences are clear.

As no craniodental material is known, and the available elements are poorly known in other species, we refrain from naming new species. Moreover, all specimens are housed at Tell Arida, which means they are currently unavailable and possibly lost, and no photographs or casts exist; a holotype defined under this situation would be very problematic. The lack of craniomandibular material prevents discriminating between *Paracamelus* and *Camelus*. Nevertheless, the data we report show beyond doubt that during the Olduvai chron (1.8 Ma), a large and a small species of camelids lived in the El Kowm Basin, but by the terminal Early Pleistocene both were replaced by an intermediate-sized form, recorded in the Oldowan assemblage of Hummal.

2. Lower Hummal (Oldowan assemblage)

The two described mandibles appear to differ: Hu E-9242 (layer 16) is massive while Hu K33-381 (layer 18) is not. However, both specimens are quite damaged and the difference is not conclusive. The former specimen preserves enough morphology of the ramus to show substantial differences with *C. thomasi*, *C. cf. roris*, *C. concordiae* and extant species.

The dentition shows a mix of size and proportions; in particular, upper P4 and M3 are very small, while lower p4 and m3 are very large. However, most specimens are stratigraphically close to each other (layers 17c and 18), and the sample size is very small; it is possible that both upper teeth come from smaller individuals than those represented by lower teeth. Two specimens of m2 are close in age, but differ greatly in width (Fig. 8b). In most species (*C. bactrianus, C. dromedarius, C.thomasi, C. concordiae*), this tooth shows a regular but small degree of widening with progressive wear. However, in *C. roris* the degree of widening is greater, indicating than the basis of m2 is wider, compared to the tip, than in other species (Fig. 8c). The large difference in width in the two Oldowan specimens is compatible with a similar tooth shape as in *C. roris*, hence they might belong to a single species. The partial mandible Hu K33-381 (layer 18) bears an m2

which is comparable to worn m2 in *C. thomasi*, and an m3 which is significantly larger than in that species. This dentition is more similar to *C. bactrianus* and *C. sivalensis*; but the two upper teeth from the same complex are much smaller than either.

In summary, the mandibular and dental specimens in the Oldowan assemblage might contain either one variable species, or more than one; both interpretations are possible. The two most complete specimens differ from *C. thomasi*, and the assemblage as a whole differs from all other known camels (including later species in El Kowm). Unfortunately, the sample is small and poorly preserved, so that definite conclusions are difficult and definition of a new species is not warranted.

The single specimen of atlas has a small cranial region, but a large caudal region. It suggests a species with a small head but a strong neck, and by extension a large body.

The distal tibia has similarities to *C. thomasi* and especially *C. concordiae*, but is radically different from the Aïn al Fil specimen, proving that no continuity exists between the two.

Several carpal and tarsal bones show some morphometrical features which are characteristic for the whole assemblage, and are diagnostic in comparison to *C. bactrianus* (scaphoideum, lunatum, hamatum, calcaneus, cuboideum, naviculare), *C. dromedarius* (lunatum, pisiforme, calcaneus, naviculare), *C. roris* (scaphoideum, lunatum, calcaneus, naviculare), *C. thomasi* (calcaneus, naviculare), *C. moreli* (cuboideum), *C. concordiae* and the Yabroudian assemblage (naviculare). The calcaneus is the most homogeneous element in the assemblage; several specimens, from layers 15 to 18, share a large number of characters which together are unique. On the other hand, it is difficult to include both specimen of cuboideum within the same species.

The metacarpal is as long and slender as in *C. thomasi*, and is significantly longer than in extant species. The proximal phalanges are relatively short, while many of the intermediate phalanges are long; however, there is too much variation in this result to confidently draw any conclusions. Other characters of the phalanges help separate this form from other known *Camelus* species.

In general, remains from the Oldowan layers show a remarkable variation in proportions. This might suggest a mix of more than one species. However, the variation is not larger than in extant camel samples (although it is larger than in other fossil assemblages); there is no apparent bimodal distribution, other consistent internal separation or differences between parts of the section; and some morphological traits valid for the entire sample can be recognized. Additionally, several elements differ from all known species of *Camelus*, including others present in El Kowm.

Therefore, we tentatively include the whole Oldowan assemblage within a single species that we informally indicate as *Camelus sp. "Oldowan".*

3. Nadaouiyeh Aïn Askar

In light of the presence of *C.* cf. *concordiae* in upper Middle Pleistocene sediments of Hummal, we reinterpreted some specimens of dubious attribution from Nadaouiyeh. The specimens of tibia and the massive scapula Nad-1 E15-71 (layer 7) can be referred to *C.* cf. *roris*, while the second scapula Nad-1 H14-755 (layer 8.1b), more gracile and with a different morphology, is referred to *C.* cf. *concordiae*. The small assemblage from the "Black Hummalian" layers is similar to the almost coeval Yabroudian and Hummalian levels of Hummal, and is likewise assigned to *Camelus* cf. *roris / concordiae*.

The original conclusions can be confirmed: while *Camelus roris* was by far the most abundant species in the Middle Pleistocene of Nadaouiyeh, a second species was occasionally present and can now be identified as *Camelus* cf. *concordiae*.

4. Upper Hummal I (Yabroudian and Hummalian assemblages)

The two fragmentary mandibles from layer 11, Hu G34-1 and Hu G34-16, indicate that two different camel species coexisted in this section. The former is smaller and similar to *Camelus concordiae*, although it appears to be slightly different: the corpus is thin and the caudal mental foramen has a more caudal placement than known in *C. concordiae*. The second specimen is massive like in *C. roris* and *C. thomasi*; the latter species is older and otherwise unknown in El Kowm. *Camelus roris* is a better fit, but seems to differ by having a large p4; however, this tooth is damaged in Hu G34-16 and does not prevent inclusion in the same species.

Other remains from Yabroudian layers have dentition whose measurements fit perfectly with *C. concordiae*; however, the mandibles are larger than in this species, preventing a conclusive determination. On the other hand, isolated dentition from the Hummalian sands differs from *C. concordiae* and the Yabroudian dentition, while identification with *C. roris* is possible.

The mandible Hu E31-C01 has been found in sands reported to contain both Mousterian and Hummalian artifacts. As it is completely similar to the holotype and the rest of the assemblage of *C. concordiae*, we included it in the type assemblage of this species and suggested that the specimen originated from a Mousterian horizon. However, there is now evidence of a form similar to this

species in more ancient layer; therefore, the *C. concordiae* specimen Hu E31-C01 might indeed have the same age as the Hummalian industry.

The postcranium is equally ambiguous. The largest part of the sample shows reduced size compared to the average in *C. dromedarius* and *C. bactrianus*, which hints to the presence of the small *C. concordiae*. Morphologically, most elements are similar or identical to *C. concordiae* (pisiforme, tibia, astragalus, naviculare, proximal phalanx), *C. roris* (radioulnare, lunatum, intermediate phalanx), or both (scaphoideum, trapezoideum, calcaneus, cuboideum, triquetrum, hamatum). One astragalus (Hu A28-2, Hummalian sands) does not resemble any other form. No other specimen can clearly be separated from *C. concordiae*, while the naviculare and the proximal phalanx differ from *C. roris*. Unlike for the mandibular and dental material, there is no indication that two species coexisted (except for the mentioned astragalus).

The largest part of the postcranial material originates from the Yabroudian cultural levels; the few elements that are found both in Hummalian and Yabroudian layers are similar to each other, except for the unidentified astragalus Hu A28-2 (Hummalian sands), which differs from the Yabroudian sample as well as from all other species. Material from the "Acheuleo-Tayacien" layer 13 (older than the Yabroudian layers) is very scarce; only the lunatum and the hamatum are represented by informative specimens, and both are similar to the Yabroudian assemblage or to *Camelus roris*.

In conclusion, the material from the late Middle Pleistocene layers in Hummal ("Acheuleo-Tayacien", Yabroudian and Hummalian) cannot be convincingly assigned to one species. Mandibular and dental remains show that in this period of time two distinct forms, similar but not identical to the type assemblages of *C. roris*, respectively *C. concordiae*, frequented the region of El Kowm. They might have coexisted or alternated with each other repeatedly over time, as dentition similar to *C. roris* is found in the Hummalian layers, younger than dentition similar to *C. concordiae* from the Yabroudian layers but older than the type assemblage of the latter in Mousterian layers. Postcranial fossils are similar to either *C. roris*, or *C. concordiae*, or (in many cases) both of them; they suggest mixing of these two species, or a descent of the latter species from the former. However, dental characters do not suggest an especially close relationship between them.

5. Upper Hummal II (Mousterian assemblage)

The new observations on the complete Hummal sequence do not offer new insight on the Mousterian remains; most unidentified elements are too fragmentary. The distal tibia Hu S-12442 (layer 5b3) and the astragali Hu SM-18 (Mousterian sands) and Hu ZZ33-8 (layer 5b1) cannot be referred to *C. moreli*, *C. concordiae*, nor to *C. roris* and further finds are needed to elucidate their systematic position.

Conclusions

The El Kowm Basin contains fossiliferous sediments spanning the last 1.8 Ma (Fig. 15). We studied the Camelidae remains from three sites in the basin: Aïn al Fil, Hummal and Nadaouiyeh and demonstrate the presence of at least six species, of which three (*Camelus roris, C. concordiae,* and *C. moreli*) were named in previous articles (Martini et al. in preparation-a; Martini et al. in preparation-b).

The Early Pleistocene is less intensely sampled: we detected the presence of two species of different sizes at Aïn al Fil (1.8 Ma), and at least another distinct species in the lower section of Hummal (0.8-1.2 Ma). Unfortunately, these assemblages consist of scarce material without well-preserved cranial remains; therefore, we did not define any new species. The late Early Pleistocene African species *Camelus thomasi* is not recorded in El Kowm.

The Middle Pleistocene is represented at Nadaouiyeh and in the upper section of Hummal, and is further subdivided into several archaeological complexes. Unit F (layer 13) of Hummal and the base of Unit F in Nadaouiyeh might represent the earlier part of the Middle Pleistocene, but both are poor in fossils. The main sequence of Nadaouiyeh (units B to E) is bracketed between 0.55 Ma and 0.35 Ma, in the central part of the Middle Pleistocene. In this sequence the species *Camelus roris* is dominant. Unit A/B ("Doline 3") is included between 0.35 Ma and 0.2 Ma but contains *C. roris* as well; therefore, the age of this material is likely closer to the lower boundary of the time span. Rare finds in Nadaouiyeh that cannot be assigned to *C. roris* might represent the oldest *Camelus* cf. *concordiae*. The late Middle Pleistocene is best known in Hummal, subdivided in Unit E and Unit D which archaeologically correspond to the Yabroudian industry (~0.3 Ma) and Hummalian industry (~0.2 Ma). In Nadaouiyeh, few fossils are known from the "Black Hummalian" sands and from Unit A (~0.15 Ma). These camelid assemblages are not homogeneous and cannot be subdivided between different complexes; the cranial material indicates the presence

of two separate species which we propose to identify as *Camelus* cf. *roris* and *Camelus* cf. *concordiae*.

The Late Pleistocene corresponds to Unit C of Hummal (layer 5), also known as the Mousterian complex. Here we record the presence of two species of different sizes, as is the case in the much older Aïn al Fil site, and likely in the late Middle Pleistocene Yabroudian and Hummalian assemblages. Unlike the latter, the Mousterian complex has yielded abundant cranial and postcranial material of both species that were described as *Camelus moreli* and *Camelus concordiae*. The former is a giant species, while the latter is smaller than extant dromedaries. Both have been mentioned before in the Levant, but were not recognized as new species.

Our identifications suggest that *Camelus roris* was present in El Kowm over most of the Middle Pleistocene; it was by far the dominant species in the middle Middle Pleistocene, while later it coexisted with *Camelus concordiae*. The latter might have appeared earlier as well. At the transition between Middle and Late Pleistocene, *Camelus roris* seems to disappear and be replaced by the giant *Camelus moreli*, while *Camelus concordiae* becomes the most abundant species in El Kowm and possibly in the entire Levant (Martini et al. in preparation-b). However, this situation did not last long; both species went extinct before the end of the Late Pleistocene, as no camel remains are known in the well-known Natufian archaeological context (Grigson 1983; Payne and Garrard 1983).

The Late Pleistocene also saw the disappearance of African camelids, as well as the giant Siberian species *Camelus knoblochi*. Apparently, *C. knoblochi* and the Levantine camels were not adapted to extreme desert climate, but rather to steppe-like environment (Payne and Garrard 1983; Titov 2008). In this, they differ from the species that survived into the Holocene: the dromedary *C. dromedarius*, which was domesticated in south-western Arabia, the Bactrian camel *C. bactrianus*, probably domesticated in eastern Central Asia, and the Mongolian wild camel *C. ferus*, which is genetically distinct from the other two species (Burger 2016). Therefore, steppe camels can be included into the Late Pleistocene mass extinction of large mammals, which is widely considered to include human hunting among its main factors (Koch and Barnosky 2006). Species with slow reproduction and species in easily accessible habitats were at a higher risk of extinction (Johnson 2002). In fact, extant *Camelus bactrianus* and *C. dromedarius* have slow life history traits (Nowak 1999) (Faye et al. 2004; Peters and Driesch 1997) which could have made them vulnerable, but their adaptation to extremely inhospitable desert might have protected both their population until they were domesticated; ironically, only domestication of camels allowed the colonization of

deserts (Peters and Driesch 1997) and possibly led to the demise of their wild relatives, with exception of the endangered Mongolian camel. On the other hand, steppe camels were likely more exposed to human hunting, which is attested in the El Kowm basin itself (Reynaud Savioz 2011), and probably had a similarly slow life history. It is tempting to suggest that hunting pressure might have led to the extinction of camel species such as *C. concordiae, C. moreli* and *C. knoblochi*, in the Levant and elsewhere.

Acknowledgements

We thank Chloé Lecompte for sharing measurements on the Tell Arida fossils, Bastien Mennecart for fruitful discussions, Denis Geraads for access to the Tighennif collection and for providing Soviet literature and Inna Popko for help with Russian and Ukrainian translation. The Syro-Swiss research in El Kowm would not have been possible without the logistic support of the Tell Arida staff, led by Ahmed Taha, and all the participants to the excavations.

This study is part of P. Martini's doctoral thesis, which is supported by the Swiss National Science Foundation, the Isaac Dreyfus-Bernheim Stiftung, and the Freiwillige Akademische Gesellschaft Basel. These institutions and the Tell Arida Foundation have also funded excavations in El Kowm.

References

ALÇIÇEK, M. C., S. MAYDA, and V. V. TITOV. 2013. Lower Pleistocene stratigraphy of the Burdur Basin of SW Anatolia. Comptes Rendus Palevol 12:1-11.

BAR-YOSEF, O., and M. BELMAKER. 2011. Early and Middle Pleistocene Faunal and hominins dispersals through Southwestern Asia. Quaternary Science Reviews 30:1318-1337.

BURGER, P. A. 2016. The history of Old World camelids in the light of molecular genetics. Tropical animal health and production.

COLBERT, E. H. 1935. Siwalik Mammals in the American Museum of Natural History. Transactions of the American Philosophical Society, New Series 26:1-401.

COLOMBERO, S., et al. 2014. The upper Messinian assemblages of fossil vertebrate remains of Verduno (NW Italy): Another brick for a latest Miocene bridge across the Mediterranean. Neues Jahrbuch für Geologie und Paläontologie - Abhandlungen 272:287-324.

FALCONER, H., and C. MURCHISON. 1868. Palæontological memoirs and notes of the late Hugh Falconer: With a biographical sketch of the author. R. Hardwicke.

FAYE, B., S. GRECH, and T. KORCHANI. 2004. Le dromadaire, entre féralisation et intensification. Anthropozoologica 39:7-14.

GENTRY, A. W., and A. GENTRY. 1969. Fossil Camels in Kenya and Tanzania. Nature 222.

GERAADS, D. 2014. *Camelus grattardi*, sp. nov., a new camel from the Shungura Formation, Omo Valley, Ethiopia, and the relationships of African fossil Camelidae (Mammalia). Journal of Vertebrate Paleontology 34:1481-1485.

GRATTARD, J.-L., F. C. HOWELL, and Y. COPPENS. 1976. Remains of *Camelus* from the Shungura Formation, lower Omo Valley. Pp. 268–274 in Earliest Man and Environments in the Lake Rudolf Basin. (Y. Coppens, F. C. Howell, G. L. Isaac and R. E. Leakey, eds.). University of Chicago Press, Chicago.

GRIGSON, C. 1983. A very large camel from the upper Pleistocene of the Negev Desert. Journal of Archaeological Science 10:311-316.

HARRIS, J. M. 1987. Fossil Giraffidae and Camelidae from Laetoli. Pp. 358-377 in Laetoli, a Pliocene site in northern Tanzania (M. D. Leakey and J. M. Harris, eds.). Clarendon Press, Oxford.

HARRIS, J. M., D. GERAADS, and N. SOLOUNIAS. 2010. Camelidae. Pp. 815-820 in Cenozoic Mammals of Africa (L. Werdelin and W. J. Sanders, eds.). University of California Press, London.

HAUCK, T. C. 2011. Mousterian technology and settlement dynamics in the site of Hummal (Syria). Journal of Human Evolution 61:519-37.

HAVESSON, Y. I. 1954. Третичные Верблюды Восточного Полушария (Род *Paracamelus*) [Tertiary camels from the Eastern Hemisphere (Genus *Paracamelus*)]. Trudy Paleontologicheskovo Instituta, Akademiya Nauk SSSR 47:100-162.

HONEY, J. J., J. A. HARRISON, D. R. PROTHERO, and M. S. STEVENS. 1998. Camelidae. Pp. 439-462 in Evolution of Tertiary Mammals of North America: Terrestrial Carnivores, Ungulates, and Ungulatelike Mammals (C. M. Janis, K. Scott and L. L. Jacobs, eds.). Cambridge University Press, Cambridge.

HOWELL, F. C., L. S. FICHTER, and R. WOLFF. 1969. Fossil Camels in the Omo Beds, Southern Ethiopia. Nature 223:150-152.

JAGHER, R. 2011. Nadaouiyeh Aïn Askar - Acheulean variability in the Central Syrian Desertin The Lower and Middle Palaeolithc in the Middle East and Neighbouring Regions (J. M. Le Tensorer, R. Jagher and M. Otte, eds.). Etudes et Recherches Archéologiques de l'Université de Liège (ERAUL), Liège.

JAGHER, R. 2016. Nadaouiyeh Aïn Askar, an example of Upper Acheulean variability in the Levant. Quaternary International 411:44-58.

JAGHER, R., H. EL SUEDE, and J. M. LE TENSORER. 2015. El Kowm Oasis, human settlement in the Syrian Desert during the Pleistocene. L'Anthropologie 119:542-580.

JAGHER, R., and J.-M. LE TENSORER. 2011. El Kowm, a key area for the palaeolithic of the Levant in Central Syriain The Lower and Middle Palaeolithc in the Middle East and Neighbouring Regions (J. M. Le Tensorer, R. Jagher and M. Otte, eds.). Etudes et Recherches Archéologiques de l'Université de Liège (ERAUL), Liège.

JOHNSON, C. N. 2002. Determinants of loss of mammal species during the Late Quaternary 'megafauna' extinctions: life history and ecology, but not body size. Proceedings. Biological sciences / The Royal Society 269:2221-7.

KOCH, P. L., and A. D. BARNOSKY. 2006. Late Quaternary Extinctions: State of the Debate. Annual Review of Ecology, Evolution, and Systematics 37:215-250.

KOSTOPOULOS, D. S., and S. SEN. 1999. Late Pliocene (Villafranchian) mammals from Sarikol Tepe, Ankara, Turkey. Mitteilungen der Bayerischen Staatssammlung für Paläontologie und Historische Geologie 39:165-202.

KOZHAMKULOVA, B. S. 1986. The Late Cenozoic Two-Humped (Bactrian) Camels of Asia. Quartärpaläontologie 6:93-97.

LE TENSORER, J.-M., V. VON FALKENSTEIN, H. LE TENSORER, and S. MUHESEN. 2011a. Hummal: A very long Paleolithic sequence in the steppe of Central Syria - Considerations on Lower Paleolithic and the beginning of Middle Paleolithicin The Lower and Middle Palaeolithc in the Middle East and Neighbouring Regions (J. M. Le Tensorer, R. Jagher and M. Otte, eds.). Etudes et Recherches Archéologiques de l'Université de Liège (ERAUL), Liège.

LE TENSORER, J.-M., V. VON FALKENSTEIN, H. LE TENSORER, P. SCHMID, and S. MUHESEN. 2011b. Étude préliminaire des industries archaïques de faciès Oldowayen du site de Hummal (El Kowm, Syrie centrale). L'Anthropologie 115:247-266.

LE TENSORER, J. M., H. LE TENSORER, P. MARTINI, V. VON FALKENSTEIN, P. SCHMID, and J. J. VILLALAIN. 2015. The Oldowan site Aïn al Fil (El Kowm, Syria) and the first humans of the Syrian Desert. L'Anthropologie 119:581-594.

MARTINI, P. 2011.A metrical analysis of the morphological variation in extant and fossil camels. Master's thesis, University of Zürich, Zürich.

MARTINI, P., L. COSTEUR, R. JAGHER, and J. M. LE TENSORER. in preparation-a. A new species from Nadaouiyeh Aïn Askar (Syria) contributes to the diversity of Pleistocene Camelidae.

MARTINI, P., L. COSTEUR, J.-M. LE TENSORER, and P. SCHMID. 2015. Pleistocene camelids from the Syrian Desert: The diversity in El Kowm. L'Anthropologie 119:687-693.

MARTINI, P., L. COSTEUR, P. SCHMID, and J. M. LE TENSORER. in preparation-b. A giant and a small camel lived side by side in the Late Pleistocene of Syria.

MARTINI, P., and D. GERAADS. 2018. *Camelus thomasi* Pomel, 1893, from the Pleistocene type-locality Tighennif (Algeria): Comparisons with modern *Camelus*. Geodiversitas 40:115-134.

MARTINI, P., P. SCHMID, and L. COSTEUR. 2017. Comparative Morphometry of Bactrian Camel and Dromedary. Journal of Mammalian Evolution.

MATTHEW, W. D. 1929. Critical Observations Upon Siwalik Mammals. Bulletin American Museum of Natural History 56:437-560.

MAUL, L. C., K. T. SMITH, G. SHENBROT, A. A. BRUCH, F. WEGMÜLLER, and J. M. LE TENSORER. 2015. Microvertebrates from unit G/layer 17 of the archaeological site of Hummal (El Kowm, Central Syria): Preliminary results. L'Anthropologie 119:676-686.

MORALES, J. 1984.Venta del Moro: su Macrofauna de Mamíferos y Biostratigrafía Continental del Mioceno Terminal Mediterráneo, Universidad Complutense de Madrid, Madrid.

MORALES, J., D. SORIA, and E. AGUIRRE. 1980. Camelido finimioceno en Venta del Moro. Primera cita para Europa Occidental. Estudios Geológicos 36:139-142.

NOWAK, R. M. 1999. Walker's Mammals of the World. The Johns Hopkins University Press, Baltimore1-1936.

PAYNE, S., and A. GARRARD. 1983. *Camelus* from the Upper Pleistocene of Mount Carmel, Israel. Journal of Archaeological Science 10.

PETERS, J., and A. V. D. DRIESCH. 1997. The two-humped camel (*Camelus bactrianus*): new light on its distribution, management and medical treatment in the past. Journal of Zoology 242:651-679.

PICKFORD, M., J. MORALES, and D. SORIA. 1995. Fossil camels from the Upper Miocene of Europe: implications for biogeography and faunal change. Geobios 28:641-650.

REYNAUD SAVIOZ, N. 2011. The faunal remains from Nadaouiyeh Aïn Askar (Syria). Preliminary indications of animal acquisition in an Acheulean site.in The Lower and Middle Palaeolithc in the Middle East and Neighbouring Regions (J. M. Le Tensorer, R. Jagher and M. Otte, eds.). Etudes et Recherches Archéologiques de l'Université de Liège (ERAUL), Liège.

RICHTER, D., T. C. HAUCK, D. WOJTCZAK, J. M. LE TENSORER, and S. MUHESEN. 2011. Chronometric age estimates for the site of Hummal (El Kowm, Syria)in The Lower and Middle Palaeolithc in the Middle East and Neighbouring Regions (J. M. Le Tensorer, R.

Jagher and M. Otte, eds.). Etudes et Recherches Archéologiques de l'Université de Liège (ERAUL), Liège.

STIMPSON, C. M., et al. 2016. Middle Pleistocene vertebrate fossils from the Nefud Desert, Saudi Arabia: Implications for biogeography and palaeoecology. Quaternary Science Reviews 143:13-36.

THOMAS, H., et al. 1998. Découverte des premières faunes pléistocènes de la pénisule Arabique dans le désert du Nafoud (Arabie Saoudite). Comptes rendus de l'Académie des Sciences de Paris 326:145-152.

TITOV, V. V. 2003. Paracamelus from the Late Pliocene of the Black Sea region. Pp. 17-24 in Advances in Vertebrate Paleontology: Hen to Panta (A. Petculescu and E. Stiuca, eds.), Bucharest.

TITOV, V. V. 2008. Habitat conditions for *Camelus knoblochi* and factors in its extinction. Quaternary International 179:120-125.

TITOV, V. V., and V. N. LOGVYNENKO. 2006. Early *Paracamelus* (Mammalia, Tylopoda) in Eastern Europe. Acta zoologica cracoviensia 49A:163-178.

VISLOBOKOVA, I. A. 2008a. Main stages in evolution of Artiodactyla communities from the Pliocene-Early Middle Pleistocene of northern Eurasia: Part 2. Paleontological Journal 42:414-424.

VISLOBOKOVA, I. A. 2008b. The major stages in the evolution of artiodactyl communities from the Pliocene-early Middle Pleistocene of northern Eurasia: Part 1. Paleontological Journal 42:297-312.

WEGMÜLLER, F. 2015. The Lower Palaeolithic assemblage of Layers 15–18 (Unit G) at Hummal. An exemplary case addressing the problems placing undated, archaic-looking stone tool assemblages in the Early and Lower Palaeolithic record by techno-typological classification. L'Anthropologie 119:595-609.

WOJTCZAK, D., and K. ISMAIL-MEYER. 2017. Palimpsests and Palaeolithic living floors around the well of Hummal (Syria). A taphonomical approach combining lithic and microstratigraphical analysis. Pp. 365-379 in Vocation préhistoire: Hommage à Jean-Marie Le Tensorer (D. Wojtczak, M. Al Najjar, R. Jagher, H. El Suede, F. Wegmüller and M. Otte, eds.), Liège.

ZDANSKY, O. 1926. *Paracamelus gigas*, Schlosser. Palaeontologia Sinica 2:1-44, 4 tables.

Figures

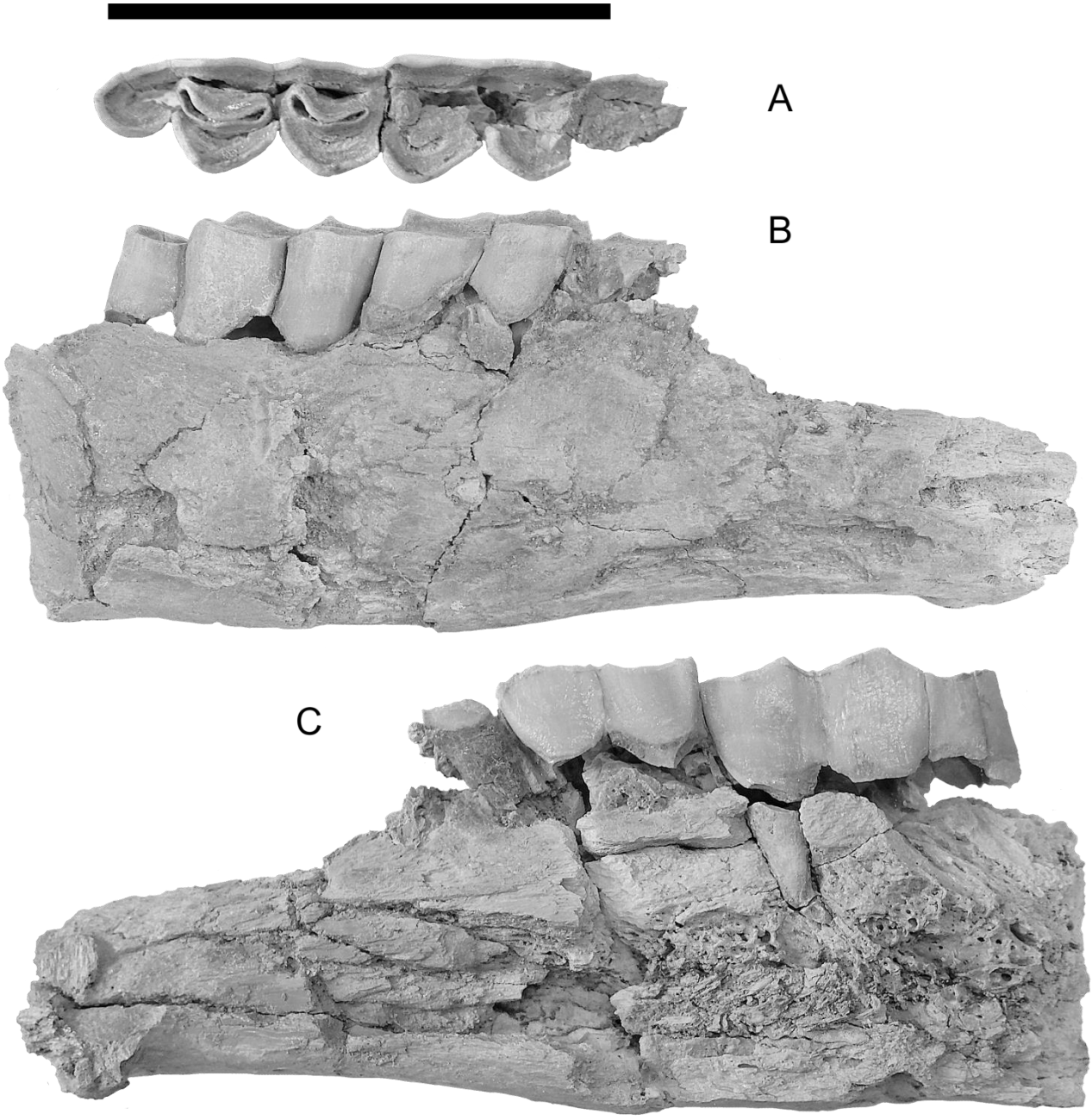

Fig. 1 Right hemimandible Hu K33-381 (*Camelus sp.*, Oldowan assemblage). **A** Occlusal view. **B** Labial view. **C** Lingual view. Scale bar equals 10 cm.

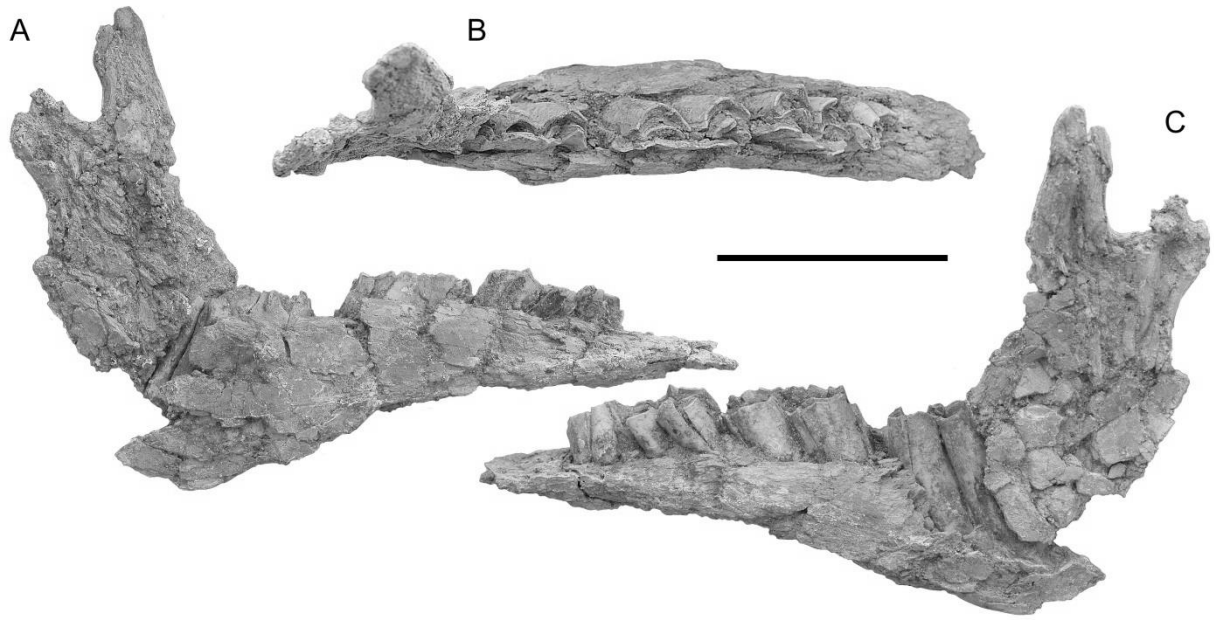

Fig. 2 Left hemimandible Hu E-9242 (*Camelus sp.*, Oldowan assemblage). **A** Lingual view. **B** occlusal view. **C** labial view. Scale bar equals 10 cm.

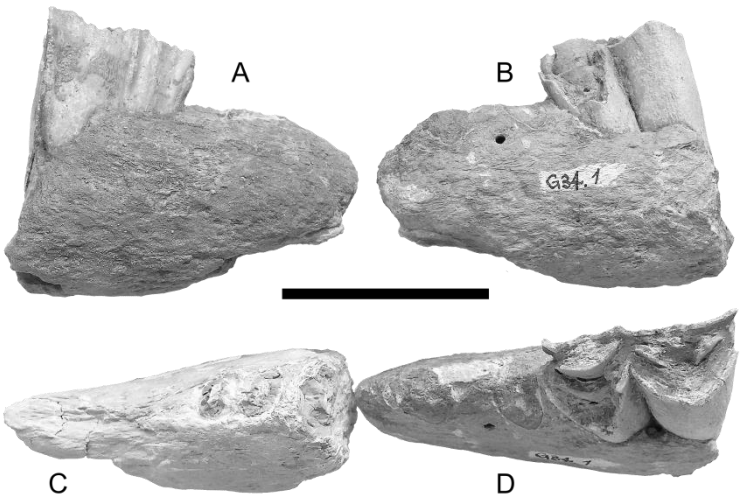

Fig. 3 Fragmentary left hemimandibles G34-1 (**A** Lingual view; **B** Labial view; **D** Occlusal view) and G34-16 (**C** Occlusal view) (both *Camelus sp.*, Yabroudian assemblage). In the lower half of the figure, **C** and **D** compare both specimens placed at their approximate position within the mandibula. Scale bar equals 5 cm.

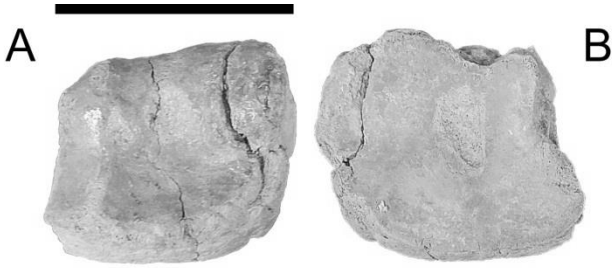

Fig. 4 Fused right capitatum and trapezoideum Hu K33-195 (*Camelus sp.*, Oldowan assemblage). **A** Proximal view. **B** Distal view. Scale bar equals 5 cm.

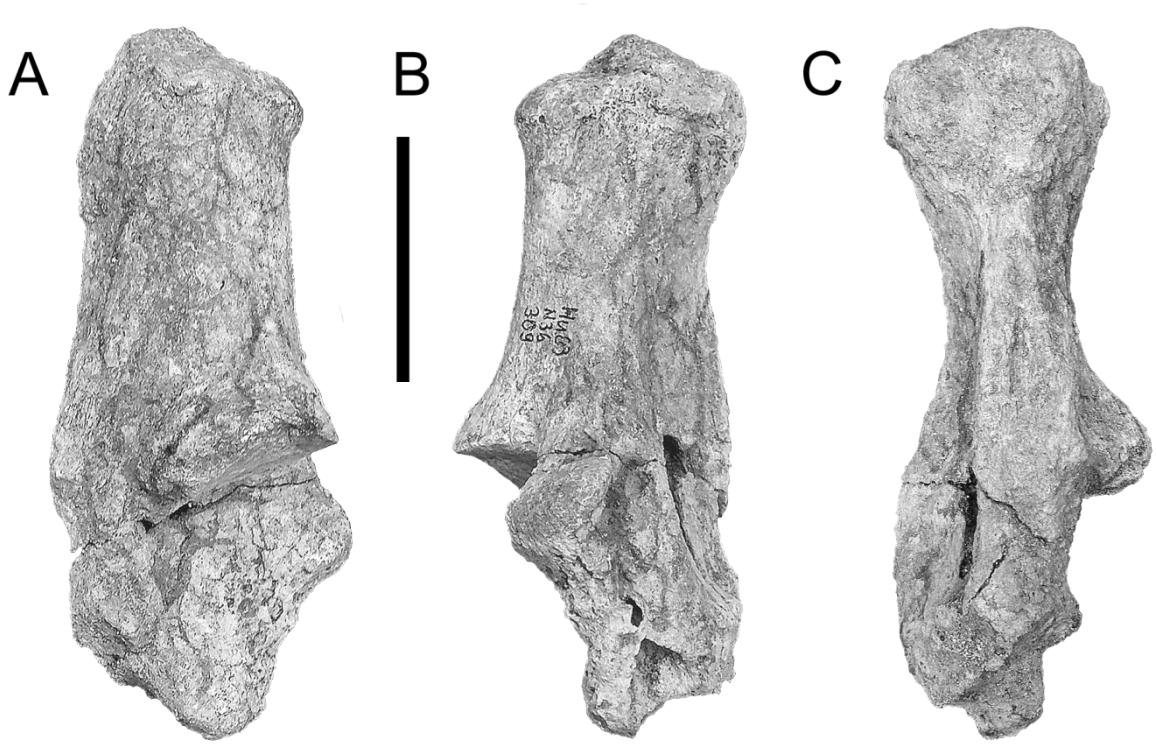

Fig. 5 Left calcaneus Hu N36-309.1 (*Camelus sp.*, Yabroudian assemblage). **A** Medial view. **B** Dorsolateral view. **C** Plantar view. Scale bar equals 5 cm.

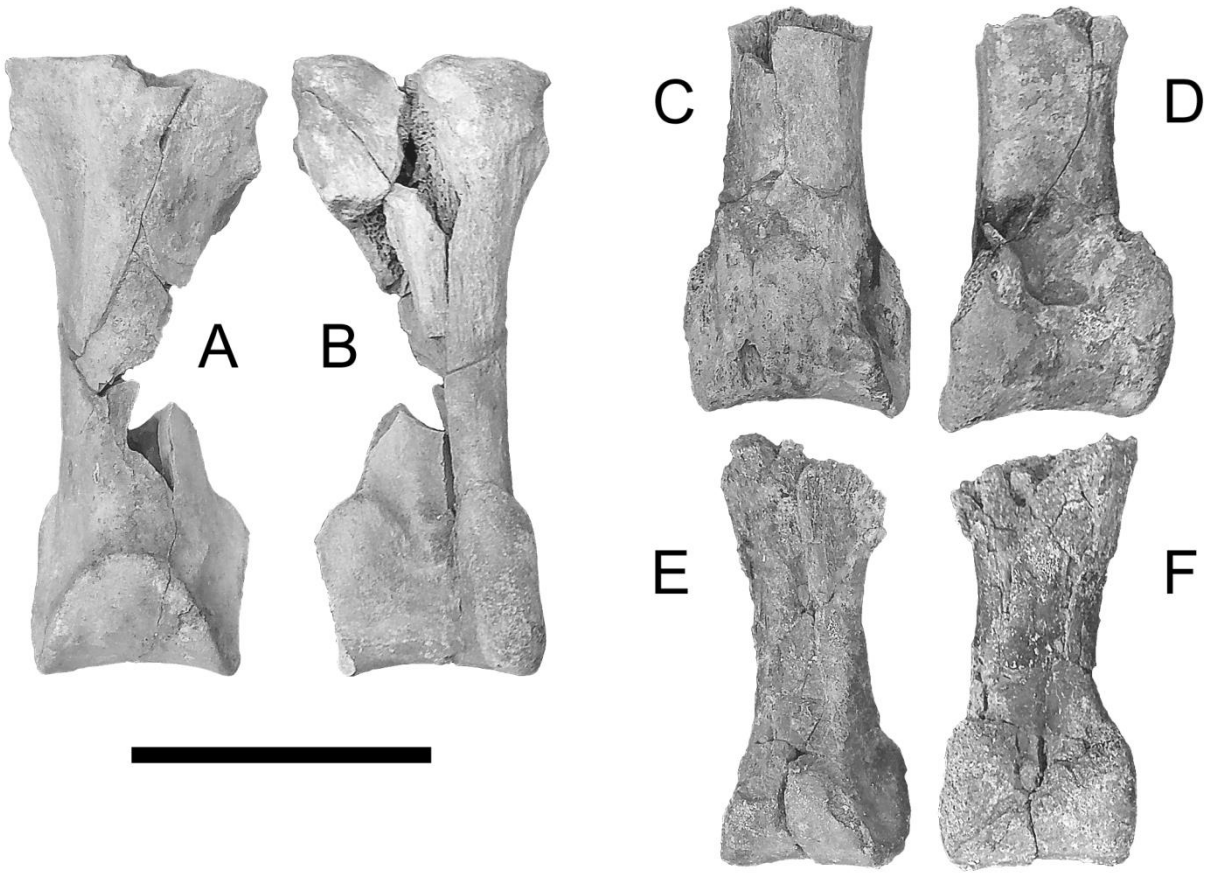

Fig 6 Proximal phalanges (*Camelus sp.*). Complete phalanx Hu 99W-100 (Yabroudian assemblage). **A** Dorsal view. **B** Palmar view. Distal fragment Hu 99W-95 (Yabroudian assemblage). **C** Dorsal view. **D** Plantar view. Distal fragment Hu E32-26 (Oldowan assemblage). **E** Dorsal view. **F** Plantar view. Scale bar equals 5 cm.

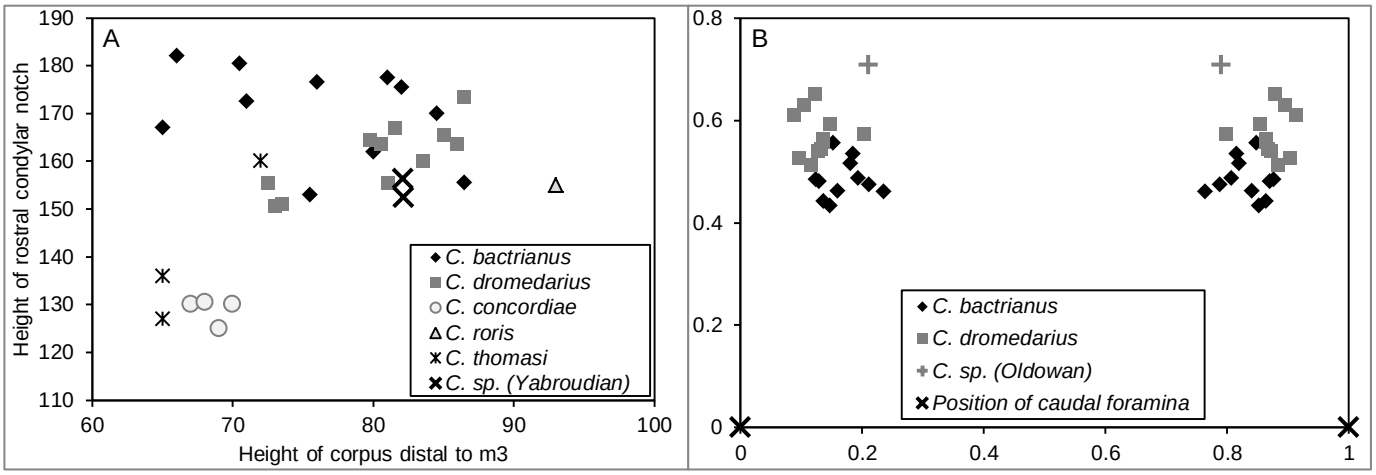

Fig. 7 Bivariate scatterplots of mandibular and vertebral measurements in *Camelus* species. **A** Height proportions of the mandibula (in mm): height of the corpus distal to m3 vs. height of the ramus at the rostral condylar notch. **B** Placement of both cranial dorsal foramina in the atlas, relatively to the standardized placement of both caudal dorsal foramina (calculated from the measured distances between foramina

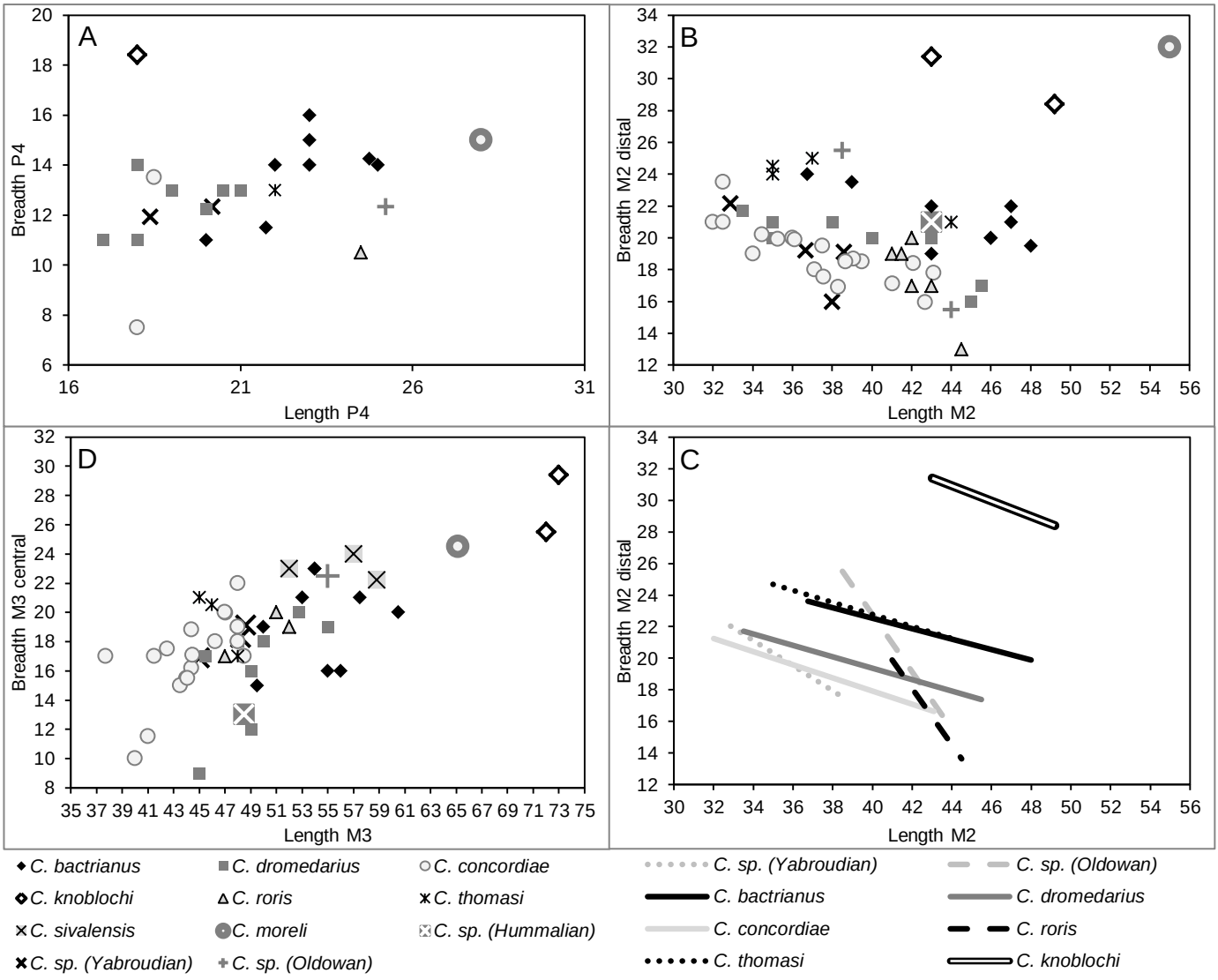

Fig. 8 Bivariate scatterplots of lower dentition measurements in *Camelus* species (in mm): occlusal length vs. occlusal breadth. **A** Length and breadth of p4. **B** Length and breadth of m2 (distal lobe). **C** Linear regression line of the data in B. **D** Length and breadth of M3 (central lobe).

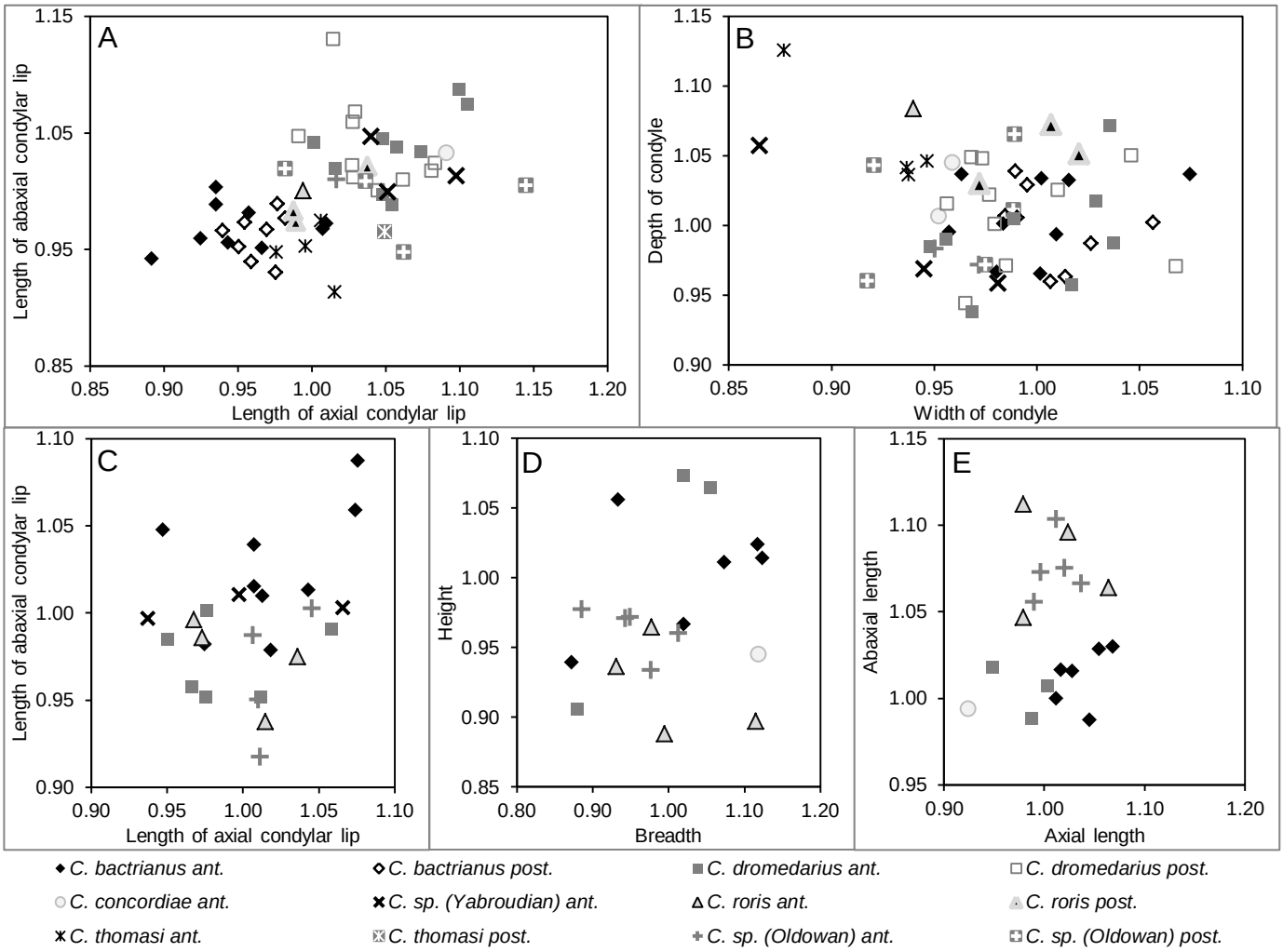

Fig. 9 Bivariate scatterplots of phalanx measurements in *Camelus* species (harmonic scores). **A** Length of condylar lips in proximal phalanges: axial lip vs abaxial lip. **B** Proportions of the condyle in proximal phalanges: width vs. depth. **C** Length of condylar lips in intermediate phalanges: axial lip vs abaxial lip. **D** Proportions of distal phalanges: breadth vs. height. **E** Simmetry of distal phalanges: length of axial side vs length of abaxial side. Abbreviations: ant., anterior; post, posterior.

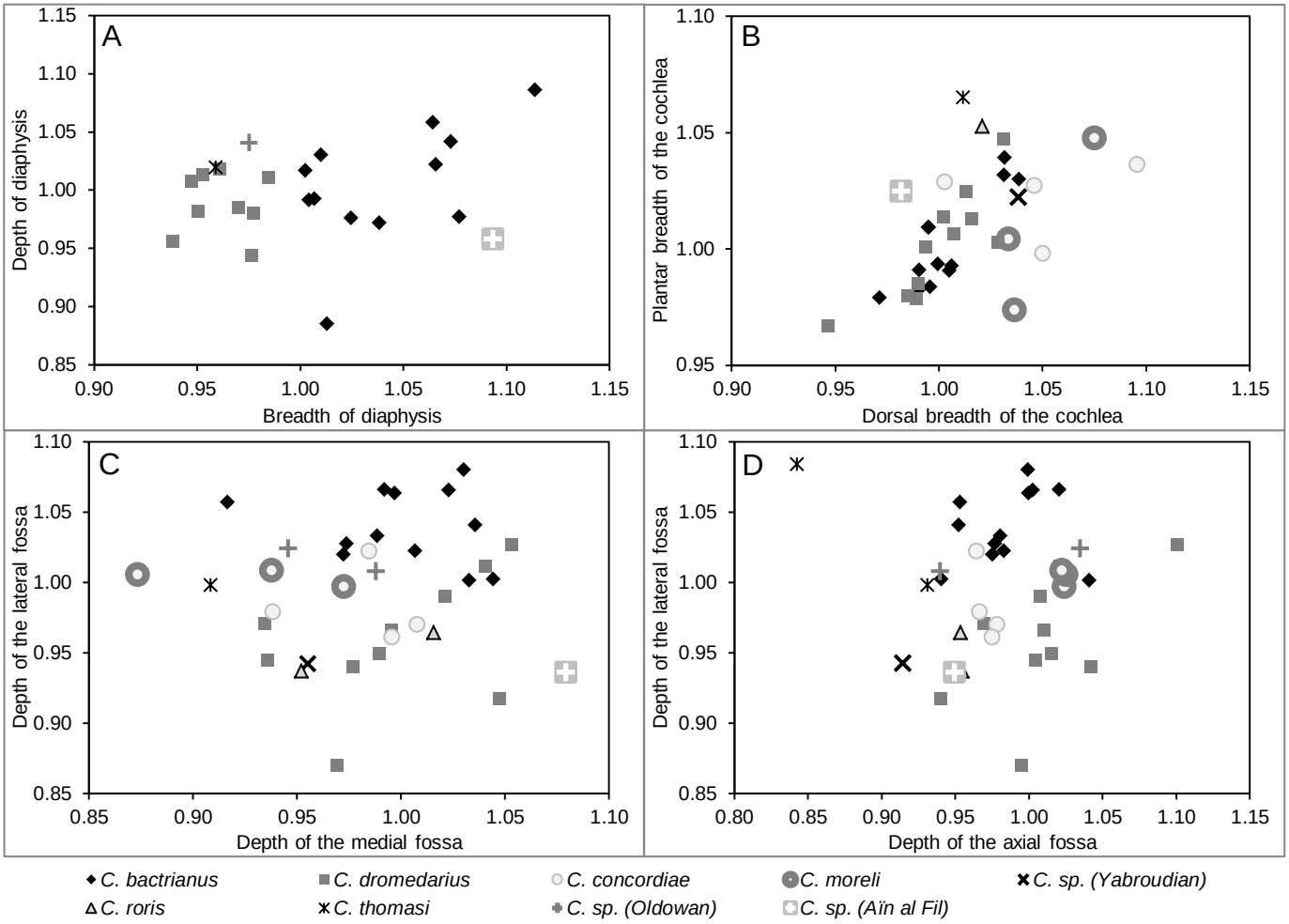

Fig. 10 Bivariate scatterplots of tibia measurements in *Camelus* species (harmonic scores). **A** Proportions of the diaphysis: minimal breadth vs. minimal depth. **B** Breadth proportions of the cochlea: dorsal vs. plantar. **C** Relative depth of articular fossae: medial fossa vs. lateral fossa. **C** Relative depth of articular fossae: axial fossa vs. lateral fossa.

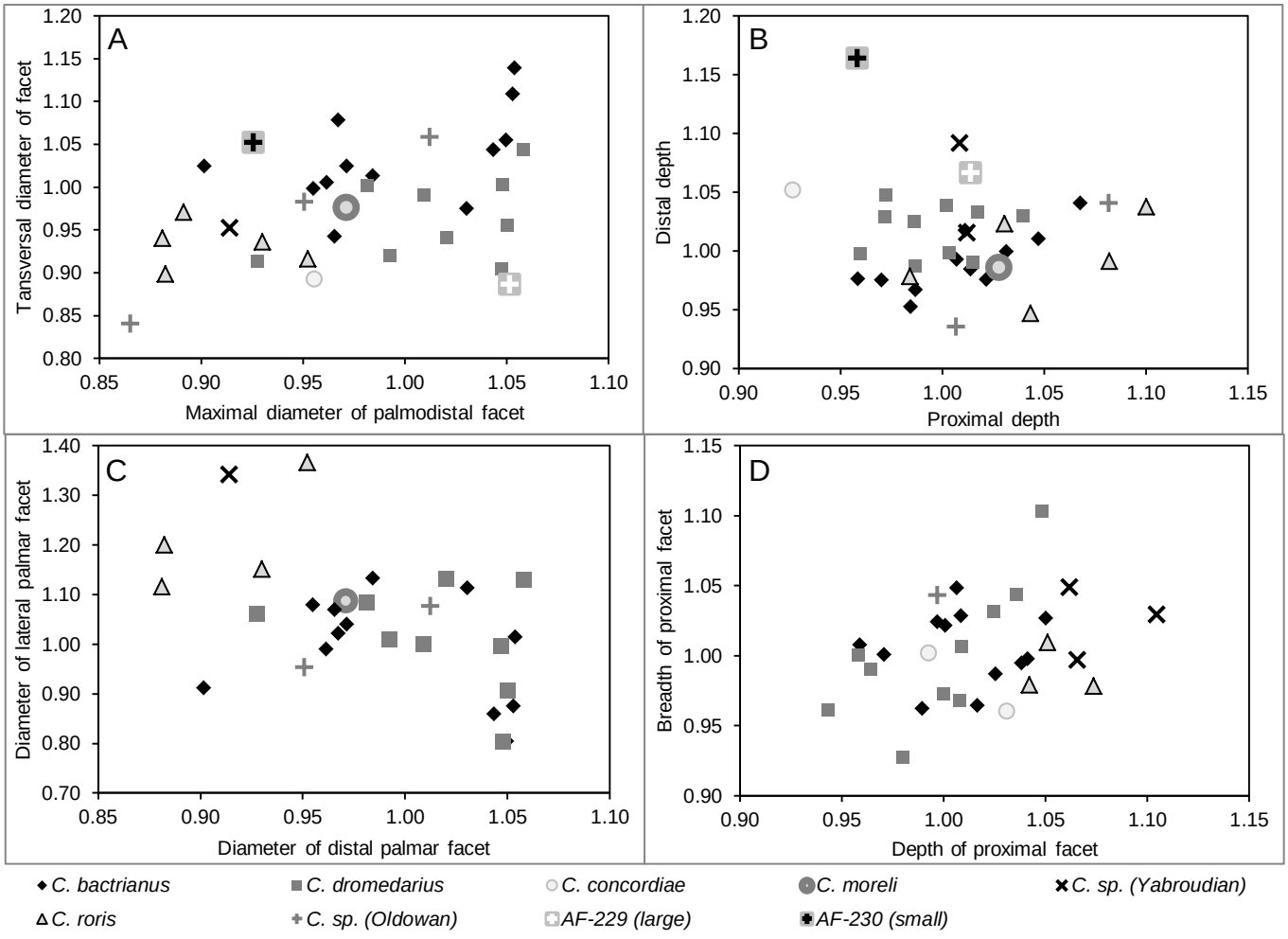

Fig. 11 Bivariate scatterplots of carpal bone measurements (proximal row) in *Camelus* species (harmonic scores). **A** Proportions of the palmodistal facet (for the trapezoideum) of the scaphoideum: maximal diameter vs. transversal breadth. **B** Depth proportions of the scaphoideum: proximal depth vs. distal depth. **C** Facet proportions of the scaphoideum: maximal diameter of palmodistal facet (for the trapezoideum) vs maximal diameter of palmolateral facet (for the lunatum). **D** Proportions of the proximal facet of the triquetrum: depth vs. breadth

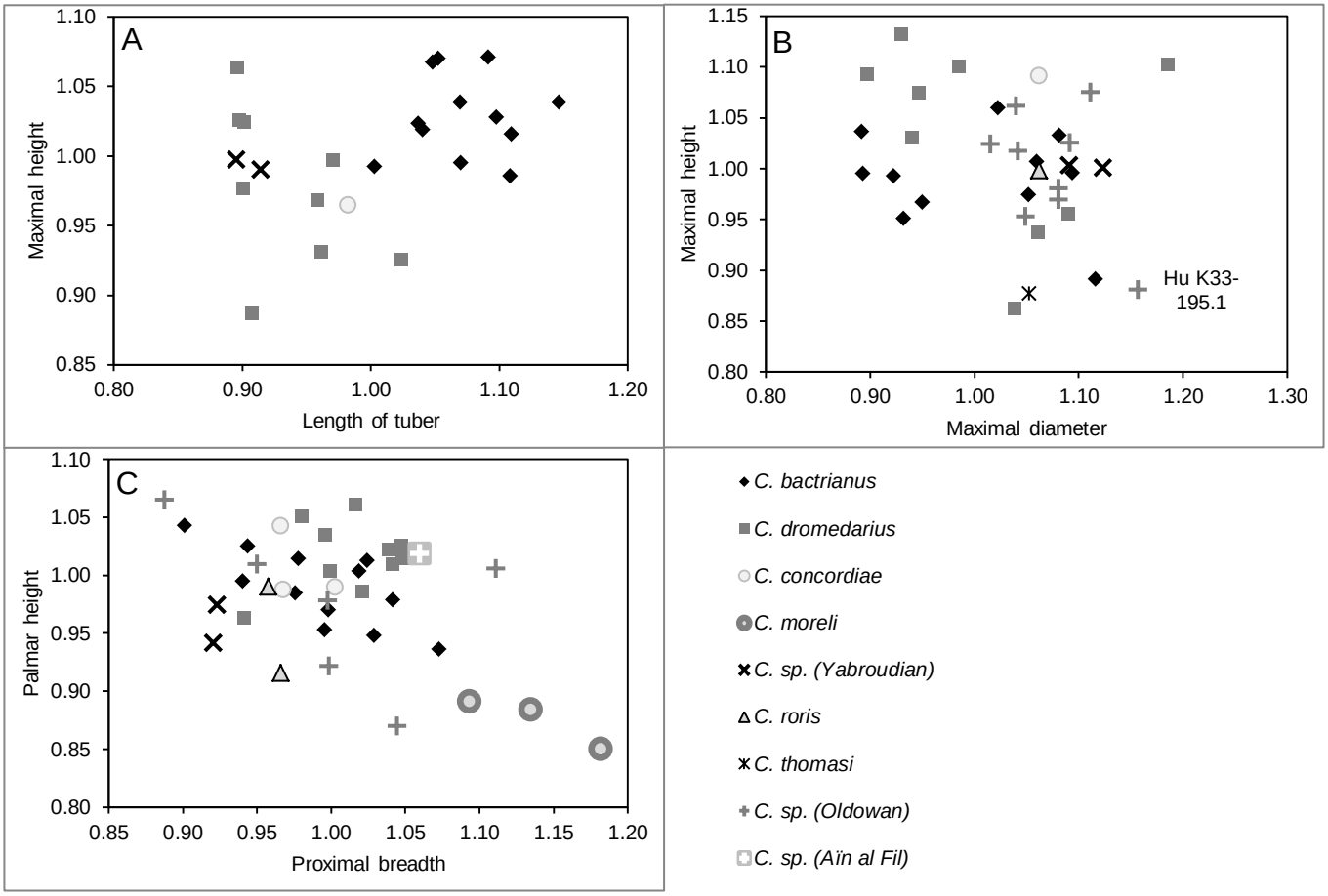

Fig. 12 Bivariate scatterplots of carpal bone measurements (distal row) in *Camelus* species (harmonic scores). **A** Proportions of the pisiforme: length of the tuber vs. maximal height. **B** Proportions of the trapezoideum: maximal diameter vs. maximal height. **C** Proportions of the hamatum: breadth of proximal facet vs. plantar height.

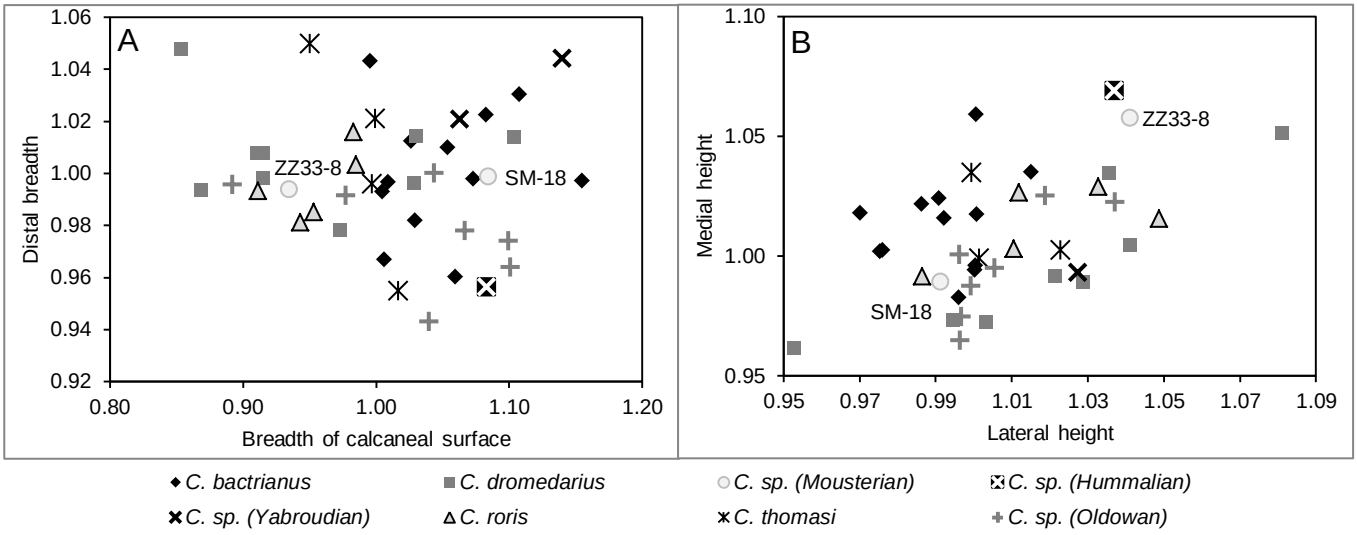

Fig. 13 Bivariate scatterplots of astragalus measurements in *Camelus* species (harmonic scores). **A** Breadth proportions: breadth of calcaneal surface vs. breadth of the distal trochlea. **B** Height proportions: lateral height vs. medial height.

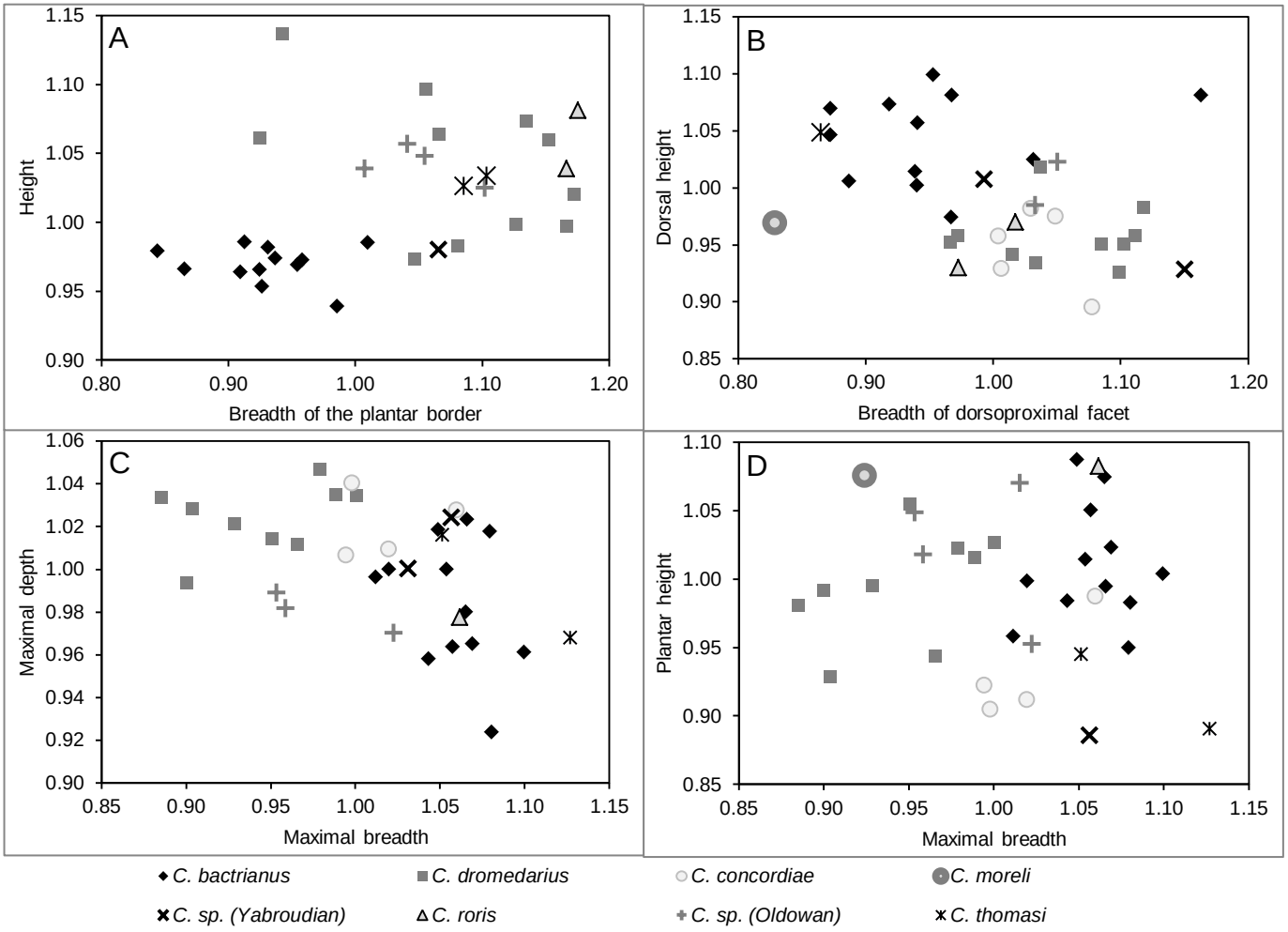

Fig. 14 Bivariate scatterplots of tarsal bones measurements in *Camelus* species (harmonic scores). **A** Proportions of the calcaneus: breadth of the plantar border vs. maximal height. **B** Dorsal proportions of the cuboideum: breadth of dorsoproximal facet (for the astragalus) vs. dorsal height. **C** Proportions of the naviculare: maximal breadth vs. maximal depth. **D** Proportions of the naviculare: maximal breadth vs. plantar height.

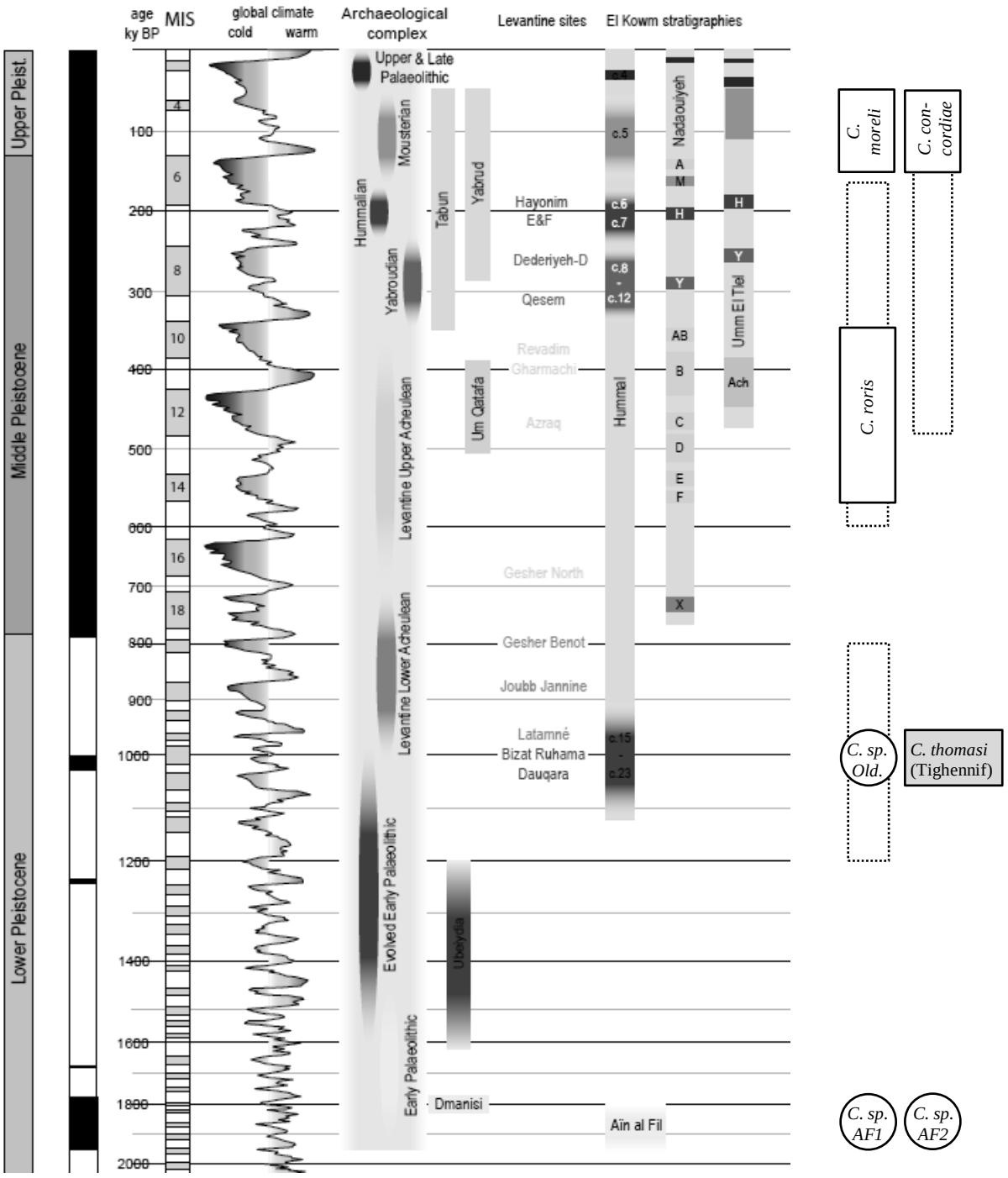

Fig. 15 Stratigraphic distribution of Camelus species discussed in this study. Square boxes indicate named species; circles indicate distinct, unnamed species; dotted borders indicate uncertain presence. *Camelus thomasi* (grey box) does not occur in the El Kowm fauna. Abbreviation: AF1 = Aïn al Fil, large species; AF2 = Aïn al Fil, small species; Old. = Oldowan assemblage. Stratigraphic chart of the EL Kowm Basin adapted from Jagher et al. (2015).

Tables

Table 1 List of specimens included in this study. The total of 170 specimens is divided into six assemblages, termed Aïn al Fil (Unit AF; total 4 specimens), Oldowan (Unit G; total 153), Acheuleo-Tayacien (Unit F; total 8), Yabroudian (Unit E; total 61), Hummalian (Unit D; total 15), and uncertain stratigraphic position (Unit ?; total 13). See text for specific identification of assemblages. Former # indicates former inventory number, which might have been used in former reports; it is given for reference. Current # indicates the correct number according to our revision, which is used in this study. Layer "6x" indicates reworked Hummalian sands (although not corresponding to layer 6). "Housed" indicates most recent housing of the specimen, either in Basel (IPNA) or in El Kowm (Tell Arida Center).

Former #	Current #	Unit	Layer	Element	Side	Description	Housed
B30-27	B30-28	E	11a	Maxilla		Fragments	Basel
H33-65	H33-65	G	16	Petrosum	sin	Fragment	Basel
G34-1	G34-1	E	11	Mandibula	sin	& m2	Basel
G34-16	G34-16	E	11	Mandibula		& roots p4	Basel
E-9045	E-9045	E	10c	Mandibula	dex	& m2-m3	El Kowm
J32-66	I32-66	F	13b	Mandibula	sin	& roots m3	Basel
E-9242	E-9242	G	16	Mandibula	sin	Fragments	El Kowm
E-9296	E-9296	G	16	Mandibula	sin	& m3	El Kowm
K33-381	K33-381	G	18	Mandibula	dex	& m1-m3; including P4 sup dex	Basel
L33-138	L33-138	G	18	Mandibula	dex	& m1-m2 or m2-m3	Basel
M31-1	M31-99.2	G	16	Dens		Fragment unidentified	Basel
-	99E-11	G	16	Dens		Molar fragment	Basel
L31-	L31-x1	G	16	Dens		Molar fragment	Basel
L31-165	L31-188	G	17	Dens		Fragment unidentified	Basel
L31-179	L31-202	G	17	Dens		Fragment unidentified	Basel
M33-51	M33-51	G	18	Dens		Fragment unidentified	Basel
L31-186	L31-210	G	17b	Dens		Fragment unidentified	Basel
-	P7-13	?	?	Dens ant		Incisive	Basel
L31-151	L31-174	G	17	Dens ant		Incisive, fragments	Basel
D32-51	D32-51	G	18	Dens ant	sin	Incisive, small (juvenile?)	Basel
-	99W-22	G	19	Dens ant		Incisive, fragments	Basel
-	P7-4	?	?	Dens inf	sin	Molar fragment	Basel
-	P7-6	?	?	Dens inf	dex	m2, incomplete	Basel
-	P7-10	?	?	Dens inf	dex	m2, half of P7-12	Basel
-	P7-12	?	?	Dens inf	dex	m2, half of P7-10	Basel
-	P7-8	?	?	Dens inf	sin	m3	Basel
D29-2	D29-2	D	6x	Dens inf	sin	m2	Basel
D29-	D29-x1	D	6x	Dens inf	dex	m3	Basel
E30-16	E30-16	D	6x	Dens inf	dex	m3	Basel
-	Db97-24	E	8a?	Dens inf	dex	m2, fragment (lingual wall)	Basel
L33-140	L33-140	G	18	Dens inf	dex?	m1, fragments	Basel
K33-417	K33-417	G	18	Dens inf	dex	p4	El Kowm
K33-218	K33-218	G	17c	Dens inf	dex	m2, fragments	Basel
-	P7-14	?	?	Dens sup	dex	M3	Basel
-	P7-15	?	?	Dens sup	sin	P3	Basel
K33-235	K33-235	G	17c	Dens sup	dex	M3	Basel
E-10561	E-10561	G	19	Atlas			El Kowm
C26-51	C26-51	?	?	Axis		Fragment odontoid process	El Kowm
L32-157	L32-157	G	17	Vertebra		Fragment spina, thoracal or lumbar	Basel
L32-13	L32-34	G	16	Vertebra cervical		Fragment zygapophysis	Basel
H33-50	H33-50	G	16	Vertebra cervical		Cervical 6	Basel
M32-108	M32-108	G	17	Vertebra lumbar		Fragment, thoracal 12 or lumbar 1-4	Basel
D32-6.2	D32-6.2	E	11-13	Vertebra thoracal		Fragment thoracal 5-8, juvenile	Basel
B30-coupe verte	B30-22	E	11a	Vertebra thoracal		Fragment cranial	Basel
B30-37	B30-80	E	11a	Vertebra thoracal		Fragment corpus, juvenile	Basel
N37-36	N37-36	E	8a	Vertebra thoracal		Fragment thoracal 2	El Kowm
W/N-65	W/N-65	E	8b	Vertebra thoracal		Fragment thoracal 4-6	Basel
L32-9	L32-30	G	16	Vertebra thoracal		Fragment corpus	Basel
-6079	E-6079	E	8a	Scapula	sin		El Kowm
E32-500	E32-500	G	18	Scapula	sin	Fragment distal	El Kowm
S07-24	S07-24	?	?	Humerus	sin	Fragment distal	El Kowm
H37-99	H37-99	E	8	Humerus	dex	Fragment distal	El Kowm

W/N-64	W/N-64	E	8b	Humerus	dex	Fragment distal	Basel
K32-103	K32-145	G	17	Humerus	sin	Fragment condyle	Basel
G01-	G01-X	?	?	Radioulnare	dex	Fragment distal	Basel
S-12192	S-12192	D	6a2	Radioulnare	?	Fragment distal	El Kowm
-	99W-76	D	6x	Radioulnare		Fragment distal	Basel
F34-10	F34-10.1	E	12	Radioulnare	dex	Distal fragment	Basel
B30-20.1	B30-21	E	11a	Radioulnare	dex	Fragment distal	Basel
-	B30-19	E	11b	Radioulnare		Fragment olecranon	Basel
-	99E-3	G	16	Radioulnare		Fragment distal	Basel
E-9396	E-9396	G	16	Radioulnare	sin	Fragment distal, juvenile epiphysis	El Kowm
-	99W-3	G	18	Radioulnare		Fragment distal	Basel
F32-16	F32-16	G	18	Radioulnare	dex	Fragments	Basel
Sondage/E-1	Sond E-1	G	16?	Radioulnare	dex	Fragment distal	Basel
J33-16	I33-16.0	F	13a	Radioulnare?		Fragment diaphysis	Basel
F34-10	F34-10.2	E	12	Cars	sin		Basel
	AF229	AF	L1b	Scaphoideum			El Kowm
	AF230	AF	L1b	Scaphoideum			El Kowm
D32-5	D32-5	E	11-13	Scaphoideum	sin		Basel
N37-94	N37-94.1	E	8a	Scaphoideum	dex		Basel
-	99E-16	G	16	Scaphoideum	dex		Basel
E-9381	E-9381	G	16	Scaphoideum	sin	Fragment dorsal	El Kowm
E-9425	E-9425	G	16	Scaphoideum	sin		El Kowm
P57-P57-04	P57-4	G	16	Scaphoideum	sin		El Kowm
K32-63	K32-105	G	17	Scaphoideum	sin	Fragment dorsal	Basel
E32-27	E32-27	G	18	Scaphoideum	sin		Basel
S07-20	S07-20	?	?	Lunatum	dex		El Kowm
E-11293	E-11293	E	10	Lunatum	sin		El Kowm
F34-10	F34-10.3	E	12	Lunatum	sin		Basel
-	99E-35	F	13	Lunatum	dex		Basel
E-9380	E-9380	G	16	Lunatum	sin		El Kowm
E-9618	E-9618.1	G	16	Lunatum	sin		El Kowm
P57-P57-02	P57-2	G	16	Lunatum	sin		El Kowm
H33-146	H33-146	G	17	Lunatum	dex		Basel
K32-110.6	K32-152.6	G	17	Lunatum	sin		El Kowm
L32-130	L32-130	G	17	Lunatum	sin		Basel
E-10897	E-10897	G	18b	Lunatum		Fragment dorsal	El Kowm
S-12258	S-12258	D	6b	Triquetrum	dex		El Kowm
E-11067	E-11067	E	10	Triquetrum	dex		El Kowm
F34-10	F34-10.4	E	12	Triquetrum	sin		Basel
E-11035	E-11035	G	15	Triquetrum	sin	Fragment dorsal	El Kowm
E-10214	E-10214	G	16	Triquetrum	dex		El Kowm
E-10633	E-10633	G	18a	Triquetrum	sin		El Kowm
E-10898	E-10898	G	18b	Triquetrum	dex	Fragment dorsal	El Kowm
-	99W-84	E	10	Pisiforme	sin		Basel
A30-3.02	A30-3.2	E	11b	Pisiforme	dex		Basel
-	99E-4	G	16	Pisiforme	sin?	Fragment	Basel
	AF221	AF	L2	Hamatum	sin		El Kowm
B30-21.2	B30-21.2	E	11a	Hamatum	dex		Basel
-	99E-18	F	13b	Hamatum	dex		Basel
E-11395	E-11395	G	15	Hamatum	sin		El Kowm
-	99E-7	G	16	Hamatum	.	Fragment palmar	Basel
E-11330	E-11330	G	16	Hamatum	sin		El Kowm
H33-44	H33-44	G	16	Hamatum	dex	Fragments	Basel
L31-f01	L31-f01	G	16	Hamatum	sin	Fragment	El Kowm
P57-SK-03.3	P57-SK02.3	G	16	Hamatum	dex		El Kowm
J32-2	I32-72	G	17	Hamatum	dex		Basel
K32?-290903-47	K32-89	G	17	Hamatum	sin		El Kowm
K32-f03	K32-f03	G	17	Hamatum	dex		El Kowm
E32-33	E32-33	G	18	Hamatum	dex	Fragment dorsal	Basel
E-10877	E-10877	G	18a	Hamatum	sin	Fragments	El Kowm
SK-Os-SK06.02	SK06-2	E	10	Capitatum	dex	Juvenile	El Kowm
F34-7	F34-7	E	12	Capitatum	sin	Fragment	Basel
G34-32	G34-32	E	12	Capitatum	dex		Basel
-6160	E-6160	E	8a	Capitatum	dex	Fragment	El Kowm
E-11366	E-11366.2	G	16	Capitatum	sin		El Kowm
P57-P57-14	P57-14	G	16	Capitatum	dex	Fragment	El Kowm
-	K33-195.1	G	17c	Capitatum	dex	Fused with trapezoideum	Basel
E-11311	E-11311	E	10	Trapezoideum			El Kowm
-	N37-94.2	E	8a	Trapezoideum	dex		Basel
E-11034	E-11034	G	15	Trapezoideum	dex		El Kowm
E-11038	E-11038	G	15	Trapezoideum	sin		El Kowm
E-10126	E-10126	G	16	Trapezoideum	sin		El Kowm
E-11366	E-11366.1	G	16	Trapezoideum	sin		El Kowm
-	99W-27	G	17	Trapezoideum	dex		Basel
E-9532	E-9532	G	18	Trapezoideum	sin		El Kowm
E32-57	E32-57	G	18	Trapezoideum	dex		Basel
E-11110	E-11110	G	21	Trapezoideum	sin		El Kowm
-	S07-43	G	15?	Trapezoideum	dex		El Kowm
-	K33-195.2	G	17c	Trapezoideum	dex	Fused with capitatum	Basel
S-12179	S-12179	D	6a	Femur	sin	Fragment distal	El Kowm
H33-42	H33-42	G	16	Femur		Fragment medial condyle	Basel
	AF178	AF	L	Tibia	sin		El Kowm
B30-33	B30-34	E	11a	Tibia	sin	Fragment distal	Basel

E-11336	E-11336	G	16	Tibia	sin	Fragment distal	El Kowm
E-9903	E-9903	G	18	Tibia	sin	Fragment distal	El Kowm
S07-19	S07-19	?	?	Fibula	dex		El Kowm
C31-11A.1	C31-x1	E	11a	Fibula	dex		Basel
E-11363	E-11363	G	16	Fibula	?		El Kowm
L33-f03	L33-f03	G	16	Fibula	dex		El Kowm
M31-8	M31-106	G	17	Fibula	sin		Basel
E-9610	E-9610	G	18	Fibula	sin		El Kowm
E32-31	E32-31	G	18	Fibula	dex		Basel
M32-128	M32-128	G	18	Fibula	sin		El Kowm
E-10379	E-10379	G	18a	Fibula	sin		El Kowm
E-10579.2	E-10579.2	G	18a	Fibula	sin		El Kowm
N35-671	N35-671	E	8a	Fibula?	sin	Fragment	Basel
S-12402	S-12402	D	7	Astragalus	dex		El Kowm
A28-2	A28-2	D	6x	Astragalus	sin		Basel
H40-9	H40-9	D	7d	Astragalus	sin		Basel
N36-313	N36-313	E	8a	Astragalus	sin		Basel
N37-57	N37-57	E	8a	Astragalus	dex	Fragment	Basel
E-9164	E-9164	G	15	Astragalus	dex		El Kowm
E-9442	E-9442	G	16	Astragalus	sin		El Kowm
E-9804	E-9804	G	16	Astragalus	sin		El Kowm
L33-f01	L33-f01	G	16	Astragalus	dex		El Kowm
E-9611	E-9611	G	18	Astragalus	dex		El Kowm
E-9828	E-9828	G	18	Astragalus	sin		El Kowm
K33-347	K33-347	G	18	Astragalus	dex		Basel
D31-3a	D31-3a	G	15a	Astragalus	sin		El Kowm
K33-18.7	K33-18.7	E	10	Calcaneus	dex	Fragments tuber	Basel
N36-309.1	N36-309.1	E	8a	Calcaneus	sin	Fragments	Basel
N38-128	N38-128	E	8a	Calcaneus	dex	Fragments	El Kowm
E-9166	E-9166	G	15	Calcaneus	dex	Fragment	El Kowm
E-11106	E-11106	G	16	Calcaneus	sin	Fragment	El Kowm
E-11107	E-11107	G	16	Calcaneus	sin	Juvenile	El Kowm
L32-22	L32-43	G	16	Calcaneus	dex	Fragment tuber	Basel
L32-24	L32-45	G	16	Calcaneus	dex	Fragment distal	Basel
J32-f00	I32-f00	G	17	Calcaneus	dex		El Kowm
M31-3	M31-101	G	17	Calcaneus	sin	Fragments medial and proximal	Basel
E32-59	E32-59	G	18	Calcaneus		Fragments tuber	Basel
L33-116	L33-116	G	18	Calcaneus	dex		Basel
K33-217	K33-217	G	17c	Calcaneus	dex	Fragments tuber	Basel
K33-224	K33-224	G	17c	Calcaneus	sin	Fragment distal	Basel
G34-26	G34-26	E	12	Calcaneus?		Fragment distal?	Basel
E32-19	E32-19	G	18	Calcaneus?		Fragment tuber?	Basel
-	AB28-D07	D	6x	Cuboideum	dex		Basel
-	99W-67	E	8	Cuboideum	dex		Basel
E-11066	E-11066	E	10	Cuboideum	sin	Fragment	El Kowm
K32-1.5	K32-1.5	E	10	Cuboideum	sin	Fragment	Basel
P57-P57-03	P57-3	G	16	Cuboideum	sin		El Kowm
E-10579.1	E-10579.1	G	18a	Cuboideum	dex		El Kowm
E-11310	E-11310	E	10	Naviculare	sin		El Kowm
D32-1.1	D32-1.1	E	11-13	Naviculare	sin	Fragment	Basel
M35-36	M35-36	E	8b	Naviculare	sin		Basel
E-10196	E-10196	G	16	Naviculare	dex		El Kowm
E-10247	E-10247	G	16	Naviculare	dex		El Kowm
-	99W-28	G	17	Naviculare	dex	Fragment	Basel
M31-12	M31-110.2	G	17	Naviculare	dex	Completed by fragment M31-169	Basel
M31-9a	M31-169	G	17	Naviculare	dex	Dorsal fragment, belongs to M31-110	Basel
E-10875	E-10875	G	18a	Naviculare	dex		El Kowm
J40-4	I40-4	D	7d	Cuneiforme medial		Fragment	Basel
J32-61	I32-61	F	13b	Cuneiforme medial		Fragments	Basel
A28-C17	A28-C17	D	6x	Cuneiforme intermediolateral	sin		Basel
E-11304	E-11304	E	10	Cuneiforme intermediolateral	sin	Fragment	El Kowm
E32-21	E32-21	G	18	Cuneiforme intermediolateral	sin		Basel
E32-23	E32-23	G	18	Cuneiforme intermediolateral	dex		Basel
E-10899	E-10899	G	18b	Cuneiforme intermediolateral	dex	Fragment	El Kowm
N37-75	N37-75	E	8a	Metacarpale	dex	Fragment distal	El Kowm
J33-16.3	I33-16.3	F	13a	Metacarpale	sin	Fragment proximal	Basel
E-10948	E-10948	G	15	Metacarpale	sin		El Kowm
D31-25	D31-25	G	16	Metacarpale		Fragment condyle	Basel
H33-65	H33-111	G	18	Metacarpale		Fragment condyle	Basel
S-12401	S-12401	D	7	Metatarsale	?	Fragment distal	El Kowm
D32-4	D32-4	E	11-13	Metatarsale	sin	Fragment proximal	Basel
E-10485	E-10485	G	16	Metatarsale	dex	Fragment proximal	El Kowm
L31-175	L31-198	G	17	Metatarsale		Fragment condyle	Basel
F32-14	F32-14	G	18	Metatarsale		Fragments	Basel
K33-365	K33-365	G	18	Metatarsale	sin	Fragment proximal	Basel
A28-C16	A28-C16	D	6x	Metapodium		Fragment proximal	Basel
-	99W-30	G	17	Metapodium		Fragment diaphysis	Basel
K32-25	K32-67	G	17	Metapodium		Fragment condyle	Basel
D32-52	D32-52	G	18	Metapodium		Fragment distal	Basel
K33-410	K33-410	G	18	Metapodium		Fragments diaphysis	Basel
-	99W-69	E	8	Metapodium?		Fragment diaphysis	Basel
C31-21	C31-21	E	11a	Phalanx I		Fragment condyle, juvenile?	Basel
-	99E-10	G	16	Phalanx I		Fragment condyle	Basel

E32-13	E32-13	G	16	Phalanx I	Fragment proximal	Basel
-	99W-100	E	11	Phalanx I ant		Basel
-	99W-95	E	11	Phalanx I ant	Fragment distal	Basel
M31-200	M31-60	F	13b	Phalanx I ant	Fragment distal	Basel
E-10949	E-10949	G	15	Phalanx I ant		El Kowm
K32-86	K32-128	G	17	Phalanx I ant	Fragment distal	Basel
E-9883	E-9883	G	18	Phalanx I ant		El Kowm
B30-35	B30-36	E	11a	Phalanx I ant?	Fragment diaphysis proximal	Basel
H36-158	H36-158	E	8b	Phalanx I post	Fragment proximal	Basel
E-10969	E-10969	G	15	Phalanx I post		El Kowm
-	99W-11	G	16	Phalanx I post	Fragment diaphysis	Basel
K32-95	K32-138	G	17	Phalanx I post	Fragment distal	Basel
K32-201	K32-201	G	17	Phalanx I post	Fragment proximal	Basel
E32-26	E32-26	G	18	Phalanx I post	Fragments	Basel
L33-252	L33-252	G	18	Phalanx I post	Fragment condyle	El Kowm
E-10829	E-10829	G	18a	Phalanx I post		El Kowm
-	99W-98	E	11	Phalanx I post?	Fragment distal	Basel
-	99W-59	F	13	Phalanx I post?	Fragment condyle, juvenile?	Basel
-	99E-5	G	16	Phalanx I?	Fragment proximal	Basel
-	99E-20	E	8	Phalanx II	Fragment proximal, juvenil	Basel
D32-6	D32-6	E	11-13	Phalanx II	Fragment proximal, juvenil	Basel
B30-19.2	B30-20	E	11a	Phalanx II	Fragment distal	Basel
H38-32	H38-32	E	8b	Phalanx II		Basel
E-9317	E-9317	G	15	Phalanx II	Juvenile	El Kowm
-	99E-14	G	16	Phalanx II	Fragment proximal	Basel
E-11357	E-11357	G	16	Phalanx II		El Kowm
H33-73	H33-73	G	16	Phalanx II		Basel
M32-4	M32-4	G	16	Phalanx II		Basel
E-10690	E-10690	G	17	Phalanx II		El Kowm
K32-110.4	K32-152.4	G	17	Phalanx II		El Kowm
SK08-1	SK08-1	G	16-18	Phalanx II		El Kowm
-	99W-12	G	16	Phalanx III		Basel
E-10802	E-10802	G	16	Phalanx III		El Kowm
E-11382	E-11382	G	16	Phalanx III		El Kowm
E-10558.1	E-10558.1	G	17	Phalanx III		El Kowm
E32-18	E32-18	G	18	Phalanx III		Basel

Table 2 Measurements of *Camelus* remains from Hummal, except Mousterian layers. Details on the specimens are given in Table 1. ~ indicates approximated measurements; § indicates measurements that might be either mesial or lateral, or one of two possible positions.

	MANDIBULA	**E-6114** **E: 8a**	**E-6115** **E: 8a**	**G34-1 sin** **E: 11**	**L33-138 dex** **G: 18**			
M13	Length from m3 distal to angular process		105.47					
M15	Thickness of the corpus measured between m1 and m2			24	39			
M16	Thickness of the corpus measured between m2 and m3				39			
M20	Height of the corpus between m1 and m2			39 ~				
M21	Height of the corpus distal to m3	82.11	82.16					
M22	Height of the ramus from coronoid process to ventral border	200.78	202.58					
M23	Height of the ramus from rostral notch to ventral border	156.36	152.39					
M24	Height of the ramus from condylar process to ventral border	168.9	154.28					
-	Length m1-m3	109.63	115.04					
	UPPER DENTITION	**K33-235 dex** **G: 17c**	**K33-381 dex** **G: 18**	**P7-14** **?**	**DBN-2** **?**	**NE-4** **?**	**NE-29** **?**	**P7-15** **?**
Ds9	Occlusal length of P3							16
Ds10	Occlusal breadth of P3							13
Ds11	Alveolar length of P4		18					
Ds12	Alveolar breadth of P4		23					
Ds13	Occlusal length of P4		20					
Ds14	Occlusal breadth of P4		19					
Ds15	Alveolar length of M1				37.93			
Ds18	Occlusal length of M1				35.24			
Ds21	Occlusal breadth of mesial lobe of M1				21.76			
Ds23	Alveolar length of M2					31.97	25.75	
Ds26	Occlusal length of M2					39.02	36.09	
Ds29	Occlusal breadth of mesial lobe of M2					23.73	28.33	
Ds31	Alveolar length of M3	33 ~						
Ds32	Alveolar breadth of mesial lobe of M3	28 ~						
Ds33	Alveolar breadth of distal lobe of M3	23.5 ~						
Ds34	Occlusal length of M3	37 ~		35				
Ds35	Occlusal length of mesial lobe of M3	19.5 ~		18				
Ds36	Occlusal length of distal lobe of M3	19 ~		18				
Ds37	Occlusal breadth of mesial lobe of M3	22		19				
Ds38	Occlusal breadth of distal lobe of M3	16.5		14.5				

	LOWER DENTITION (P4-M1)	E-6114 E: 8a	E-6115 E: 8a	K33-417 G: 18	P7-10/12 dex ?
Di8	Alveolar length of p4	17.19	16.52	22.58	
Di10	Occlusal length of p4	20.19	18.38	25.22	
Di11	Occlusal breadth of p4	12.33	11.93	12.34	
Di12	Alveolar length of m1	27.7	25.74		
Di15	Occlusal length of m1	28.13	28.61		34 § ~
Di16	Occlusal length of mesial lobe of m1				16 § ~
Di17	Occlusal length of distal lobe of m1				17 §
Di18	Occlusal breadth of mesial lobe of m1				16 §
Di19	Occlusal breadth of distal lobe of m1	20.83	21.02		17 §

	LOWER DENTITION (m2)	D29-2 sin D: 6x	Db97-24 dex E: 8a	E-6114 E: 8a	E-6115 E: 8a	E-9045 E: 10c	G34-1 sin E: 11	K33-218 dex G: 17c	K33-381 dex G: 18	P7-6 dex ?	P7-10/12 dex ?
Di20	Alveolar length of m2			28.94	36.33	35.9	37 ~				
Di21	Alveolar breadth of mesial lobe of m2						21 ~				
Di22	Alveolar breadth of distal lobe of m2						20				
Di23	Occlusal length of m2	43	39 ~	32.86	36.64	38.6	38	44 ~	38.5	40 ~	34 § ~
Di24	Occlusal length of mesial lobe of m2	21					18 ~	22 ~	20	21 ~	16 § ~
Di25	Occlusal length of distal lobe of m2	22					21	22.5 ~	19	21	17 §
Di26	Occlusal breadth of mesial lobe of m2	21							24		16 §
Di27	Occlusal breadth of distal lobe of m2	21		22.17	19.21	19.1	16	15.5 ~	25.5	13	17 §

	LOWER DENTITION (m3)	E30-16 dex D: 6x	D29-x1 dex D: 6x	E-6114 D: 8a	E-6115 D: 8a	E-9045 D: 10c	K33-381 dex G: 18	P7-8 sin juv ?	Db97-5 ?	DBN-1 ?	NE-21 ?
Di28	Alveolar length of m3			48.63	49.17	47.5			45.72	46.1	
Di32	Occlusal length of m3	50	48.5	48.63	48.21	45	55	49 ~	46.93	44.11	39.68
Di33	Occlusal length of mesial lobe of m3		23				21				
Di34	Occlusal length of central lobe of m3		18				21				
Di35	Occlusal length of distal lobe of m3		10				16				
Di36	Occlusal breadth of mesial lobe of m3		15 ~				22	14 ~			
Di37	Occlusal breadth of central lobe of m3		13 ~	19.12	18.26	16.9	22.5	15 ~	20.27	18.6	
Di38	Occlusal breadth of distal lobe of m3		7				14.5	8			

	ATLAS	E-10561 axial G: 19
at2	Lateral length (length of the wings)	115.5 ~
at3	Length between cranial and caudal dorsal foramina	65
at4	Distance from cranial dorsal foramina to cranial lateral tip	41.5
at5	Breadth between cranial dorsal foramina	51
at6	Maximal cranial breadth	88
at7	Dorsal breadth of the cranial opening (between the articular surfaces)	29
at9	Maximal diagonal height of cranial articular cavity	62.25
at11	Breadth of the caudal articular surface	88
at12	Dorsal breadth of the caudal opening (between the dorsal tips of the articular surfaces)	58
at13	Breadth between caudal dorsal foramina	88
at15	Maximal diagonal height of caudal articular surface	52
at16	Length of the ventral arch	56
at17	Maximal diameter of the ventral foramen	22.25

	SCAPULA	E-6079 sin E: 8a	E32-500 sin G: 18
sc7	Depth of the neck	71	
sc8	Maximal distal depth	103	
sc11	Depth of the glenoid fossa	64.5	61
sc12	Breadth of the glenoid fossa		48

	HUMERUS	W/N-64 dex E: 8b	S07-24 sin ?
hu14	Distal medial depth (medial epicondyle to trochlea)		107
hu17	Distal breadth (trochlea to capitulum)	76	

	RADIOULNARE	S-12192 ? D: 6a2	99W-76 ? D: 6x	B30-21 dex E: 11a	F34-10 dex E: 12	E-9396 sin G: 16	Sond E-1 dex G: 16?	99E-3 ? G: 16	G01-X dex ?
ru17	Distal medial depth (transversal crest included)	51	42			50			
ru18	Distal axial depth (transversal crest included)	45	42 ~			50			
ru19	Distal lateral depth (ulnar articular surface)	26	23	24	22	23	25.5	25	30
ru20	Maximal distal breadth	99							
ru21	Breadth of the distal articular surface	82	68 ~						
ru27	Breadth of the distal lateral (ulnar) articular surface)				24		33 ~	29	

	METACARPALE	E-10948 sin G: 15	D31-25 cond. G: 16	H33-111 cond. G: 18
mp1	Length on the medial side	410		
mp2	Length on the lateral side	405		
mp5	Breadth of the proximal articulation	84		
mp13	Depth of the medial condyle	47	45	41
mp14	Depth of the lateral condyle	46		41
mp15	Breadth of the medial condyle	49	42	44 ~
mp16	Breadth of the lateral condyle	45		44 ~
mp17	Maximal distal breadth	106		

	FEMUR	S-12179 Sin D: 6a
fe11	Distal medial depth (medial condyle to trochlea)	102 ~
fe12	Breadth of medial condyle	31 ~
fe13	Depth of the trochlea (groove to intercondylar fossa	72 ~
fe14	Distal cranial breadth (breadth of the trochlea)	39
fe15	Distal lateral depth (lateral condyle to trochlea)	98
fe16	Breadth of lateral condyle	42
fe17	Distal maximal breadth (condyle to condyle)	93

	TIBIA	B30-34 sin E: 11a	E-11336 sin G: 16	E-9903 sin G: 18	AF-178 sin AF: L	P. gigas	
ti2	Length axial (from epicondylar eminence)				650 ~	600 *	* = Maximal length
ti4	Proximal breadth				136	148	
ti5	Depth of the lateral condyle				43		
ti6	Depth of the medial condyle				80		
ti10	Medial proximal depth (medial condyle to tibial tuberosity)				133		
ti11	Depth of the tubercle (to palmar side)				89		
ti12	Minimal depth of the diaphysis	34 ~		26	32		
ti13	Minimal breadth of the diaphysis			40	60		
ti14	Depth of the medial fossa of the cochlea (maximal)	44	44	39	57	60 * ~	* = Greatest distal depth
ti15	Depth of the axial fossa of the cochlea (maximal)	42	48	37	50		
ti16	Depth of the lateral fossa of the cochlea	36	39.5	33	41		
ti17	Dorsal breadth of the cochlea	83		72.5	90		
ti18	Palmar depth of the cochlea	87	86		100	102 *~	* = Greatest distal width
ti19	Breadth of the medial fossa of the cochlea	22.5					
ti20	Breadth of the axial fossa of the cochlea	27					
ti21	Breadth of the lateral fossa of the cochlea	16					

Data on Paracamelus gigas *from Zdansky (1926)*

	METATARSALE	S-12401 D: 7	D32-4 sin 11-13?	E-10485 dex G: 16	K33-365 sin G: 18	L31-198 G: 17
mp18	Length of the triangular process			24.5		
mp19	Breadth of the triangular process			24		
mp20	Depth of the medioplantar proximal facet		13 ~	13.5	16.5	
mp21	Depth of the medial proximal facet		31	31	32	
mp22	Depth of the lateral proximal facet			39	40	
mp5	Breadth of the proximal articulation		59 ~	59.5	61	
mp6	Breadth of the medial proximal facet				22	
mp8	Depth of the proximal articulation				44 ~	
mp11	Minimal depth of the diaphysis	23				
mp13	Depth of the medial condyle	33				32 ~
mp14	Depth of the lateral condyle	36				32 ~
mp15	Breadth of the medial condyle	34				28 ~
mp16	Breadth of the lateral condyle	33				28 ~
mp17	Maximal distal breadth	72				

	ANTERIOR PROXIMAL PHALANX	99W-100 E: 11	99W-95 E: 11	M31-60 F: 13b	E-10949 G: 15	E-9883 G: 18	K32-128 G: 17
pp1	Length of the axial side	98.5			116	100	
pp2	Length of the abaxial side	99			114		
pp3	Proximal depth (articular surface)	32.5			40		
pp4	Proximal breath (articular surface)	40			50	44	
pp5	Depth of the diaphysis	18	17		22.5		19.5
pp6	Breadth of the diaphysis	22 ~	21.5		27	24	23.5
pp7	Depth of the condyle	23.5	23 ~	26.5	28.5	25	
pp8	Breadth of the condyle	37 ~	38	35 ~	46 ~	39	
pp9	Length of the axial lip of the condyle	33	33	36	39		
pp10	Length of the abaxial lip of the condyle	36	34	36	42		

	POSTERIOR PROXIMAL PHALANX	H36-158 E: 8b	99W-98 E: 11	E-10969 G: 15	99W-11 G: 16	K32-138 G: 17	K32-201 G: 17	E32-26 G: 18	L33-252 G: 18	E-10829 G: 18a
pp1	Length of the axial side			97.5						85
pp2	Length of the abaxial side			94.5						83.5
pp3	Proximal depth (articular surface)	30		33.5			31			29
pp4	Proximal breath (articular surface)	39		43			37			33.5
pp5	Depth of the diaphysis			19	17.5			15		16
pp6	Breadth of the diaphysis			21	19			18.5		19
pp7	Depth of the condyle		21	25		23		20	22.5	22
pp8	Breadth of the condyle		31			33		31	34	30
pp9	Length of the axial lip of the condyle		31.5 ~					27.5 ~	27.5	27.5
pp10	Length of the abaxial lip of the condyle		31 ~	33		29		27.5 ~	32	30

	INTERMEDIATE PHALANX	H38-32 E: 8b	D32-6 11-13?	B30-20 E: 11a	E-9317 G: 15	E-11357 G: 16	H33-73 G: 16	M32-4 G: 16	E-10690 G: 17	K32-152.4 G: 17	SK08-1 16-18
ip1	Length of the axial side	50			49.5	58.5	50	54	48		55
ip2	Length of the abaxial side	53 ~			51	62	52	58	49.5		58.5
ip3	Length of the plantar side	59			58.5	70	58	64.5	55		
ip4	Proximal depth (maximal)	22.5			26	31	24	27	25	27	32
ip5	Proximal breath (articular surface)	29.5			30	34	28	32 ~	28	29.5	37
ip6	Minimal breadth of the diaphysis	26	20		20	25	23	25	23	27	28
ip7	Depth of the condyle		13	16.5	15	15	16 ~	16	13		17
ip8	Breadth of the condyle	33 ~	27	33	27	35	34.5		30		37
ip9	Length of the axial lip of the condyle	23 ~	22.5	26 ~		28	26		23.5		29
ip10	Length of the abaxial lip of the condyle	26 ~	22.5	28	22.5	27	26.5 ~		24.5		29

	DISTAL PHALANX *(not included in Martini et al. 2017)*	99W-12 G: 16	E-10802 G: 16	E-11382 G: 16	E32-18 G: 18	E-10558.1 G: 17
dp1	Maximal length	29	23	23	21	24
dp2	Maximal breadth	25	21	21	16.5	20
dp3	Maximal height	21	17.5	19	16	18
dp4	Height of the axial side	24	18	20	15	18
dp5	Height of the abaxial side	26	22.5	21.5	17	22
dp6	Length of the axial side	25.5	21	22	18	20.5
dp7	Length of the abaxial side	28	22.5	25	20	23
dp8	Dorsal length	28	24	26	19	24
dp9	Distance from the facet to the axial lateral foramen	8.5				7.5
dp10	Distance from the facet to the abaxial lateral foramen	7.5	5.5		9	6

	SCAPHOIDEUM	N37-94.1 dex E: 8a	D32-5 sin E: 11	F34-10.2 sin E: 12	E-9425 sin G: 16	P57-4 sin G: 16	E-9381 sin G: 16	99E-16 dex G: 16	E32-27 sin G: 18	AF229 AF: L1b	AF230 AF: L1b
Ks1	Height dorsal	35	32	29 ~	37.5	35	35	35	36.5	43.5	37
Ks2	Height in the middle	24	24.5		30	24		25	27.5		24.5
Ks3	Height palmar	29 ~	29		35.5	32			32	37	30.5
Ks4	Depth maximal	52	50		60	54.5			55	64	53
Ks5	Depth proximal	45	45	39 ~	57	47			49	56.5	45
Ks6	Breadth of proximal facet, dorsal	29.5	29	27 ~	34.5	28.5	30	29	28	38	28
Ks7	Breadth of proximal facet, palmar	27 ~	24 ~		31	26	27		27	32	26.5
Ks8	Total depth of distal facets	41 ~	38		44.5	41			38 ~	50	46
Ks9	Depth of dorsal distal facet	21.5	23		27	21.5		23		25 ~	25 ~
Ks10	Breadth of dorsal distal facet		25		33	27		24	26 ~	32	26
Ks11	Breadth of palmar distal facet		18		22	21			16 ~	21	21
Ks12	Maximal diameter of palmar distal facet	22.5 ~	21.5		26.5	25			20.5 ~	31	23
Ks13	Length of lateral (palmar) facet		19 ~		16	16					
Ks14	Lateral (palmar) facet to lateral dorsal distal corner		34 ~		37 ~	36.5 ~				41.5 ~	39 ~

	LUNATUM	E 11293 sin E: 10	F34-10.3 sin E: 12	99E-35 dex F: 13	E-9380 sin G: 16	E-9618.1 sin G: 16	P57-2 sin G: 16	H33-146 dex G: 17	L32-130 sin G: 17	K32-152.6 sin G: 17b	E-10897 ? G: 18b	S07-20 dex ?
Kl1	Height maximal	42	35	39	41		38	37.5	36.5	41		40
Kl2	Lateral depth of the proximal facet	34.5	30 ~	37				33.5	35	40		
Kl3	Medial depth of the proximal facet		25 ~	29				26	28	33		
Kl4	Dorsal breadth of the proximal facet	21	22	24.5	29		21.5	23	22	24	23	
Kl5	Minimal breadth of the proximal facet		10 ~	16.5		17.5		15.5	12	18		
Kl6	Maximal diagonal			52				49	50	57		
Kl7	Depth of the distal facet			41				40.5	42	47		
Kl8	Dorsal breadth of the distal facet		18	20.5	25		16	20	17	20		
Kl9	Minimal breadth (in the middle) of the distal facet		13.5	15.5			14	17	13	16		
Kl10	Distance from distal lateral tip, to distal dorsomedial tip		26.5	32				32		35.5		
Kl11	Distance from distal lateral tip, to distal palmar tip			33		33		34		36		
Kl12	Distance from distal dorsolateral, to the central eminence of the distal facet		20	19				21	22.5	22.5		

	TRIQUETRUM	S-12258 dex D: 6b	E-11067 dex E: 10	F34-10.4 sin E: 12	E-11035 sin G: 15	E-10214 dex G: 16	E-10633 sin G: 18a	E-10898 dex G: 18b
Kq1	Dorsal maximal height	38	40	36.5	37	44	38	27
Kq2	Dorsal height, between tips of both facets	24	24	21	22.5	28	23	21
Kq3	Height in the middle	26.5	31	24.5		32	27.5	
Kq4	Palmar height	32	38.5	31		39	33	
Kq5	Depth of proximal facet	49	50	44		51.5	48.5	
Kq6	Breadth of proximal facet	30.5	33 ~	27.5		36		
Kq7	Depth of distal facet	39	38	35		42.5	37	
Kq8	Breadth of distal facet	20.5	21	21		25.5	21	

	PISIFORME	99W-84 ? E: 10	A30-3.2 ? E: 11b	99E-4 ? G: 16
Kp1	Diameter of the tuberosity	51	48	
Kp2	Proximal depth	55	50	
Kp3	Maximal depth	58.5	57	
Kp4	Maximal height	47.5	46	
Kp5	Breadth of the articular facet	36	34	32.5
Kp6	Height of the articular facet		28	22

	TRAPEZOIDEUM	N37-94.2 dex E: 8a	E-11311 ? E: 10	E-11034 dex G: 15	E-11038 sin G: 15	S07-43 G: 15?	E-10126 sin G: 16	E-11366.1 sin G: 16	99W-27 sin G:17	K33-195.1 dex G: 17c	E-9532 G: 18	E32-57 dex G: 18	E-11110 sin G: 21
Kt1	Maximal height	26	26	23	24	26	27	27	27	25	28.5	30	29
Kt2	Maximal diagonal	31	32	25	29		29	31.5	33 ~	36 ~	32	34 ~	35
Kt3	Maximal diameter of the distal facet	23	23	21.5	22.5		23	24	26.5		25.5	24 ~	27
Kt4	Breadth of the proximal facet	19 ~	20	15	17	17	19	20	21.5		21	19 ~	23.5
Kt5	Minimal diameter of the distal facet	16	15	15	16		15	15	16		17		19.5

	CAPITATUM	E-6160 dex E: 8a	SK06-2 E: 10	F34-7 sin E: 12	G34-32 sin E: 12	E-11366.2 sin G: 16	P57-14 dex G: 16	K33-195.1 dex G: 17c
Kc1	Height of the palmar region				26	27		29
Kc2	Height of the dorsomedial region	20.5	22.5		21		23	19.5
Kc3	Maximal diameter	46		41				50
Kc4	Depth of the lateral part	37			38			43 ~
Kc5	Depth of the proximal lateral ridge	31			32			
Kc6	Depth of the distal facet	27	24		30			38
Kc7	Maximal breadth	36.5	37.5					50
Kc8	Breadth of the distal facet	34.5	34					47 ~
Kc9	Maximal diagonal of the palmar proximal facet	16			16.5	18		
Kc10	Diagonal of the palmar lateral facet	14			12	12		

	HAMATUM	B30-21.2 dex E: 11a	99E-18 dex F: 13b	E-11395 sin G: 15	E-11330 sin G: 16	H33-44 dex G: 16	L31-f01 sin G: 16	P57-SK02.3 dex G: 16	I32-72 dex G: 17	K32-89 sin G: 17	K32-f03 dex G: 17	E-10877 sin G: 18a	AF221 AF: L2
Kh1	Height of the dorsal region	24 ~	25.5	23.5				26	22	23	25.5	24	27.5
Kh2	Height of the palmar region	26 ~	28	27	27.5	24 ~	26	30	25.5	23	30.5		34
Kh3	Maximal diameter (including the hamulus)	51 ~		50					52.5		53		
Kh4	Depth of the proximal facet	47	44	46.5			43.5	46	46 ~	43.5	44		54
Kh5	Depth of the distal facet	44	42	38.5				41	43	37	41.5		49.5
Kh6	Maximal breadth (from medial notch)	35	30.5	31			28	33	31	28.5	30		38
Kh7	Breadth of the proximal facet (in palmar region)	23	24	23			24	30	25	25	23		32
Kh8	Breadth of the distal facet	28 ~	33	27	23	30 ~	30		32	30	31.5		34.5
Kh9	Diagonal of the palmar medial facet		16	13.5	15				14	14.5	17		16

	FIBULA	C31-x1 dex E: 11a	E-11363 ? G: 16	L33-f03 dex G: 16	M31-106 sin G: 17	E-9610 sin G: 18	E32-31 dex G: 18	M32-128 sin G: 18	E-10379 sin G: 18a	E-10579.2 sin G: 18a	S07-19 dex ?
fi1	Height dorsal		31	29	33	27.5	26	30.5 ~	39	30.5	31
fi2	Height in the middle (height of the process)	29.5	28		30	28.5		22 ~	31	27.5	29
fi3	Height plantar	20	20.5	19.5	22	19	21	18 ~	24	21	21
fi4	Maximal depth	41	44.5	41	45	39.5	42.5		51	46.5	42
fi5	Depth of the proximal facet	38	40	39.5	39	37	38		44	41	40
fi6	Depth of the distal facet	34	35	31	35	33	33	31	41	37.5	32
fi7	Dorsal breadth of the proximal facet		27	22.5	27.5	21	27.5	26	33	25	25
fi8	Plantar breadth of the proximal facet	15	16	15	16.5	17.5	18.5		21	17	21
fi9	Breadth of the distal facet	21	20	18	20	15	20	20	22	19	20
fi10	Depth of the medial (astragalus) facet	33.5	39	33.5	34	29.5	35	32	40	36.5	35

	ASTRAGALUS	A28-2 sin D: 6x	S-12402 dex D: 7	H40-9 sin D: 7d	N36-313 sin E: 8a	N37-57 dex E: 8a	E-9164 dex G: 15	D31-3a sin G: 15a	E-9442 sin G: 16	E-9804 sin G: 16	L33-f01 dex G: 16	E-9611 dex G: 18	E-9828 sin G: 18	K33-347 dex G: 18
Ta1	Height of the lateral side	77 ~	70		73	68	77 ~		82	85	78	75	78.5	80
Ta2	Height axial	61.5	53	54	55		59	68	64	64.5	61.5	57.5	61	63
Ta3	Height of the medial side	72	61	63 ~	64		69	80	72	76	70	66.5	71.5	73
Ta4	Proximal depth of the lateral side	33	29		32.5	27	32		35	36	33.5	32.5	33	32 ~
Ta5	Distal depth of the lateral side	22 ~	20				25		26	26	23	24	28	26
Ta6	Middle depth of the lateral side	37	32.5		34	32	38		40.5	41	36	37	37	40
Ta7	Proximal breadth	45	41		42	42 ~	44.5		53	48	48	43	43.5	48
Ta8	Breadth of the calcaneal surface	33 ~	32.5		31		33		33	30	35	34	34.5	33.5
Ta9	Breadth at the lateral (calcaneal) process				47 ~					56	52			
Ta10	Distal breadth	47 ~	48		48		51	51	54	54	50	48	51	49
Ta11	Greater maximal diameter (dorsolateral-distomedial)	90	80		82		87		92	98	90	85.5	90.5	90
Ta12	Lesser maximal diameter (dorsomedial-distolateral)	76	73		73	70 ~	79	86	84	84	81	76.5	78	83
Ta13	Minimal depth of the proximal trochlea (groove)	22		19 ~	20									
Ta14	Breadth of the medial part of the distal trochlea													30 ~
Ta15	Breadth of the lateral part of the distal trochlea													20
Ta16	Medial depth of the distal trochlea	25												27
Ta17	Axial depth of the distal trochlea (groove)	16			16									17
Ta18	Lateral depth of the distal trochlea	21			25									28
Ta19	Height of the calcalneal surface	54			48 ~									

	CALCANEUS	N36-309.1 sin E: 8a	N38-128 dex E: 8a	K33-18.7 dex E: 10	G34-26 ? E: 12	E-9166 dex G: 15	E-11106 sin G: 16	E-11107 sin G: 16	I32-f00 dex G: 17	M31-101 sin G: 17	L32-43 dex G: 16	L32-45 dex G: 16	K33-224 sin G: 17c	L33-116 dex G: 18
Tc1	Maximal height (greatest length)	140 ~				148	157		140.5					165
Tc2	Depth of the tubercle	45		41		48	52		48	45	52			48
Tc3	Maximal breadth of the tubercle	46		37		41	45.5		40	44	39			43
Tc4	Minimal breadth of the tubercle	25		19 ~		21	22		17		21			25
Tc5	Depth medial (plantar border to substentaculum)	56				63	66	59.5						65
Tc6	Breadth of the substentaculum	45				46	46.5	43						47.5
Tc7	Medial distal height	72 ~				74	77	73						80
Tc8	Depth lateral (plantar border to fibular trochlea)	64				69	75.5	67	64					76
Tc9	Height of the fibular trochlea	31 ~	30			31	35	33	30				34	34
Tc10	Breadth of the fibular trochlea	20					20	20	19			20.5	19	21
Tc11	Distal lateral height (fibular trochlea to distal facet)	56 ~	56.5			56.5	63	60	52				61	66.5
Tc12	Breadth of the plantar border	22 ~				23	22	18.5	20					24
Tc13	Height of the distal (cuboid) facet	40 ~	39.5		41.5 ~	40	45 ~	38	38			42		46
Tc14	Breadth of the distal (cuboid) facet	22.5 ~	21		23.5 ~		20	22	21			25		26.5

	CUBOIDEUM	AB28-D07 dex D: 6x	99W-67 dex E: 8	E-11066 sin E: 10	K32-1.5 sin E: 10	P57-3 sin G: 16	E-10579.1 dex G: 18a
Tq1	Dorsal height		29	33		35	31
Tq2	Medial height (proximal process to centrodistal medial facet)				37		28
Tq3	Plantar diagonal (proximal process to plantar tuberosity)						45
Tq4	Proximal depth (proximal dorsal border to plantar tuberosity)		55			60 ~	56
Tq5	Distal depth (distal dorsal border to plantar tuberosity)		52			54 ~	51
Tq6	Lateral depth (proximal dorsolateral border to plantar tuberosity)		47			52 ~	47
Tq7	From the plantar border of the proximal facet, to the dorsal border of the distal facet		50			50 ~	51
Tq8	From the dorsal border of the proximal facet, to the plantar border of the distal facet		45 ~			52.5	48
Tq9	Depth of the proximal facet		47 ~			50	47
Tq10	Depth of the distal facet	37 ~	35			40	35
Tq11	Length of the lateral groove (laterodorsal border of the proximal facet to distal facet)	41	38			45	36
Tq12	Length of the plantar tubercle (centrodistal medial facet to plantar tuberosity)		34				35
Tq13	Proximal breadth (centrodistal medial facet to lateral border of proximal facet)		41				41
Tq14	Distal breadth (centrodistal medial facet to lateral border of distal facet)		39				40
Tq15	Maximal diagonal breadth (proximal process to lateral border of distal facet)						46
Tq16	Breadth of the main proximal facet		33			34 ~	35
Tq17	Breadth of the distal facet	27 ~	24			29	22.5
Tq18	Breadth of the dorsal proximal facet		21	19		21	19

	NAVICULARE	M35-36 sin E: 8b	E-11310 sin E: 10	D32-1.1 sin E/F: 11-13?	E-10196 dex G: 16	E-10247 dex G: 16	M31-110.2 dex G: 17	E-10875 dex G: 18a
Tn1	Dorsal height	18 ~	16 ~	18	17		20.5	19
Tn2	Lateral height		18 ~	17	15.5		16 ~	14
Tn3	Plantar height		27 ~		31	30	35 ~	31
Tn4	Maximal depth	48.5	47 ~		45	46		44
Tn5	Maximal breadth	33	32 ~	32 ~	29	32	33 ~	28
Tn6	Depth of the distal dorsal and lateral facet	43	39 ~	41	40.5	43		40
Tn7	Depth of the distal dorsal facet	35	35 ~	34	34	35		33
Tn8	Depth of the distal plantar facet	13.5			13	12	13 ~	12
Tn9	Breadth of the distal dorsal facet	20	20 ~	19	20	20		18

	INTERMEDIOLATERAL CUNEIFORME	A28-C17 sin D: 6x	E-11304 sin E: 10	E32-21 sin G: 18	E32-23 dex G: 18	E-10899 dex G: 18b
Tl1	Maximal breadth	37	35	35	34	
Tl2	Proximal breadth	21	19	19	19	
Tl3	Proximal depth	38	32	34	35	37
Tl4	Diameter of the plantar lateral facet	11 ~		9.5	7	
Tl5	Diameter of the dorsal lateral facet	17 ~	13.5	15	14.5 ~	
Tl6	Lateral depth	33	30	29	27 ~	
Tl7	Lateral height	16.5	19.5	19.5	20	
Tl8	Breadth of distal facet	25	22	23	21	
Tl9	Depth of distal facet	34	30.5	32	32	

Conclusion

This thesis brings some important contributions to the paleontological history of Old World camelids. The two extant species of this group, the Bactrian camel and the dromedary, are among the most important domestic animals, yet their evolutionary history is still very poorly understood: hence, this work starts to fill a relevant scientific void. The thesis includes a morphometric comparison of the skeleton of both extant species, finding statistically significant differences in most bones; a description of the Algerian species *Camelus thomasi*, which is represented by abundant cranial and postcranial material from its type locality Tighennif, but was known only through short description of few elements; and a detailed analysis of the rich camelid fauna in El Kowm, Syria. This site complex holds a prominent place in the Quaternary paleontology of the Middle East, as it represents a rare instance of arid steppe fauna, in contrast to most other sites in the region which sample other habitats - Mediterranean scrub or montane forest.

A minimum of six unique species are detected in El Kowm over the span of the last 1.8 Ma. Three species are well defined, well represented by cranial and postcranial material, and are therefore described and named as new species. Another species is postcranially distinctive, but the lack of well preserved cranial material dissuaded me from creating a formal name for it. The last two forms, the oldest, are represented by convincing but scarce postcranial material, and remain unnamed as well. No specimen can be referred to any already known camel species, extant or extinct. Outside of El Kowm, only five fossil *Camelus* species are known: they originate from three continents (Africa, Europe and Asia) and cover a time span longer than 3 Ma. These numbers highlight the richness and importance of the camelid fauna from El Kowm.

However, much work remains to be done. Concretely, the studies included in this thesis can be further expanded to additional material or topics. The fossil collection which is stored in Tell Arida might become available again, once the political situation in Syria allows resuming the fieldwork in the El Kowm region. The investigated sample might be further extended to include the material from Umm el Tlel and of other species, such as the extant wild camel (*Camelus ferus*) and the fossils *Camelus knoblochi, "Camelus" sivalensis,* and the *Paracamelus* species. A systematic study of these additional Old World camelid samples will then allow the elaboration of a meaningful phylogeny. My position is that attempting a phylogenetic reconstruction using only the El Kowm material and the sketchy informations available on other forms would have been a rather futile endeavour. Looking even further, the study of Camelidae might be extended to the North American species, especially the huge and largely unstudied Frick Collection at the American

Museum of Natural History, New York. Finally, the methods here presented, focusing on the uses of the Harmonic Score data transformation, might be applied to other paleontological topics, as they have the potential to shed new light on other groups of similar, size-overlapping species.

But in general, the greatest need is for additional research on the field. Old World camels lived and still live in regions where the paleontological effort has been relatively shallow, such as the Middle East, Northern Africa and Central Asia: regions where the population is scarce to begin with, and where the influence of Western scientific interest has been less than in other continents. This also helps explaining the lack of evolutionary knowledge about camels, compared with other livestock, but also compared with the abundant veterinary research on camels that has been stimulated by practical economical interests. It is to hope that in the future, more effort and resources will be dedicated to the origins of such unusual, unique, and important animals.